

Revision of the “*Chloritis delibrata* (Benson, 1836)” group (Gastropoda, Stylommatophora, Camaenidae)

Barna Páll-Gergely¹, Jonathan D. Ablett², Márton Szabó³, Eike Neubert^{4,5}

1 Plant Protection Institute, Centre for Agricultural Research, Herman Ottó Street 15, Budapest, H-1022, Hungary **2** Mollusca Section, Invertebrates Division, Department of Life Sciences, The Natural History Museums, London SW7 5BD, UK **3** Hungarian Natural History Museum, Department of Paleontology and Geology, Ludovika tér 2, Budapest 1083, Hungary **4** Natural History Museum of the Burgergemeinde Bern, Bernastr. 15, CH-3005 Berne, Switzerland **5** Institute of Ecology and Evolution, University of Bern, 3012 Bern, Switzerland

Corresponding author: Barna Páll-Gergely (pallgergely2@gmail.com)

Academic editor: Martin Haase | Received 27 October 2021 | Accepted 22 November 2021 | Published 15 February 2022

<http://zoobank.org/0AFF7CFB-9400-477F-8116-0120C393C4FD>

Citation: Páll-Gergely B, Ablett JD, Szabó M, Neubert E (2022) Revision of the “*Chloritis delibrata* (Benson, 1836)” group (Gastropoda, Stylommatophora, Camaenidae). ZooKeys 1086: 1–31. <https://doi.org/10.3897/zookeys.1086.77180>

Abstract

Chloritis delibrata (Benson, 1836), known from northeastern India, was believed to have three varietal forms, sometimes mentioned as subspecies: *C. delibrata* var. *khasiensis* (Nevill, 1877) and *C. delibrata* var. *fasciata* (Godwin-Austen, 1875) from the Khasi Hills, India, and *C. delibrata* var. *procumbens* (Gould, 1844) from Dawei in Myanmar. The reproductive anatomy of the latter form is known and does not match with those of any continental camaenid genera, but does with that of the newly examined *Chloritis platytropis* Möllendorff, 1894 from Thailand. The latter species is conchologically similar to *Bouchetcamaena huberi* Thach, 2018 (synonym of *Helix fouresi* Morlet, 1886), which is the type species of the genus *Bouchetcamaena* Thach, 2018. Thus, *Bouchetcamaena* can provisionally host the entire *Chloritis delibrata*-group with the exception of var. *fasciata*, which is transferred to *Burmochloritis* Godwin-Austen, 1920 due to the multiple reddish bands on its shell. The examination of shells deposited in the Natural History Museum, London revealed that seven morphologically distinguishable forms are present, which are accepted here as representing distinct species. Four new species are described from India: *Bouchetcamaena foveata* Páll-Gergely **sp. nov.**, *B. fusca* Páll-Gergely **sp. nov.**, *B. raripila* Páll-Gergely **sp. nov.**, and *B. subdelibrata* Páll-Gergely **sp. nov.**

Keywords

Bouchetcamaena, *Burmochloritis*, conchology, India, Myanmar, new combinations, new species, shell morphology, systematics, taxonomy

Introduction

Chloritis (*Trichochloritis*) *delibrata* (Benson, 1836) was considered to be a variable camaenid species inhabiting a relatively large area from Assam in India to Dawei (= Tavoy) in Myanmar (Stoliczka 1871; Gude 1914). The distance between these two sites is approximately 1500 km as the crow flies. The last overview of this species was published over a century ago in the Fauna of British India by Gude (1914) who listed three varieties: var. *khasiensis* (Nevill, 1877) and var. *fasciata* (Godwin-Austen, 1875) from the Khasi Hills, India, and var. *procumbens* (Gould, 1844) from Tavoy, Myanmar. The two Indian varieties were listed as subspecies of *Chloritis delibrata* in the latest Indian checklist (Ramakrishna et al. 2010).

Examination of specimens assigned to *Chloritis delibrata* and its forms in the Natural History Museum, London, revealed that at least seven species can be distinguished based on the shape the shell and, most importantly, its fine sculpture. Thus, we here give an overview of the *C. delibrata* group, and describe the morphologically recognisable, distinct entities as species.

Generic position

Placing the *Chloritis delibrata*-group in its appropriate genus turned out to be challenging. The morphology of the jaw and the radular teeth, along with the outer characters of the reproductive anatomy of “var. *procumbens*” from Moulmein were described by Stoliczka (1871) [redrawn by Pilsbry (1894) and in this manuscript (Fig. 1)]. Based on these descriptions, the penis is spindle-shaped, the epiphallus is longer than the penis, slender, cylindrical, the retractor muscle inserts at the penis-epiphallus transition, and there is a slender, pointed, moderately short flagellum. We needed to examine the possible placement of the *Chloritis delibrata*-group in *Chloritis* Beck, 1837, *Trichochloritis* Pilsbry, 1891, and *Trachia* Martens, 1860, since this species complex had previously been placed in those genera, along with *Bellatrachia* Schileyko, 2018, *Bouchetcamaena* Thach, 2018, *Burmochloritis* Godwin-Austen, 1920, *Neotrachia* Schileyko, 2018, *Planispira* Beck, 1837, *Satsuma* A. Adams, 1868, and *Sinochloritis* M. Wu & Z. Chen, 2019, which inhabit the same or adjacent geographic areas. The key traits of the reproductive anatomy are summarized in Table 1.

The anatomy of the type species of *Trichochloritis* (*Helix breviseta* Pfeiffer, 1862) is known based on Stoliczka (1873) (see also Páll-Gergely and Neubert 2019). The most obvious difference is the presence of a slender but relatively long penial caecum, which is absent in *C. delibrata* var. *procumbens*. Further differences include the following: flagellum shorter, vagina longer in *Trichochloritis*, and bursa of bursa copulatrix more ovoid, less elongated.

Some species of *Satsuma* (type species: *Helix japonica* L. Pfeiffer, 1847; SD, Kuroda and Habe 1949) from China are similar to the *delibrata*-group in terms of the thin shell with a single band, but *Satsuma* is characterized by a well-developed penial caecum (Wang et al. 2014; Zhang et al. 2019). We note that those Chinese *Satsuma*

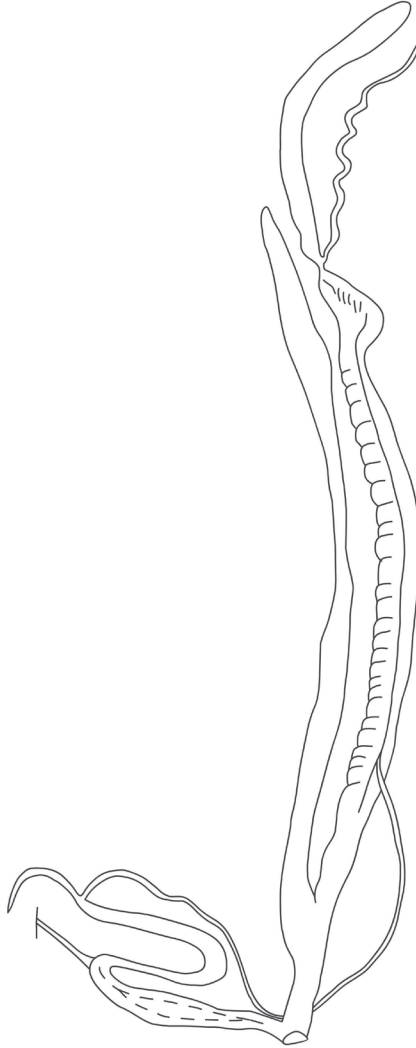


Figure 1. Reproductive anatomy of *Chloritis delibrata* var. *procumbens* (Gould, 1844). Redrawn from Stoliczka (1871).

species possess a short, vestigial flagellum, which is well developed, rather long in the type species of *Satsuma* (see Emura 1933; Azuma 1995; unpublished information); thus, the generic status of the Chinese *Satsuma* species requires a revision.

Sinochloritis, known only from the Chinese Sichuan Province, also possesses a large penial caecum. Thus, we do not consider the *C. delibrata*-group to belong to any of those three genera (*Trichochloritis*, *Satsuma*, *Sinochloritis*).

The type species of *Trachia* Martens, 1860 (*Helix asperella* L. Pfeiffer, 1846) is not known anatomically. The anatomy of *Trachia vittata* (O. F. Müller, 1774) was

Table 1. Most important character states of camaenid genera relevant for this study.

	References	Penis	Inner structure of the penis	Penial sheath	Epiphallus	Insertion of retractor muscle	Penial caecum	Flagellum	Additional organ
<i>Bouchetamaena</i> Thach, 2018	this study	long, apically thickened	parallel folds and a vestigial verge	absent	long, cylindrical	on distal epiphallus	absent	long, slender	absent
Continental " <i>Chloritis</i> "	Sutcharit and Panha (2010), Páll-Gergely et al. (2020)	long, apically thickened	parallel folds and a large verge	absent	long, cylindrical	on distal epiphallus	absent	medium length, gradually becoming slender	absent
<i>Neotrachia</i> Schileyko, 2018	Schileyko (2018)	short, thick	longitudinal pilasters, broken into series of tubercles	absent	swollen, ovoid	penis-epiphallus transition	absent	medium length, gradually becoming slender	absent
<i>Trachia</i> Martens, 1860 (based on <i>T. vittata</i>)	Schileyko (2003)	short, swollen	chaotically arranged pilasters	covers entire penis	rather short, thick	incorporated into penial sheath	absent	rather long, gradually becoming slender	–
<i>Trichochloritis</i> Pilsbry, 1891	Collinge (1903), Páll-Gergely and Neubert (2019)	long, apically thickened	unknown	absent	long, cylindrical	on distal epiphallus	moderately long, slender	very short, pointed	absent
<i>Burmochloritis</i> Godwin-Austen, 1920	Godwin-Austen (1920), unpublished information	long, thick, cylindrical	wavy folds, verge absent	absent	long, cylindrical	bounds penis and epiphallus at some distance from their junction	short, pointed	long, slender	long, cylindrical, derives from wall of vagina
<i>Satsuma A.</i> Adams, 1868	Wang et al. (2014), Zhang et al. (2020)	long, cylindrical	wavy folds, verge absent	absent	long, cylindrical	on distal epiphallus	well-developed, tapering	long to short	absent
<i>Sinochloritis</i> M. Wu & Z. Chen, 2019	Wu & Chen, 2019	thick, cylindrical	parallel folds, verge absent	absent	long, cylindrical	on distal epiphallus, and also covers proximal part of penis	large, internally with "peach shaped epiphallic papilla"	long, slender, tapering	absent
<i>Bellatrachia</i> Schileyko, 2018	Schileyko (2018), Páll-Gergely and Neubert (2019)	long, cylindrical	parallel folds	absent	long, cylindrical	penis-epiphallus transition	absent	thick, somewhat swollen, with slender tip	absent
<i>Planispira</i> Beck, 1837	Schileyko (2003)	short, apically thickened	folds and an ovoid, large verge	absent	long, cylindrical	middle of epiphallus	absent	short, conical	absent

described by Schileyko (2003), who revealed that it is entirely different from that of *Chloritis delibrata*, since the retractor muscle joins the fibrous sheath around the penis. Later, Schileyko (2018) claimed that since the shell of *Trachia asperella* is similar to that of "*Helix*" *delibrata*, their anatomy is also probably similar, and thus, classified *C. delibrata* in *Trachia*. However, *Trachia vittata* possesses multiple spiral bands, whereas only a single band is present in the *delibrata*-group. More importantly, *Trachia vittata* is known from central and southern India (Gude 1904; Mitra et al. 2004), whereas the *delibrata*-group is restricted to the areas southeast of the Himalaya, a biogeographically very distinct region. Moreover, most other species named by Schileyko (2018) as possible *Trachia* species also inhabit the Indian subcontinent.

Thus, it is improbable that *Trachia vittata* and the species of the *C. delibrata*-group would belong to the same genus.

Bellatrachia differs from Stoliczka's (1871) drawing of *C. delibrata* var. *procumbens* by the much longer penis and epiphallus, the well-developed flagellum, and the thickened base of the bursa copulatrix.

Burmochloritis Godwin-Austen, 1920 (type species: *Burmochloritis kengtungensis* Godwin-Austen, 1920, OD) possesses a long flagellum, a well-developed, large penial caecum is, and an additional organ (homologous with dart sac?) originating from the wall of the vagina (Godwin-Austen 1920; and unpublished information).

The genital anatomy of *Neotrachia* is very different from that of *C. delibrata* var. *procumbens* due to its short penis and swollen epiphallus (Schileyko 2018).

The type species of *Planispira* Beck, 1837 (*Helix zonaria* Linnaeus, 1767) was re-described by Schileyko (2003) as having penis swollen and epiphallus relatively short and thick (spindle-shaped penis and long, slender epiphallus in *C. delibrata*), and stalk or bursa copulatrix very long, convoluted.

This makes it improbable that the *C. delibrata*-group belongs to any of the genera *Bellatrachia*, *Burmochloritis*, *Neotrachia*, and *Planispira*.

The type species of the genus *Chloritis* is *Helix unguolina* Linnaeus, 1758 (SD, Gray 1847), which was described without stating the type locality. Subsequently it turned out to inhabit Indonesia (Zilch 1966). Although the anatomy of *Chloritis unguolina* is unknown, it is highly unlikely that the *Chloritis delibrata*-group would belong to the same genus due to the geographical separation of the two species. Some continental (Thailand, Vietnam) species are classified in *Chloritis*, and their genitalia largely agree with Stoliczka's drawing (Sutcharit and Panha 2010; Páll-Gergely and Neubert 2019; Páll-Gergely et al. 2020). However, the presence of a penial caecum distinguishes continental *Chloritis* from *Bouchetcamaena* (see below).

We examined the reproductive anatomy of a specimen of *Chloritis platytropis* Möllendorff, 1894 from Thailand (Figs 2A, 3, 4), which is conchologically similar to the type species of *Bouchetcamaena* Thach, 2018 (*Bouchetcamaena huberi* Thach, 2018 [Fig. 5A]: synonym of *Helix fouresi* Morlet, 1886). Consequently, the anatomy of *Chloritis platytropis* can be used to characterize *Bouchetcamaena*. *Chloritis platytropis* differs from the *C. delibrata*-group only in the keeled shell, whereas their reproductive anatomy is similar. Moreover, *Chloritis gabata* (Gould, 1844) (Fig. 5B), which was described from Dawei, Myanmar (the type locality of *Chloritis delibrata* var. *procumbens*), is similar to the type species of *Bouchetcamaena* in shell shape, size and sculpture (including the prominent keel), and differs from the *C. delibrata*-group only in the presence of a keel on the body whorl. We here move *Chloritis gabata* (Gould, 1844) and *Chloritis platytropis* to the genus *Bouchetcamaena*, comb. nov.

Thus, *Bouchetcamaena* can host the entire *Chloritis delibrata*-group with the exception of var. *fasciata*, which is transferred to *Burmochloritis* Godwin-Austen, 1920, comb. nov. due to the multiple narrow spiral bands on its shell. The anatomical characters are summarized in Table 1.

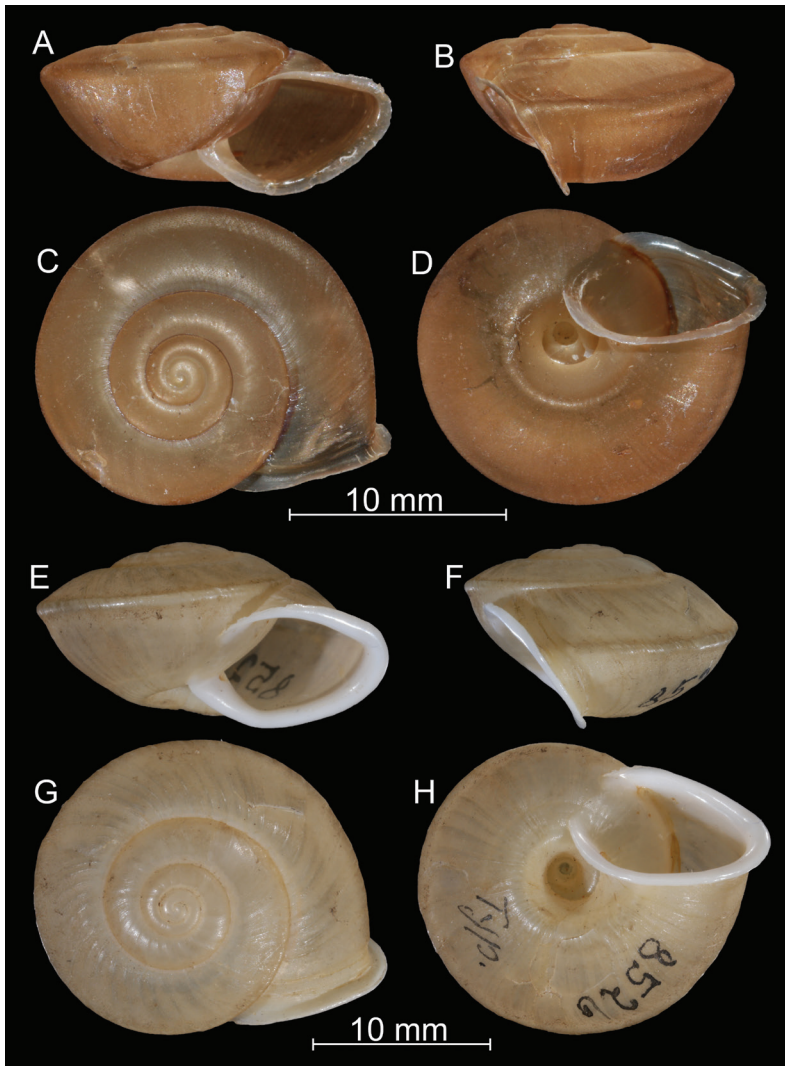


Figure 2. *Bouchetcamaena platytropis* Möllendorff, 1894 **A–D** anatomically examined specimen (ZMH 51934) **E–H** lectotype (SMF 8526). All photos: B. Páll-Gergely.

Materials and methods

Determination of the number of shell whorls (precision to 0.25 whorl) follows Kerney and Cameron (1979: p. 13). In the case of close-up images, multilayer close-up photographs were taken of each shell.

Locality data presented with the specimen examined data are cited as verbatim from the specimen labels. For Indian and Burmese localities see Páll-Gergely et al. (2015a, 2015b). Measurements were taken on the visually selected largest and smallest

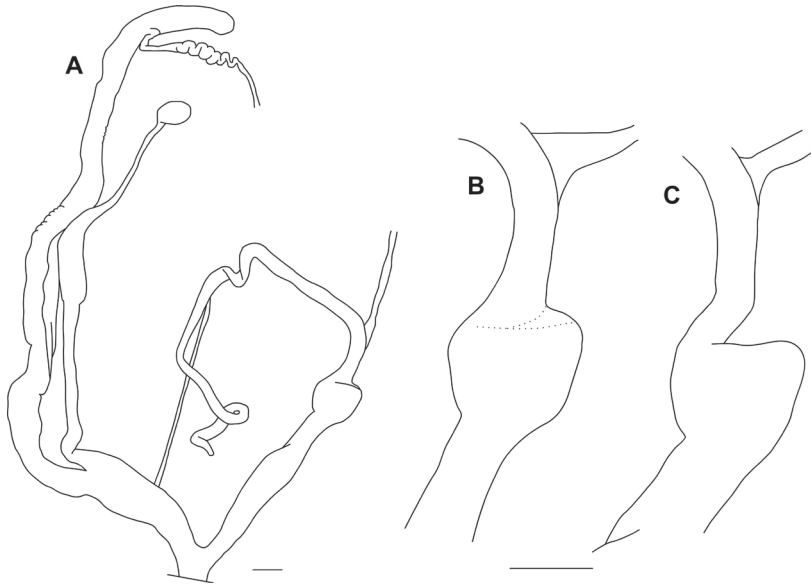


Figure 3. Reproductive anatomy of *Bouchetcamaena platytropis* Möllendorff, 1894 (ZMH 51934) **A** entire genitalia **B** penis before cutting the weak fibres connecting proximal end of penis to distal part of epiphallus; **C** after removing the weak fibres. Scales represent 1 mm.

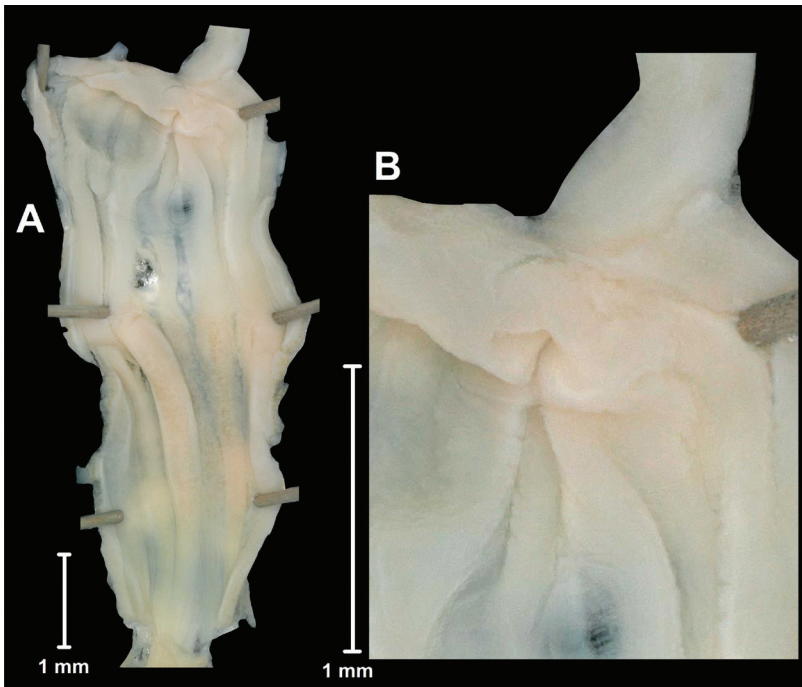


Figure 4. Inner wall of the penis of *Bouchetcamaena platytropis* Möllendorff, 1894 (ZMH 51934) **A** entire penis **B** penis-epiphallus transition.

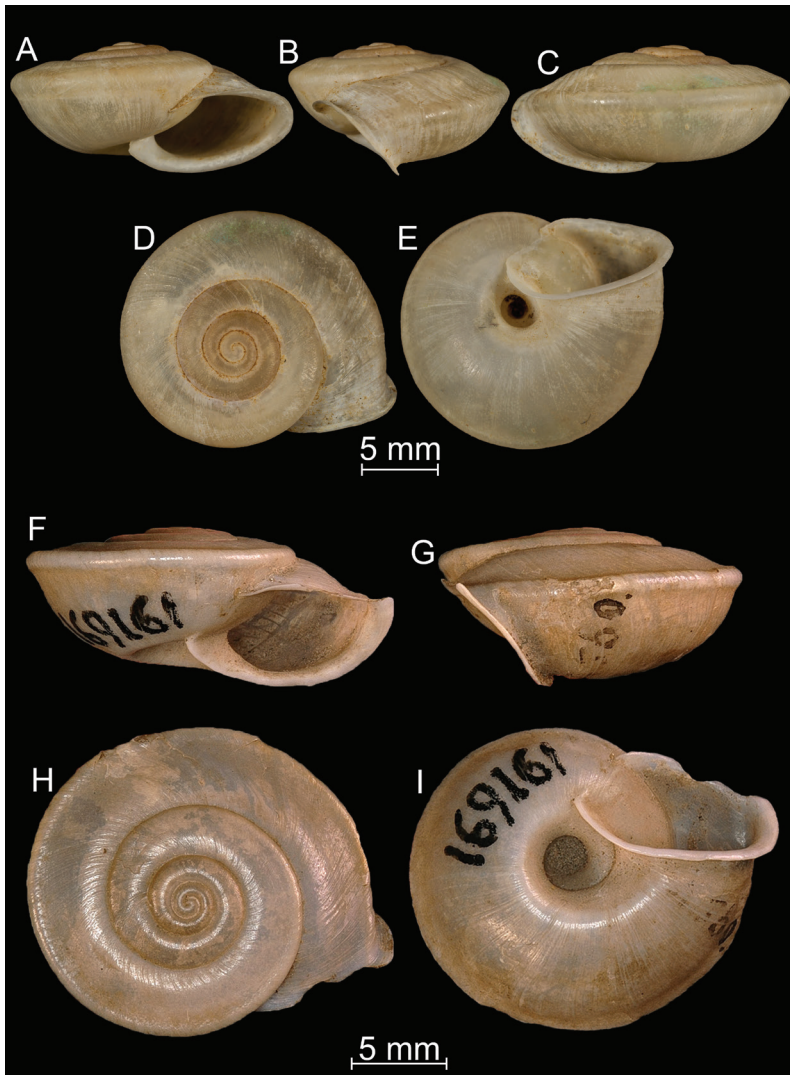


Figure 5. Shells of *Bouchetcamaena* species **A–E** *Bouchetcamaena huberi* Thach, 2018 (synonym of *B. fouresi* (Morlet, 1886), type species of *Bouchetcamaena*) **F–I** *Bouchetcamaena gabata* (Gould, 1844) (MCZ Mala 169161). Photos: M. Caballer, MNHN (**A–E**) and downloaded from MCZ website (**F–I**).

specimens. Figure 6 presents the exact position of shell details that have to be checked when identifying species of *Bouchetcamaena*.

Abbreviations

BSNH	Boston Society of Natural History (Boston, USA)
D	Shell diameter
H	Shell height

MCZ	Museum of Comparative Zoology (Cambridge, USA)
NHM	The Natural History Museum (London, UK)
NHMKUK	when citing lots deposited in the NHM
SMF	Senckenberg Forschungsinstitut und Naturmuseum (Frankfurt am Main, Germany)
UMZC	University Museum of Zoology (Cambridge, UK)
USNM	Smithsonian National Museum of Natural History (Washington, D.C., USA)
ZSI	Zoological Survey of India (Kolkata, India)

Taxonomy and systematics

Camaenidae Pilsbry, 1895

Genus *Bouchetcamaena* Thach, 2018

Bouchetcamaena Thach, 2018: 65.

Type species. *Bouchetcamaena huberi* Thach, 2018, by original designation (synonym of *Helix fouresi* Morlet, 1886 – see Páll-Gergely et al. 2020).

Diagnosis. The shell characters are similar to those of most other *Chloritis*-like groups. Shell depressed to depressed globular (sometimes with a sunken apex), body whorl rounded, colour uniform with a single peripheral band, shell surface covered by hair scars (pits) of variable density (in some cases these are more or less absent on the last whorl) and deciduous periostracum of variable thickness, aperture rounded to oval/subrectangular, peristome expanded, parietal callus only indicated, umbilicus relatively narrow (narrower than one fourth of the shell's width).

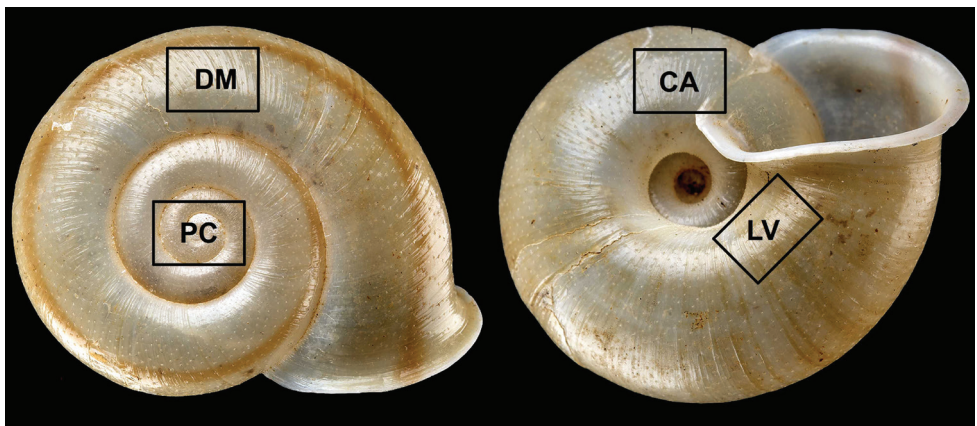


Figure 6. Positions of close-up images. Abbreviations: CA: callus; DM: middle of dorsal side; LV: last whorl; PC: protoconch. Not to scale.

The genital organs [based on *B. procumbens* (Stoliczka 1871) and *B. platytropis* (this study)] are characterized by an elongated penis (spindle-shaped or with slightly swollen proximal end), the absence of a penial verge, a slender, cylindrical epiphallus longer than the penis, a retractor muscle inserted at the penis-epiphallus transition or on the distal end of the epiphallus, and a slender, pointed, elongated flagellum.

Remarks. We only move the few species revised here to this genus. However, several other camaenid species from Southeast Asia may belong to *Bouchetcamaena*, which will be revealed by future studies.

***Bouchetcamaena delibrata* (Benson, 1836), comb. nov.**

Figures 7–10

Helix delibratus Benson, 1836: 352.

Chloritis (*Trichochloritis*) *delibrata* Gude, 1914: 172.

Chloritis delibrata Richardson, 1985: 92.

Chloritis delibrata Ramakrishna et al., 2010: 326.

Type locality. “North-East frontier of Bengal”.

Types examined. UMZC 2387 (1 syntype).

Additional material examined. Khasi Berge, coll. Möllendorff, SMF 27140/1; Hinterindien, coll. Möllendorff, SMF 27141 (2 shells, mixed sample with an-

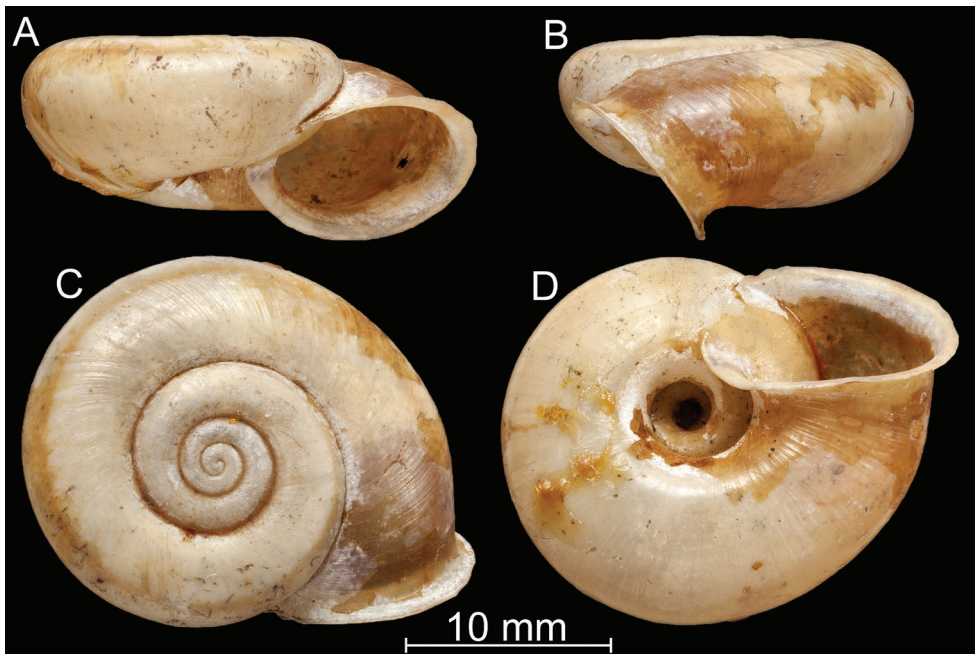


Figure 7. *Bouchetcamaena delibrata* (Benson, 1836), comb. nov. UMZC 2387 (syntype).

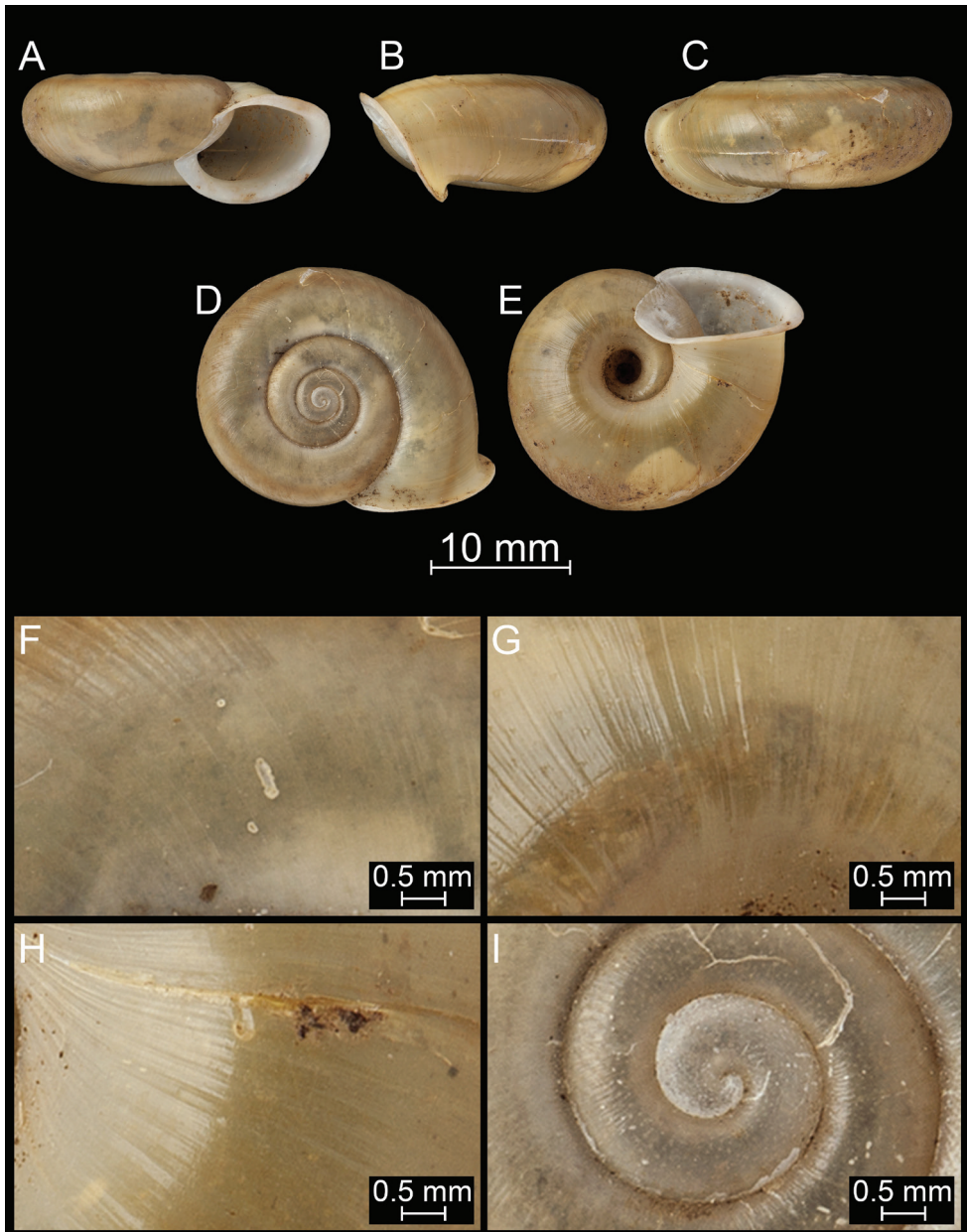


Figure 8. *Bouchetamaena delibrata* (Benson, 1836), comb. nov. NHMUK 1903.7.1.381. For positions of close-up images see Fig. 6 (F = DM, G = CA, H: LV, I: PC).

other species); India, NHMUK 1871.9.23.99/1 (1 shell, mixed lot with *B. foveata*: NHMUK 1871.9.23.99/2); Khasi Hills, blue label 7/12/06, NHMUK 20191138 (1 shell); Khasi Hills, coll. Godwin-Austen, NHMUK 1903.7.1.381/2 (1 shell, mixed lot with *B. fasciata*, NHMUK 1903.7.1.381/1, this is the syntype lot of *fasciata*); Khasi

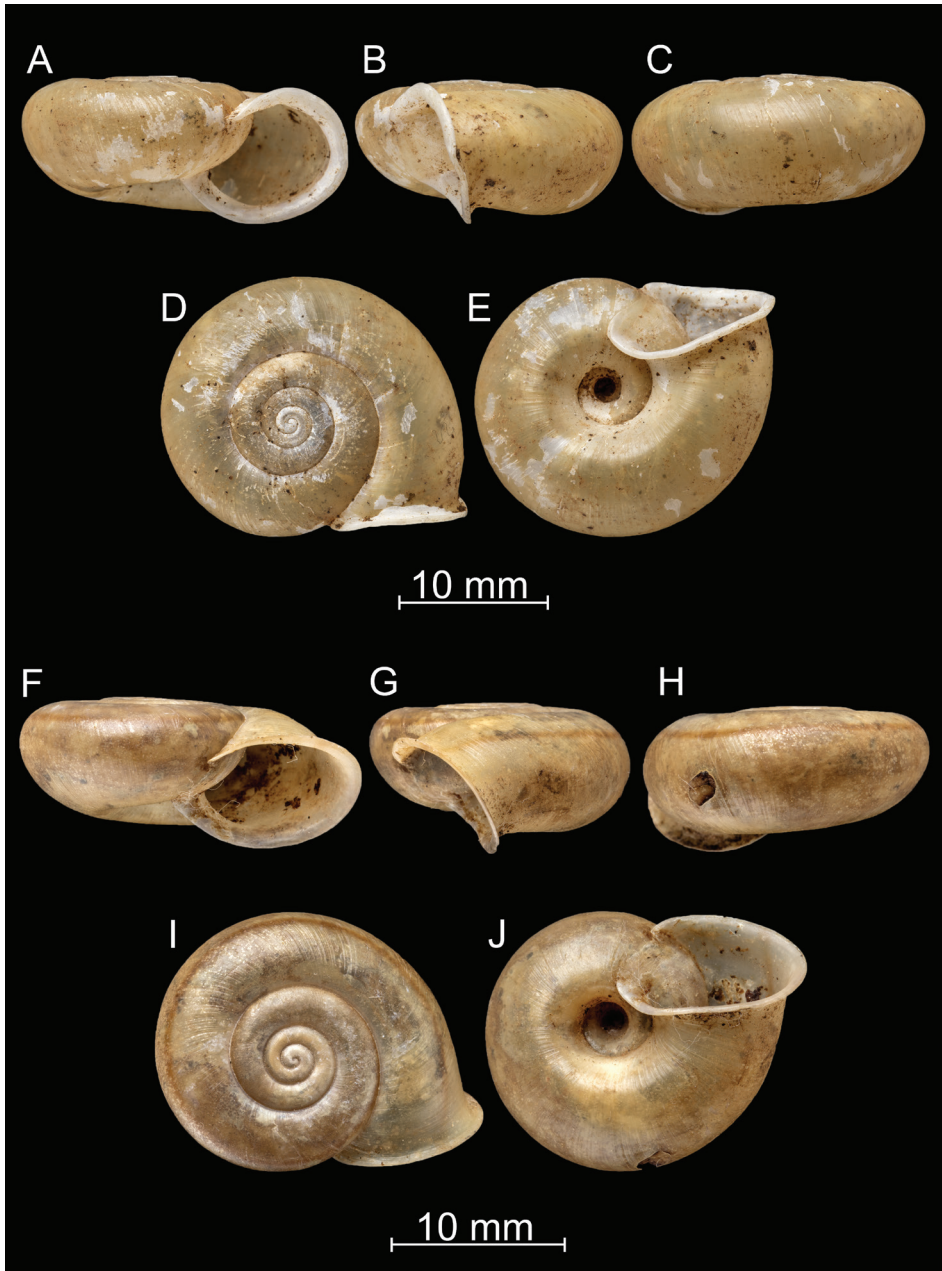


Figure 9. *Bouchetcamaena delibrata* (Benson, 1836), comb. nov. **A–E** NHMUK 1903.7.1.61 **F–J** 1903.7.1.381.a.

Hills, coll. Godwin-Austen, no. 183, NHMUK 1903.7.1.381a/1 (1 shell, mixed lot with *B. fusca*: NHMUK 1903.7.1.381a/2); Khasi Hills, NHMUK 1920.1.28.12-13/1 (1 shell, mixed lot with *B. foveata*: NHMUK 1920.1.28.12-13/2); Manipur, coll. Godwin-Austen, NHMUK 1903.7.1.391/1 (1 shell, mixed lot with *B. fusca*: NHMUK 1903.7.1.391/2); Sibsagar, Assam, coll. Godwin-Austen, NHMUK 1909.3.15.23 (2

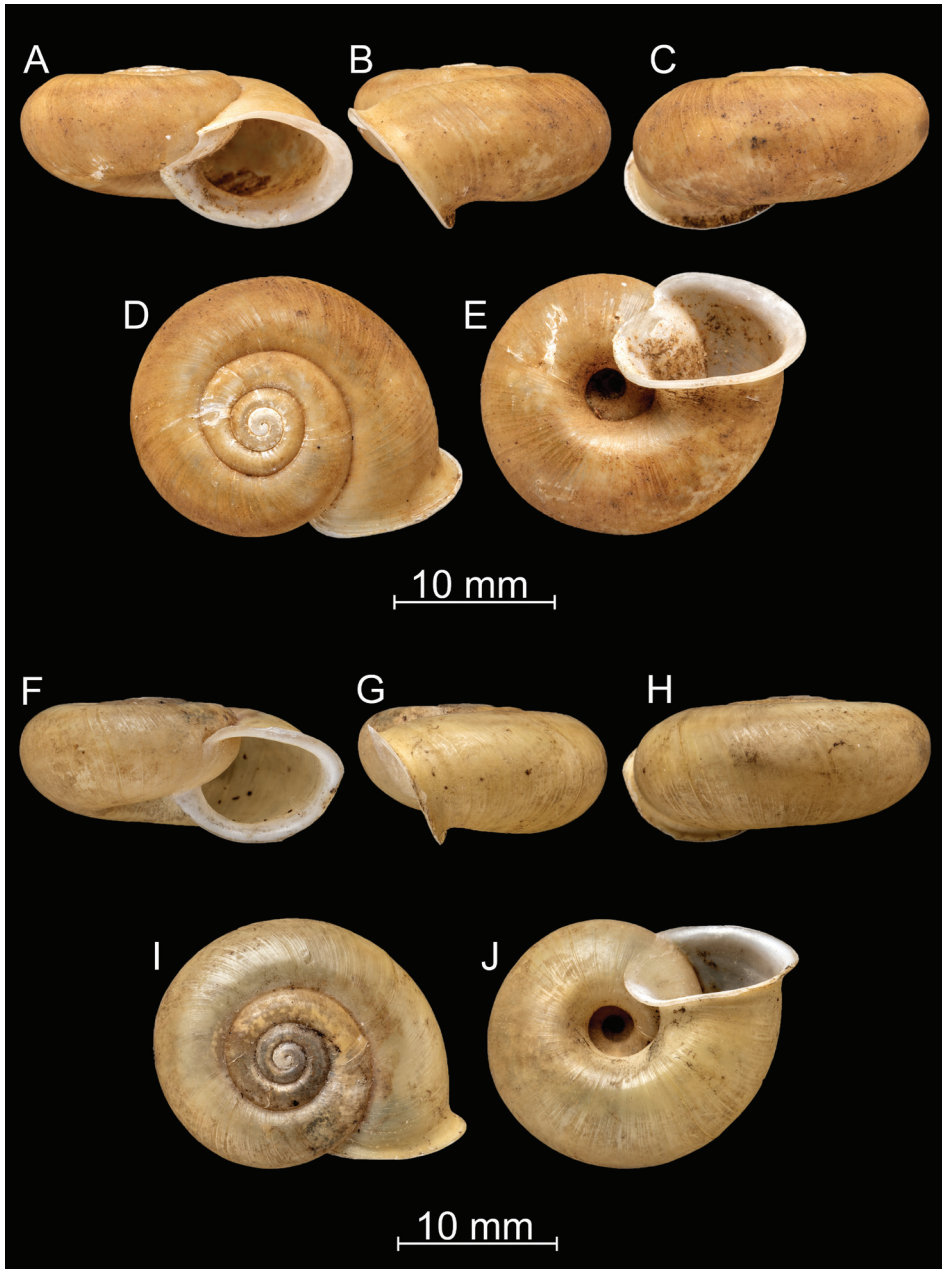


Figure 10. *Bouchetcamarena delibrata* (Benson, 1836), comb. nov. **A–E** NHMUK 1920.1.28.12–13 **F–J** NHMUK 23-iii-15.

shells); South Sylhet Hills, coll. W Chennell, NHMUK 1903.7.1.61/1 (1 shell, mixed lot with *B. subdelibrata*: NHMUK 1903.7.1.61/2).

Diagnosis. Shell large, flat, olive green, glossy, last whorl practically without hair scars, or widely-spaced hair scars near the parietal callus, aperture oval.

Description. Shell relatively large, rather thin-walled; depressed, dorsal side usually entirely flat, rarely very slightly elevated; colour greenish-olive to greenish-yellowish with an obscure, reddish band just above the blunt keel (rarely missing); protoconch consists of 1.75 whorls, with very fine radial ribs and regularly arranged hair scars (pits); entire shell with 4 whorls; separated by a moderately deep suture; teleoconch overall glossy, with irregular, fine growth lines, dorsal side of first 2.0–2.5 whorls covered by widely-spaced hair scars (= pits), and short hairs near suture; ventral side of body whorl without hair scars or widely spaced (in some specimens somewhat denser than in others) pits near the parietal callus only; aperture oval/subrectangular; peristome strongly expanded and slightly reflected in direction of umbilicus; palatal part with very thin, whitish, semi-transparent layer, showing hair scars on penultimate whorl; umbilicus open, relatively wide, funnel-shaped, peri-umbilical keel only very slightly indicated.

Measurements. D = 21.4–24.4 mm, H = 9.2–10.3 mm (n = 4).

Differential diagnosis. *Bouchetcamaena subdelibrata* sp. nov. differs from *B. delibrata* mainly in the presence of hair scars on the entirety of the last whorl. For further differences, see under that species.

Distribution. This species is apparently widespread in the southwestern Himalaya (Khasi Hills, Manipur, Silhet).

***Bouchetcamaena foveata* Páll-Gergely, sp. nov.**

<http://zoobank.org/768A3926-C993-458D-8D27-CC787DCE6633>

Figure 11

Type material. Holotype: Khasia Hills [Meghalaya, India], 183, Assam, coll. Godwin-Austen, NHMUK 20191130/2 (D: 20.5 mm, 9.1 mm, mixed lot with *B. fasciatus*: NHMUK 20191130/1).

Paratypes: Assam, coll. C. Bosch ex coll. H. Rolle, SMF 297336 (2 paratypes, labelled as *delibrata* f. *major*); Assam: Chenapoongu, coll. Jetschin ex coll. Gude 1900, SMF 91157 (2 paratypes); Assam: Khasia Hills, coll. C. Bosch ex coll. H. Rolle ex coll. Schlüter, SMF 297335 (2 paratypes); (1) Khasi Hills, Assam, (2) Burma, A.S. Kennard coll., Acc. No. 1824, NHMUK 20191136/2 (2 paratypes, mixed lot with *B. procumbens*: NHMUK 20191136/1, the Khasi Hills probably refers to *foveata*, whereas Burma refers to *procumbens*); India, NHMUK 1871.9.23.99/2 (1 paratype, mixed lot with *B. delibrata*: NHMUK 1871.9.23.99/1); India, Laity (?) valley, H.F./W.T. Blanford coll., acc. 1944, NHMUK 20191135 (2 paratypes); Khasi Hills, blue label, 13/II/00, NHMUK 20191140 (2 paratypes, shells corroded by Byrne's disease); Khasi Hills, NHMUK 1920.1.28.12-13/2 (1 paratype, mixed lot with *B. delibrata*: NHMUK 1920.1.28.12-13/1); Nemotha, blue label, 7/3/91, NHMUK 20191139 (2 paratypes).

Diagnosis. Shell relatively large, fragile, thin-walled, dorsal side flat or even slightly sunken, colour light yellow to whitish, with a faint peripheral band; hair scars represented as elevated knobs (like strawberry seeds), or even hair scars represented as truncated hairs or short, slender, pointed hairs; aperture oval, umbilicus relatively narrow.

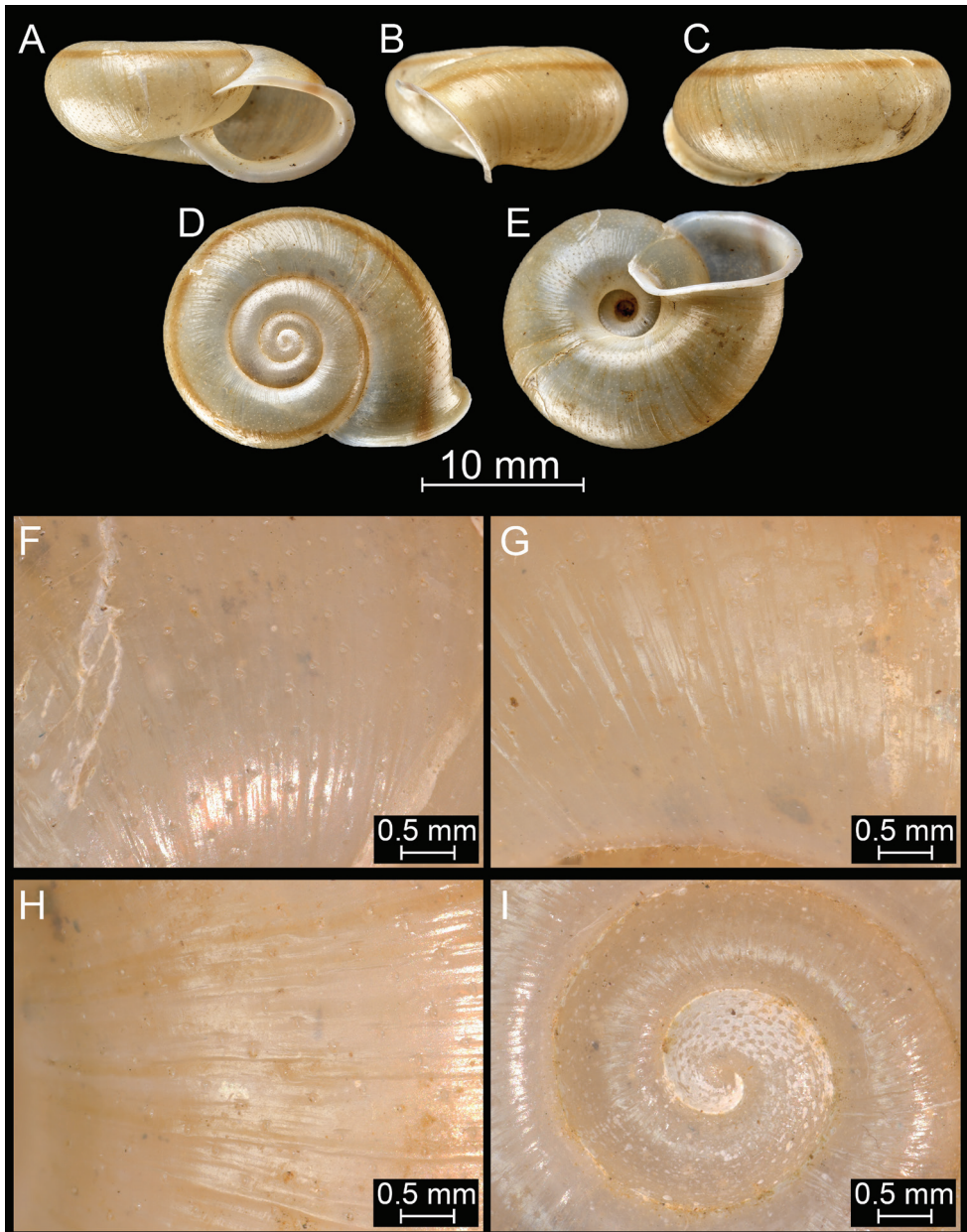


Figure 11. *Bouchetcamaena foveata* Páll-Gergely sp. nov., holotype (NHMUK 20191130/2). For positions of close-up images see Fig. 6 (F = DM, G = CA, H: LV, I: PC).

Description. Shell medium-sized to large, thin-walled; dorsal side flat or even sunken; basic colour light yellowish to whitish, a peripheral band of various thickness present in all specimens, running around the shoulder or the body whorl; protoconch consisting of 1.50–1.75 whorls, finely wrinkled and covered by widely-spaced hair scars

reminiscent of strawberry seeds; entire shell consisting of slightly less or more than 3.75–4 whorls, separated by a relatively deep suture; teleoconch very finely and irregularly wrinkled; hair scars (reminiscent of strawberry seeds) widely-spaced, clearly visible on the entire teleoconch; occasionally (near suture, behind expanded peristome, inside umbilicus, etc.) short, slender, pointed hairs remaining; hairs inside umbilicus denser than elsewhere on the teleoconch; aperture oval/subrectangular; peristome strongly expanded and slightly reflected, especially in direction of umbilicus; palatal part with thin, whitish, semi-transparent layer, which allows hair scars of penultimate whorl to be seen; umbilicus open, normally wide, funnel-shaped, peri-umbilical keel blunt.

Measurements. D = 20.3–20.5 mm, H = 9.1–10.5 mm (n = 3).

Differential diagnosis. This new species differs from that which is the most similar, *B. delibrata*, in having a flatter dorsal side, glossier shell, and deep hair scars on the entire surface. The hair scars of *B. subdelibrata* sp. nov. are much finer and denser on the entire shell surface.

Etymology. The new species is named after its conspicuously pitted (= *foveatus* in Latin) surface.

Distribution. All samples with relatively precise localities were collected in the Khasi Hills.

***Bouchetcamaena fusca* Páll-Gergely, sp. nov.**

<http://zoobank.org/75255BD2-CBD1-4BA5-B0C0-82DD4E88F5CE>

Figure 12

Type material. Holotype: Manipur [India, Manipur], coll. Godwin-Austen, NHMUK 1903.7.1.391/2 (D: 16.8 mm, H: 8 mm, mixed lot with *B. delibrata*, NHMUK 1903.7.1.391/1).

Paratypes: same data as holotype, NHMUK 1903.7.1.391/3 (1 shell: paratype); Gaziphima, Naga Hills, Manipur frontier line, coll. Godwin-Austen, NHMUK 1903.7.1.385 (2 paratypes); Khasi Hills, coll. Godwin-Austen, no. 183, NHMUK 1903.7.1.381a/2 (1 shell, mixed lot with *B. delibrata*, NHMUK 1903.7.1.381a/1); Manipur, coll. Godwin-Austen, NHMUK 20191134 (1 shell).

Diagnosis. Shell small to medium-sized, with flat dorsal side or very slightly elevated spire; thick, brown, matt periostracum makes hair scars practically invisible, aperture oval.

Description. Shell small to medium-sized; depressed-globular, dorsal side flat or spire very slightly elevated; body whorl slightly or relatively strongly but bluntly shouldered; colour brownish due to thick, matt periostracum; protoconch consists of 1.5 whorls, finely wrinkled, with short hairs near suture; in some specimens wrinkles only visible in the middle of whorls, whereas in others hair scars (pits) are also discernible; entire shell consisting of 3.75–4 whorls, suture moderately deep; short hairs visible in the suture and inside umbilicus; hair scars practically invisible due to thick periostracum; in one paratype (NHMUK 1903.7.1.391) periostracum of lighter colour around each hair scar on the ventral side, making the density of scars visible; very few hair scars visible at

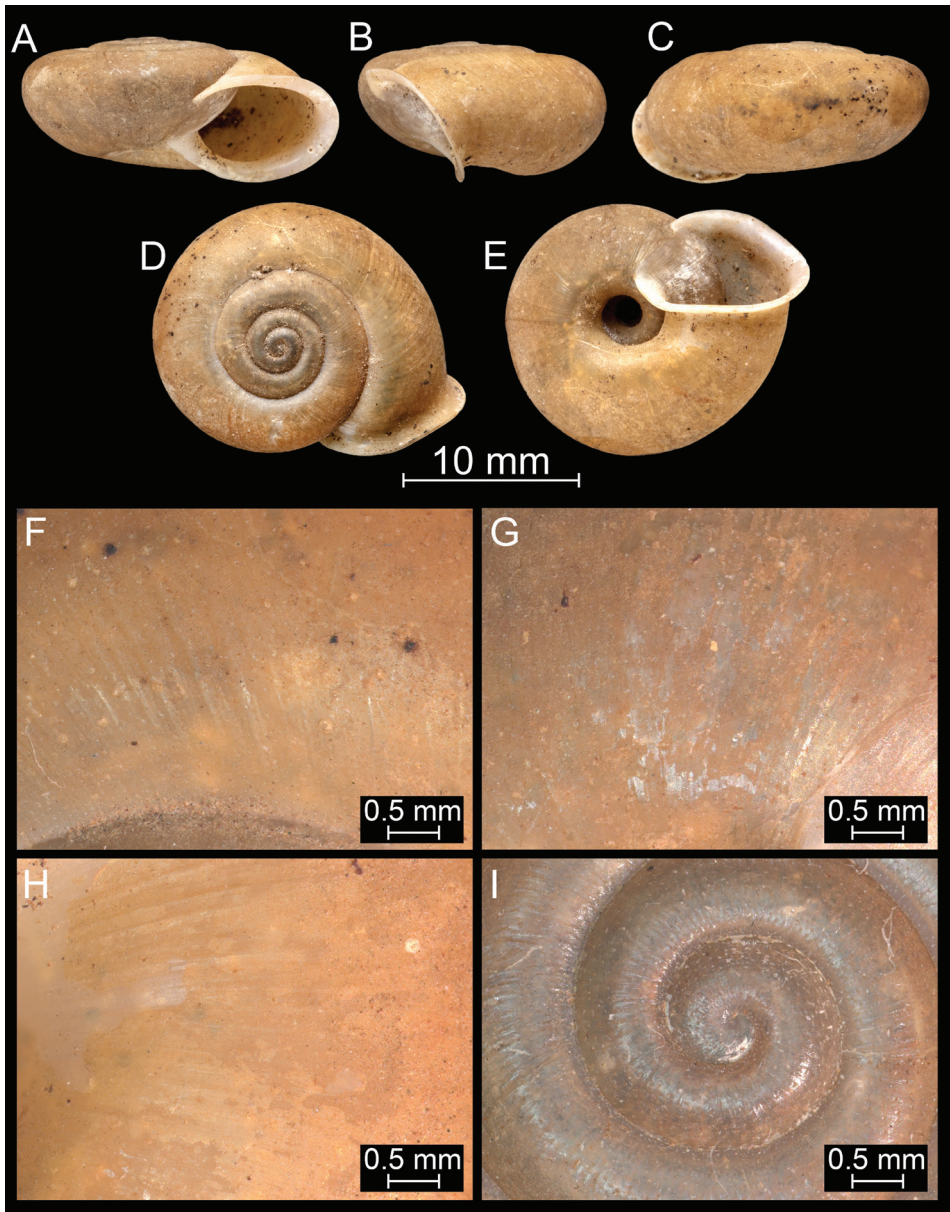


Figure 12. *Bouchetcamana fusca* Páll-Gergely sp. nov., holotype (NHMUK 1903.7.1.391/2). For positions of close-up images see Fig. 6 (F = DM, G = CA, H: LV, I: PC).

the parietal callus, but to a much lesser degree than in other species; aperture oval/subrectangular; peristome expanded and slightly reflected in direction of umbilicus; palatal part with a very thin, whitish, semi-transparent layer; hair scars not visible beneath parietal callus; umbilicus open, relatively narrow, peri-umbilical keel only very slightly indicated.

Measurements. D = 15.3–18.7 mm, H = 7.8–8.8 mm (n = 5).

Differential diagnosis. *Bouchetcamaena raripila* sp. nov. is most similar to *B. fusca* sp. nov. in having a relatively small shell, narrow umbilicus and brown periostracum, but it differs in the strong, sparsely standing hair scars. All other *Bouchetcamaena* species have larger, lighter-coloured shells and a wider umbilicus.

Etymology. The new species is named after its dark (*fuscus* in Latin) periostracum.

Distribution. Seems to be restricted to Manipur, the Khasi and the Naga Hills (India).

Helix (Trachia) delibrata var. *khasiensis* Nevill, 1877, taxon inquirendum

Helix delibrata (?) var. Hanley & Theobald, 1870: pl. 14, fig. 9.

Helix (Trachia) delibrata Var. *khasiensis* Nevill, 1877: 21.

Chloritis (Tricho-chloritis) delibrata var. *khasiensis* Gude, 1914: 173.

Chloritis delibrata var. *khasiensis* Richardson, 1985: 93.

Chloritis delibrata khasiensis Ramakrishna et al., 2010: 326.

Type locality. “Khasi Hills”.

Types. Not found in the NHM or in the ZSI (Sheikh Sajan, pers. comm. April 2020).

Remarks. Nevill (1877) named the form illustrated in Hanley and Theobald’s (1870) *Conchologia Indica* (pl. 14, fig. 9) as var. *khasiensis*, and mentioned that it has more raised and rounded whorls and a less open umbilicus than the typical *H. delibrata*. Nevill’s (1877) description was as follows: “The raised and rounded whorls, less open umbilicus, and contracted aperture will distinguish the form; it has sometimes a single brown band, but is often without it; it is tolerably abundant in the Naga and Khasi Hills. (...) Var. *khasiensis*, from Khasi Hills, axis 8.5, diam. 19.5 (apert. 9, diam 10.5) mm”.

Bouchetcamaena fusca sp. nov. agrees with some parts of Nevill’s description (more raised spire and narrower umbilicus than in other similar species), and the Naga and Khasi Hills also match, but the specimens we described above as *B. fusca* sp. nov. possessed no band and are all smaller than the size mentioned by Nevill. Furthermore, the shell illustrated by Hanley and Theobald (1870) possesses a subsutural furrow (a furrow running between the middle of the body whorl and the suture), which is absent in all *B. fusca* sp. nov. shells we examined. Thus, we decided to describe these specimens as a new species and consider the name *Helix (Trachia) delibrata* var. *khasiensis* as a taxon inquirendum.

Bouchetcamaena platytropis (Möllendorff, 1894), comb. nov.

Figures 2–4

Chloritis platytropis Möllendorff, 1894: 150.

Chloritis (Tricho-chloritis) platytropis platytropis Zilch, 1966: 304, pl. 10, fig. 34.

Chloritis platytropis platytropis Maassen, 2001: 121.

Types examined. Siam, Tschaya, coll. O. Möllendorff ex coll. Roebelen, SMF 8526/1 (lectotype of *Chloritis platytropis*); same data, SMF 8527/1 (paralectotype of

Chloritis platytropis); Golf von Siam, Insel Samui, coll. O. Möllendorff ex coll. Roebelen, SMF 8524/1 (lectotype of *Chloritis platytropis* var. *samuiana*); same data, SMF 8525/1 (paralectotype of *Chloritis platytropis* var. *samuiana*).

Additional material examined. Thailand, Phangnga: Thai Mueang: Ton Prai waterfall, 90 m, 08°26'11"N, 098°18'33"E, leg. Hausdorf, 02.08.2010, ZMH 51934 (1 dry shell + ethanol-preserved body).

Description of the genitalia. Penis long, cylindrical, with swollen proximal part connected to adjacent epiphallic area by weak fibres; internally with ca. 6 wide, longitudinal, low folds; no penial verge present, although the folds form a circular ring with slightly elongated margin; epiphallus slightly longer than penis; retractor muscle slender, inserting on the distal end of epiphallus near its joint with penis; flagellum long, slender, pointed; no penial caecum present; vagina shorter and thicker than penis; spermiduct elongated, stalk of bursa copulatrix very long, with some central swelling, bursa small, rounded; albumen gland long, banana-shaped, talon small.

***Bouchetcamaena procumbens* (Gould, 1844), comb. nov.**

Figures 13–15

Helix procumbens Gould, 1844: 453, pl. 24, fig. 1.

Helix delibrata Hanley & Theobald, 1870: pl. 14, fig. 10.

Chloritis (*Trichochloritis*) *delibrata* var. *procumbens* Gude, 1914: 172–173.

Trachia delibrata f. *procumbens* Stoliczka, 1871: 225, pl. 16, figs 1–3 (reproductive anatomy, jaw, radula).

Chloritis delibrata var. *procumbens* Richardson, 1985: 93.

Type locality. "Province of Tavoy in British Burmah" (from the title).

Types examined. Tavoy, British Burmah, leg. F. Mason, MCZ 169311 (lectotype: labelled as holotype, see remarks).

Additional material examined. white type: (1) Khasi Hills, Assam, (2) Burma, A.S. Kennard coll., Acc. No. 1824, NHMUK 20191136/1 (1 shell, mixed lot with *B. foveata*: NHMUK 20191136/2; the Khasi Hills material probably refers to *foveata*, whereas the Burma material refers to *procumbens*); India, "Khasi Hills", NHMUK 1862.11.19.12 (2 shells); Moulmain, Tenasserim, coll. Stoliczka, NHMUK 1903.7.1.387 (1 shell); Pegu, ex coll. Godwin-Austen, NHMUK 1903.7.1.386 (1 shell); Pegu, NHMUK 1888.12.4.1114–1115 (2 shells); Tavoy, Burmah, Museum Cuming, NHMUK 20191137 (1 shell). **darker type:** Arakan, coll. H.F. Blanford, NHMUK 1909.3.15.25 (1 shell); Mutan, Tenasserim, coll. Godwin-Austen, NHMUK 20191133 (1 shell); Pegu, Arakan Hills, NHMUK 1906.2.2.121 (4 shells, one of them with widely-spaced pits, others with hardly visible scars, see remarks).

Diagnosis. Shell small to medium-sized, with flat dorsal side or slightly sunken or very slightly elevated spire; aperture oval, peristome strongly expanded, umbilicus narrow and deep; sculpture variable: in some shells the thick, brown, matt periostracum

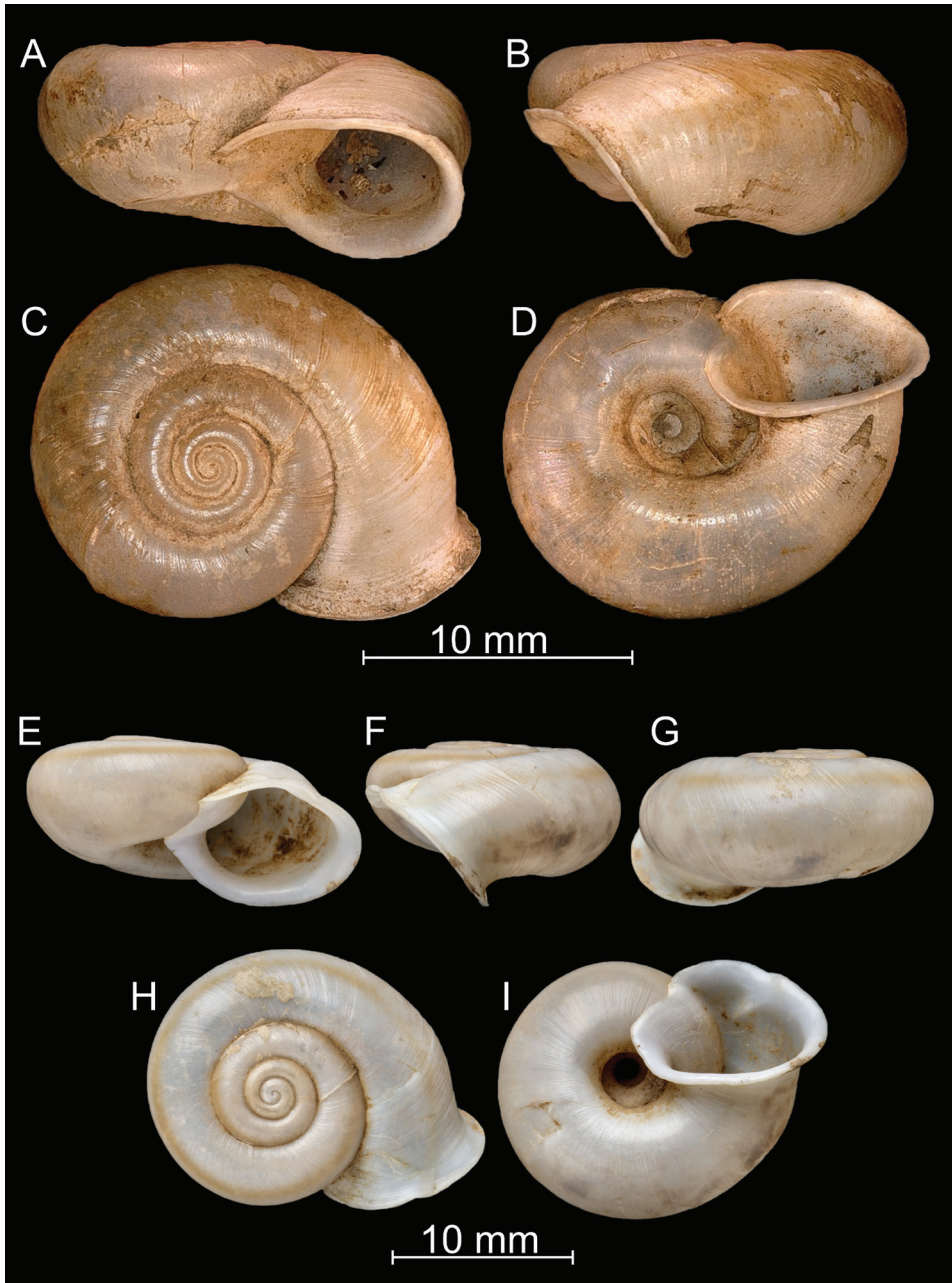


Figure 13. *Bouchetcamaena procumbens* (Gould, 1844), comb. nov. **A–D** lectotype (MCZ 169311) **E–I** NHMUK 1862.11.19.12.

makes hair scars practically invisible, in other shells the hair scars (pits) are usually densely arranged on the entire shell.

Description. Shell medium-sized, rather thin-walled; dorsal side flat, very rarely (NHMUK 1906.2.2.121) slightly domed; shell shape “nautiliform” (i.e., initial whorls

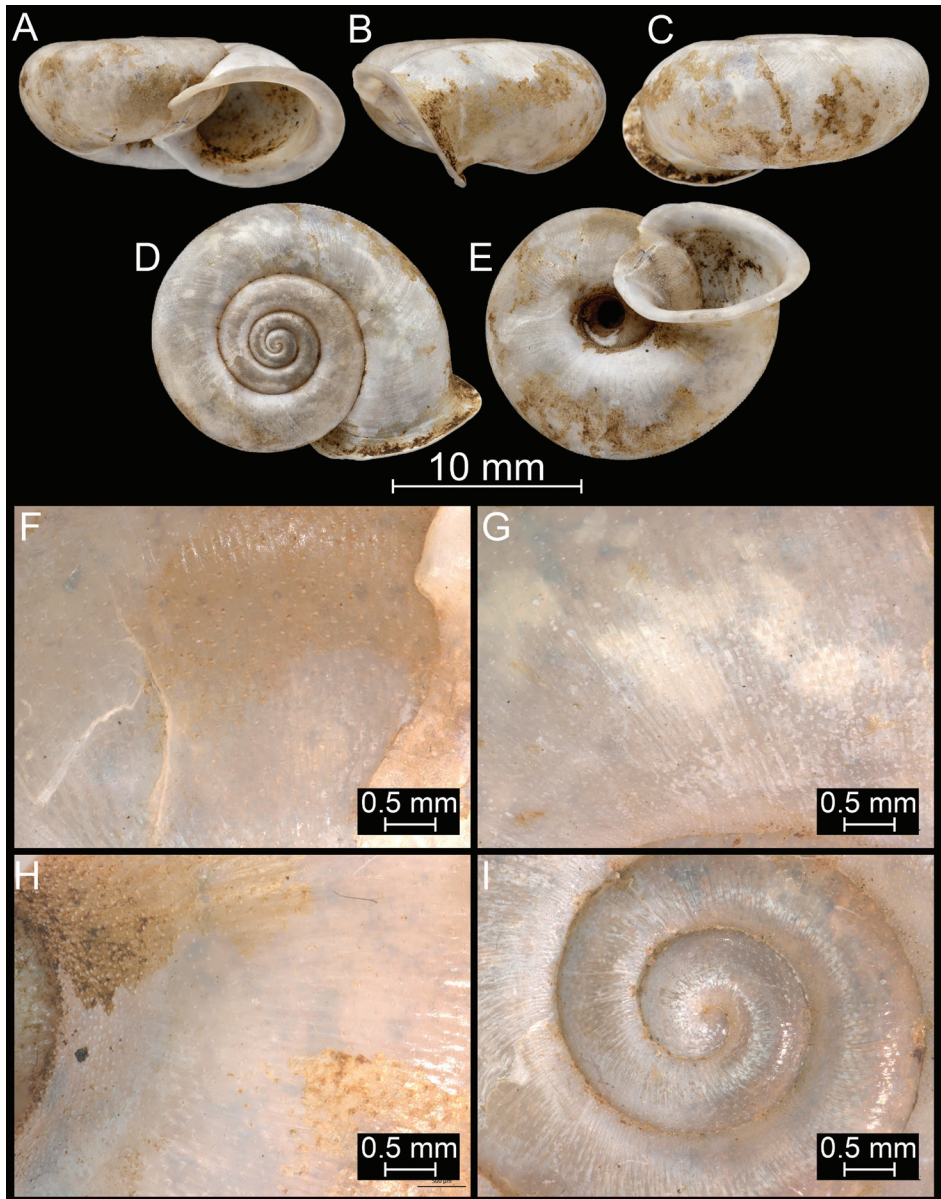


Figure 14. *Bouchetcamaena procumbens* (Gould, 1844), comb. nov. NHMUK 1903.7.1.386. For positions of close-up images see Fig. 6 (F = DM, G = CA, H: LV, I: PC).

closely coiled, body whorl conspicuously expanded); colour whitish to light yellowish with somewhat darker yellowish, matt (dull) periostracum in some places, or, as in one sample (Mutan, Tenasserim), on the entire shell; a normally wide, faint reddish-brown belt running around the shoulder of the body whorl (can be entirely absent); protoconch consisting of 1–1.5 whorls, finely wrinkled and covered by hair scars (pits) or small, mamilla-like hairs; entire shell consisting of 3.75–4.75 whorls, separated by a deep su-

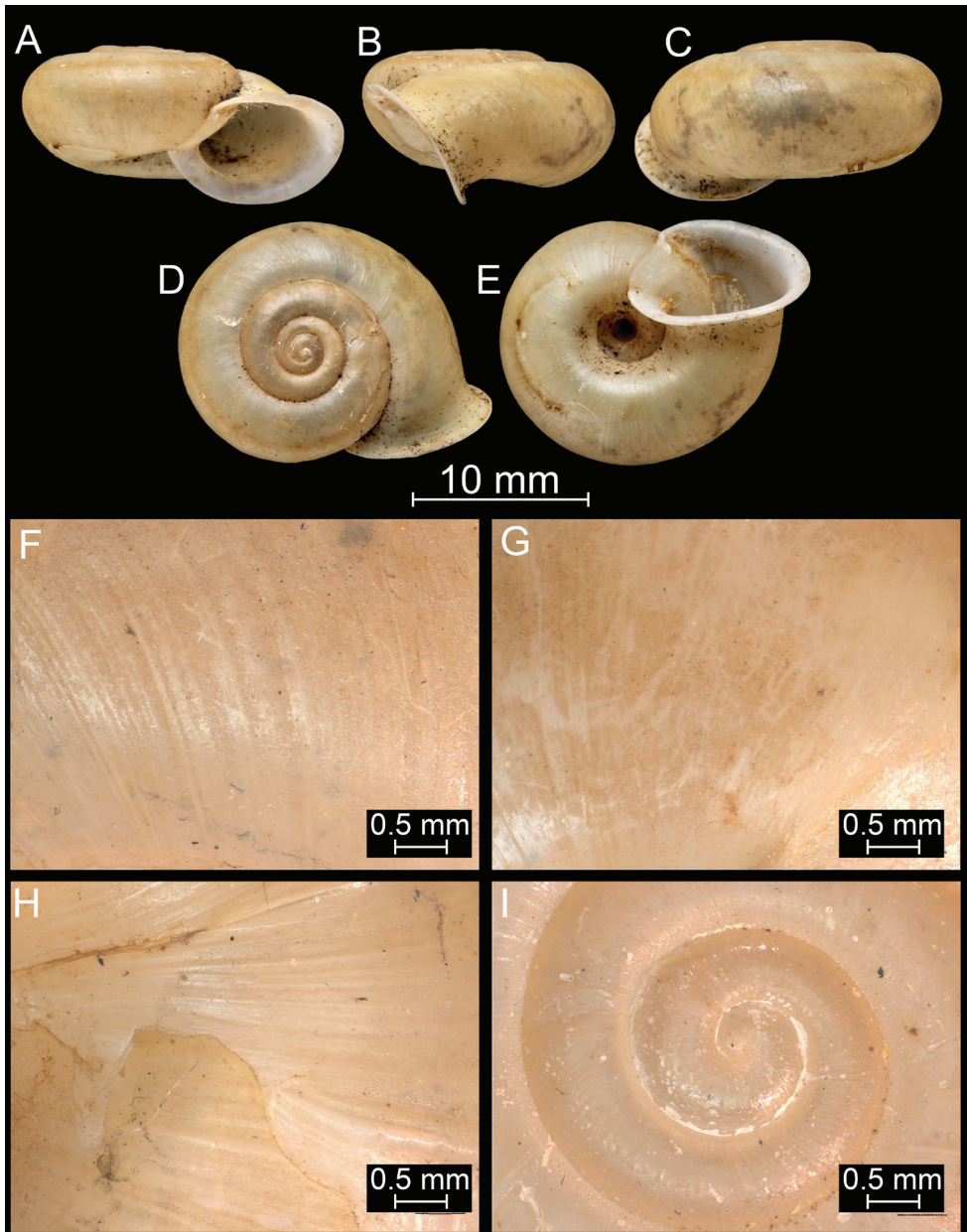


Figure 15. *Bouchetcamaena procumbens* (Gould, 1844), comb. nov. NHMUK 1906.2.2.121. For positions of close-up images see Fig. 6 (F = DM, G = CA, H: LV, I: PC).

ture; teleoconch finely and irregularly wrinkled; sculpture variable: in typical shells some darker yellowish-light brownish periostracum covers parts of the teleoconch, and the densely arranged hair scars are only visible in the suture on the dorsal side and near the parietal callus on the ventral side; in the “pitted form”, hair scars densely arranged on entire shell and clearly visible on both the dorsal and ventral sides; aperture oval/subrec-

tangular; peristome strongly expanded and slightly reflected in direction of umbilicus; palatal part with a thin, whitish, semi-transparent layer, with hair scars visible on penultimate whorl; umbilicus open, narrow, funnel-shaped, peri-umbilical keel blunt.

Measurements. D = 15.8–19.5 mm, H = 7.8–9.4 mm (n = 7).

Differential diagnosis. The smaller shell size and the more reflected peristome distinguish this species from the most similar species, *B. delibrata*. Furthermore, the “white type” *B. procumbens* differs from *B. delibrata* in the presence of dense and prominent hair scars.

Distribution. Seems to be restricted to southern Myanmar.

Remarks. Johnson (1964) mentioned that the figured “holotype” (MCZ 169311) is from the NYSM 232 (original no. A 567), and that there is a “paratype” (USNM 611226) from the same NYSM lot. Johnson’s listing of the specimen as a “holotype” has to be accepted as an indirect lectotype designation by inference of holotype (see ICZN Art. 74.6). Furthermore, two additional “paratypes” (= paralectotypes) are found in the MCZ (reg. no.: 87935, ex BSNH).

There are two forms of this species. One is lighter in colour, some of the specimens have a slightly sunken spire and possess uniformly arranged, strong hair scars on the entire surface of the shell (“white type”), whereas the other type has a darker shell (yellowish to light brownish) with hardly visible hair scars (“darker type”). The sample NHMUK 1906.2.2.121 contains four shells of identical appearance; however, one of them has widely-spaced pits, whereas the other three have only some pits on the callus area but otherwise no hair scars. Thus, it seems that the strength of the hair scars is variable within this species, unlike in all other species of this group. Since the shell and aperture shape are, with the exception of spire height, practically identical, and there are transitional forms between the two types in terms of shell sculpture, we provisionally treat them as one species. There are no clearly visible hair scars on the lectotype. Thus, the form without prominent hair scars is considered typical *procumbens*, and the “pitted form” is considered atypical.

***Bouchetcamaena raripila* Páll-Gergely, sp. nov.**

<http://zoobank.org/CE6219D5-7470-43D8-BDC2-D07137D2ED37>

Figure 16

Type material. Holotype: Kopanedza, coll. Godwin-Austen, NHMUK 20191131 (D: 15.4 mm, H: 8.1 mm).

Diagnosis. Shell small, with slightly elevated spire; periostracum thick, brown, hair scars (truncated hairs or strawberry seed-like scars) extremely sparsely arranged on the body whorl; aperture oval, almost rounded.

Description. Shell small; depressed-globular, with very slightly elevated spire (low domed dorsal side); body whorl rounded; colour brown due to thick, matt (dull) periostracum, locally worn locally making the nude whitish shell surface visible; protoconch consists of 1.5 whorls, finely wrinkled, with hair scars reminiscent of strawberry seeds; entire shell consisting of 4.25 whorls, suture moderately deep; inside of umbilicus and

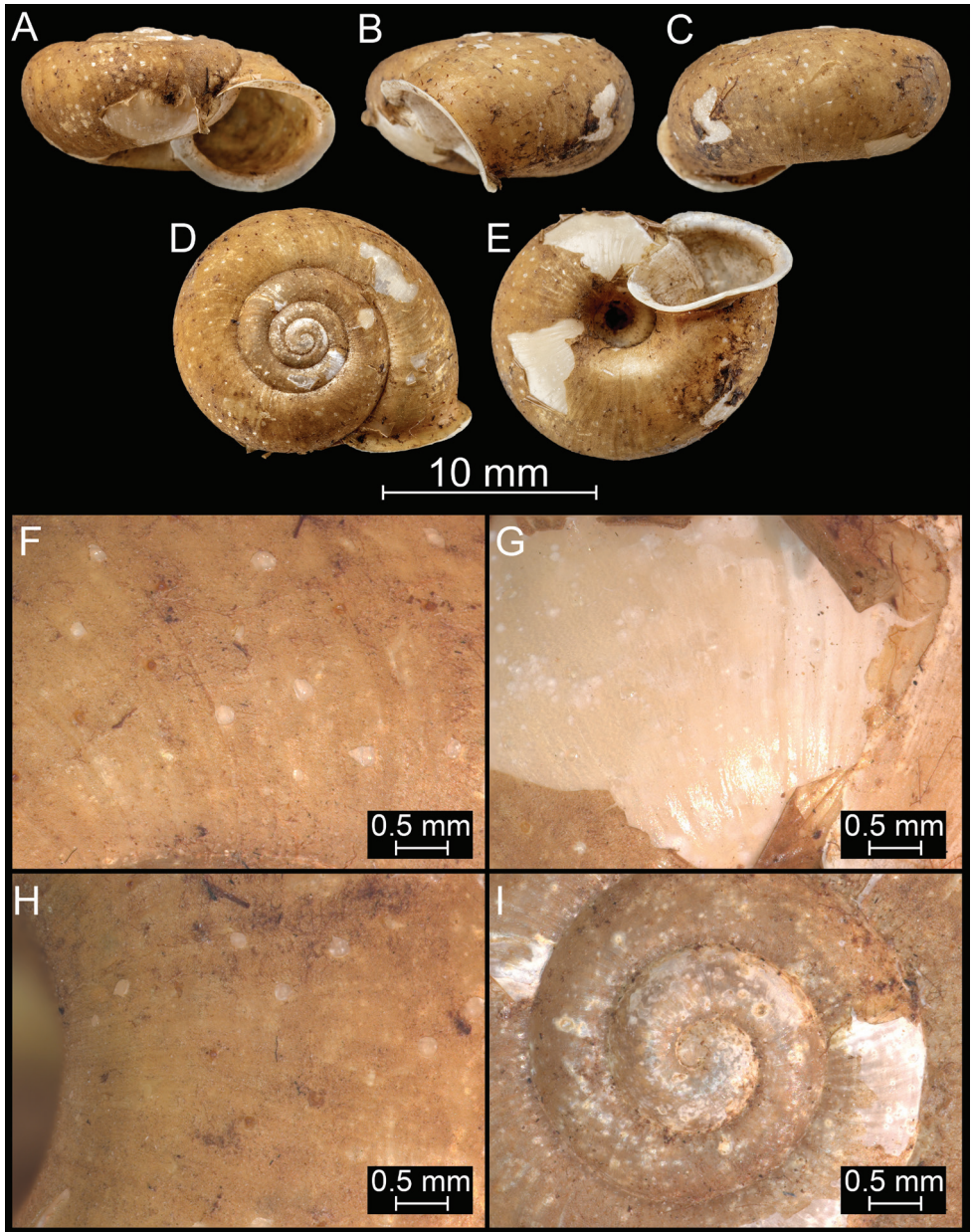


Figure 16. *Bouchetcamaena raripila* Páll-Gergely sp. nov., holotype (NHMUK 20191131). For positions of close-up images see Fig. 6 (F = DM, G = CA, H: LV, I: PC).

suture with mamilla-like, relatively densely arranged hair scars; other parts of teleoconch with extremely widely-spaced hairs (truncated, reddish-brown hairs or strawberry seed-like scars, and very few, relatively long, conical hairs); aperture oval, almost rounded; peristome strongly expanded and slightly reflected in direction of umbilicus; palatal part

with a very thin, whitish, semi-transparent layer, which allows hair scars of the penultimate whorl to be seen; umbilicus open, narrow, funnel-shaped, peri-umbilical keel blunt.

Measurements. D = 15.4 mm, H = 8.1 mm (n = 1).

Differential diagnosis. Differs from *B. procumbens* by having a more rounded shell shape and the last whorl is also more rounded. Most important are the extremely widely-spaced and prominent hair scars. This latter trait distinguishes *B. raripila* sp. nov. from all other similar species.

Etymology. The name *raripila* refers to the few hairs/hair scars on the shell surface (*rarus*: few, *pilus*: hair in Latin).

Distribution. The new species is known from the type locality only. Kopanedza (also spelled Kopamedza) is situated in the Barail Range, Daffa Hills (India), although its exact locality is unknown (Páll-Gergely et al. 2015b).

***Bouchetcamaena subdelibrata* Páll-Gergely, sp. nov.**

<http://zoobank.org/BADF67BD-2D56-40D2-8378-823B52F21352>

Figure 17

Type material. Holotype: S. Silhet, leg. Chennell, coll. Godwin-Austen, NHMUK 20191132/1 (D: 17.7 mm, 8.6 mm).

Paratypes: Same data as holotype, NHMUK 20191132/2 (1 paratype); Habiang, Garo Hills, coll. Godwin-Austen 183, ex coll. W. Blanford, NHMUK 1906.1.1.714 (3 paratypes); South Sylhet Hills, coll. W Chennell, NHMUK 1903.7.1.61/2 (1 paratype, mixed lot with *B. delibrata*: NHMUK 1903.7.1.61/1).

Additional material examined. Same data as holotype, NHMUK 20191132/3 (7 juvenile shells).

Diagnosis. Shell medium-sized, nearly flat, greenish, glossy, entire shell with densely arranged hair scars (mostly hardly visible), aperture oval, peristome not particularly expanded.

Description. Shell medium-sized, rather thin walled; depressed, dorsal side entirely flat (type series), or slightly elevated (Habiang); colour greenish to dark yellowish with an obscure, reddish band just above the blunt keel; protoconch consisting of 1.5 whorls, with densely arranged, clearly visible, knob-like hair scars; entire shell with 3.50–3.75 whorls; separated by a rather deep suture; teleoconch overall glossy, with irregular, fine growth lines, ventral side and edge of body whorl (except for last quarter whorl) covered with densely-arranged hair scars, some hair scars also recognizable on the last quarter whorl, but not regular as on the preceding areas; last whorl of dorsal side dominated by wrinkles, and regular hair scars only visible in areas before the last half whorl; aperture almost rounded, slightly oval; peristome strongly expanded and slightly reflected in direction of umbilicus; palatal part with a very thin, whitish, semi-transparent layer, which allows hair scars on penultimate whorl to be seen; umbilicus open, normally wide, funnel-shaped, peri-umbilical keel blunt, only very slightly indicated.

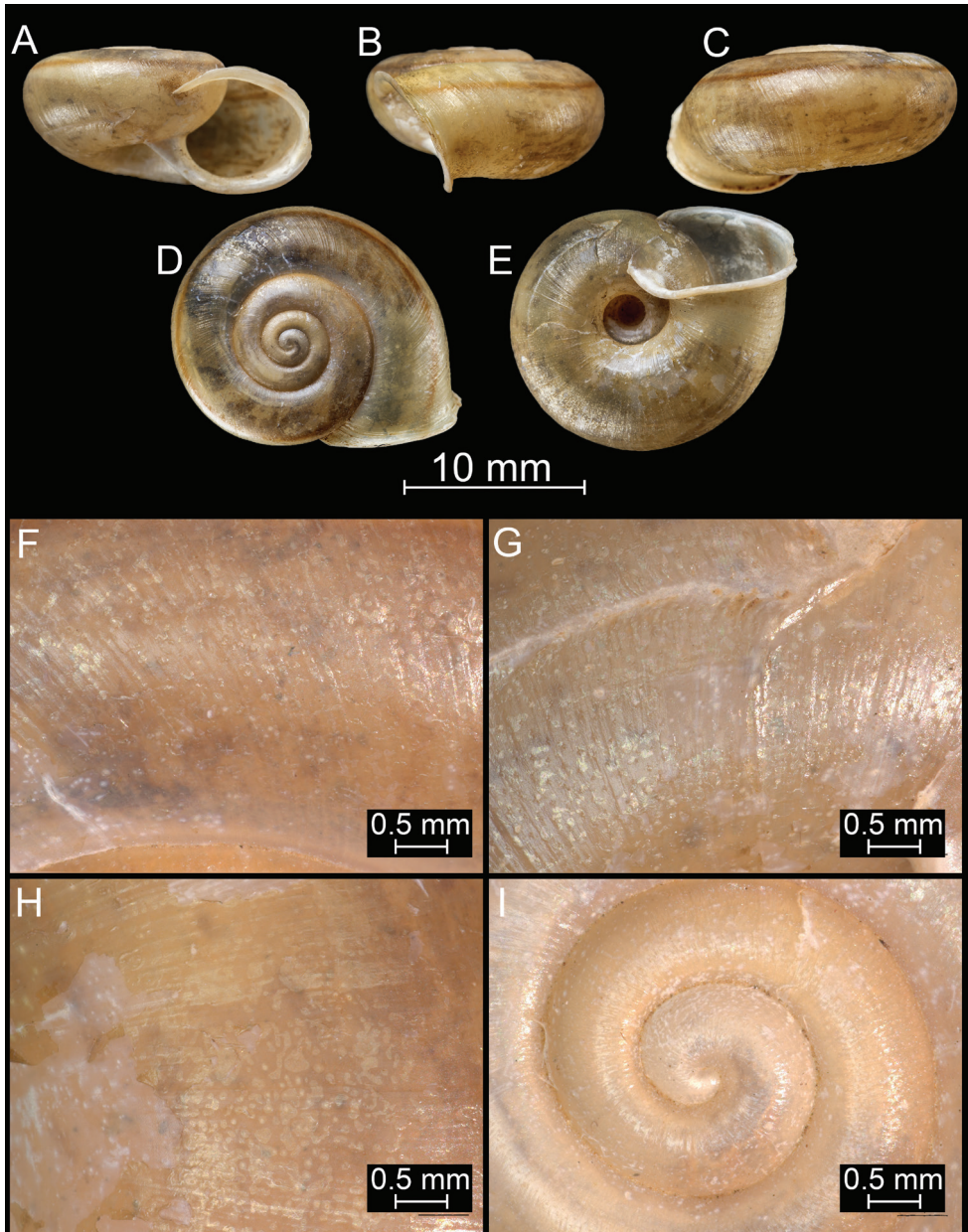


Figure 17. *Bouchetcamena subdelibrata* Páll-Gergely sp. nov., holotype (NHMUK 20191132). For positions of close-up images see Fig. 6 (F = DM, G = CA, H: LV, I: PC).

Measurements. D = 17.7–19.3 mm, H = 8.6–9.9 mm (n = 4).

Differential diagnosis. *Bouchetcamena delibrata* is most similar to the new species, but it is larger, has a more strongly depressed shell, elongated aperture and expanded peristome, and lacks hair scars on the last half whorl. The hair scars of *B. delibrata* are more widely-spaced than those of *B. subdelibrata* sp. nov.

Etymology. The specific epithet refers to the most similar species.

Distribution. The new species is known from the Garo Hills (Meghalaya, India), and the neighbouring Silhet Hills to the south.

Genus *Burmochloritis* Godwin-Austen, 1920

Burmochloritis Godwin-Austen, 1920: 9.

Burmochloritis Schileyko, 2003: 1518.

Type species. *Burmochloritis kengtungensis* Godwin-Austen, 1920, OD.

Remarks. *Burmochloritis* Godwin-Austen, 1920 possesses a long flagellum, has penial caecum well-developed, and a large, additional organ originating from the wall of the vagina (Godwin-Austen 1920; and unpublished information). See also Table 1.

Burmochloritis fasciata (Godwin-Austen, 1875), comb. nov.

Figure 18

Helix delibrata var. *fasciata* Godwin-Austen, 1975: 1, pl. 1, fig. 1.

Chloritis (*Trichochloritis*) *delibrata* var. *fasciata* Gude, 1914: 173.

Chloritis delibrata var. *fasciata* Richardson, 1985: 93.

Chloritis delibrata fasciata Ramakrishna et al., 2010: 326.

Type locality. "On the high open grassy country of the West Khasi Hills".

Types examined. Khasi Hills, coll. Godwin-Austen, NHMUK 1903.7.1.381/1 (syntype, mixed lot with *B. delibrata*: NHMUK 1903.7.1.381/2).

Additional material examined. Khasia Hills, 183, Assam, coll. Godwin-Austen, NHMUK 20191130/1 (1 shell, mixed lot with *B. foveata*: NHMUK 20191130/2).

Diagnosis. Shell medium-sized, dorsal side domed, greenish-yellowish with a slender main spiral band and several thinner ones; last whorl with dense hair scars (pits) only near the parietal calls, aperture almost rounded.

Description. Shell medium-sized, rather thick-walled; depressed globular, with slightly domed dorsal side; colour greenish-yellowish, with a main but still slender reddish band just above the blunt keel and several even thinner belts on both the dorsal and ventral surfaces; protoconch consists of 1.25 whorls, with very fine radial ribs and regularly arranged hair scars; entire shell consists of slightly more than 4 whorls, separated by a moderately deep suture; teleoconch covered with a matt periostracum, dense hair scars (and short hairs near suture) visible only near parietal callus; aperture rounded/subrectangular; peristome strongly expanded and slightly reflected in direction of umbilicus; parietal part with thin, whitish, semi-transparent layer, which allows hair scars of penultimate whorl to be seen; umbilicus open, relatively narrow, funnel-shaped, with blunt peri-umbilical keel.

Remarks. This species was described as a variety of *B. delibrata*, but differs in numerous shell characters (smaller, more globular shell, smaller protoconch, domed

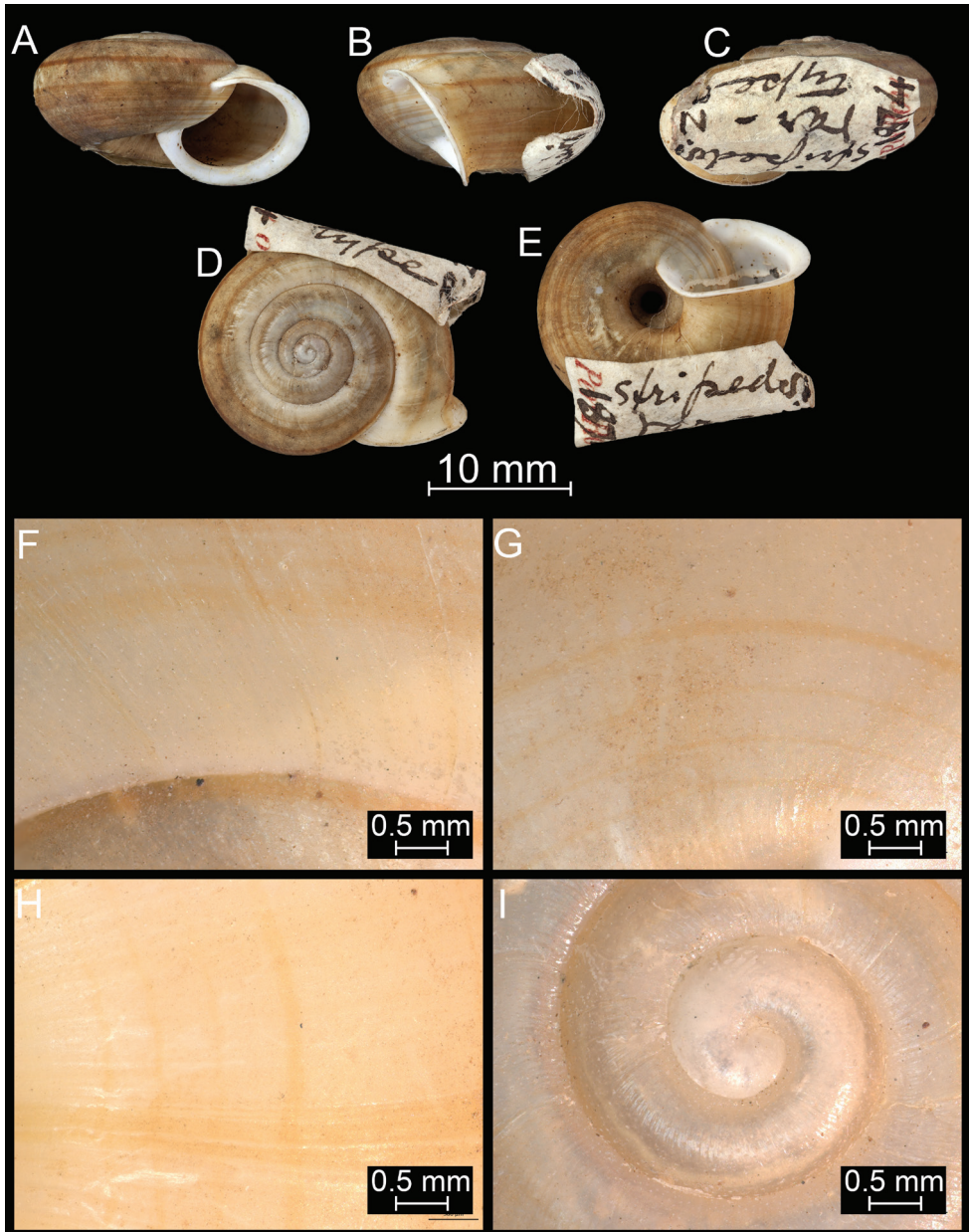


Figure 18. *Burmochloritis fasciata* (Godwin-Austen, 1875), comb. nov., syntype (NHMUK 1903.7.1.381/1). For positions of close-up images see Fig. 6 (F = DM, G = CA, H: LV, I: PC).

dorsal side, comparatively smaller, more rounded aperture, narrower umbilicus, denser hair scars). Thus, it should be handled as a species in its own right. Moreover, based on the multiple spiral bands (*Bouchetcamaena* species have no band or a single band), this species is transferred to the genus *Burmochloritis*, although this placement requires confirmation through anatomical examination.

Acknowledgements

We are grateful to Adam Baldinger (MCZ) and Thomas White (NHM) for providing photographs of types, to Sigrid Hof and Ronald Janssen (SMF) for providing access to their museum collection, to Kevin Webb and Richard Turney (NHM) for photos, to Bernhard Hausdorf (ZMH) for loaning specimens of *Bouchetcamaena platytropis*, to Sheikh Sajjan (ZSI) for searching for type specimens in the collection of the ZSI, and to Attila Gonda for his help with Latin etymology. This study was supported by the Bolyai Research Scholarship of the Hungarian Academy of Sciences, and grants from the SYNTHESYS Project (GB-TAF-2523) and the Hungarian Research Fund (OTKA FK 135262) to B. P.-G. We are indebted to The Biodiversity Heritage Library (www.biodiversitylibrary.org) for the multitude of rare literature made available to us.

References

- Adams A (1868) On the species of Helicidae found in Japan. *Annals and Magazine of Natural History*. ser. 4(1): 459–472. <https://doi.org/10.1080/00222936808695731>
- Albers JC, Martens E von (1860) Die Heliceen nach natürlicher Verwandtschaft systematisch geordnet von Joh. Christ. Albers. Ed. 2. Engelmann, Leipzig, 369 pp. <https://doi.org/10.5962/bhl.title.11218>
- Azuma M (1995) Colored illustrations of the land snails of Japan. Enlarged revised edition. Hoikusha Publishing, Osaka, 343 pp.
- Beck H (1837) Index molluscorum praesentis aevi musei principis augustissimi Christiani Frederici, Hafniae [Copenhagen], 124 pp. <https://doi.org/10.5962/bhl.title.77331>
- Benson WH (1836) Descriptive catalogue of terrestrial and fluviatile Testacea, chiefly from the North-East frontier of Bengal. *The Journal of the Asiatic Society of Bengal* 5(54): 350–358.
- Emura S (1933) On the copulatory organ of *Ganesella japonica* (PFEIFFER), with special reference to the function of appendix of penis: Observations on the morphology and physiology of the reproductive system of the Japanese pulmonates 1. *Venus* 4(1): 17–24.
- Godwin-Austen HH (1875) Descriptions of new species of Mollusca of the genera *Helix* and *Glessula* from the Khasi Hills and Manipur. *The Journal of the Asiatic Society of Bengal*, Part II 44 (1): 1–4, pl. 1.
- Godwin-Austen HH (1920) Notes on the genus *Chloritis* Beck, with the description of the animal of a new genus (*Burmochloritis*). *Records of the Indian Museum* 19(1): 9–11.
- Gould AA (1844) Descriptions of land shells from the province of Tavoy, in British Burmah. *Boston journal of natural history* 4(4): 352–359.
- Gray JE (1847) A list of the genera of recent Mollusca, their synonyms and types. *Proceedings of the Zoological Society of London* 15: 129–219.
- Gude GK (1902–1904) A classified list of the Helicoid land shells of Asia. *Journal of Malacology*, 9(1): 1–11 (10-IV-1902); 9(2): 51–59 (30-VI-1902); 9(3): 97–104 (29-IX-1902); 9(4): 112–129 (24-XII-1902); 10(1): 5–16 (31-III-1903); 10(2): 45–62 (30-VI-1903); 10(3): 83–98 (20-X-1903); 10(4): 129–136 (21-XII-1903); 11(4): 93–97 (28-XII-1904).

- Gude GK (1914) Mollusca-II. Trochomorphidae-Janellidae. In: Shipley, A. E. & Marshall, G. A. K. (eds.): The Fauna of British India, including Ceylon and Burma. Taylor & Francis, London, 520 pp. <https://doi.org/10.5962/bhl.title.12891>
- Hanley SCT, Theobald W (1870–1876) Conchologia Indica; Being Illustrations of the Land and Freshwater Shells of British India. L. Reeve & Co., London, I–CLX, 1–65. <https://doi.org/10.5962/bhl.title.14456>
- Johnson RI (1964) The recent Mollusca of Augustus Addison Gould. Smithsonian Institution, Washington DC, 239: 1–182. <https://doi.org/10.5479/si.03629236.239>
- Kerney MP, Cameron RAD (1979) A field guide to the land snails of Britain and North-west Europe. Collins, London, 288 pp.
- Kuroda T, Habe T (1949) Helicacea. Sanmeisha, Tokyo. 6 + 129 pp., 1 pl.
- Linnaeus C (1758) Systema Naturae per regna tria naturae, secundum classes, ordines, genera, species, cum characteribus, differentiis, synonymis, locis. Editio decima, reformata [10th revised edition]. Laurentius Salvius, Holmiae, vol. 1, 824 pp. <https://doi.org/10.5962/bhl.title.542>
- Linnaeus C (1766–1767) Systema naturae per regna tria naturae: secundum classes, ordines, genera, species, cum characteribus, differentiis, synonymis, locis. Ed. 12. 1., Regnum Animale. 1 & 2. Laurentii Salvii, Holmiae [Stockholm], 532 pp. <https://doi.org/10.5962/bhl.title.156772>
- Maassen WJM (2001) A preliminary checklist of the non-marine molluscs of West-Malaysia: “a Hand List”. De Kreukel, Extra Editie 2001, 1–155.
- Mitra SC, Dey A, Ramakrishna (2004) Pictorial Handbook-Indian Land Snails (Selected Species). Director, Zoological Survey of India, Kolkata, 344 pp.
- Möllendorff OF von (1894) On a collection of land-shells from the Samui Islands, Gulf of Siam. Proceedings of the Zoological Society of London, 1894: 146–156.
- Morlet L (1886) Diagnoses molluscorum novorum Cambodgiae. Journal de Conchyliologie 34(1): 74–75.
- Müller OF (1774) Vermium terrestrium et fluviatilium, seu animalium infusorium, Helminthi-
corum, et testaceorum, non marinorum, succincta historia. vol 2, apud Heineck et Faber,
ex officina Molleriana, Havniae et Lipsiae, I–XXXVI, 1–214, 10 unnumbered pages. <https://doi.org/10.5962/bhl.title.12733>
- Nevill G (1877) List of the Mollusca brought back by Dr. J. Anderson from Yunnan and Upper Burma, with descriptions of new species. The Journal of the Asiatic Society of Bengal, Part II 46(1): 14–41.
- Páll-Gergely B, Budha PB, Naggs F, Backeljau T, Asami T (2015b) Review of the genus *Endothyrella* Zilch, 1960 with description of five new species (Gastropoda, Pulmonata, Plecto-
pylidae). ZooKeys 529: 1–70. <https://doi.org/10.3897/zookeys.529.6139>
- Páll-Gergely B, Fehér Z, Hunyadi A, Asami T (2015a) Revision of the genus *Pseudopoma-
tias* and its relatives (Gastropoda: Cyclophoroidea: Pupinidae). Zootaxa 3937(1): 1–49.
<https://doi.org/10.11646/zootaxa.3937.1.1>
- Páll-Gergely B, Neubert E (2019) New insights in *Trichochloritis* Pilsbry, 1891 and its relatives (Gastropoda: Pulmonata: Camaenidae). ZooKeys 865: 137–154. <https://doi.org/10.3897/zookeys.865.36296>
- Páll-Gergely B, Hunyadi A, Auffenberg K (2020) Taxonomic vandalism in malacology: Com-
ments on molluscan taxa recently described by N. N. Thach and colleagues (2014–2019).
Folia Malacologica 28(1): 35–76. DOI: <https://doi.org/10.12657/folmal.028.002>

- Pfeiffer L (1847) Diagnosen neuer Landschnecken. Zeitschrift für Malakozoologie 4(10): 145–151.
- Pfeiffer L (1846) Symbolae ad historiam Heliceorum. Sectio tertia. Th. Fischer, Cassellis, 100 pp.
- Pfeiffer L (1862) Diagnoses de neuf espèces nouvelles provenant de Siam. Journal de Conchyliologie 10(1): 39–46.
- Pilsbry HA (1890–1891) Manual of Conchology, structural and systematic, with illustrations of the species. Ser. 2, Pulmonata. Vol. 6: Helicidae, vol. 4. 1–324, pls 1–69. Philadelphia, published by the Conchological Section, Academy of Natural Sciences
- Pilsbry HA (1893–1895) Manual of Conchology, (2) 9. Helicidae, vol. VII. Guide to the study of Helices. Academy of Natural Sciences, Conchological Section, Philadelphia, 366 + 126 pp. <https://biodiversitylibrary.org/page/1102607>
- Ramakrishna, Mitra SC, Dey A (2010) Annotated checklist of Indian land molluscs. Zoological Survey of India, Kolkata, 359 pp.
- Richardson L (1985) Camaenidae: Catalog of species. Tryonia, Miscellaneous Publications of the Department of Malacology of the Academy of Natural Sciences of Philadelphia. 12: 1–479.
- Schileyko AA (2003) Treatise on Recent terrestrial pulmonate molluscs. Part 11. Trigonochlamydidae, Papillodermidae, Vitrinidae, Limacidae, Bielziidae, Agriolimacidae, Boettgerillidae, Camaenidae. Ruthenica. Supplement 2: 1467–1626.
- Schileyko A (2018) On the genus *Trachia* auct. (Gastropoda, Pulmonata, Camaenidae). Ruthenica 28(4): 169–174. <https://www.biotaxa.org/Ruthenica/article/view/41985>
- Stoliczka F (1871) Notes on terrestrial Mollusca from the neighbourhood of Moulmein (Tenasserim Provinces), with descriptions of new species. The Journal of the Asiatic Society of Bengal, Part II 40(3): 217–259, pl. 15–19.
- Stoliczka F (1873) On the land-shells of Penang Island, with descriptions of the animals and anatomical notes; part second, Helicacea. Journal of the Asiatic Society of Bengal 42: 11–38. <https://biodiversitylibrary.org/page/35545891>
- Sutcharit C, Panha S (2010) Taxonomic re-evaluation of *Chloritis bifoveata* (Benson 1856) and *C. diplochone* Möllendorff 1898 (Pulmonata: Camaenidae). Journal of Conchology 40(3): 277–285. <https://conchsoc.org/node/4851>
- Thach NN (2018) New shells of South Asia. Seashells-Landsnails-Freshwater Shells. 3 New Genera, 132 New Species & Subspecies. 48HRBooks Company, Akron, Ohio, USA. 173 pp.
- Wang P, Xiao Q, Zhou W-C, Hwang C-C (2014) Revision of three camaenid and one bradybaenid species (Gastropoda, Stylommatophora) from China based on morphological and molecular data, with description of a new bradybaenid subspecies from Inner Mongolia, China. ZooKeys 372: 1–16. <https://doi.org/10.3897/zookeys.372.6581>
- Wu M, Chen Z, Zhu X (2019) Two new camaenid land snails (Eupulmonata) from Central China. ZooKeys 861: 129–144. <https://doi.org/10.3897/zookeys.861.35430>
- Zhang L-J, Zhu Y-J, Lyu Z-T (2019) A new sinistral species of the land-snail genus *Satsuma* (Pulmonata: Camaenidae) from China. Molluscan Research 40(1): 93–100. <https://doi.org/10.1080/13235818.2019.1644721>
- Zilch A (1966) Die Typen und Typoide des Natur-Museums Senckenberg, 35: Mollusca, Camaenidae. Archiv für Molluskenkunde 95(5/6): 293–319.

A review of the genus *Laeocathaica* Möllendorff, 1899 (Gastropoda, Pulmonata, Camaenidae)

Barna Páll-Gergely¹, András Hunyadi², Kaibaryer Meng³, Judit Fekete^{4,5}

1 Centre for Agricultural Research, Plant Protection Institute, Eötvös Loránd Research Network, Herman Ottó út 15, H-1022, Budapest, Hungary **2** Adria sétány 10G 2/5., Budapest 1148, Hungary **3** National Zoological Museum of China, Institute of Zoology, Chinese Academy of Sciences, Beijing, China **4** University of Pannonia, Centre of Natural Science, Research Group of Limnology, H-8200 Veszprém, Egyetem u. 10, Hungary **5** Centre for Ecological Research, Institute of Aquatic Ecology, Department of Tisza Research, 18/c Bem square, H-4026 Debrecen, Hungary

Corresponding author: Barna Páll-Gergely (pallgergely2@gmail.com)

Academic editor: Thierry Backeljau | Received 31 October 2021 | Accepted 5 January 2022 | Published 15 February 2022

<http://zoobank.org/6C32148C-A014-4AC4-88EA-82A1509E44F8>

Citation: Páll-Gergely B, Hunyadi A, Meng K, Fekete J (2022) A review of the genus *Laeocathaica* Möllendorff, 1899 (Gastropoda, Pulmonata, Camaenidae). ZooKeys 1086: 33–76. <https://doi.org/10.3897/zookeys.1086.77408>

Abstract

In this paper an overview of the *Laeocathaica* species is provided, and the intraspecific variability of several *Laeocathaica* species demonstrated on multiple shells. *Laeocathaica hisanoi* Páll-Gergely, **sp. nov.** and *L. minwui* Páll-Gergely, **sp. nov.** are described based on specimens found in museum collections. Five new synonyms are recognized: *L. prionotropis albocincta* Möllendorff, 1899 is a new synonym of *L. prionotropis* Möllendorff, 1899, *L. stenochone* Möllendorff, 1899 is a new synonym of *Laeocathaica carinifera* (H. Adams, 1870). *Laeocathaica distinguenda* Möllendorff, 1899, *L. tropidorhapse* Möllendorff, 1899, and *L. dangchanensis* Chen & Zhang, 2004 are moved to the synonymy of *Laeocathaica amdoana* Möllendorff, 1899. Furthermore, photos of paratypes of *Cathaica bizonalis* Chen & Zhang, 2004 are published for the first time.

Keywords

Intraspecific variability, shell, systematics, taxonomy

Introduction

The genus *Laeocathaica* Möllendorff, 1899 consists of approximately 20 species, and inhabits west China. Most of the species assigned to this genus were reported from the southern part of Gansu Province and the neighbouring Sichuan. A single species,

L. filippina (Heude, 1882) is known from Hubei Province, more than 500 km south-east from southern Gansu.

The monophyly of this genus is questionable for several reasons. First, *Laeocathaica* is defined by the sinistral shell coiling, whereas species with dextral shells of otherwise similar appearance (large, depressed shells with white base colour and brownish spiral bands) are included in other genera such as *Cathaica* Möllendorff, 1884, *Bradybaena* Beck, 1837, and *Euhadra* Pilsbry, 1890 (Chen and Zhang 2004). The type species of the latter is *Helix peliomphala* L. Pfeiffer, 1850 from Japan, which makes it questionable that the same large-bodied land snail genus could inhabit such a vast area covering ca. 3500 km. Moreover, species similar to *Laeocathaica* species (e.g., *Bradybaena haplozona* Möllendorff, 1899) have been classified in genera different from *Laeocathaica* (Möllendorff 1899; Chen and Zhang 2004). Second, the genus *Laeocathaica* as understood by Möllendorff (1899) and Chen and Zhang (2004) is variable in terms of shells characters. Some are large, with a white base colour, keeled or rounded body whorl, and without apertural barriers, others are keeled with apertural barriers, and some are small, transparent, and also possess apertural teeth. The genital anatomy is known in a handful of species only: *L. prionotropis* (see Chen and Zhang 2004), *L. polytyla* (see Schileyko 2004) and *L. filippina* (see Wu 2004), providing little basis of our understanding of the systematics of *Laeocathaica* and related genera.

In this paper we provide an overview of the genus *Laeocathaica* after consulting all available types and newly collected samples. We provide precise localities for most species, and photographs of multiple shells showing intraspecific variability for the first time in this genus.

Materials and methods

We counted the whorls of adult shells according to Kerney and Cameron (1979). Of the newly collected specimens and the ones deposited in the Senckenberg Museum, 10–20 photographs were taken of each shell using Canon EOS 6D camera and a Canon Macro Lens EF 100 mm 1: 2.8 and merged to create a single image using Photoshop. Shells deposited in other museums were photographed by the respective museum staff.

Abbreviations

D shell diameter;
H shell height.

Depositories

ANSP Academy of Natural Sciences (Philadelphia, USA);
HA Collection András Hunyadi (Budapest, Hungary);

- IZCAS** National Zoological Museum of China, Institute of Zoology, Chinese Academy of Sciences (Beijing, China);
- MNHN** Muséum National d'Histoire Naturelle (Paris, France);
- NHM** The Natural History Museum (London, UK);
- NHMMUK** When citing lots deposited in the NHM;
- PGB** Collection Barna Páll-Gergely (Budapest, Hungary);
- SMF** Senckenberg Forschungsinstitut und Naturmuseum (Frankfurt am Main, Germany);
- USNM** Smithsonian National Museum of Natural History (Washington, USA).

Taxonomy and systematics

Family Camaenidae Pilsbry, 1895

Genus *Cathaica* Möllendorff, 1884

Type species. *Helix pyrrhozona* Philippi, 1845; OD.

Cathaica (Cathaica) bizonalis Chen & Zhang, 2004

Figure 1

Cathaica (Cathaica) bizonalis Chen & Zhang, 2004: 238 [Chinese description], fig. 219 (erroneous figure showing *L. carinalis* specimen); 439 [English description].

Type locality. 陕西洛川县黑木沟. “Hemugou twon [sic!], Luochuan County (35°7'N, 109°04'E), Shaanxi Province”.

Remarks. Chen and Zhang (2004) described two species relevant for the present study: *Cathaica (Cathaica) bizonalis* Chen & Zhang, 2004 and *Laeocathaica carinalis* Chen & Zhang, 2004. According to the original description of *Cathaica bizonalis* (page 238 for Chinese, page 439 for English description), it is a dextral species characterised by a keel and two spiral bands (one above and one below the keel), and it is known from Shaanxi Province. The accompanying figure (Chen and Zhang 2004: fig. 219), however, shows a sinistral *Laeocathaica* species, identified here as *L. carinalis*.

According to the original description of *Laeocathaica carinalis*, that species is characterised by a sinistral, strongly depressed, keeled shell with a broad umbilicus. However, the provided photo (Chen and Zhang 2004: fig. 334) shows a sinistral juvenile shell of probably a *Laeocathaica* species with blunt keel and narrow umbilicus.

Examining the specimens deposited in IZCAS revealed the following:

1. The shell labelled as the holotype of *Cathaica bizonalis* is a dextral, juvenile shell.

2. A jar labelled as paratypes of *Cathaica bizonalis* (IZCAS TM 006579–006595) contains several probably conspecific juvenile specimens in ethanol.

3. Another jar labelled as paratypes of *Cathaica bizonalis* (IZCAS TM 097575–097587) contained 13 dry adult shells of a *Laeocathaica carinalis* (sinistral, strongly keeled species).

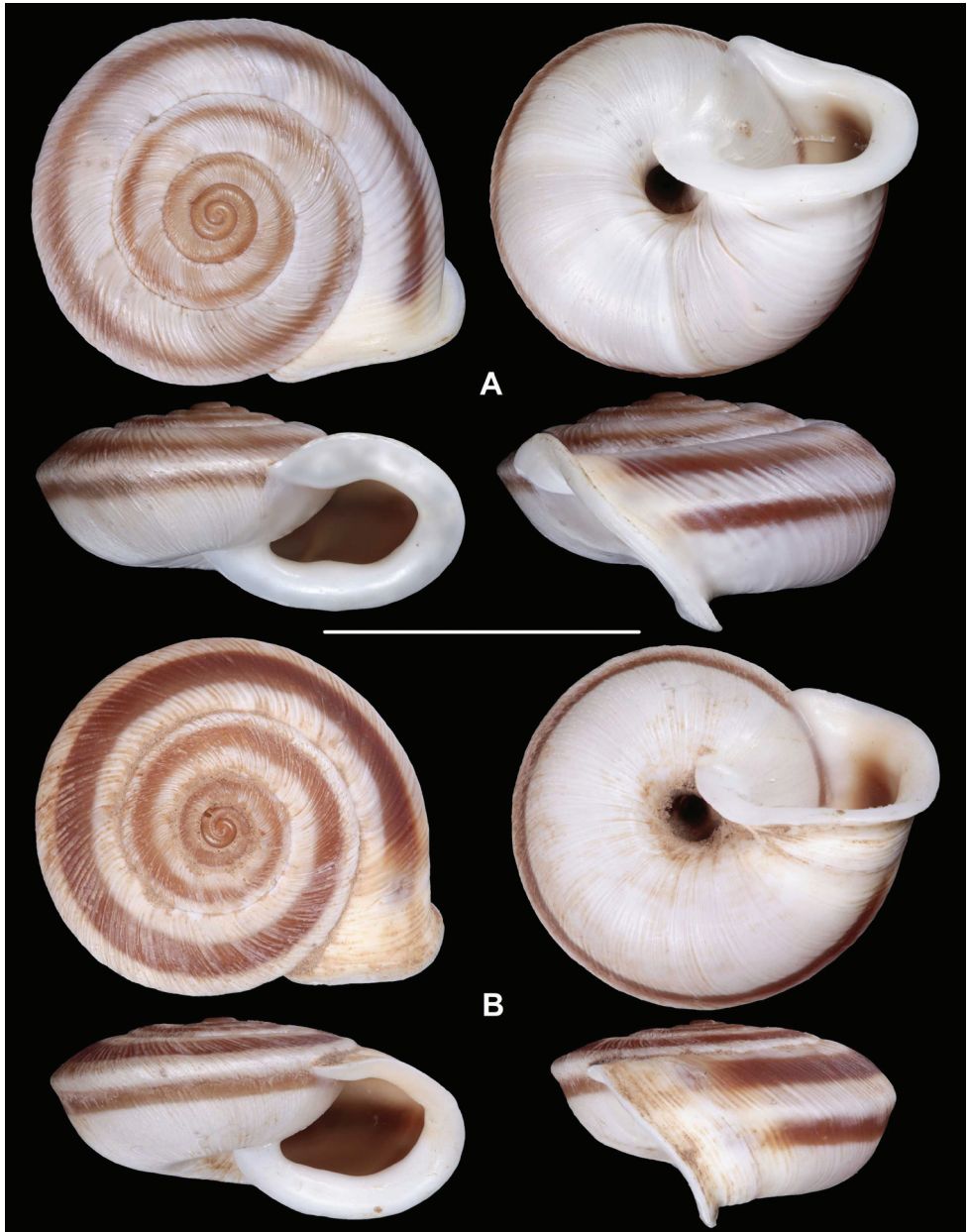


Figure 1. Paratypes of *Cathaica (Cathaica) bizonalis* Chen & Zhang, 2004 **A** IZCAS TM 097593 **B** IZCAS TM 097600. Scale bar: 10 mm. Photographs: Kaibaryer Meng.

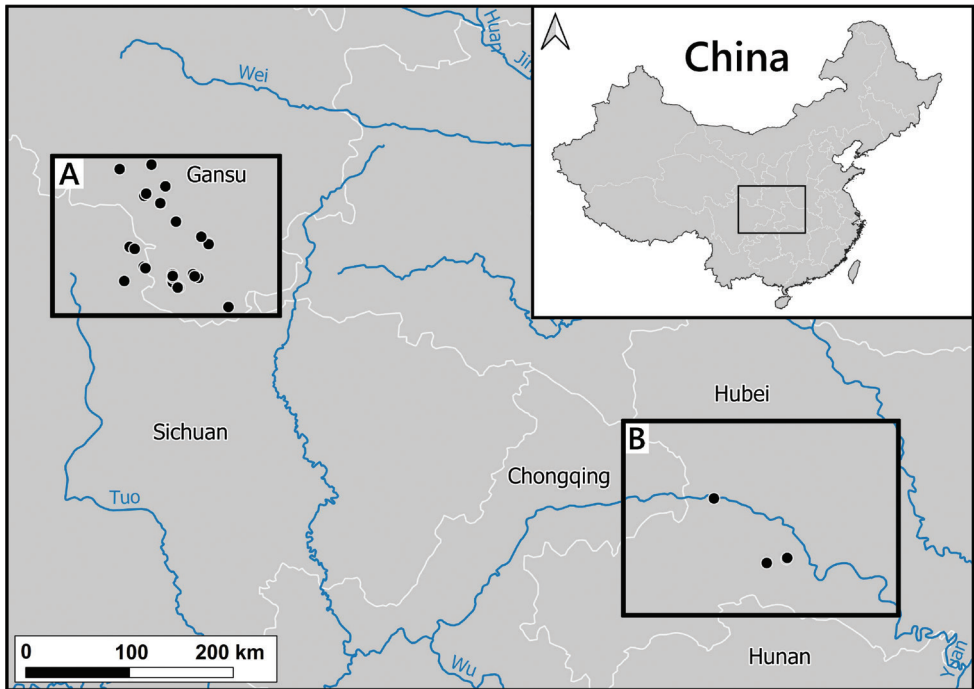


Figure 2. Distribution of the genus *Laeocathaica* in China **A** see Figs 8, 11, 17, 24 for details **B** see Fig. 14 for detail.

4. Among those shells (IZCAS TM 097575–097587), specimen IZCAS TM 097578 is exactly the same shell as in fig. 219 of Chen and Zhang (2004).

5. A jar labelled as paratypes of *Laeocathaica carinalis* (IZCAS TM 006612–006625) contained several adult specimens of *L. carinalis* in ethanol.

6. Another jar labelled as paratypes of *Laeocathaica carinalis* (IZCAS TM 097588–097602) contained several dry adult shells of *Cathaica bizonalis* (two of them figured in this work, see Fig. 1). This clearly shows that shells of the above taxa have been confused even before the publication. As a result, not only were the different samples mixed up with the labels in the collection, but also in the original descriptions.

Based on Chen and Zhang (2004) and the examination of the specimens deposited in IZCAS, we conclude the following:

1. Fig. 219 in Chen and Zhang (2004) shows the holotype of *Laeocathaica carinalis* Chen & Zhang, 2004 instead of *Cathaica bizonalis*.

2. Fig. 334 in Chen and Zhang (2004) shows an unidentifiable juvenile *Laeocathaica* species, and not *Laeocathaica carinalis*.

3. A holotype was designated in the original description of *Cathaica bizonalis*, so a lectotype cannot be chosen later. The holotype cannot be located because there is no photograph in the original description, and because the paratypes are of similar

size (i.e., the given measurements of the holotype are insufficient to recognize the shell). So, we treat it as lost (perhaps in the lot of paratypes). Since all the paratypes belong to one single species, and are consistent with the original description, we know what the authors intended by the taxon, so designation of a neotype is not needed.

Genus *Laeocathaica* Möllendorff, 1899

Laeocathaica Möllendorff, 1899: 86; Richardson 1983: 77; Schileyko 2004: 1686; Chen and Zhang 2004: 312.

Type species. *Helix (Plectotropis) christinae* H. Adams, 1870 (by original designation).

Laeocathaica amdoana Möllendorff, 1899

Figures 3–7

Laeocathaica amdoana Möllendorff, 1899: 92–93, pl. 5, fig. 5.

Laeocathaica distinguenda Möllendorff, 1899: 93, pl. 5, fig. 6. **new synonym**

Laeocathaica tropidorhaphe Möllendorff, 1899: 94, pl. 5, fig. 7. **new synonym**

Laeocathaica amdoana. – Yen 1939: 148, pl. 15, fig. 31.

Laeocathaica distinguenda. – Yen 1939: 149, pl. 15, fig. 32.

Laeocathaica tropidorhaphe. – Yen 1939: 149, pl. 15, fig. 33.

Laeocathaica (Laeocathaica) amdoana. – Zilch 1968: 173.

Laeocathaica (Laeocathaica) distinguenda. – Zilch 1968: 173.

Laeocathaica (Laeocathaica) tropidorhaphe. – Zilch 1968: 175.

Laeocathaica amdoana. – Chen & Zhang 2004: 316, fig. 303.

Laeocathaica distinguenda. – Chen & Zhang, 2004: 318, fig. 305.

Laeocathaica tropidorhaphe. – Chen & Zhang 2004: 319, fig. 307.

Laeocathaica dangchangensis Chen & Zhang, 2004: 339 [Chinese description], 443 [English description], fig. 332. **new synonym**

Type material. China (Gansu), Ho-dshi-gou, coll. Möllendorff ex coll. Potanin 853, SMF 8952 (lectotype of *amdoana*, Fig. 3A, B) • China (SO-Gansu), Wen-Hsien, coll. Möllendorff ex coll. Potanin 907, SMF 8953 (paralectotype of *amdoana*) • China (Sytshuan): Thal des Pui-hob. Lum-du, coll. Möllendorff ex coll. Potanin 906, SMF 8959 (lectotype of *distinguenda*, Fig. 5A) • SO-Gansu (NW China), coll. C.R. Boettger ex coll. Möllendorff, SMF 95024/1 paralectotype of *distinguenda* • SO-Gansu: Nanping, coll. Möllendorff ex coll. Potanin 8, 64, 846, SMF 8958/5 paratypes of *distinguenda* • SO-Gansu, Yü-Lin-Guam, u. Wen-hsien, coll. Möllendorff ex coll. Potanin 11, 521, 565, SMF 8955/3 paralectotypes of *distinguenda* • China: SO-Gansu, coll. Möllendorff ex coll. Potanin 725a, SMF 8957/3 paralectotypes of *distinguenda* • Shy-Pu am Pui-hu, coll. Möllendorff ex coll. Potanin 69, 653, SMF 8956/2 paralectotypes of *distinguenda* • SO-Gansu, zw. Li-dshia-pu u. Hsi-gu-tsheng, coll. Möllendorff ex coll. Potanin 923,

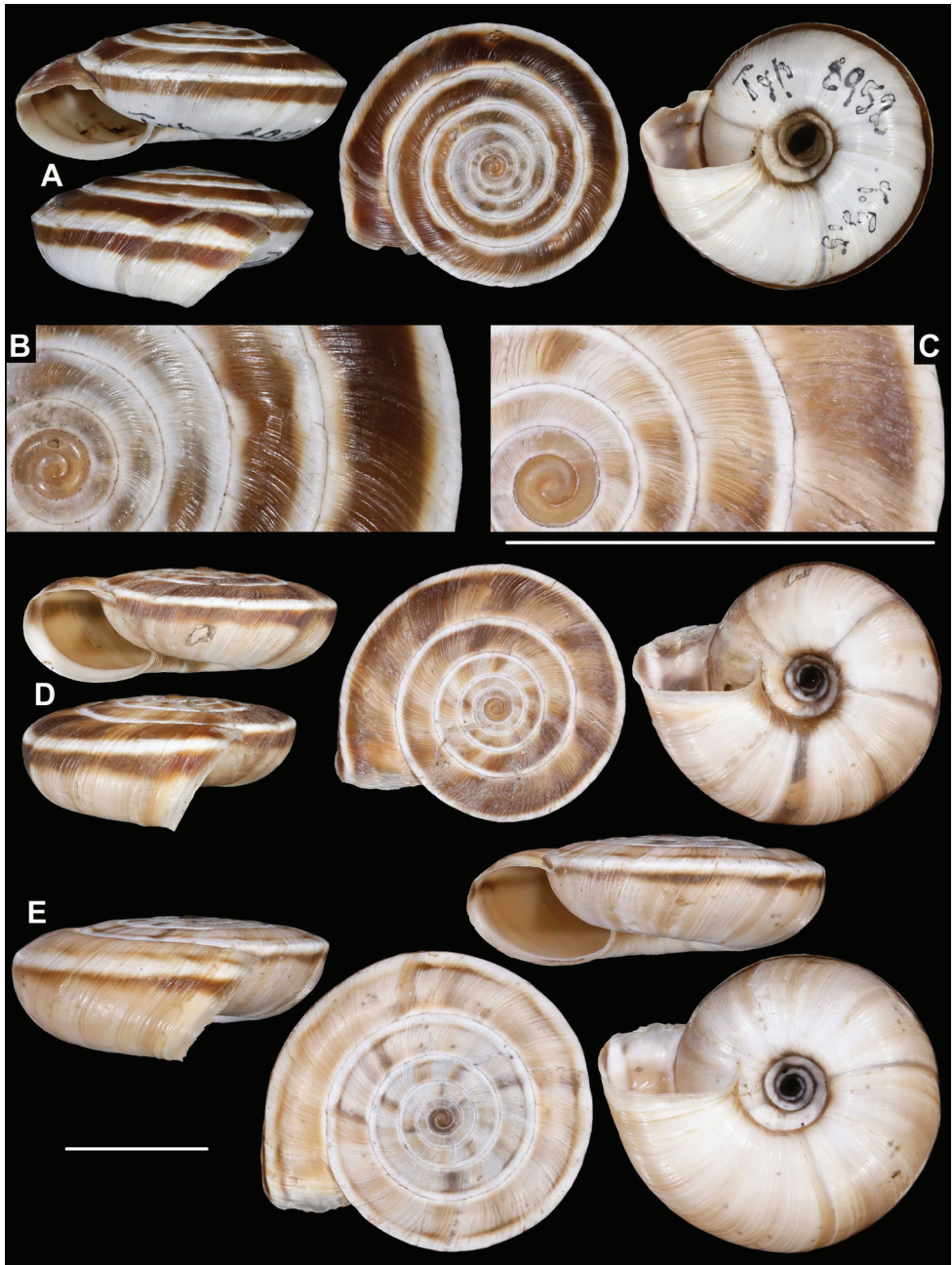


Figure 3. *Laeocathaica amdoana* **A, B** lectotype (SMF 8952) **C, D** 2016/74, specimen2 **E** 2016/74, specimen1. Scale bars: 10 mm. All photographs: B. Páll-Gergely.

SMF 9074 (lectotype of *L. tropidorhapse*, Fig. 7A) • Same data, SMF 9077/2 paralectotypes • NW-China, SO-Gansu, coll. C.R. Boettger 1904 ex coll. Möllendorff SMF 95126/1 (paralectotype of *L. tropidorhapse*) • SO-Gansu, Tan-tshang, coll. Möllen-



Figure 4. *Laeocathaica amdoana* Möllendorff, 1899, 2016/75 (4 different shells of the same sample). Scale bar: 10 mm. All photographs: B. Páll-Gergely.

dorff ex coll. Potanin 545, 623, 808, SMF 9075/4 (paralectotypes of *L. tropidorhapse*)
 • Gansu: Dshie-dshou, coll. Möllendorff ex coll. Potanin 119, SMF 9076/1 (paralectotype of *L. tropidorhapse*)
 • IZCAS TM 095895 (labelled as holotype of *L. dangchangensis*, but its measurements do not match with the ones given in the original



Figure 5. *Laeocathaica amdoana* Möllendorff, 1899 **A** lectotype of *L. distinguenda* (SMF 8959) **B** 2016/72, specimen1 **C** 2016/72, specimen2 **D** 2016/76. Scale bar: 10 mm. All photographs: B. Páll-Gergely.

description, see also remarks, Fig. 7D) • IZCAS TM 095843–095894 + IZCAS TM 095896–095950 (103 paratypes of *L. dangchangensis* in ethanol).

Museum material. Szechwan, coll. Möllendorff, SMF 42564/1 • Tan-Tschan, coll. Möllendorff, SMF 24269/1 (“*tropidorhapa*”).

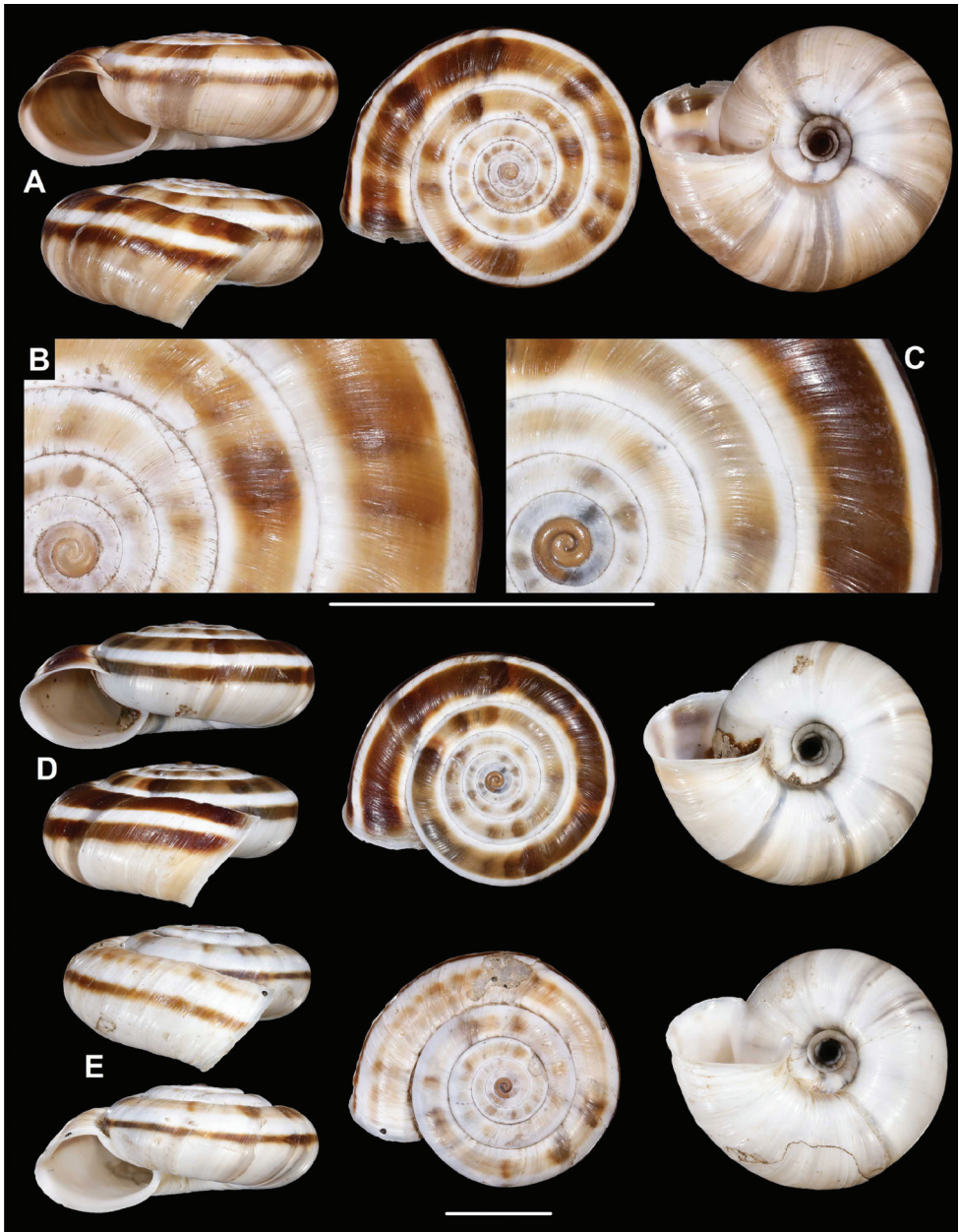


Figure 6. *Laeocathaica amdoana* Möllendorff, 1899 **A, B** 2016/70a **C, D** 2016/71 **E** 2016/69. Scale bars: 10 mm. All photographs: B. Páll-Gergely.

New material (typical tropidorhaphe). CHINA • 2 shells; Gansu, Longnan Shi, Dangchang Xian, Chengguan Zhen, Wenchangmiao, temple hill (locality code: 2016/87); 34°02.394'N, 104°23.499'E; 1835 m a.s.l.; 02 June 2016; A. Hunyadi

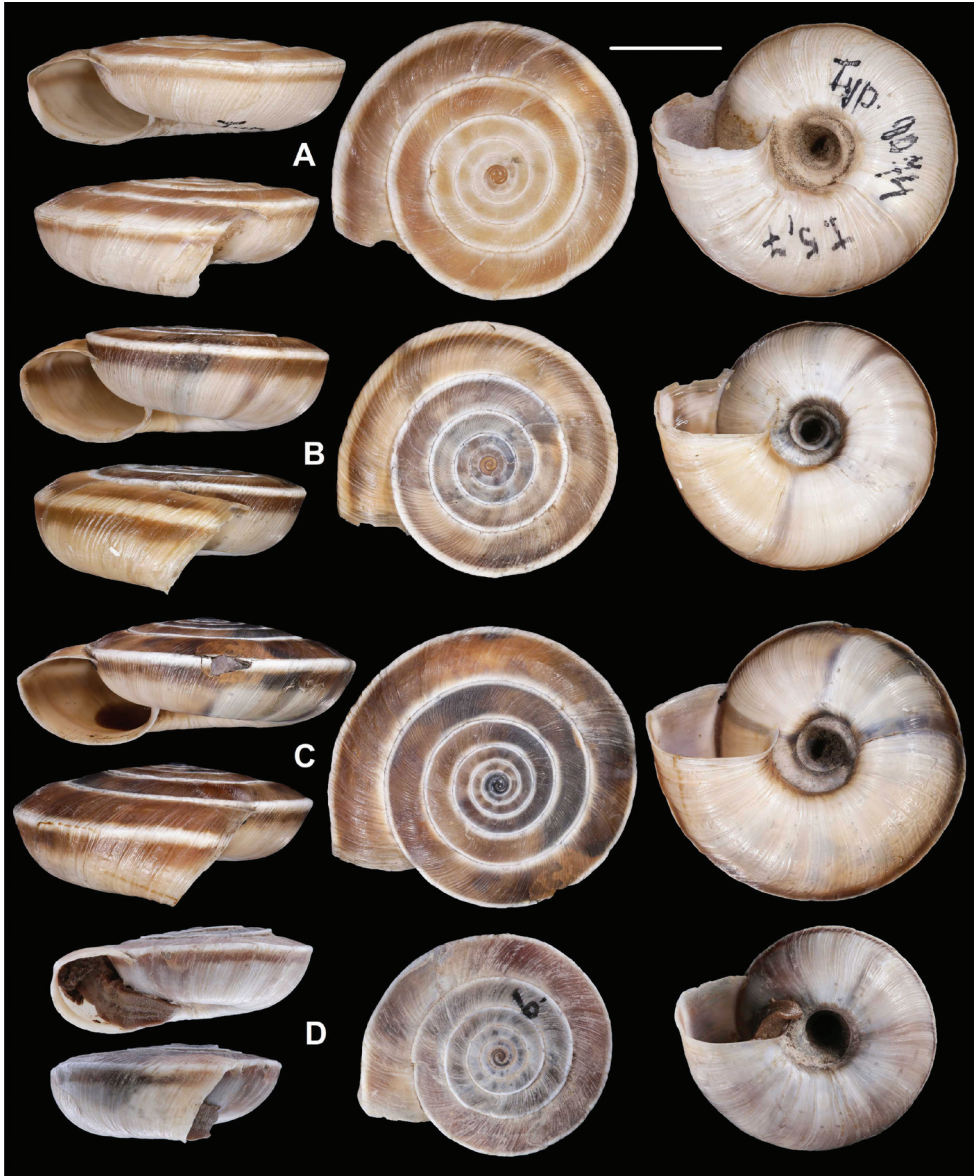


Figure 7. *Laeocathaica amdoana* Möllendorff, 1899 **A** lectotype of *Laeocathaica tropidorhapse* (SMF 9074) **B** 2016/88 **C** 2016/89 **D** paratype of *Laeocathaica dangchangensis* Chen & Zhang, 2004 (labelled as holotype). Scale bar: 10 mm. Photographs: K. Meng (**D**) and B. Páll-Gergely (**A–C**).

leg.; HA • 2 shells; Gansu, Longnan Shi, Dangchang Xian, Lianghekou Xiang, Lianghekou Cun, rock above the intersection (locality code: 2016/89); 33°41.808'N, 104°29.182'E; 1245 m a.s.l.; 02 June 2016; A. Hunyadi leg.; HA (Fig. 8C) • 2 shells; Gansu, Longnan Shi, Dangchang Xian, Guanting Zhen, 1.5 km north of Guanting towards Dangchang (locality code: 2016/88); 33°50.803'N, 104°32.470'E; 1815 m

a.s.l.; 02 June 2016; A. Hunyadi leg.; HA (Fig. 7B) • 2 shells; Gansu, Longnan Shi, Zhugqu Xian, 2.5 km west of Suoertou Cun, northern bank of Bailong He (locality code: 2016/91); 33°46.906'N, 104°20.106'E; 1235 m a.s.l.; 03 June 2016; A. Hunyadi leg.; HA • 2 shells; Gansu, Longnan Shi, Wudu Xian, Jiaogong Zhen, 1.5 km west of Chenjiaba Cun, Zhaoyangdong, below the cave (locality code: 2016/95); 33°31.924'N, 104°39.286'E; 1175 m a.s.l.; 04 June 2016; A. Hunyadi leg.; HA.

New material (other morphs). 6 shells; Sichuan, Aba, Jiuzhaigou Xian, Baihe Xiang, southern edge of Taiping Cun, rock wall facing north (locality code: 2016/72); 33°18.026'N, 104°09.500'E; 30 May 2016; A. Hunyadi leg.; HA (Fig. 5B, C) • 1 shell; Sichuan, Aba, Jiuzhaigou Xian, Baihe Xiang, Taiping Cun, eastern bank of Baishui He (locality code: 2016/73); 33°18.366'N, 104°09.413'E; 30 May 2016; A. Hunyadi leg.; HA • 4 shells; Sichuan, Aba, Jiuzhaigou Xian, Anle Xiang, ca. 1.5 km east of Zhongtianshan Cun towards Jiuzhaigou Shi (locality code: 2016/74); 33°17.279'N, 104°12.702'E; 1445 m a.s.l.; 30 May 2016; A. Hunyadi leg.; HA (Fig. 3C–E) • 4 shells; Sichuan, Aba, Jiuzhaigou Xian, Guoyuan Xiang, 1 km from Guoyuanyi Cun towards Lengshuishan Cun (locality code: 2016/75); 33°07.681'N, 104°18.489'E; 1220 m a.s.l.; 30 May 2016; A. Hunyadi leg.; HA (Fig. 4) • 1 shell; Sichuan, Aba, Jiuzhaigou Xian, Guoyuan Xiang, Guoyuaner Cun, environment of the bridge (locality code: 2016/76); 33°06.922'N, 104°19.617'E; 1200 m a.s.l.; 30 May 2016; A. Hunyadi leg.; HA (Fig. 5D) • 3 shells; Gansu, Longnan Shi, Wenxian, Buziba Xiang, southern edge of Buziba Cun, western bank of the river (locality code: 2016/77); 33°03.592'N, 104°37.094'E; 1215 m a.s.l.; 31 May 2016; A. Hunyadi leg.; HA • 1 shell; Gansu, Longnan Shi, Wenxian, Buziba Xiang, northern edge of Taojiaba Cun, 200 m towards Buziba (locality code: 2016/78); 33°02.706'N, 104°37.157'E; 1200 m a.s.l.; 31 May 2016; A. Hunyadi leg.; HA • 4 shells; Gansu, Longnan Shi, Wenxian, Buziba Xiang, 1 km south of Taojiaba Cun towards Dongyukou Cun (locality code: 2016/79); 33°01.865'N, 104°37.329'E; 1150 m a.s.l.; 31 May 2016; A. Hunyadi leg.; HA • 4 shells; Gansu, Longnan Shi, Wenxian, Chengguan Zhen, next to a museum (locality code: 2016/64); 32°56.471'N, 104°40.379'E; 960–970 m a.s.l.; 28 May 2016; A. Hunyadi leg.; HA • 3 shells; Gansu, Longnan Shi, Wenxian, Chengguan Zhen, cemetery hill above the city (locality code: 2016/65); 32°57.026'N, 104°40.527'E; 1090 m a.s.l.; 28 May 2016; A. Hunyadi leg.; HA • 4 shells; Gansu, Longnan Shi, Wenxian, Jianshan Xiang, 1200 m south of Hekou Cun, eastern bank of Bailong He (locality code: 2016/68); 33°01.703'N, 104°53.602'E; 810 m a.s.l.; 29 May 2016; A. Hunyadi leg.; HA • 2 shells; Gansu, Longnan Shi, eastern edge of Wenxian, northern bank of the river (locality code: 2016/66); 32°56.459'N, 104°41.372'E; 28 May 2016; A. Hunyadi leg.; HA • 4 shells; Gansu, Longnan Shi, Wenxian, Jianshan Xiang, southern edge of Hekou Cun, western bank of Bailong He (locality code: 2016/67); 33°02.014'N, 104°53.478'E; 800 m a.s.l.; 29 May 2016; A. Hunyadi leg.; HA • 3 shells; Gansu, Longnan Shi, Wenxian, Shifang Xiang, 800 m from the northwestern edge of Baiyiba Cun towards Dongyukou Cun, left bank of the river (locality code: 2016/83); 32°58.985'N, 104°37.503'E; 970 m a.s.l.; 31 May 2016; A. Hunyadi leg.; HA • 4 shells; Gansu, Longnan Shi, Wenxian, Shifang Xiang, 1300 m northwest from Baiyiba Cun towards Dongyukou Cun (locality code: 2016/82); 32°59.346'N, 104°37.233'E; 980 m a.s.l.; 31 May 2016; A. Hunyadi

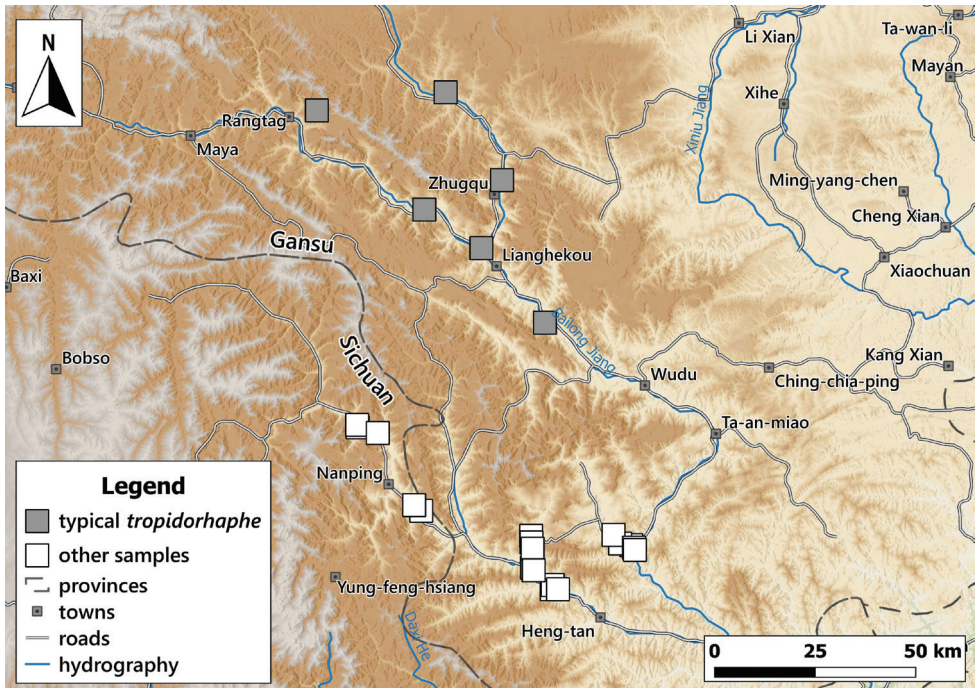


Figure 8. Distribution of *Laeocathaica amdoana* Möllendorff, 1899 in China (detail from Fig. 2A).

leg.; HA • 9 shells; Gansu, Longnan Shi, Wenxian, Jianshan Xiang, western edge of He-kou Cun towards Caojiaba, along road no. 212 (locality code: 2016/69); 33°2.343'N, 104°53.045'E; 29 May 2016; A. Hunyadi leg.; HA (Fig. 6E) • 8 shells; Gansu, Longnan Shi, Wenxian, Jianshan Xiang, 600 m west of Jianshan towards Diaohuya (locality code: 2016/70a); 33°02.559'N, 104°51.254'E; 850 m a.s.l.; 29 May 2016; A. Hunyadi leg.; HA (Fig. 6A, B) • 4 shells; Gansu, Longnan Shi, Wenxian, Jianshan Xiang, 200 m north of Lvjiaba, along road no. 212 (locality code: 2016/71); 33°03.712'N, 104°50.209'E; 29 May 2016; A. Hunyadi leg.; HA (Fig. 6C, D).

Distribution. This species is known from several sites in southwestern Gansu Province and the neighbouring areas in Sichuan (Fig. 8).

Remarks. *Laeocathaica amdoana* was described from Pass Ho-Dshi-Gou bei Mu-gua-tshi (the exact locality could not be located on the map) near Wenxian at the border with Sichuan province, and characterised by a domed, brown, dorsal side with a relatively broad, sharp, distinctly bordering, white band of the keel. We did not find shells identical to typical *Laeocathaica amdoana*, but have found similar ones that can be identified as conspecific (Figs 3C, D, 4).

Laeocathaica distinguenda is represented in the Senckenberg Museum by several samples. Strangely, the lectotype is the most “untypical” among the lots labelled as *L. distinguenda* due to its pale caramel colour, the blurry border of light and dark stripes, and the rounded body whorl. Our samples from the vicinity of Wenxian (Fig. 5B–D) are more similar to the paralectotypes of *L. distinguenda*.

Laeocathaica tropidorhaphae was described from the north (Tanchang and its vicinity), and is characterised by a large, keeled shell with a flat dorsal side and a thick brown spiral band. The northernmost populations we collected (samples 2016/87, 2016/88, 2016/89, 2016/91, 2016/95) agree with the types of *L. tropidorhaphae* in size, shape, and colouration, but their spire height is variable. However, some shells from much further south are also similar (i.e., samples 2016/74, 2016/75, see Fig. 4). The characteristic colouration of *L. tropidorhaphae* (brown dorsal side with slender white band on the keel) is also not unique to the northern *L. tropidorhaphae* populations, but can be found in more southern populations as well (compare Fig. 4a with Fig. 7).

Overall, there is a continuous variation across most of the historical and newly collected samples in terms of shape of dorsal side, shape of body whorl, size, colour, and sculpture (see Figs 3B, C; 6B, C). *Laeocathaica amdoana* and the lectotype of *L. distinguenda* (but not the paralectotypes!) seem to be slightly out of the morphological continuum, but not to a degree that a species-level distinction should be applied.

Colouration can be extremely variable even within a single population (see Fig. 4). Therefore, colour is of minor importance in species distinction within this group of *Laeocathaica*. It is a general trend that towards the southeastern part of the distribution of these “species”, the peripheral keel disappears and the body whorl becomes rounded.

Because of the aforementioned reasons, and until anatomical and DNA sequence data become available, we do not find the names *L. distinguenda* and *L. tropidorhaphae* meaningful, and so we provisionally synonymise them with *L. amdoana*. Table 1 summarises the key traits that are variable across and within newly collected populations.

Laeocathaica dangchangensis Chen & Zhang, 2004 is also a junior synonym of *L. amdoana*, because it shows the same characteristic conchological features (large shell size, acute, white keel, almost flat dorsal side) as *L. tropidorhaphae*. Moreover, its type locality (Shawan town, Dangshang county (34°0'N, 104°3'E), Gansu Province, China) is situated close to the known sites of *L. tropidorhaphae*, whose two closest populations are situated at ca. 31 km and 35 km from the type locality of *L. dangchangensis*.

According to the original description of *Laeocathaica dangchangensis*, the holotype has a shell width of 27.22 mm. However, the shell labelled as the holotype is 23 mm wide. Moreover, the number 6 is written on that specimen's dorsal side, whereas “Holotype: Sp8” is written on the label. We have not found any shells bearing the number 8. Consequently, the shell labelled as the holotype is a paratype, and the real holotype is probably one of the specimens labelled as paratypes, or lost.

***Laeocathaica carinalis* Chen & Zhang, 2004**

Figures 9–10

Laeocathaica carinalis Chen & Zhang, 2004: 341 [Chinese description], fig. 334 (erroneous! Shows a juvenile *Laeocathaica* shell belonging to another species); 444 [English description].

Type locality. “Town of Wenxian County, (33°0'N, 104°6'E), Gansu Province, China”.

Type material. The shell we examined (IZCAS TM 097578) is exactly the same as the one figured by Chen and Zhang (2004: fig. 219) as the holotype of *Cathaica bizonalis* Chen & Zhang, 2004. Therefore, we understand this situation as a confusion of specimens and photographs before publication, and consider the figured shell (IZCAS TM 097578, Fig. 9) as the holotype. See also under *Cathaica bizonalis* Chen & Zhang, 2004.

New material. CHINA • 4 shells; Gansu, Longnan Shi, Wenxian, Jianshan Xi-ang, 1800 m west of Jianshan towards Diaohuya, right side of road no. 212 (locality code: 2016/70b); 33°2.922'N, 104°50.840'E; 29 May 2016; A. Hunyadi leg.; HA (Fig. 10A, B) • 10 shells; Gansu, Longnan Shi, Wenxian, Shifang Xiang, 1300 m northwest from Baiyiba Cun towards Dongyukou Cun, right side of the road (locality code: 2016/82); 32°59.346'N, 104°37.233'E; 980 m a.s.l.; 31 May 2016; A. Hunyadi leg.; HA (Fig. 10E) • 4 shells; Gansu, Longnan Shi, Wenxian, Shifang Xiang, 800 m from the northwestern edge of Baiyiba Cun towards Dongyukou Cun, left bank of the river (locality code: 2016/83); 32°58.985'N, 104°37.503'E; 970 m a.s.l.; 31 May 2016; A. Hunyadi leg.; HA (Fig. 10F) • 7 shells; Gansu, Longnan Shi, Wenxian, Buziba Xiang, 1 km south of Taojiaba Cun towards Dongyukou Cun (locality code: 2016/79); 33°01.865'N, 104°37.329'E; 1150 m a.s.l.; 31 May 2016; A. Hunyadi leg.; HA • 5 shells; Gansu, Longnan Shi, Wenxian, Buziba Xiang, southern edge of Liangjiaba (locality code: 2016/81); 33°00.262'N, 104°36.712'E; 1005 m a.s.l.; 31 May 2016; A. Hunyadi leg.; HA (Fig. 10C, D) • 1 shell; Gansu, Longnan Shi, Wenxian, Cheng-

Table 1. Shell morphological traits of *Laecathaica amdoana* Möllendorff, 1899 populations.

Locality no.	D (in mm)	H (in mm)	Dorsal side	Body whorl
2016/64	21.9–27.1	12–14.7	domed	rounded to slightly keeled
2016/65	25.5–26.2	13.3–14.7	domed	rounded to slightly keeled
2016/66	23.7–24.5	11.2–12.9	domed	rounded
2016/67	19.9–23.3	8.8–11	slightly domed	rounded
2016/68	24.3–25.4	10.4–10.7	flat to slightly domed	rounded
2016/69	27.4–30.7	12.2–14.1	slightly domed	rounded
2016/70a	30–31.3	13.1–14.9	slightly domed	rounded
2016/71	28.5–29.7	13–13.6	slightly domed	rounded
2016/72	19.8–24.2	9.1–12.2	domed	slightly keeled
2016/73	21.8	10	domed	slightly keeled
2016/74	21.4–25.4	9–10.7	flat to slightly domed	strongly to slightly keeled
2016/75	25.1–27.4	9.8–12.5	slightly domed to domed	strongly to slightly keeled
2016/76	20.8	9	flat	strongly keeled
2016/77	20.8–21.6	10.5–11.5	domed	slightly keeled
2016/78	22.7	11.6	slightly domed	slightly keeled
2016/79	20.7–21.7	10–10.3	slightly domed to domed	strongly to slightly keeled
2016/82	20.6–23	9.8–11.6	slightly domed to domed	rounded to slightly keeled
2016/83	27.7–28.3	13–13.7	slightly domed	rounded
2016/87	23–26.9	8.1–11.4	flat to slightly domed	strongly keeled
2016/88	26.6–27.7	10.9–11.3	flat to slightly domed	strongly keeled
2016/89	27.9–30.6	11.3–12.1	flat to slightly domed	strongly keeled
2016/91	27.5–30	10.4–11.5	flat	strongly keeled
2016/95	23.6–27.4	9–10.1	flat	strongly keeled



Figure 9. *Laeocathaica carinalis* Chen & Zhang, 2004 (IZCAS TM 097578, holotype). Scale bar: 10 mm. Photographs: Kaibaryer Meng.

guan Zhen, next to a museum (locality code: 2016/64); 32°56.471'N, 104°40.379'E; 960–970 m a.s.l.; 28 May 2016; A. Hunyadi leg.; HA.

Description. Shell sinistral, depressed, strongly keeled, dorsal side with flat, scalariform whorls; ventral side widely conical; dorsal side chocolate brown, ornamented with a white keel on all whorls; ventral side primarily white, below the white keel there is a chocolate brown belt, white part ornamented with greyish radial stripes that sometimes reach the umbilicus, but sometimes thin and stop before umbilicus; umbilicus inside with a chocolate-brown and a white belt; entire shell consists of 7.25–7.75 whorls; protoconch consists of 1.5–1.75 whorls, brownish, seemingly smooth, extremely finely granulose, rather matte, slightly protruding above first whorls of teleoconch; white keels of every whorl slightly elevated from dorsal surface, but dorsal surface flat with usually the last one being scalariform; dorsal side with fine, irregular wrinkles and between the main wrinkles there are very fine radial lines; ventral surface with less prominent wrinkles; umbilicus rather narrow, funnel-shaped, shows all whorls; periumbilical keel absent; aperture oblique to shell axis, semilunar, with pointed incision at the keel; peristome expanded and slightly thickened, but not reflexed; palatal swelling whitish, with a low, blunt basal tooth; parietal callus practically absent, in some old specimens with translucent calcareous layer.

Measurements (in mm): D: 18.6–22.9; H: 6.8–9.8 ($n = 13$, newly collected shells from multiple samples).

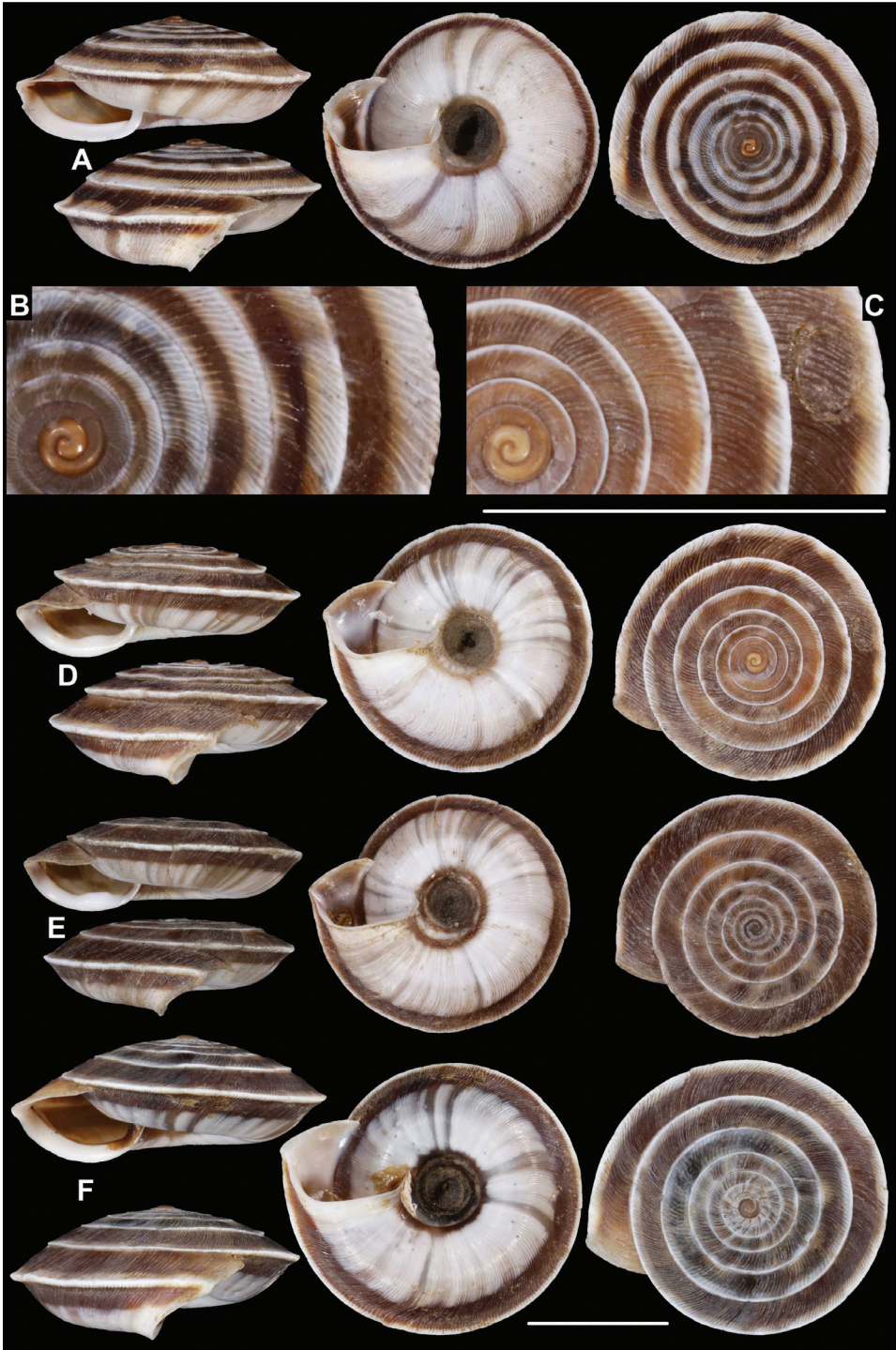


Figure 10. *Laeocathaica carinalis* Chen & Zhang, 2004 **A, B** 2016/70b **C, D** 2016/81 **E** 2016/82 **F** 2016/83. Scale bars: 10 mm. All photographs: B. Páll-Gergely.

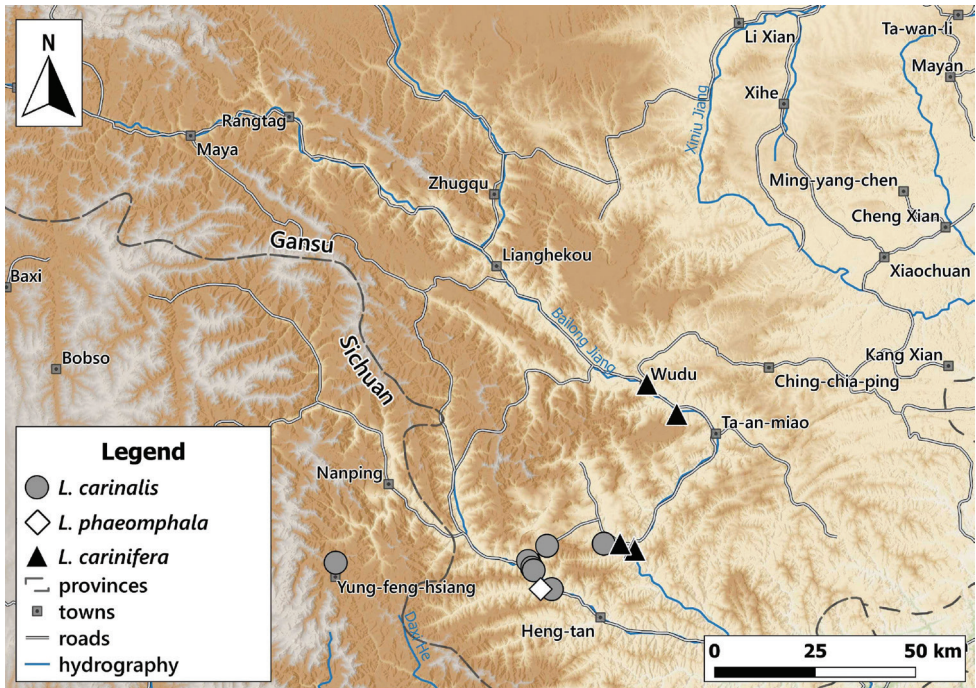


Figure 11. Distribution of *Laeocathaica* species in China (detail from Fig. 2A).

Differential diagnosis. The most similar species is *L. pewzowi*, which is smaller, paler in colour, has a wider umbilicus, a more domed (and not scalariform) dorsal side, stronger radial sculpture, and a more oblique aperture with a more pointed basal tooth. Furthermore, there is a second broken belt between the main belt and the umbilicus in *L. pewzowi*, which is not present in any specimens of this species. *Laeocathaica potanini* has a more scalariform, uniformly light brown shell, and the basal tooth (when present) is situated closer to the columella than in *L. carinalis*. *Laeocathaica amdoana* is also similar in colouration, but it is larger, has a blunter keel, a weaker sculpture, and its whorls are never scalariform.

Distribution. Most precise locality data are from the rocky area along the Baishui River, whereas one sample was collected on the bank of the Yangtang River (Fig. 11). The type locality is situated ca. 50 km west in a straight line.

Remarks. We here provide a redescription, an updated differential diagnosis, and notes on the differences between different populations (Table 2).

Laeocathaica carinifera (H. Adams, 1870)

Figure 12

Helix (Plectotropis) christinae var. *carinifera* H. Adams, 1870: 377.

Helix subsimilis Deshayes, 1874: 10, pl. 2, figs 28–29.

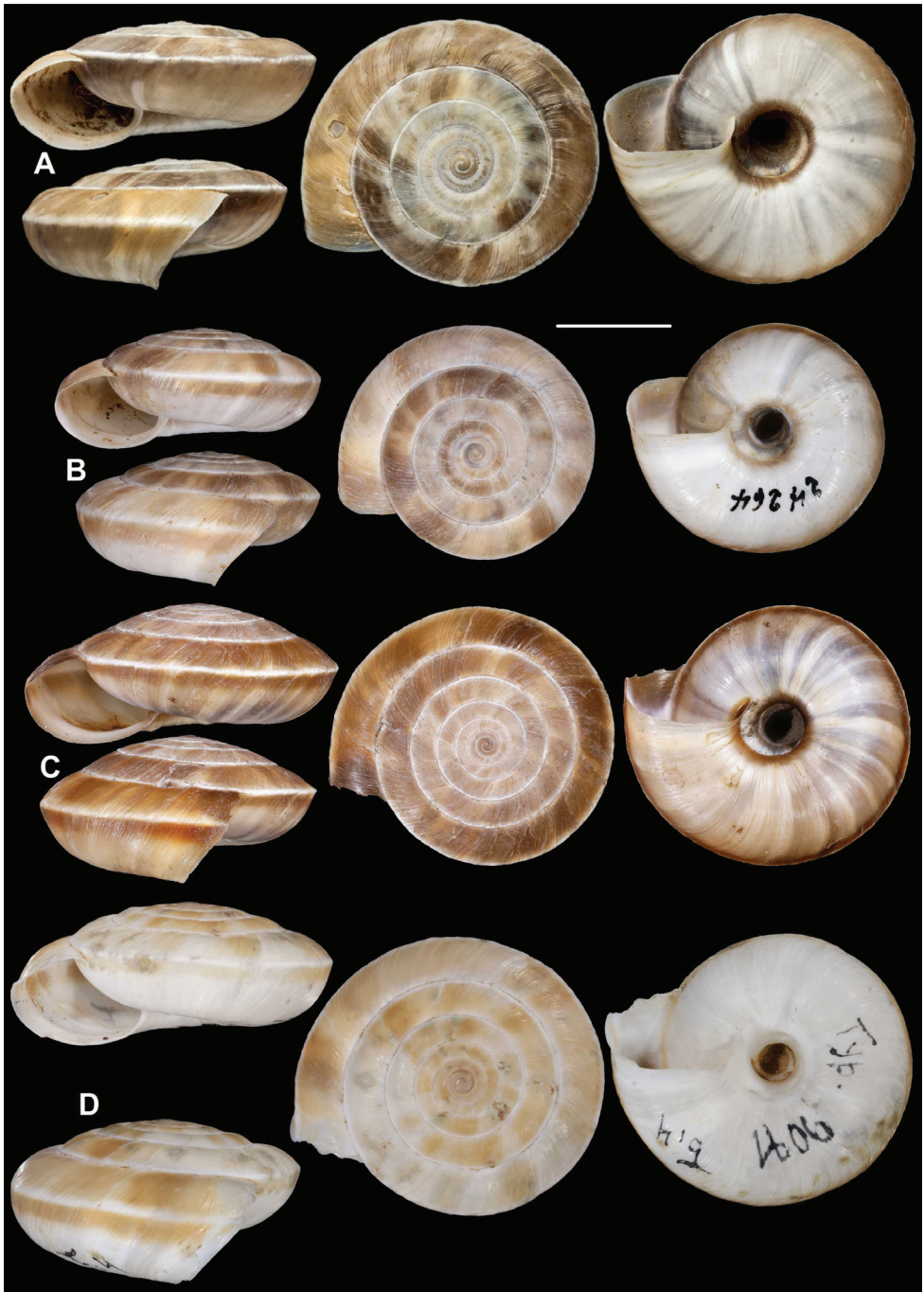


Figure 12. *Laecathaica carinifera* (H. Adams, 1870) **A** syntype, NHMUK 1870.7.16.7 **B** SMF 24264 **C** 2016/70a **D** lectotype of *L. stenochone* (SMF 9071). Scale bar: 10 mm. Photographs: B. Páll-Gergely (**C, D**), Kevin Webb, NHM (**A**).

Helix christinae. – Möllendorff 1884: 351.

Helix subsimilis. – Gredler 1884: 264.

Helix christinae var. *carinifera*. – Möllendorff 1884: 351.

Laeocathaica subsimilis. – Möllendorff 1899: 89.

Laeocathaica stenochone Möllendorff 1899: 91, pl. 5, fig. 4. **new synonym**

Laeocathaica subsimilis subsimilis. – Yen 1939: 148, pl. 15, fig. 28.

Laeocathaica stenochone. – Yen 1939: 148, pl. 15, fig. 30.

Laeocathaica (Laeocathaica) stenochone. – Zilch 1968: 175.

Laeocathaica (Laeocathaica) subsimilis. – Zilch 1968: 175.

Laeocathaica subsimilis. – Chen and Zhang 2004: 313, fig. 299 (treats *filippina* as a synonym).

Laeocathaica stenochone. – Chen and Zhang 2004: 314, fig. 301.

Laeocathaica subsimilis subsimilis. – Wu 2004: 86, 89, 98, 112, fig. 17 (figure labelled as *L. filippina*).

Type material. China, Woushan, coll. Swinhoe, NHMUK 1870.7.16.7 (3 shells, probably syntypes of *Helix christinae* var. *carinifera*, labelled as “christinae var”) (Fig. 12A) • China, coll. Swinhoe, NHMUK 1870.7.16.8 (3 shells, probably syntypes of *Helix christinae* var. *carinifera*, labelled as “christinae var”) • Thibet, leg. Abbé David, 1870, MNHN/1 syntype of *H. subsimilis* (broken) • Thibet (Moupin), leg. Abbé David, 1869, MNHN/12 syntypes of *H. subsimilis* (some of them are juvenile/broken) • Chine, leg. Abbé David, 1874, MNHN/1 syntype of *H. subsimilis* • China (SO-Gansu): Moupin, Thibet Oriental, leg. David, coll. Deshayes, 1872 in coll. Crosse, MNHN-IM-2014-7944/2 syntypes of *H. subsimilis* • Hsi-gu-tseng, coll. Möllendorff ex coll. Potanin 577, SMF 9071 (lectotype of *L. stenochone*, Fig. 12D) • Same data, SMF 9072/1 (paralectotype of *L. stenochone*) • SO-Gansu, Zw. Yü-lin-guan u. Wenhsien, SMF 8951/1 (paralectotype of *L. stenochone*) • Sy-tchuan, coll. Möllendorff ex coll. Berezowski, 908c, SMF 24270/1 (paralectotype of *L. stenochone*).

Museum material. China, Yangtze-Tal, coll. Jetschin ex coll. Beddome, SMF 95020/1 (mixed sample with *L. christinae*) • Lü-feng-kou b. Guan-yüan, coll. Möllendorff ex coll. Potanin 270, SMF 24264/4 (Fig. 12B) • China (Sy-tchuan): zw. Guan-yüan u. Dshau-hoa, coll. Möllendorff ex coll. Potanin 275, SMF 24256/3 • WM-China, Sy-tchuan, Chung-King, coll. O. Boettger ex coll. Möllendorff, SMF

Table 2. Shell morphological traits of *Laeocathaica carinalis* Chen & Zhang, 2004 populations.

Locality no.	Shell diameter	Belt below keel	White belt on keel	Dorsal side	Denticle
2016/64	20.2	medium	thin	flat/not scalariform	strong
2016/70b	20.3–21.5	thin	thick	domed/scalariform	only low thickening
2016/79	19.1–20.3	thick	moderate	flat/scalariform	strong
2016/81	19.8–20.4	thick	moderate	flat/scalariform	1 out of 5 shells
2016/82	18.6–19.8	medium	thin	flat/scalariform	present
2016/83	21.2–22.9	thick	moderate	moderately domed/ slightly scalariform	only low thickening

24262/4 • China: Badung, Hubei, coll. Möllendorff ex coll. L. Fuchs, SMF 24259/2; O-Sy-tschuan, coll. Möllendorff, SMF 24255/4 • China: W-Hupé, ex Gredler, SMF 294293/2 • China: Kwan-juön-hszién (Kuan-yuan-hsien), Prov. Sze-csuen, China, ex coll. T. Kormos, SMF 24260/1 • China, Coll. H. Rolle, SMF 294294/1; China: Sytchuan, coll. C. Bosch ex coll. H. Rolle, SMF 294292/2 (mixed sample with *L. filippina*) • W-China: Prov. Sy-chuan, coll. C.R. Boettger, SMF 95117/1 • Sytschuan: Tal des Lu-fyn-kou nördlich von der Stadt Juanj-juan, leg. Potanin, coll. Jetschin, SMF 95116/1 • Same locality, MNHN-IM-2014-7935/2 • China: Yang-dsy Gebiet, coll. Möllendorff ex coll. Heude, SMF 24265/2 • China: Shen-hsi, Liu-ba-ting, coll. Möllendorff ex coll. Potanin 451, SMF 24261/2 • O-Sytchuan, coll. Kobelt (alte Schau-Sammlung) ex coll. Möllendorff, SMF 24258/3 • O-Sy-tchuan, coll. Möllendorff ex coll. B. Schmacker, SMF 24257/4 • Paoning, Szechuan, Don: Tomlin, 1946, MNHN-IM-2014-7931/4 adult + 2 juvenile shells • Chine, Chungking, Sytschouan, coll. Letellier, 1949, MNHN-IM-2014-7936/1 • Chine, coll. Denis, 1945, MNHN-IM-2014-7937/2 • China, Baoning, MNHN-IM-2014-7941/1 juvenile shell • Turkestan, leg. Potanin, MNHN-IM-2014-7943/1 adult + 1 juvenile shell • Chine, collector's name not readable, 1878, MNHN-IM-2014-7938/1 • Chine, coll. Fischer, MNHN/1 • Hupé, China, MNHN-IM-2014-7940/1 • Hupé, China, coll. Staadt, 1969, MNHN-IM-2014-7929/1 + 2 *L. filippina* shell (mixed sample, erroneous locality for *L. carinifera*).

New material. CHINA • 3 shells; Gansu, Longnan Shi, Wenxian, Bikou Zhen, above the hydroelectric power plant, northern side of Bailong He (locality code: 2016/63); 32°45.966'N, 105°13.005'E; 28 May 2016; A. Hunyadi leg.; HA • 1 shell; Gansu, Longnan Shi, Wenxian, Jianshan Xiang, 1800 m west of Jianshan towards Diaohuya, right side of road no. 212 (locality code: 2016/70b); 33°2.922'N, 104°50.840'E; 29 May 2016; A. Hunyadi leg.; HA • 3 shells; Gansu, Longnan Shi, Wenxian, Jianshan Xiang, southern edge of Hekou Cun, western bank of Bailong He (locality code: 2016/67); 33°02.014'N, 104°53.478'E; 800 m a.s.l.; 29 May 2016; A. Hunyadi leg.; HA • 3 shells; Gansu, Longnan Shi, Wenxian, Jianshan Xiang, 600 m west of Jianshan towards Diaohuya (locality code: 2016/70a); 33°02.559'N, 104°51.254'E; 850 m a.s.l.; 29 May 2016; A. Hunyadi leg.; HA (Fig. 12C) • 3 shells; Gansu, Longnan Shi, Wenxian, Jianshan Xiang, 1200 m south of Hekou Cun, eastern bank of Bailong He (locality code: 2016/68); 33°01.703'N, 104°53.602'E; 810 m a.s.l.; 29 May 2016; A. Hunyadi leg.; HA • 2 shells; Gansu, Longnan Shi, Wudu Xian, Hanwang Zhen, Wanxiangdong, path below the cave (locality code: 2016/85); 33°19.824'N, 105°00.273'E; 1160 m a.s.l.; 01 June 2016; A. Hunyadi leg.; HA • 2 shells; Shaanxi, Hanzhong Shi, Lueyang Xian, Gaojiaba, along the highway (locality code: 2016/96); 33°22.090'N, 106°10.116'E; 06 June 2016; A. Hunyadi leg.; HA • 3 shells; Gansu, Longnan Shi, Wudu Xian, Chengguan Zhen, northwest of Jiezhou Botanical Garden, hill above the city (locality code: 2016/86); 33°23.809'N, 104°55.524'E; 1035 m a.s.l.; 01 June 2016; A. Hunyadi leg.; HA • 2 shells; Sichuan, Chengdu Shi, Chengdu, Nanda Jie, stone fence (locality code: 2015/78); 30°39.228'N, 104°3.659'E; 23 June 2015; A. Hunyadi & M. Szekeres leg.; HA.

Distribution. The original description *Helix christinae* var. *carinifera* was published together with that of the nominotypical form, without any specification of a type locality. However, on one of the boxes of var. *carinifera* in the NHM, the locality Woushan (probably Wushan, Chongqing at 31°5'N, 109°53'E) was mentioned. The type locality of *Helix subsimilis* is Moupin (Baoxing, at 30°22'N, 102°49'E) in Tibet. Furthermore, Wu (2004) dissected *Laeocathaica subsimilis* specimens collected at Nanchong, Sichuan. All precise locality data are known from southern Gansu and from the centre of Chengdu city in Sichuan (probably introduced?). Therefore, it is possible that *L. carinifera* is a widespread species, or the locality data from 250–450 km from southern Gansu are the results of imprecise labelling. On the map (Fig. 11) we only indicate the newly reported samples from southern Gansu.

Remarks. Adams (1870) described *Helix christinae* and *Helix christinae* var. *carinifera*. According to the original description, var. *carinifera* differs from the nominotypical form by the smaller shell, the more acute keel, and the narrower umbilicus. We found a sample labelled *Helix christinae* and two labelled as “*Helix christinae* var.” in the NHM. The latter two samples differ from the former one exactly in the traits mentioned by Adams. Thus, although they are not labelled as var. *carinifera*, it is clear that they represent syntypes of that taxon.

The syntypes of *Helix christinae* var. *carinifera* are identical with the types of *Helix subsimilis*, and thus, the latter is a junior synonym of the former. Although both Möllendorff (1884) and Gredler (1884) synonymised *H. subsimilis* with *H. carinifera*, this species (*L. carinifera*) has been mentioned in the literature as *Laeocathaica subsimilis*. *Laeocathaica stenochone* is also identical with both *Helix christinae* var. *carinifera* and *Helix subsimilis*, and therefore, it is also treated as a junior synonym.

***Laeocathaica christinae* (H. Adams, 1870)**

Figure 13

Helix (Plectotropis) christinae H. Adams, 1870: 377, pl. 27, figs 4, 4a.

Helix christinae. – Gredler 1884: 264.

Laeocathaica christinae. – Möllendorff 1899: 88.

Laeocathaica (Laeocathaica) christinae christinae. – Zilch, 1968: 173.

Laeocathaica christinae. – Chen and Zhang 2004: 334, fig. 326.

Type material. China, coll. Swinhoe, NHMUK 1870.7.16.6 (3 shells, probably syntypes, Fig. 13A) • Chine, Ichang & Fungsiang, Achat Sallé, MNHN-IM-2014-7932/3 (probably syntypes).

Museum material. Asia Centrale, MNHN-IM-2014-7933/3 • Asia Centrale, MNHN-IM-2014-7934/7 • Hupé, China, coll. Staadt, 1969, MNHN-IM-2014-7929/2 + 1 *L. carinifera* shell (mixed sample, erroneous locality for *L. carinifera*) • Moupin, leg. Abbé David, coll. Deshayes, 1872, MNHN-IM-2014-7945/2 (probably erroneous locality).



Figure 13. Shell of *Laeocathaica christinae* (H. Adams, 1870) **A** probable syntype, NHMUK 1870.7.16.6 **B** 2010/29. Scale bar: 10 mm. Photographs: B Páll-Gergely (**B**), Kevin Webb, NHM (**A**).

New material. CHINA • 10 shells; Hubei, Enshi Tujiazu Miaozu Zizhizhou, Badong Xian, east of Badong, Bashan Senlin Gongyuan, (next to Xinlingzhen) (locality code: 2010/29); 31°01.472'N, 110°25.284'E; 225 m a.s.l.; 03 November 2010; A. Hunyadi leg.; HA (Fig. 13B).

Distribution. The type localities and the newly collected sample suggest that this species lives more upstream in the Yangtze valley than *L. filippina*. The samples from Moupin (Baoting County, Sichuan) are probably erroneous. We indicated only the newly collected sample on the map (Fig. 14).

Remarks. We found three samples in the NHM. One of them, containing two shells, was labelled *Helix christinae*. The other two lots, labelled “*Helix christinae* var.,” contained three shells each. The latter two samples are probably syntypes of *Helix christinae* var. *carinifera*, described in the same publication (Adams 1870; see further details under that species). None of the two *Helix christinae* shells (NHMUK 1870.7.16.6) are identical with the shells figured in the original description (Adams 1870: pl. 27, figs 4, 4a). However, the indication of the collector

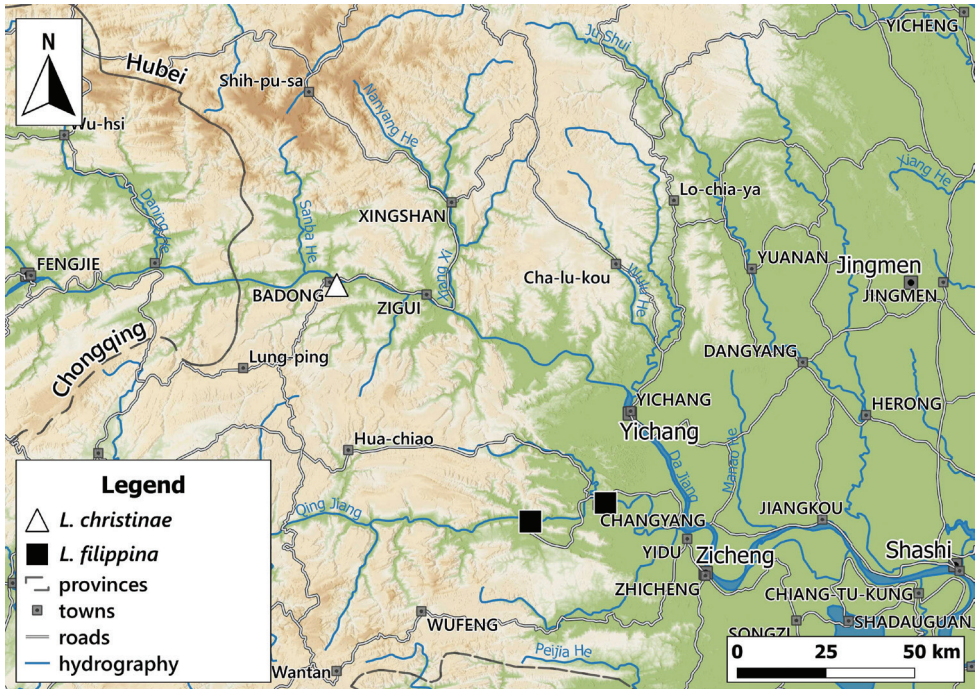


Figure 14. Distribution of *Laeocathaica* species in China (**B** in Fig. 2).

(Swinhoe) agrees with the collector mentioned in the original description. Thus, we treat the two shells of that lot as syntypes.

Adams (1870) gave two type localities: “Ichang and Fungsiang gorges, China”. The former is situated upstream of Yichang City in Hubei (30°56'N, 110°48.7'E), whereas the latter is Fengxiangxia, Fengjie County in Chongqing (31°2'N, 109°35'E). Our sample 2010/29 is geographically located between the two type localities. The shells of this sample are identical with the types, but they are smaller.

Laeocathaica dejeana (Heude, 1882)

Figure 15

Helix dejeana Heude, 1882: 21, pl. 20, fig. 17.

Cathaica (*Campylocathaica*) *dejeana*. – Chen and Zhang 2004: 270–272, fig. 255.

Laeocathaica dejeana. – Chen and Zhang 2004: 337, fig. 330.

Type material. According to Johnson (1973) there is a paratype in the USNM (inv. number: 472128), which was not examined by us.

Museum material. China: Da-tshien-lu am Ya-lung, coll. Möllendorff ex coll. Potanin 380, SMF 23919/4 (Fig. 15) • Sy-tschuan, Umgebungen der Stadt Da-zsjan-lu, det. Möllendorff, MNHN-IM-2014-7946/1.



Figure 15. *Laeocathaica dejeana* (Heude, 1882), SMF 23919. Scale bar: 10 mm. All photographs: B. Páll-Gergely.

Laeocathaica dityla Möllendorff, 1899

Figure 16

Laeocathaica dityla Möllendorff, 1899: 99–100, pl. 6, fig. 8.

Laeocathaica dityla. – Yen 1939: 149, pl. 15, fig. 42.

Laeocathaica (*Laeocathaica*) *dityla*. – Zilch 1968: 174.

Laeocathaica dityla. – Chen and Zhang 2004: 332, fig. 324.

Type material. SO-Gansu, zw. Li-tshia-pu u. Hsi-gu-tsheng, coll. Möllendorff ex coll. Potanin 776, SMF 9086 (lectotype, Fig. 16A) • Same data, SMF 9087 (paralectotype); Tshiu-dsei-dsy, coll. Möllendorff ex coll. Potanin 22, SMF 9088/1 (paralectotype).

New material. CHINA • 4 shells; Gansu, Longnan Shi, Dangchang Xian, Guanting Zhen, 1.5 km north of Guanting towards Dangchang (locality code: 2016/88); 33°50.803'N, 104°32.470'E; 1815 m a.s.l.; 02 June 2016; A. Hunyadi leg.; HA (Fig. 16C) • 5 shells; Gansu, Longnan Shi, Wudu Xian, Hanwang Zhen, Wanxiangdong, serpentine leading to the cave (locality code: 2016/84); 33°20.383'N, 104°59.876'E; 1010 m a.s.l.; 01 June 2016; A. Hunyadi leg.; HA (Fig. 16B) • 1 shell; Gansu, Longnan Shi, Dangchang Xian, Lianghekou Xiang, eastern edge of Lianghekou Cun (locality code: 2016/90); 33°41.587'N, 104°29.379'E; 02 June 2016; A. Hunyadi leg.; HA



Figure 16. *Laeocathaica dityla* **A** lectotype (SMF 9086) **B** 2016/84 **C** 2016/88. Scale bar: 10 mm. All photographs: B. Páll-Gergely.

• 9 shells; Gansu, Longnan Shi, Wudu Xian, Jiaogong Zhen, 1.5 km west of Chenjiaba Cun, Zhaoyangdong, below the cave (locality code: 2016/95); 33°31.924'N, 104°39.286'E; 1175 m a.s.l.; 04 June 2016; A. Hunyadi leg.; HA • 1 shells; Gansu, Longnan Shi, Wudu Xian, Chengguan Zhen, northwest of Jiezhou Botanical Garden, hill above the city (locality code: 2016/86); 33°23.809'N, 104°55.524'E; 1035 m a.s.l.; 01 June 2016; A. Hunyadi leg.; HA • 2 shells; Gansu, Dangchangxian, Shawanxiang, 401 km point along R212 (locality code: 20110422C); 33°38.067'N, 104°33.240'E; 1258 m a.s.l.; 21 April 2011; Y. Nakahara, K. Okubo & K. Otani leg.; PGB.

Distribution. Newsamples were collected along the Bailong and Minjiang rivers (Fig. 17).

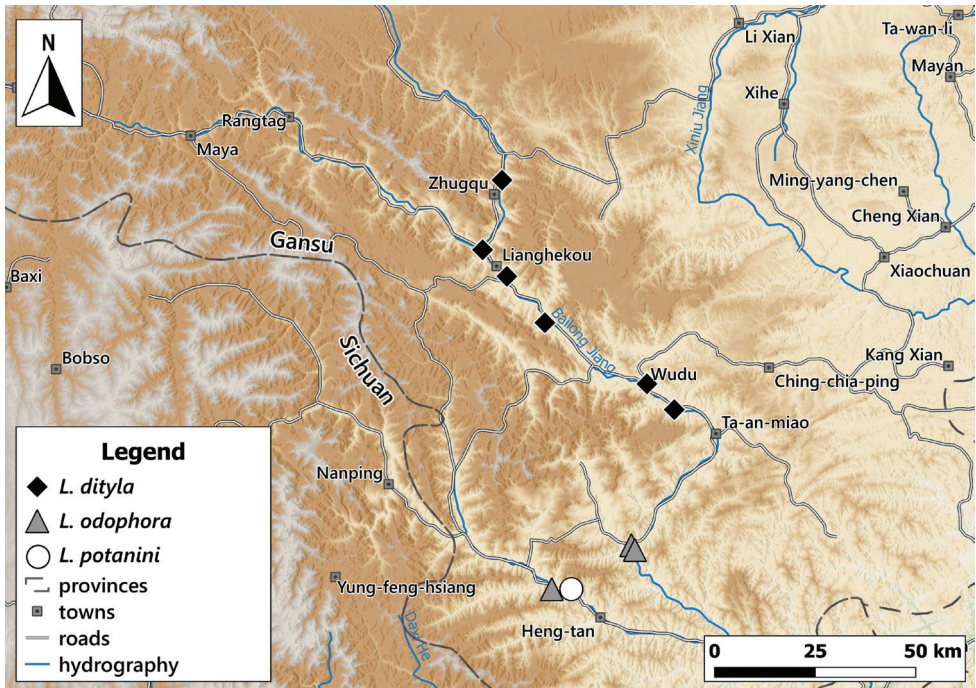


Figure 17. Distribution of *Laeocathaica* species in China (A in Fig. 2).

Laeocathaica dolani (Pilsbry, 1934)

Figure 18A

Cathaica (*Laeocathaica*) *dolani* Pilsbry, 1934: 16, pl. 3, figs 4, 4a–c.

Laeocathaica dolani. – Chen and Zhang 2004: 335, fig. 328.

Type material. China, Szechuan, Romichengu, Brooke Dolan, W. China Expedition 1931, ANSP 162061 (holotype in Fig. 18A + 3 paratypes).

Laeocathaica filippina (Heude, 1882)

Figure 19

Helix filippina Heude, 1882: 23, pl. 20, fig. 19.

Helix (*Plectopylis*) *subchristinae* Ancey, 1882: 44.

Helix subsimilis var. *filippina*. – Gredler 1884: 264.

Laeocathaica filippina. – Möllendorff 1899: 88–89.

Laeocathaica subsimilis filippina. – Yen 1939: 148, pl. 15, fig. 29.

Laeocathaica (*Laeocathaica*) *christinae filippina*. – Zilch 1968: 173.

Type material. Patong, Heude type coll., USNM 472127, (1 syntype, Fig. 19A).



Figure 18. Shells of *Laeocathaica* species **A** *Laeocathaica dolani* Pilsbry, 1934 (holotype, ANSP 162061) **B** *Laeocathaica leucorhaphe* (Möllendorff, 1899), lectotype (SMF 9073) **C** *Laeocathaica phaeomphala* Möllendorff, 1899, lectotype (SMF 9089). Scale bar: 10 mm. All photographs: B. Páll-Gergely.

Museum material. China, W-Hupei, coll. K. Hashagen, SMF 24226/3 • Hubei, Badung, coll. Möllendorff, SMF 24266/4 (Fig. 19B) • China: Badung, Hubei: coll. Kobelt (alte Schau-Sammlung) ex coll. Möllendorff, SMF 24266a/3 • W-Hupei, China, coll. Naegle ex coll. Gredler 1906, SMF 50089/2 (labelled as



Figure 19. Shells of *Laeocathaica filippina* (Heude, 1882) **A** syntype, USNM 427127 **B** SMF 24266 **C** 2010/25. Scale bar: 10 mm. Photographs: downloaded from the webpage of USNM (**A**), B. Páll-Gergely (**B–C**).

L. filippina, det. Wu 2008) • China, SMF 24227/1 (labelled as *L. subsimilis*, det. Wu 2008) • China, Sytchuan, Changyang, coll. O. Boettger ex coll. B. Schmacker 1893, SMF 24267/2 • China: Badung, Hubei: coll. C.R. Boettger 1904, SMF 95118/5 • China: Changyang, coll. C. Bosch ex coll. Sowerby ex coll. Fulton, SMF 294296/3 • China: Changyang, coll. Ehrmann ex coll. Sowerby ex coll. Fulton, SMF 294295/1 • Changyang, Coll. Denis 1945, MNHN-IM-2014-7942/2 • China: Sytchuan, coll. C. Bosch ex coll. H. Rolle, SMF 294292/1 (mixed sample with *L. carinifera*).

New material. CHINA • 7 shells; Hubei, Yichang Shi, Changyang Tujiazu Zizhixian, Qingjiang Hualang Fengjingqu, Geheyan Shuiku, Wuluozhongli Shan (locality code: 2010/25); 30°25.805'N, 110°59.254'E; 260 m a.s.l.; 31 October 2010; A. Hunyadi leg.; HA (Fig. 19C) • 3 broken shells; Hubei, Yichang Shi, Changyang Tujiazu Zizhixian, eastern edge of Changyang, environment of Hukouwan, rocks around the

budhist temple (locality code: 2010/23); 30°28.622'N, 111°12.421'E; 95 m a.s.l.; 31 October 2010; A. Hunyadi leg.; HA.

Distribution. The newly collected samples, and the several museum samples from Changyang (at 30°28'N, 111°12'E), suggest that this species lives downstream along the river Yangtze compared to *L. christinae* (Fig. 13). The type locality of *L. filippina* (Badong) is situated more upstream, within the area of *L. christinae*. However, it may be erroneous, as at the time of the description the nearest large city was usually mentioned on the labels.

Remarks. We did not examine the types of *Helix subchristinae* Ancey, 1882, and treat it as a synonym of *L. christinae* following Gredler (1884), while Richardson (1983) listed it under *L. christinae*.

***Laeocathaica hisanoi* Páll-Gergely, sp. nov.**

<http://zoobank.org/F273CAC1-E575-426C-ACA6-A16F6CB80171>

Figure 20D

Type material. *Holotype* China • S Kansu, China, coll. S. Hisano, 24.05.204, SMF 336708 (D: 11.6 mm, H: 5.2 mm) (Fig. 20D). *Paratype* CHINA • Same data as for holotype; SMF 363469.

Diagnosis. A small *Laeocathaica* species with many (8.5) whorls, conical dorsal side, rounded body whorl and single, small basal tooth that is situated close to the columella.

Description. Shell sinistral, depressed, dorsal side conical with protruding apex, body whorl shouldered; colour chalk white with a single brownish belt below shoulder; entire shell consists of 8.5 whorls, protoconch consists of 1.75–2 whorls, very finely granulose, conspicuously elevated compared to first teleoconch whorls; teleoconch with fine, irregular growth lines, without any notable sculpture, although both examined shells were corroded; last quarter whorl with slight sub-sutural furrow; aperture semilunar, very strongly oblique to shell axis; peristome sharp, very slightly expanded dorsally, with thickening situated behind peristome edge; basal tooth blunt, elongated, situated ca. at the middle of basal peristome; parietal callus inconspicuous, appears only as thick calcareous layer; umbilicus open, narrow, shows all whorl, with the last half of body whorl extremely widened, resulting in a “9”-shape.

Measurements (in mm): D: 11.5–11.6; H: 5.2–5.3 ($n = 2$).

Differential diagnosis. The most similar species is *L. polytyla*, which is usually larger, has one whorl more, has a more elevated spire with a domed dorsal side, a rounded body whorl, and a comparatively smaller basal tooth situated closer to the columella.

Etymology. This new species is named after S. Hisano, who collected the type material.

Distribution. This new species is known from a single museum sample only, consisting of two shells.

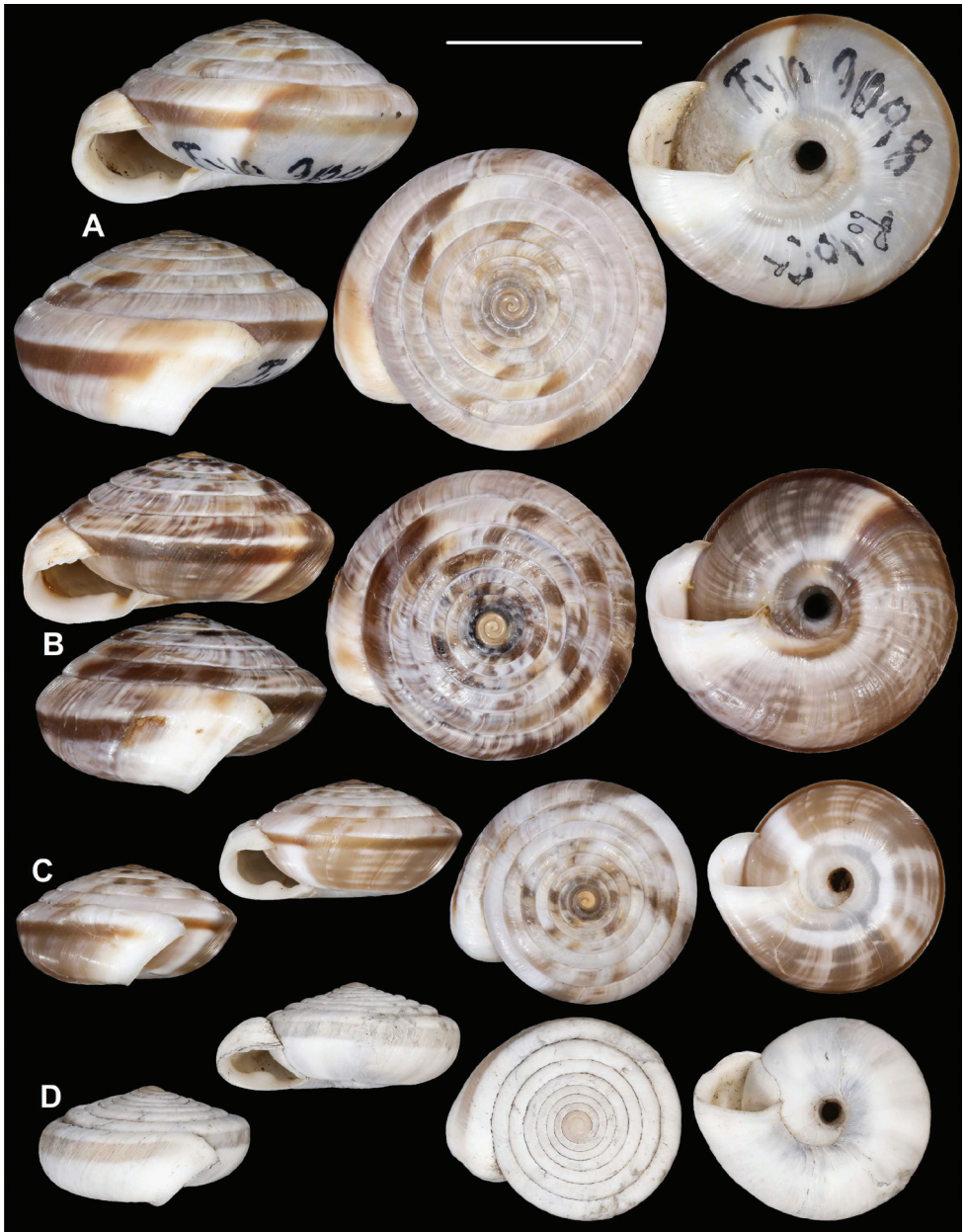


Figure 20. *Laeocathaica* species **A** *Laeocathaica polytyla* Möllendorff, 1899, lectotype (SMF 9198) **B** *Laeocathaica polytyla*, 2016/78 **C** *Laeocathaica polytyla*, 2016/65 **D** *Laeocathaica hisanoi* sp. nov. (holotype, SMF 336708). Scale bar: 10 mm. All photographs: B. Páll-Gergely.

***Laeocathaica leucorhapse* Möllendorff, 1899**

Figure 18B

Laeocathaica leucorhapse Möllendorff, 1899: 95–96, pl. 6, fig. 2.

Laeocathaica leucorhapse. – Yen 1939: 149, pl. 15, fig. 36.

Laeocathaica (Laeocathaica) leucorhapse. – Zilch 1968: 174.

Laeocathaica leucorhapse. – Chen and Zhang 2004: 323, fig. 312.

Types examined. N-Sytschuan: am Tung-ho, coll. Möllendorff ex coll. Potanin 312b, SMF 9073 (lectotype, Fig. 18B).

***Laeocathaica minwui* Páll-Gergely, sp. nov.**

<http://zoobank.org/C96CE473-3692-4306-9AB2-2AEFDA307824>

Figure 21

Type material. *Holotype* CHINA • China, O. Sy-tshuan, coll. C.R. Boettger ex coll. Möllendorff ex coll. L. Fuchs, SMF 95019 (D = 23.1, H = 9.1) (Fig. 21). *Paratypes* CHINA • Yangtze-Tal, coll. Jetschin ex coll. Beddome, SMF 95020/1 (mixed sample with *L. carinifera*) • W. China, Sy-tshuan, coll. Kobelt ex coll. Möllendorff, SMF 6920/1 (det. Wu 2008, labelled as *L. christinae*) • China: Hupei: Kao-cha-hien, coll. O. Boettger ex coll. B. Schmacker, 1893, SMF 24263/1 (det. Wu 2008, labelled as *L. christinae*) • China, O. Sy-tshuan, coll. Möllendorff, SMF 24255a/5 • China: Chang-Yang, coll. O. Boettger ex coll. M. Schmacker, SMF 42563/2 • Moupin, leg. Abbé David, MNHN-IM-2014-7939/14 (probably erroneous locality).

Diagnosis. A rather large *Laeocathaica* species with a sharp keel, a domed dorsal side, an oval aperture and a marmorated ventral side.

Description. Shell sinistral, depressed, with domed dorsal side, keel strong, situated in the middle of body whorl, whitish; dorsal side latte-coloured, with darker and paler areas alternating as the shell grows; ventral side with white and pale brownish (latte) spiral bands forming a marmorated colour pattern; inner side of umbilicus with brownish spiral band; protoconch light brownish, ca. 1.5 whorls, finely granulate, slightly protrudes above first whorls of teleoconch; entire shell consists of six whorls; dorsal side finely ribbed, ventral side smoother, only with growth lines; umbilicus ca. one third of shell width; shows all whorls; periumbilical keel absent; aperture oblique to shell axis, oval, without incision at the position of keel; peristome white, expanded and slightly thickened, but not reflexed (only in direction of umbilicus); parietal callus practically absent, only with some additional translucent calcareous layer.

Measurements (in mm): D = 23.1, H = 9.1 (holotype).

Differential diagnosis. *Laeocathaica minwui* sp. nov. has been confused with *L. christinae* in museum collections, probably due to the lack of examination of the types of *L. christinae*. However, *L. christinae* has a flatter dorsal side, a more upper-situated peripheral keel, a darker brown (instead of latte) colour, a more uniformly white ventral side with a brown spiral band inside the umbilicus, and brownish spots. In contrast, in the new species the ventral side is characterised by a marmorated (marbled-like) pattern resulted by the fusing of whitish and pale brown spiral bands. *Laeocathaica filippina* has a notched aperture at the position of the peripheral keel, a more brownish colour, and a less marmorated ventral side. See also Table 3.



Figure 21. *Laeocathaica minwui* sp. nov. (holotype, SMF 95019). Scale bar: 10 mm. Photographs: B. Páll-Gergely.

Table 3. Differences between *L. carinifera*, *L. christinae*, *L. filippina*, and *L. minwui* sp. nov.

Species	Dorsal surface	Keel on body whorl	Aperture (palatal part)	Colour of dorsal side	Ventral side
<i>L. carinifera</i>	domed	acute, in the middle of body whorl	rounded	lighter and darker brownish patches alternate rather abruptly resulting in a mosaic-like structure	umbilicus narrow, colour pale, or light and darker stripes alternate
<i>L. christinae</i>	nearly flat/ slightly domed	blunt to acute, upper part of body whorl	rounded	same as in <i>carinifera</i> , just brown colour darker and there is usually a brown and a white spiral band	umbilicus wider, mostly white with slender darker radial stripes and dark dots
<i>L. filippina</i>	domed	acute, upper part of body whorl	notched	paler than <i>carinifera</i> and <i>christinae</i> , light and brown patches alternate smoothly	umbilicus wider, similar to <i>minwui</i> sp. nov., but paler and less nicely marmorated
<i>L. minwui</i> sp. nov.	domed	acute, upper part of body whorl	rounded	mostly cream/latte-coloured, lighter and darker patches alternate smoothly	umbilicus wider, latte and white spiral bands form a marmorated pattern

Etymology. This new species is dedicated to and named after Dr. Min Wu, the leading expert of Chinese Camaenidae.

Distribution. This new species is only known from historical samples from the Yangtze valley. Other samples labelled as being collected from Sichuan are not precise enough to understand their geographic origin.

Laeocathaica odophora Möllendorff, 1899

Figure 22

Laeocathaica odophora Möllendorff, 1899: 97–98, pl. 6, fig. 6.

Laeocathaica odophora. – Yen 1939: 149, pl. 15, fig. 39.

Laeocathaica (Laeocathaica) odophora. – Zilch 1968: 174.

Laeocathaica odophora. – Chen and Zhang 2004: 328, fig. 318.

Type material. S-Gansu, Dshie-dshou, coll. Möllendorff ex coll. Potanin 254, SMF 8954 (holotype = juvenile shell, Fig. 22A).

New material. CHINA • 1 photographed shell; Gansu, Longnan Shi, Wenxian, Jianshan Xiang, 1800 m west of Jianshan towards Diaohuya, right side of road no. 212 (locality code: 2016/70b); 33°2.922'N, 104°50.840'E; 29 May 2016; A. Hunyadi leg.; HA (Fig. 22B) • 5 adult + 2 juvenile shells; Gansu, Longnan Shi, Wenxian, Jianshan Xiang, 1200 m south of Hekou Cun, eastern bank of Bailong He (locality code: 2016/68); 33°01.703'N, 104°53.602'E; 810 m a.s.l.; 29 May 2016; A. Hunyadi leg.; HA • 1 shell; Gansu, Longnan Shi, Wenxian, Jianshan Xiang, western edge of Hekou Cun towards Caojiaba, right side of road no. 212 (locality code: 2016/69); 33°2.343'N,



Figure 22. *Laeocathaica odophora* Möllendorff, 1899 **A** holotype (SMF 8954) **B** 2016/70b. Scale bar: 10 mm. All photographs: B. Páll-Gergely.

104°53.045'E; 29 May 2016; A. Hunyadi leg.; HA • 1 juvenile shell; Gansu, Longnan Shi, Wenxian, Chengguan Zhen, next to a museum (locality code: 2016/64); 32°56.471'N, 104°40.379'E; 960–970 m a.s.l.; 28 May 2016; A. Hunyadi leg.; HA.

Description. Shell sinistral, depressed, strongly keeled, dorsal side domed, ventral side conical; shell colour basically brownish, greyish, latte-coloured, with whitish stripes; as a result dorsal surface mosaic-like, ventral side striped; keel always white, there is always a brownish belt just below the keel, periumbilical keel always white; entire shell consists of 9–9.5 whorls; protoconch consists of 1.5 whorls, brownish, seemingly smooth, extremely finely granulose, rather matte; white keels of every whorl slightly elevated from dorsal surface, but dorsal surface almost continuous, suture practically absent; dorsal side with fine, irregular wrinkles (most wrinkles stand alone, but some of them unite to each other); ventral surface with less prominent wrinkles; umbilicus rather narrow, regular funnel-shaped, shows all whorls; periumbilical keel blunt; aperture semilunar, peristome very slightly expanded, but not reflexed or thickened; palatal swelling whitish, with two prominent denticles, situated in some distance from peristome; parietal wall with some whitish thickening in adult shells. Juveniles reverse conical in shape; several apertural barriers are built during lifetime; palatal swelling of juveniles appears as a continuous ridge, although the two denticles recognisable.

Distribution. Known from a few localities in southern Gansu Province (Fig. 17).

Remarks. The single juvenile shell of sample 2016/64 has a narrower, blunter umbilical keel than the holotype, and it is possible that it belongs to another species. However, the juvenile shell of sample 2016/68 is identical with the holotype.

Laeocathaica pewzowi (Möllendorff, 1899)

Figure 23C, D

Laeocathaica pewzowi Möllendorff, 1899: 98, pl. 6, figs 4, 4a.

Laeocathaica pewzowi. – Yen 1939: 149, pl. 15, fig. 40.

Laeocathaica (*Laeocathaica*) *pewzowi*. – Zilch 1968: 174.

Laeocathaica pewzowi. – Chen and Zhang 2004: 329, fig. 320.

Laeocathaica pewzowi. – Schileyko 2004: 1686, fig. 2174a.

Type material. S-Gansu, Wen-hsien, coll. Möllendorff ex coll. Potanin 248, 661, 793, SMF 9084 (lectotype, Fig. 23C, D) • Same data, SMF 9084/3 (paralectotypes) • Same data, coll. C. Boettger, SMF 9084/1.

Museum material. Nung-dan b. Wen-Hsien, coll. Möllendorff, SMF 24268/1.

Laeocathaica phaeomphala Möllendorff, 1899

Figure 18C

Laeocathaica phaeomphala Möllendorff, 1899: 96, pl. 6, fig. 3.

Laeocathaica phaeomphala. – Yen 1939: 149, pl. 15, fig. 37.



Figure 23. *Laeocathaica* species **A, B** *Laeocathaica potanini* (lectotype, SMF 9082) **C, D** *Laeocathaica pewzowi* (lectotype, SMF 9084). Scale bars: 10 mm. All photographs: B. Páll-Gergely.

Laeocathaica (Laeocathaica) phaeomphala. – Zilch 1968: 174.

Laeocathaica phaeomphala. – Chen and Zhang 2004: 325, fig. 314.

Type material. S-Gansu, Wenhsien, coll. Möllendorff ex coll. Potanin 51b, 72, 741, SMF 9089 (lectotype, Fig. 18C) • Same data, SMF 9090/3+1 (paralectotypes, one of them from coll. C. Boettger).

New material. CHINA • 6 shells; Gansu, Longnan Shi, Wenxian, Chengguan Zhen, next to a museum (locality code: 2016/64); 32°56.471'N, 104°40.379'E; 960–970 m a.s.l.; 28 May 2016; A. Hunyadi leg.; HA.

***Laeocathaica polytyla* Möllendorff, 1899**

Figure 20A–C

Laeocathaica polytyla Möllendorff, 1899: 98–99, pl. 6, fig. 7.

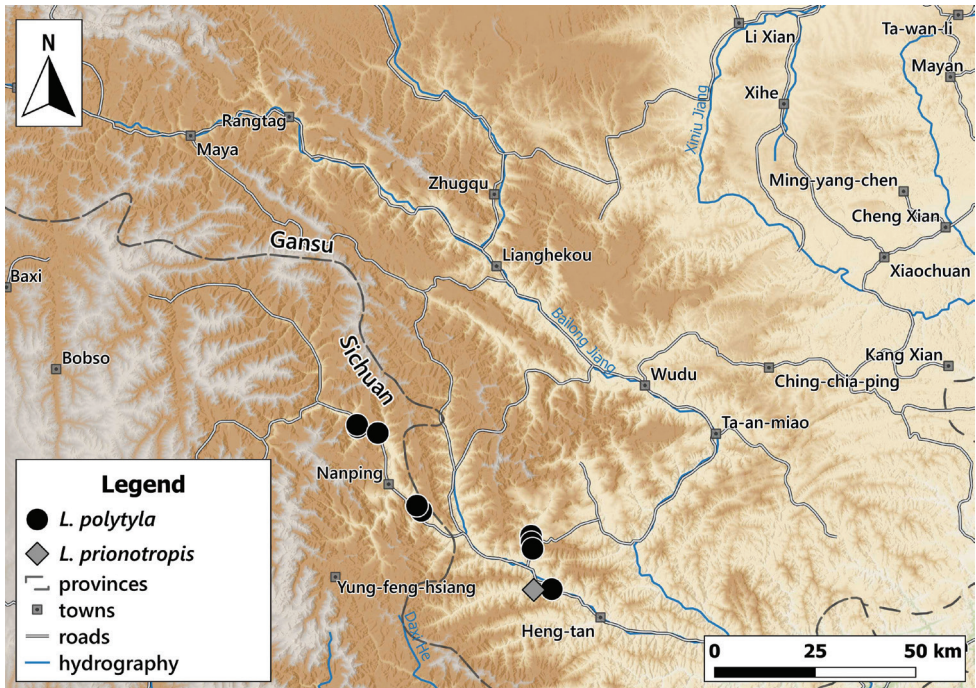


Figure 24. Distribution of *Laeocathaica* species in China (A in Fig. 2).

Laeocathaica polytyla. – Yen 1939: 149, pl. 15, fig. 41.

Laeocathaica (Laeocathaica) polytyla. – Zilch 1968: 174.

Laeocathaica polytyla. – Chen & Zhang, 2004: 331, fig. 322.

Laeocathaica polytyla. – Schileyko 2004: 1686, fig. 2174b–d.

Type material. Nan-Ping, Sung-pan, coll. Möllendorff ex coll. Potanin 725b, 744, SMF 9098 (lectotype, Fig. 20A) • Same data, SMF 9099/6 (paralectotypes) • China, S-Gansu, leg. S. Hisano, 22.06.2004, ex coll. S. Hisano, 2011, SMF 336710/1.

New material. CHINA • 4 shells; Gansu, Longnan Shi, Wenxian, Buziba Xiang, northern edge of Taojiaba Cun, 200 m towards Buziba (locality code: 2016/78); 33°02.706'N, 104°37.157'E; 1200 m a.s.l.; 31 May 2016; A. Hunyadi leg.; HA (Fig. 20B) • 11 shells; Gansu, Longnan Shi, Wenxian, Chengguan Zhen, cemetery hill above the city (locality code: 2016/65); 32°57.026'N, 104°40.527'E; 1090 m a.s.l.; 28 May 2016; A. Hunyadi leg.; HA (Fig. 20C) • 2 shells; Gansu, Longnan Shi, Wenxian, Buziba Xiang, 1 km south of Taojiaba Cun towards Dongyukou Cun (locality code: 2016/79); 33°01.865'N, 104°37.329'E; 1150 m a.s.l.; 31 May 2016; A. Hunyadi leg.; HA • 4 shells; Sichuan, Aba, Jiuzhaigou Xian, Baihe Xiang, Taiping Cun, eastern bank of Baishui He (locality code: 2016/73); 33°18.366'N, 104°09.413'E; 30 May 2016; A. Hunyadi leg.; HA • 7 shells; Sichuan, Aba, Jiuzhaigou Xian, Guoyuan Xiang, Guoyuaner Cun, environment of the bridge (locality code: 2016/76); 33°06.922'N, 104°19.617'E; 1200 m a.s.l.; 30 May 2016; A. Hunyadi leg.; HA • 2 shells; Sichuan,

Aba, Jiuzhaigou Xian, Anle Xiang, ca. 1.5 km east of Zhongtianshan Cun towards Jiuzhaigou Shi (locality code: 2016/74); 33°17.279'N, 104°12.702'E; 1445 m a.s.l.; 30 May 2016; A. Hunyadi leg.; HA • 8 shells; Sichuan, Aba, Jiuzhaigou Xian, Baihe Xiang, southern edge of Taiping Cun, rock wall facing north (locality code: 2016/72); 33°18.026'N, 104°09.500'E; 30 May 2016; A. Hunyadi leg.; HA • 3 shells; Gansu, Longnan Shi, Wenxian, Buziba Xiang, southern edge of Buziba Cun, western bank of the river (locality code: 2016/77); 33°03.592'N, 104°37.094'E; 1215 m a.s.l.; 30 May 2016; A. Hunyadi leg.; HA • 2 shells; Sichuan, Jiuzhaigouxian, Guoyuanxiang, 7.7 km from provincial border (locality code: 2011.04.25A); 33°07.616'N, 104°18.927'E; 1258 m a.s.l.; 25 April 2011; Y. Nakahara, K. Okubo & K. Otani leg.; PGB.

Distribution. Known from several precise localities in southern Gansu Province (Fig. 22).

Laeocathaica potanini Möllendorff, 1899

Figure 23A, B

Laeocathaica potanini Möllendorff, 1899: 96–97, pl. 6, fig. 5.

Laeocathaica potanini. – Yen 1939: 149, pl. 15, fig. 38.

Laeocathaica (Laeocathaica) potanini. – Zilch 1968: 174.

Laeocathaica potanini. – Chen and Zhang 2004: 326, fig. 316.

Type material. Gansu: Wenhsien, coll. Möllendorff ex coll. Potanin 251, 587, 734, SMF 9082 (lectotype, Fig. 23A, B) • Same data, SMF 9083/3+1 (paralectotypes, one of them from coll. C. Boettger) • S-Gansu, Hungadan b. Wen-hsien, coll. Möllendorff ex coll. Berezowski, SMF 8960/1.

New material. CHINA • 6 shells; Gansu, Longnan Shi, Wenxian, Chengguan Zhen, cemetery hill above the city (locality code: 2016/65); 32°57.026'N, 104°40.527'E; 1090 m a.s.l.; 28 May 2016; A. Hunyadi leg.; HA • 5 shells; Gansu, Longnan Shi, eastern edge of Wenxian, northern bank of the river (locality code: 2016/66); 32°56.459'N, 104°41.372'E; 28 May 2016; A. Hunyadi leg.; HA.

Remarks. The examined shells are identical to the types.

Laeocathaica prionotropis Möllendorff, 1899

Figures 25, 26

Laeocathaica prionotropis Möllendorff, 1899: 94–95, pl. 6, figs 1, 1a.

Laeocathaica prionotropis subsp. *albocincta* Möllendorff, 1899: 95. **new synonym**

Laeocathaica prionotropis prionotropis. – Yen 1939: 149, pl. 15, fig. 34.

Laeocathaica prionotropis albocincta. – Yen 1939: 149, pl. 15, fig. 35.

Laeocathaica (Laeocathaica) prionotropis prionotropis. – Zilch 1968: 175.

Laeocathaica (Laeocathaica) prionotropis albocincta. – Zilch 1968: 175.

Laeocathaica prionotropis. – Chen and Zhang 2004: 320, figs 309–310.



Figure 25. *Laeocathaica prionotropis* **A** lectotype (SMF 9078) **B** lectotype of *Laeocathaica prionotropis albocincta* Möllendorff, 1899 (SMF 9080). Scale bar: 10 mm. All photographs: B. Páll-Gergely.

Type material. Zw. Yü-lin-guan u. Wen-hsien, coll. Möllendorff ex coll. Potanin 520a, 908a, SMF 9078 (lectotype of *L. prionotropis*, Fig. 25A) • Same data, SMF 9079/3 (paralectotypes) • W. Sy-tshuan, Tung-ho, coll. Möllendorff ex coll. Potanin 312a, SMF 9080 (lectotype of *L. prionotropis albocincta*, Fig. 25B) • Same data, SMF 9081 (paralectotype of *L. prionotropis albocincta*).

New material. CHINA • 1 shell; Gansu, Longnan Shi, Wenxian, Bikou Zhen, above the hydroelectric power plant, northern side of Bailong He (locality code: 2016/63); 32°45.966'N, 105°13.005'E; 28 May 2016; A. Hunyadi leg.; HA (Fig. 26D, E) • 5 shells; Gansu, Longnan Shi, Wenxian, Chengguan Zhen, next to a museum (locality code: 2016/64); 32°56.471'N, 104°40.379'E; 960–970 m a.s.l.; 28 May 2016; A. Hunyadi leg.; HA (Fig. 26A–C).

Distribution. Known from two sites in Southern Gansu Province (Fig. 24).

Remarks. *Laeocathaica prionotropis* subsp. *albocincta* agrees in size and shell shape with the nominotypical form, and therefore it is here synonymised with *Laeocathaica prionotropis*.

Discussion

Although we list and publish photographs of all *Laeocathaica* species in this work, the taxonomy of this group is still far from being solved. Following previous authors, we classify only sinistral species in *Laeocathaica*. However, it is very probable that the coiling direction has changed multiple times during the evolution of Bradybaeninae inhabiting the

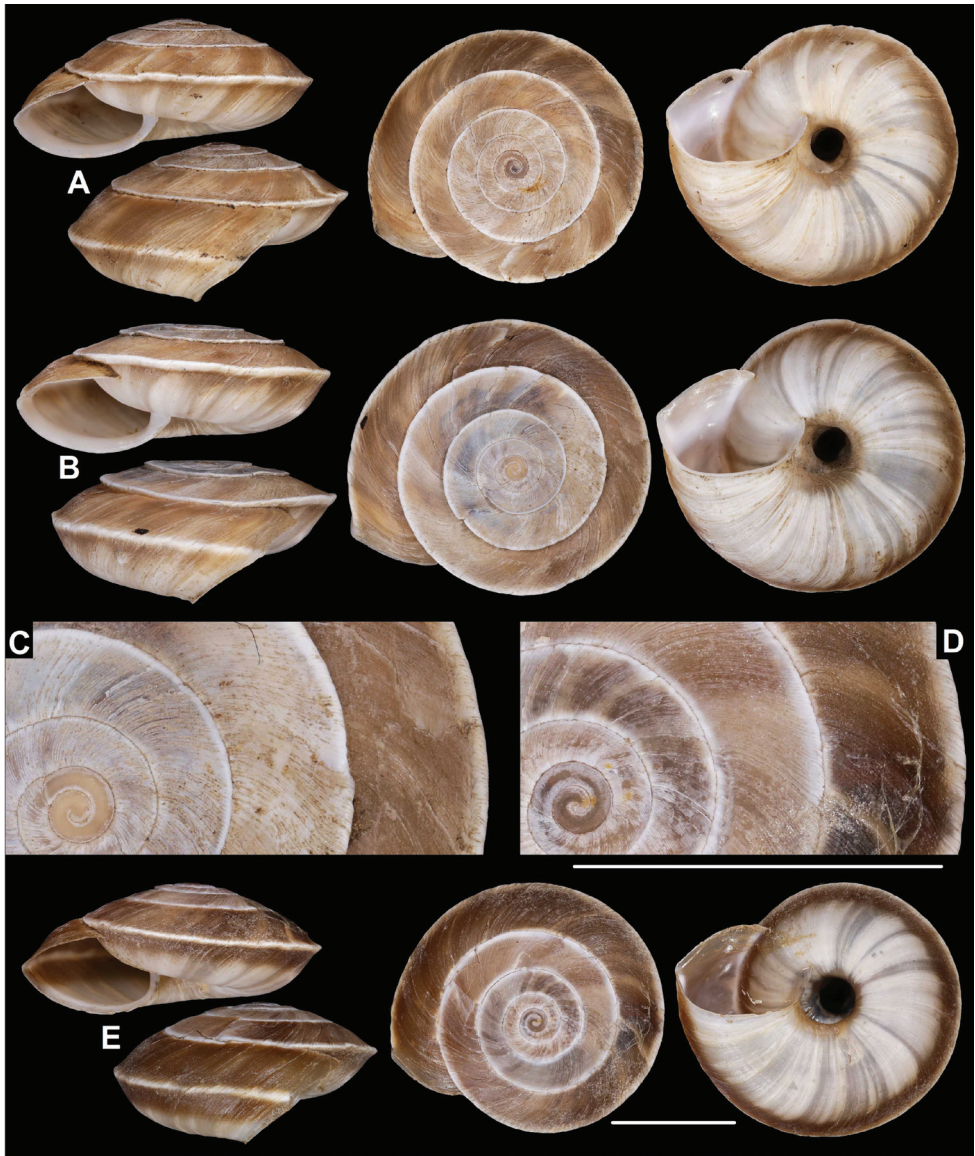


Figure 26. *Laeocathaica prionotropis* **A** 2016/64, specimen1 **B, C** 2016/64, specimen2 **D, E** 2016/63. Scale bars: 10 mm. All photographs: B. Páll-Gergely.

arid regions of central China. Furthermore, sinistral species such as *Bradybaena micromphala* (Möllendorff, 1899) and *B. eris* (Möllendorff, 1899) also inhabit southern Gansu, and are similar to *Laeocathaica* species in most traits except for the narrow umbilicus. Future investigations will probably reveal that the latter two species (and maybe some other similar ones from the region) are relatives of *Laeocathaica* rather than *Bradybaena*.

One of the main outcomes of the present paper is the clarification of some names that have been incorrectly used in the literature and in museum collections because the

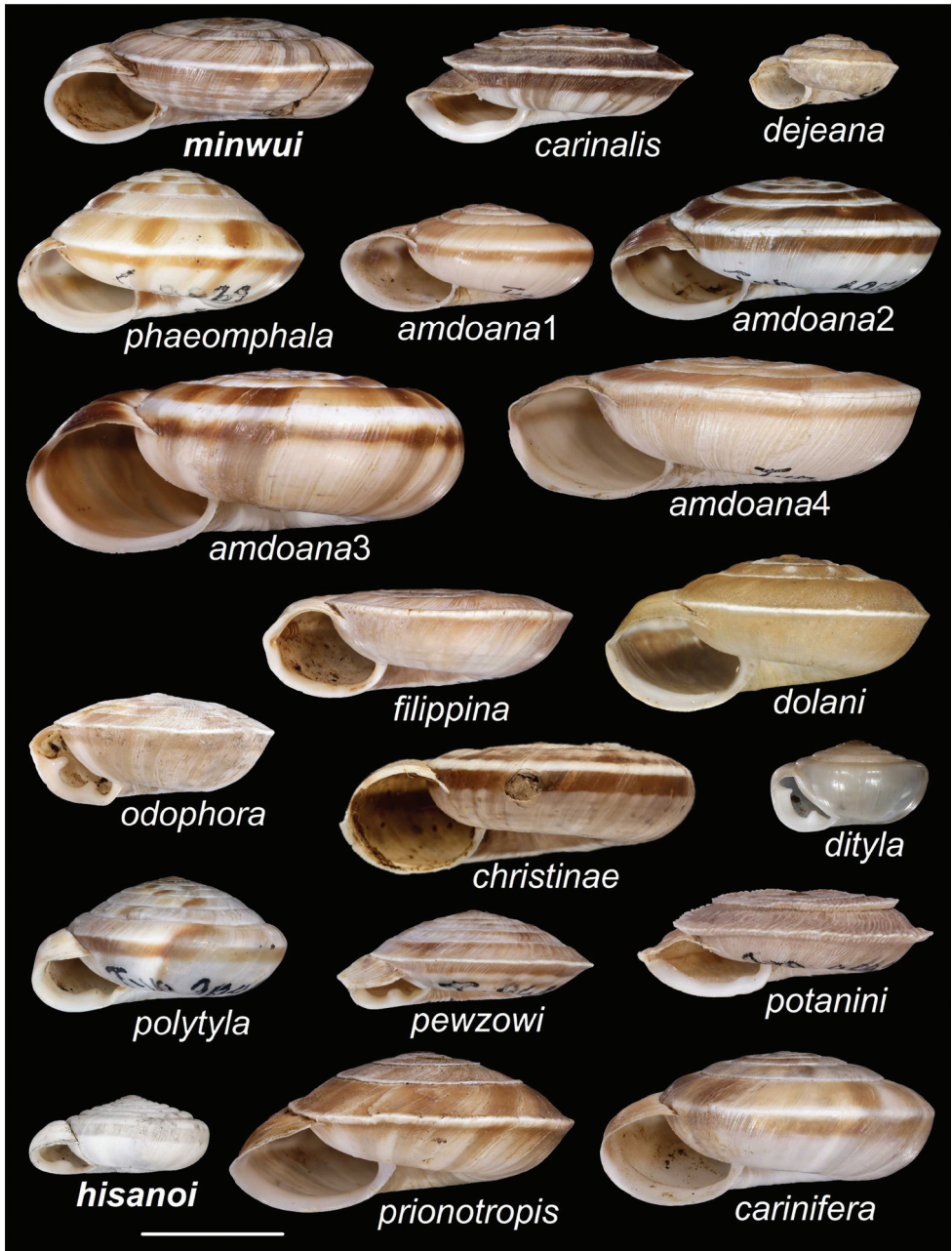


Figure 27. Synoptic view of *Laeocathaica* species. The variability of *L. amdoana* is shown on four examples. Scale bar: 10 mm. Species in bold are described here as new

types were not examined. One such case is *Helix christinae* var. *carinifera* H. Adams, 1870, which resulted in being a senior synonym of *Laeocathaica subsimilis* (Deshayes, 1874) after examination of both type species. The other case is that of *L. minwui* sp.

Table 4. Co-occurrence patterns of *Laeocathaica* species with locality codes.

	<i>L. amdoana</i>	<i>L. carinalis</i>	<i>L. carinifera</i>	<i>L. odophora</i>	<i>L. phaeomphala</i>
<i>L. carinalis</i>	2016/64, 2016/79, 2016/82, 2016/83				
<i>L. carinifera</i>	2016/67, 2016/68, 2016/70a	2016/70b			
<i>L. dityla</i>	2016/88, 2016/95		2016/86		
<i>L. odophora</i>	2016/64, 2016/68, 2016/69	2016/64, 2016/70b	2016/68, 2016/70b		
<i>L. phaeomphala</i>	2016/64	2016/64		2016/64	
<i>L. polytyla</i>	2016/65, 2016/72, 2016/73, 2016/74, 2016/76, 2016/77, 2016/78, 2016/79	2016/79	2016/78		
<i>L. potanini</i>	2016/65, 2016/66				
<i>L. prionotropis</i>	2016/64	2016/64	2016/63	2016/64	2016/64

nov., which was called *L. christinae* (H. Adams, 1870) in museum collections, because the types of the “real” *L. christinae* had not been examined.

The other important outcome of the present study is the recognition of continuous dorsal surface variability from flat to domed, the strongly keeled to rounded body whorl, the colouration, and shell size (D: 19–32 mm) across the taxa *Laeocathaica amdoana*, *L. distinguenda*, *L. tropidorhaphae*, and *L. dangchangensis*.

Table 4 summarises the co-occurrence patterns between *Laeocathaica* species, showing which species pairs are reproductively isolated, true biological species, and Fig. 27 shows all *Laeocathaica* species.

Acknowledgements

We are grateful to Zhe-Yu Chen for his help in locating historical Chinese localities on the map, to Sigrid Hof and Ronald Janssen (SMF), Philippe Bouchet and Virginie Héros (MNHN), and Jonathan Ablett (NHM) for granting access to their museum collections, and to Ellen Strong (USNM) for arranging photographs of *Laeocathaica filippina*. Philippe Bouchet and Gary Rosenberg helped in solving nomenclatural problems. Min Wu, Zhe-Yu Chen, Klaus Groh, and an anonymous reviewer corrected the manuscript.

This study was supported by the Bolyai Research Scholarship of the Hungarian Academy of Sciences, the Hungarian Research Fund (OTKA FK 135262) and grants from the SYNTHESYS Project (GB-TAF-2523) to B.P.-G. We are indebted to The Biodiversity Heritage Library for the multitude of rare literature made available to us (www.biodiversitylibrary.org).

References

- Adams H (1870) Descriptions of ten new species of land and freshwater shells collected by Robert Swinhoe, Esq., in China and Formosa. Proceedings of the Zoological Society of London 1870: 377–379. [pl. 27] <https://www.biodiversitylibrary.org/page/28555227>

- Ancey CF (1882) Coquilles de Chine Centrale nouvelles ou peu connues. *Le Naturaliste*. 4: 44–45. <https://www.biodiversitylibrary.org/page/33927196>
- Beck H (1837) *Index molluscorum praesentis aevi musei principis augustissimi Christiani Frederici. Hafniae* [Copenhagen], 124 pp. <https://doi.org/10.5962/bhl.title.77331>
- Chen D-N, Zhang G-Q (2004) *Fauna Sinica Invertebrata Vol. 37 (Mollusca: Gastropoda: Stylommatophora: Bradybaenidae)*. Science Press, Beijing, 482 pp. [pls. 1–8]
- Deshayes G-P (1874) Description de quelques espèces de mollusques nouveaux, ou peu connus envoyés de la Chine par M. l'Abbé A. David. *Bulletin des Nouvelles Archives du Muséum* 9: 1–14. <https://doi.org/10.5962/bhl.title.13038>
- Gredler VM (1884) Zur Conchylien-Fauna von China. VI. Stück. *Archiv für Naturgeschichte*. 50(2): 257–280. <https://www.biodiversitylibrary.org/page/6459964>
- Heude RPM (1882) Mémoires concernant l'histoire naturelle de l'empire chinois par des pères de la Compagnie de Jésus. Notes sur les Mollusques terrestres de la vallée du Fleuve Bleu. *Mission Catholique, Chang-Hai*, 2: 1–88. <https://doi.org/10.5962/bhl.title.50365>
- Johnson RJ (1973) Heude's Molluscan Types: or, Asian land and fresh water mollusks, mostly from the People's Republic of China, described by P. M. Heude. Cambridge, Massachusetts (Special Occasional Publication, Department of Mollusks, Museum of Comparative Zoology, Harvard University), 111 pp. <https://doi.org/10.5962/bhl.title.141074>
- Kerney MP, Cameron RAD (1979) *A Field Guide to the Land Snails of Britain and North-west Europe*. Collins, London, 288 pp.
- Möllendorff OF von (1884) Materialien zur Fauna von China. *Jahrbücher der Deutschen Malakozoologischen Gesellschaft* 11: 162–181; 307–390. <https://biodiversitylibrary.org/page/16289265>
- Möllendorff OF von (1899) Binnen-Mollusken aus Westchina und Central-Asien I. *Annuaire du Musée Zoologique de l'Académie Impériale des Sciences de Saint Pétersbourg* 4: 46–142. <https://doi.org/10.5962/bhl.title.13125>
- Pfeiffer L (1850) Einige Bemerkungen über Deshayes's Bearbeitung des Ferussacschen Werkes. *Zeitschrift für Malakozoologie* 7: 145–160. <https://biodiversitylibrary.org/page/16300445>
- Philippi RA (1845–1847) *Abbildungen und Beschreibungen neuer oder wenig gekannter Conchylien. Zweiter Band*. 2. Fischer, Cassel, 231 pp. <https://www.biodiversitylibrary.org/page/11073321>
- Pilsbry HA (1890–1891) *Manual of conchology, structural and systematic, with illustrations of the species. Ser. 2, Pulmonata. Vol. 6: Helicidae, vol. 4. Conchological Section, Academy of Natural Sciences, Philadelphia*, 324 pp. [pls. 1–69] <https://biodiversitylibrary.org/page/23626788>
- Pilsbry HA (1934) Zoological results of the Dolan West China expedition of 1931. Part II. Mollusks. *Proceedings of the Academy of Natural Sciences of Philadelphia* 86: 5–28. [6 pls]
- Richardson L (1983) Bradybaenidae: Catalog of species. *Tryonia* 9: 1–253. <https://www.biodiversitylibrary.org/page/57458375>
- Schileyko AA (2004) *Treatise on Recent terrestrial pulmonate molluscs Part 12. Bradybaenidae, Monadeniidae, Xanthonychidae, Epiphragmophoridae, Helminthoglyptidae, Elonidae, Humboldtianidae, Sphincterochilidae, Cochlicellidae*. *Ruthenica, Supplement 2*: 1627–1763.

- Wu M (2004) Preliminary phylogenetic study of Bradybaenidae (Gastropoda: Stylomatophora: Helicoidea). *Malacologica* 46: 79–125. <https://www.biodiversitylibrary.org/page/28112649>
- Yen T-C (1939) Die chinesischen Land- und Süßwasser-Gastropoden des Natur-Museums Senckenberg. *Abhandlungen der Senckenbergischen Naturforschenden Gesellschaft, Frankfurt am Main*, 233 pp. [pls. 1–16]
- Zilch A (1968) Die Typen und Typoide des Natur-Museums Senckenberg, 41: Mollusca, Bradybaenidae, Bradybaeninae. *Archiv für Molluskenkunde* 98(3/4): 155–207.

Island hoppers: Integrative taxonomic revision of *Hogna* wolf spiders (Araneae, Lycosidae) endemic to the Madeira islands with description of a new species

Luís C. Crespo^{1,2}, Isamberto Silva³, Alba Enguídanos¹,
Pedro Cardoso², Miquel Arnedo¹

1 Department of Evolutionary Biology, Ecology and Environmental Sciences (Arthropods), Biodiversity Research Institute (IRBio), Universitat de Barcelona, Av. Diagonal 643, 08028 Barcelona, Spain **2** Laboratory for Integrative Biodiversity Research (LIBRe), Finnish Museum of Natural History (LUOMUS), University of Helsinki, P.O. Box 17, 00014 Helsinki, Finland **3** Instituto das Florestas e Conservação da Natureza IP-RAM, Jardim Botânico da Madeira, Caminho do Meio, Bom Sucesso, 9064-512, Funchal, Portugal

Corresponding author: Luís C. Crespo (luiscarloscrespo@gmail.com)

Academic editor: Ingi Agnarsson | Received 28 April 2021 | Accepted 13 December 2021 | Published 16 February 2022

<http://zoobank.org/89728BCE-242A-4936-9095-E9B544F8B9F7>

Citation: Crespo LC, Silva I, Enguídanos A, Cardoso P, Arnedo M (2022) Island hoppers: Integrative taxonomic revision of *Hogna* wolf spiders (Araneae, Lycosidae) endemic to the Madeira islands with description of a new species. ZooKeys 1086: 84–135. <https://doi.org/10.3897/zookeys.1086.68015>

Abstract

Because of their ability for aerial dispersal using silk and preference for open habitats, many wolf spiders are formidable colonisers. Pioneering arachnologists were already aware of the large and colourful wolf spiders in the Madeira archipelago, currently included in the genus *Hogna* Simon, 1885. The origins were investigated and species boundaries of Madeiran *Hogna* examined by integrating target-gene and morphological information. A multi-locus phylogenetic analysis of a thorough sampling across wolf-spider diversity suggested a single origin of Madeiran endemics, albeit with low support. Divergence time estimation traced back their origin to the late Miocene, a time of major global cooling that drove the expansion of grasslands and the associated fauna. Morphological examination of types and newly collected material revealed a new species, hereby described as *H. isamberto* Crespo, **sp. nov.** Additionally, *H. blackwalli* is revalidated and three new synonymies are proposed, namely *H. biscoitoi* Wunderlich, 1992, junior synonym of *H. insularum* Kulczynski, 1899, *H. schmitzi* Wunderlich, 1992, junior synonym of *H. maderiana* (Walckenaer, 1837), and *Arctosa maderana* Roewer, 1960 junior synonym of *H. ferox* (Lucas, 1838). Species delimitation analyses of mitochondrial and nuclear markers provided additional support for morphological delineations. The species pair *H. insularum* and *H. maderiana*, however, constituted an exception: the lack of exclusive haplotypes in the examined markers, along with the discovery of intermediate forms,

pointed to hybridisation between these two species as reported in other congeneric species on islands. Finally, the conservation status of the species is discussed and candidates for immediate conservation efforts are identified.

Keywords

Endangered species, island radiation, Lycosinae, Macaronesia, morphological polymorphism, species delimitation

Introduction

Most wolf spiders (Lycosidae) are ground-dwelling cursorial hunters, with only a small portion of its species displaying sheet-web building behaviour. They are one of the most abundant and ubiquitous spiders in open terrestrial habitats, such as grass- and shrublands. It has been suggested that lycosids underwent major global diversification concomitantly with grassland expansion during the Miocene (Jocqué and Alderweireldt 2005; Piacentini and Ramírez 2019). Some groups of wolf spiders frequently use ballooning, a form of passive airborne transport mediated by silk (Bell et al. 2005). The ability for long-distance dispersal combined with their preference for open and disturbed habitats for many species, makes them formidable colonisers of oceanic islands, including the world's most remote island chain, the Hawaiian Archipelago (Suman 1964). The genus *Hogna* Sundevall, 1833 includes medium- to large-sized spiders said to have a worldwide distribution, although this fact is probably derived from a lack of any recent thorough systematic studies. Despite its size, the genus has managed to colonise and diversify on many oceanic islands, including the Galápagos (Baert et al. 2008) in the Pacific Ocean and Saint Helena, in the south Atlantic (Tongiorgi 1977). Similarly, the Madeira archipelago also harbours several endemic species of *Hogna*. Among spiders, *Hogna* (7 species) is second only to the genus *Dysdera* Latreille, 1804 (11 species) in numbers of endemic species present in the Madeira archipelago (Crespo et al. 2020), and some of its species rank among the most emblematic organisms of the islands.

Madeira is situated in the North Atlantic Ocean, approximately 500 km north of the Canary Islands, 900 km west from Morocco, and 1000 km southwest from the Iberian Peninsula (Fig. 1). It is composed of a small number of islands and islets aligned in a southwestern direction as a result of their sequential formation from a volcanic hot-spot on the oceanic crust. Among the larger islands, Porto Santo is a small and relatively flat island (maximum altitude 516 m at Pico do Facho), surrounded by several islets in a later stage of island ontogeny, its subaerial stage dating back to 14 million years ago (mya). The emergences of the two other larger islands, Madeira and Deserta Grande, date back to 7 and 5 mya, respectively (Geldmacher and Hoernle 2000; Schwarz et al. 2005; Ramalho et al. 2015). Although both islands are in an intermediate stage of the island ontogeny, they show substantially different geomorphology. Madeira is larger with a rugged, steep orography, especially in its northern side, reaching a maximum



Figure 1. Map of the Macaronesia and the Madeira archipelago (adapted from Borges et al. 2008, with authors' permission).

altitude of 1861m at Pico Ruivo. This stands at a sharp contrast with the aspect of the Deserta Grande, which together with the islets of Ilhéu Chão and Bugio constitute the Desertas islands, with a maximum altitude of only 479 m (Rocha do Barbusano), yet displaying a dramatic topographic relief, also observed in Bugio. The Madeira islands exhibit a wide variety of habitats, ranging from the humid subtropical laurel forest of Madeira to the *Erica* shrublands, high-elevation and coastal grasslands, or rocky scarps across all islands and islets. Madeiran *Hogna* spiders occur throughout all these habitats, mostly on montane or coastal grasslands and rocky scarps, as is common for the family, but also in closed-canopy laurel forest.

Due to their large size, restricted distribution, and striking appearance of some species, either in size or distinctive leg coloration, local *Hogna* spiders were known to naturalists since the early 19th century. The largest and most colourful species were the first to be described, namely *H. maderiana* (Walckenaer, 1837) and *H. ingens* (Blackwall, 1857). By the end of the 19th century, two smaller species, *H. heeri* (Thorell, 1875) and *H. insularum* (Kulczynski, 1899), were added to the checklist. The report of new endemic *Hogna* species had to wait for almost a century, until the description of *H. biscoitoi* Wunderlich, 1992, *H. schmitzi* Wunderlich, 1992, and *H. nonannulata* Wunderlich, 1995.

Although no other taxonomic work on Madeiran *Hogna* has been published for more than 25 years, a number of taxonomic problems remained to be tackled, including nomenclatural issues and the interpretation of intraspecific variability in the

context of intermediate forms (Wunderlich 1992, 1995). In addition, recent studies suggest that species delimitation in wolf spiders may be hampered by either the recent origin of some species (Ivanov et al. 2021) or introgression events among close relatives (De Busschere et al. 2015). On the other hand, the genus *Hogna* is in much need of a thorough revision (Logunov 2020). Brady (2012) has provided a diagnosis based on coloration and eye arrangement, while stating that genitalic morphology, traditionally used by taxonomists to identify species, cannot be used to separate *Hogna* from other Lycosinae genera. Descriptions of the old species are usually vague, poorly illustrated and, in some cases, the type materials have been lost. As a result, the genus has traditionally served as a dumping ground for large lycosids of uncertain placement in the Lycosinae. The lack of a clear circumscription of the genus poses a burden in terms of identifying the putative source of colonisers of the Madeiran species.

Some of the Madeira *Hogna* species are of conservation concern. The Desertas giant wolf spider, *H. ingens*, is listed as “Critically Endangered” on the IUCN Red List of Threatened Species due to its narrow distribution range and the fact that the native vegetation of the small valley it inhabits has been mostly displaced by an invasive grass (Crespo et al. 2014b). Conservation efforts involving an ex-situ breeding program and management control of the grasses are underway (Cardoso et al. 2016).

In the present study, we integrate morphological and natural history information with molecular data to (1) test the monophyly of the Madeiran *Hogna* to resolve the number and timeline of colonisation events, (2) delimitate species boundaries and (3) conduct a taxonomic revision of these iconic endemic species.

Materials and methods

Field work

The material studied here was made available through collections from expeditions to Madeira, Porto Santo and the Desertas in springs of 2017 and 2018. Additional specimens were provided by occasional collecting by one of us (IS). Sampling was done in a wide variety of habitats, especially in open areas surrounding native vegetation patches, by lifting stones and retrieving *Hogna* specimens manually. Each specimen was placed into a separate cryovial containing 96% molecular grade ethanol and stored in a freezer at -20 °C until further study. Specimens for morphological analyses were later transferred to glass vials containing 75% ethanol. The sampling coordinates, when available, are shown in decimal degrees format.

Molecular lab procedures

We extracted DNA from one leg III using commercial kits (Speedtools Tissue DNA Extraction Kit, Biotools; or DNeasy Blood & Tissue Kit, Qiagen) following the tissue protocol suggested by the respective manufacturer. We amplified partial fragments

of the mitochondrial cytochrome c oxidase subunit I (COI), i.e., the animal DNA barcode (Hebert et al. 2003), the small ribosomal subunit 12S rRNA (12S), large ribosomal subunit 16S rRNA (16S), the tRNA Leu (L1), the NADH dehydrogenase subunit 1 (*nad1*), and the nuclear large ribosomal subunit 28S rRNA (28S), the internal transcribed spacer 2 (ITS-2) and the histone 3 (H3) genes. The primers used for amplification and sequencing, as well as the PCR conditions for the loci are listed in Suppl. material 1. The final PCR product was sequenced by Macrogen Inc. (Seoul, South Korea). Sequences were edited and managed in GENEIOUS Prime 2021.0.3 (<https://www.geneious.com>). Voucher sequence data of samples used in phylogenetic analysis is available and accession numbers are available in Suppl. material 2.

Phylogenetic analyses

To test the monophyly and phylogenetic structure of Madeiran *Hogna*, we combined our newly generated sequences with the data matrix of Piacentini and Ramírez (2019) designed to infer phylogenetic relationships for the family Lycosidae using a target gene approach. Additional sequences of *Hogna* species were retrieved from GenBank. We aligned sequence fragments of COI, 12S, 16S-L1, *nad1*, 28S, and H3 individually per gene using the GENEIOUS plugin of the alignment program MAFFT v. 1.4.0 (Katoh and Standley 2013), using the G-INS-I algorithm with default options. We concatenated all genes in a super matrix for subsequent phylogenetic analyses with the help of the program SEQUENCE MATRIX (Vaidya et al. 2011).

Parsimony analysis of the matrix was conducted with the program TNT v1.5 (Goloboff and Catalano 2016). We first recoded gaps as absence/presence characters using the simple coding method proposed by Simmons and Ochoterena (2000) with the help of the computer program SEQSTATE (Müller 2005). Search strategy for shortest trees combined sectorial searches, tree fusing, drift and ratchet. Tree searches were driven to hit independently 10 times the optimal scoring, followed by Tree Bisection and Reconnection (TBR) branch swapping, saving up to 1000 trees (Soto et al. 2017). We estimated support values by jackknifing frequencies derived from 1000 resampled matrices using 15 random addition sequences, retaining 20 trees per replication, followed by TBR, and TBR collapsing to calculate the consensus. We inferred the best maximum likelihood trees with IQ-TREE v. 2.1.2 (Minh et al. 2020). We used MODELFINDER to first select the best-fit partitioning scheme and corresponding evolutionary models (Kalyaanamoorthy et al. 2017), and then to infer the best tree and estimate clade support by means of 1000 replicates of ultrafast bootstrapping (Hoang et al. 2018). For Bayesian analyses, the best partition scheme and evolutionary model was first selected with help of the computer program PARTITIONFINDER v2.1.1 (Lanfear et al. 2017). We implemented Bayesian inference with MRBAYES v3.2.6 (Ronquist et al. 2012). The analysis was run for 10 million generations, sampling every 1000, with eight simultaneous Markov Chain Monte Carlo (MCMC) chains, 'heating temperature' of 0.15. Support values were calculated as posterior probabilities. We assessed convergence of the chains, correct mixing and

the number of burn-in generations with TRACER v. 1.7 (Rambaut et al. 2018). We ran model based analyses remotely at the CIPRES Science Gateway (Miller et al. 2010). The phylogenetic tree was edited for aesthetic purposes using FIGTREE (<http://tree.bio.ed.ac.uk/software/figtree/>).

Species delimitation

We used COI and ITS-2 sequences of a larger sample of Madeiran *Hogna* to explore species boundaries using single marker molecular based approaches. We investigated three alternative methods for species delineation using COI sequences, namely a distance based algorithmic method (Barcode identification number, BIN) (Ratnasingham and Hebert 2013) and two character-explicit methods, one requiring ultrametric trees (General Mixed Yule Coalescent model with single threshold, GMYC) (Fujisawa et al. 2016) and one that does not (multi-rate Poisson tree processes, mPTP) (Kapli et al. 2017). The BIN system was implemented on-line through the BOLD v4 platform (Ratnasingham and Hebert 2007). We inferred gene trees using maximum likelihood following the same strategy specified in the previous section. In addition, we inferred an ultrametric tree using the Bayesian framework for divergence time estimation implemented in BEAST v2.6.3. We assumed a coalescent tree prior (constant population size), which has been suggested to provide a more rigorous test of delimitation since the GMYC model assumes a single species as the null option (Monaghan et al. 2009). We defined the best partition scheme and evolutionary model inferred with PARTITIONFINDER, defined a lognormal relaxed clock and used an informative prior on the mean rate under the uncorrelated lognormal relaxed molecular clock (ucl.d.mean) parameter derived from the literature (mean = 0.0199, sd. dev.=0.05) (Bidegaray-Batista and Arnedo 2011). Convergence and mixing of MCMC chains were assessed with TRACER v.1.7 (Rambaut et al. 2018). Independent runs were combined with LOGCOMBINER (10% burn-in), and TREEANNOTATOR was used to summarise the information from the sampled trees. The m-PTP model was implemented using a Markov chain Monte Carlo (mcmc) approach, which allows estimates of support values on the delimitations, on the COI matrix. The analyses were conducted on the best IQ-TREE. We ran 5 chains of 100 million generations each, removing the first 2 million as burn-in, and discarding all branches with lengths smaller or equal to 0.0012708187. We used the R package ‘SPLITS’ (Ezard et al. 2017) to fit the GMYC model. Additionally, we estimated haplotype/allele networks for the COI and ITS-2 matrices independently using the statistical parsimony method (Templeton et al. 1992; Clement et al. 2000), with a confidence limit of 95% implemented in the R package ‘HAPLOTYPES’ (Aktas 2015). The ITS-2 sequences were aligned using the phylogeny-aware algorithm implemented in WEBPRANK (Löytynoja and Goldman 2010), specially recommended for aligning closely related sequences. We determined the number of alleles in the ITS-2 matrix considering the gaps as absence/presence data. Uncorrected pairwise genetic distances were calculated in MEGA X (Kumar et al. 2018).

Divergence time estimation

In the absence of fossil evidence and to avoid using circular reasoning by using information on the island age, we estimated divergence time using published information on substitution rates in lycosids (Piacentini and Ramírez 2019). We restricted our estimates to the more exhaustively sampled COI gene. Since the COI sequences include both intra and inter-specific relationships, we used a multispecies coalescent (MSC) approach as implemented in STARBEAST2 (Ogilvie et al. 2017), which allows combining coalescent and species (Yule) tree priors. Haplotypes were assigned to species according to the results of the molecular delimitations (see results), which resulted in the combination of *H. insularum* and *H. maderiana* haplotypes in one single lineage. We included sequences of *H. radiata* and *H. ferox* as putative outgroups but did not enforce the root. We assigned unlinked evolutionary models to each codon position, as suggested by PARTITIONFINDER and defined a relaxed lognormal clock with prior rates for the ucl.d.mean rate as follows: mean = 0.1716 substitutions/mya and Stdev = 0.006. Three independent runs of 50 million generations were performed, sampling every 5000 generations. We assessed convergence and mixing of each MCMC chain and combined them as described above.

Morphological analyses

The genus *Hogna*, as shown by Piacentini and Ramírez (2019), is paraphyletic with many of its former species transferred to other genera (Brady 2012). This forbids the elaboration of an identification diagnosis based on the systematic circumscription of the genus. The genus diagnosis created by Dondale and Redner (1990) includes species that were or should probably be placed in other genera for which the only way to identify a species as *Hogna* is to follow the diagnosis provided by Brady (2012). By doing so, we identify the presented species as *Hogna*.

Morphological observations were carried out using a stereomicroscope Leica MZ 16A equipped with a digital camera Leica DFC450. Individual raw photos were taken with the help of the software Leica Application Suite v4.4 and mounted with the software Helicon Focus (Helicon Soft, Ltd.). Further editions were done with Paint Shop Pro v21 (Corel Corporation). The epigyne was removed from female specimens with the aid of hypodermic needles and forceps. To clear the membranous tissues surrounding the spermathecae and copulatory ducts, we manually removed muscular and membranous tissue with forceps and a needle. This process accidentally led to the breakage of some copulatory ducts (usually delicate in the Lycosidae) and cracking of the median septum in some specimens (e.g., Figs 16E, 29B). SEM images of the male copulatory bulb were obtained with a Q-200 (FEI Co.) scanning electron microscope (SEM). For the SEM images, each male pedipalp was excised at the joint between tarsus and tibia. Samples were sonicated for roughly 30 seconds with ultrasonic bath Nahita ZCC001, air dried and carbon or gold sputter-coated. In most cases, the position of the embolus of the SEM samples appears slightly altered (usually directed more

anteriorly, closer to the tip of the terminal apophysis) relative to the normal resting position from specimens stored in ethanol. We measured all adult specimens with an ocular micrometre in the stereoscope. All measurements are in millimetres (mm). Description format followed Baert et al. (2008) and genitalic nomenclature followed Langlands and Framenau (2010).

Abbreviations

AW	anterior eye row width;	Mt	metatarsus;
Cl	clypeus;	MW	median eye row width;
Fe	femur;	Pa	Patella;
LMP	length between hind border of posterior eye and front border of median eye;	PW	posterior eye row width;
MOQ	median ocular quadrangle;	Ti	tibia;
		TiIL/D	Length to Diameter of Tibia I.

Male genitalia

AT	apical point;	TgA	tegular apophysis;
C	cymbium;	T	tegulum;
E	embolus;	TmA	terminal apophysis;
P	palea;	VS	ventral spur.
R	Ridge;		

Female genitalia

AP	anterior pocket;	S	spermatheca;
MS	median septum;	D	diverticulum.
PTP	posterior transverse part;		

Collections

NHM	Natural History Museum, London, UK;
CRBA	Centre de Recursos de Biodiversitat Animal, University of Barcelona, Barcelona, Spain;
FMNH	Finnish Museum of Natural History, Helsinki, Finland;
LCPC	Luís Crespo's personal collection;
MIZ	Museum and Institute of Zoology, Polish Academy of Sciences, Warsaw, Poland;
MMF	Museu Municipal do Funchal, Funchal, Portugal;
MMUE	Manchester Museum, University of Manchester, Manchester, UK;
MNHN	French National Museum of Natural History, Paris, France;
OUMNH	Oxford University Museum of Natural History, Oxford, UK;

SMF Senckenberg Research Institute, Frankfurt am Main, Germany;
NHRS Swedish Museum of Natural History, Stockholm, Sweden.

Conservation

AOO Area of occupancy; **EOO** Extent of Occurrence.

Results

Phylogenetic analyses

The concatenated matrix included 2641 characters, 657 bp of the COI, 302 bp H3, and 554 bp of the nad1, and 300 and 828 aligned position for the 12S and 28S, respectively, and 173 terminals including outgroups (see Piacentini and Ramírez 2019). Inferred relationships of the concatenated data matrix are summarised in Fig. 2 (See Suppl. material 3 for full trees for each inference methods). Parsimony analysis of the concatenated data matrix with gaps scored as absence/presence characters resulted in 1,000 trees (overflow) of 16,865 steps. Bayesian maximum clade credibility tree was obtained after removing 40% of the first generations as burn-in. Preferred partition schemes differed between IQTREE2 and PARTITIONFINDER in that the first joined COI and H3 second positions, while the second split by gene and codon position in all cases. Madeiran *Hogna* were recovered as two well-supported clades, one including the species *H. maderiana* and *H. insularum*, hereafter referred as the *maderiana* clade, and the other one including the remaining species, hereafter referred as the *ingens* clade. Model-based analyses inferred the two clades as sister groups, albeit with low support (Fig. 2). Conversely, parsimony inferred the *ingens* clade to be sister to the mainland species *H. radiata*. In all analyses, *H. isambertoii* sp. nov. was supported as sister to the remaining species in the *ingens* clade, while *H. nonannulata* and *H. blackwalli* were supported as sister in model-based analyses. All analyses agreed in supporting a surprisingly close relationship between *H. ingens* and one individual identified as *H. insularum* from Madeira. Similarly, all analyses agreed in showing the genus *Hogna* as a polyphyletic assemblage. Remaining relationships within Lycosoidea including subfamilies, were similar to those reported in Piacentini and Ramírez (2019).

Molecular species delimitation

The COI data matrix included 133 terminals, including a single sequence of the non-Madeiran *Hogna radiata* (Iberian Peninsula), corresponding to 62 haplotypes (one non-Madeiran) (Suppl. material 2). The ITS-2 matrix included 40 terminals with 400 aligned positions and ten additional absence/presence characters, corresponding to 17 alleles (sequence types) (Suppl. material 2). The clustering analysis (BIN) of the COI sequences resulted in six clusters, that mostly matched the morphological circumscrip-

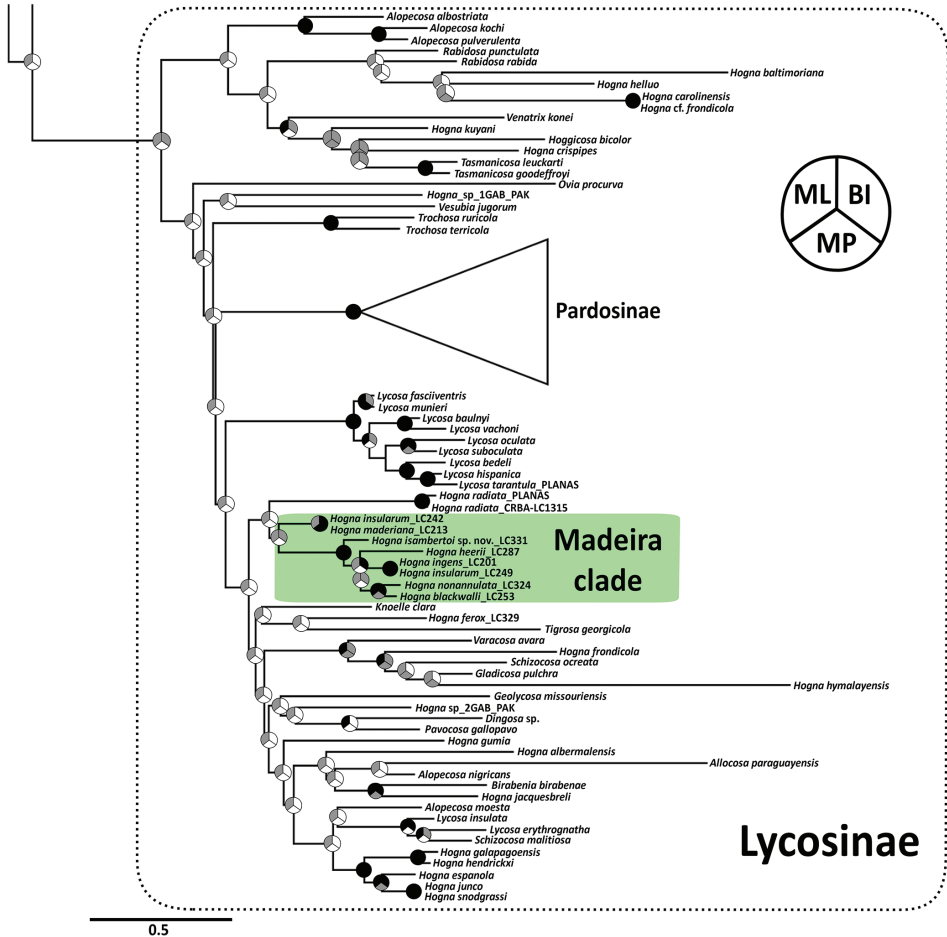


Figure 2. Best maximum likelihood tree of Lycosinae, inferred with IQTREE2 after selecting the best partition scheme and evolutionary models. Nodes are split in three sections, representing the different methods. Support on nodes should be read as follows: black: ML ultrafast bootstrap and BI posterior probability ≥ 0.95 , MP Jackknife ≥ 0.7 ; grey: ML Ultrafast Bootstrap and BI posterior probability < 0.95 , MP Jackknife < 0.7 ; white: unrecovered node.

tion, except for the merging of individuals identified as *H. maderiana* and *H. insularum* (Fig. 3). As already noted in the target multilocus phylogenetic analyses, one individual identified as *H. insularum* (DNA code LC249) clustered together with individuals morphologically assigned to *H. ingens*. Uncorrected genetic distances are shown in Table 1, with unidentified juveniles from the *H. insularum*-*maderiana* complex listed as “hx”. The genetic distance between *H. insularum* and *H. maderiana* was 1.6%, similar to the values observed within *H. insularum* (1.7%). The next lower genetic distance was observed between *H. nonannulata* and *H. maderiana* (4.3%). The largest genetic distances were found between the species pair *H. insularum* and *H. maderiana* and

Table 1. The number of base differences per site from averaging over all sequence pairs within each group are shown. This analysis involved 133 nucleotide sequences. All ambiguous positions were removed for each sequence pair (pairwise deletion option). There was a total of 676 positions in the final dataset. Evolutionary analyses were conducted in MEGA X (Kumar et al. 2018). The presence of n/c in the results denotes cases in which it was not possible to estimate evolutionary distances. *hins_mad_LC336_5* and *hins_ma_LC249_5* are included in *H. ingens*. *Hx* refers to non-identified juveniles. Grey cells refer to comparison with a continental taxon, yellow cells refer to comparison within the *ingens* clade, and green cells refer to comparison within the *maderiana* clade.

	<i>radiata</i>	<i>beeri</i>	<i>ingens</i>	<i>nonannulata</i>	<i>blackwalli</i>	<i>isambertoi</i>	<i>maderiana</i>	<i>insularum</i>	<i>hx</i>
<i>radiata</i>									
<i>beeri</i>	0.105	0.006							
<i>ingens</i>	0.111	0.065	0.004						
<i>nonannulata</i>	0.106	0.059	0.064	0.009					
<i>blackwalli</i>	0.098	0.074	0.073	0.043	0				
<i>isambertoi</i>	0.107	0.07	0.082	0.075	0.084	0.003			
<i>maderiana</i>	0.103	0.106	0.105	0.103	0.105	0.095	0.007		
<i>insularum</i>	0.102	0.104	0.108	0.099	0.104	0.098	0.016	0.017	
<i>hx</i>	0.103	0.106	0.108	0.103	0.105	0.098	0.01	0.016	0.01

the remaining endemic species (9.9–10.6%) and were similar to those observed with regard to the mainland species *H. radiata* (9.8–11.1%).

The mPTP analysis ran on the IQ-TREE inferred tree, recovered the same groupings with high support. The GMYC model delimited five groups, by merging *H. nonannulata* and *H. blackwalli* together, but the likelihood ratio test revealed that it did not provide a significantly better fit than the null model (one single species, $p = 0.7764125$).

The statistical parsimony analysis at 95% connection resulted in six independent networks that exactly matched the BIN and mPTP clusters (Fig. 4). Lowering the connection limited to 90% had no effect on the results. For the ITS alleles, a single network was obtained (both at 90% and 95%). The alleles of the species *H. maderiana* and *H. insularum* were mixed up, while the rest of alleles were exclusive to each species, except for *H. beeri*, *H. blackwalli* and *H. nonannulata* that shared one allele. The alleles of the putative *H. insularum* individuals bearing *H. ingens* COI haplotypes, were also observed to cluster close to the *H. ingens* alleles.

Divergence time estimation

The inferred species tree suggested non-monophyly of Madeiran *Hogna* albeit with low support (Fig. 5). Estimated time of split from their closest sister taxa was similar for the two Madeiran lineages (10.9 mya, 4–23 mya 95%HPD, and 10.4 mya, 2.8–24 mya, for the *ingens* and the *maderiana* clades, respectively). The most recent common ancestor of the *ingens* clade was 5.9 mya (2–13.1 mya). The coalescent times inferred from the COI tree for the different species were 0.09 mya for *H. isambertoi* sp. nov., 0.13 for *H. beeri*, 0.26 for *H. ingens*, 0.4 for *H. blackwalli* and 0.06 for *H. nonannulata*, and 1.17 for the *maderiana* clade.

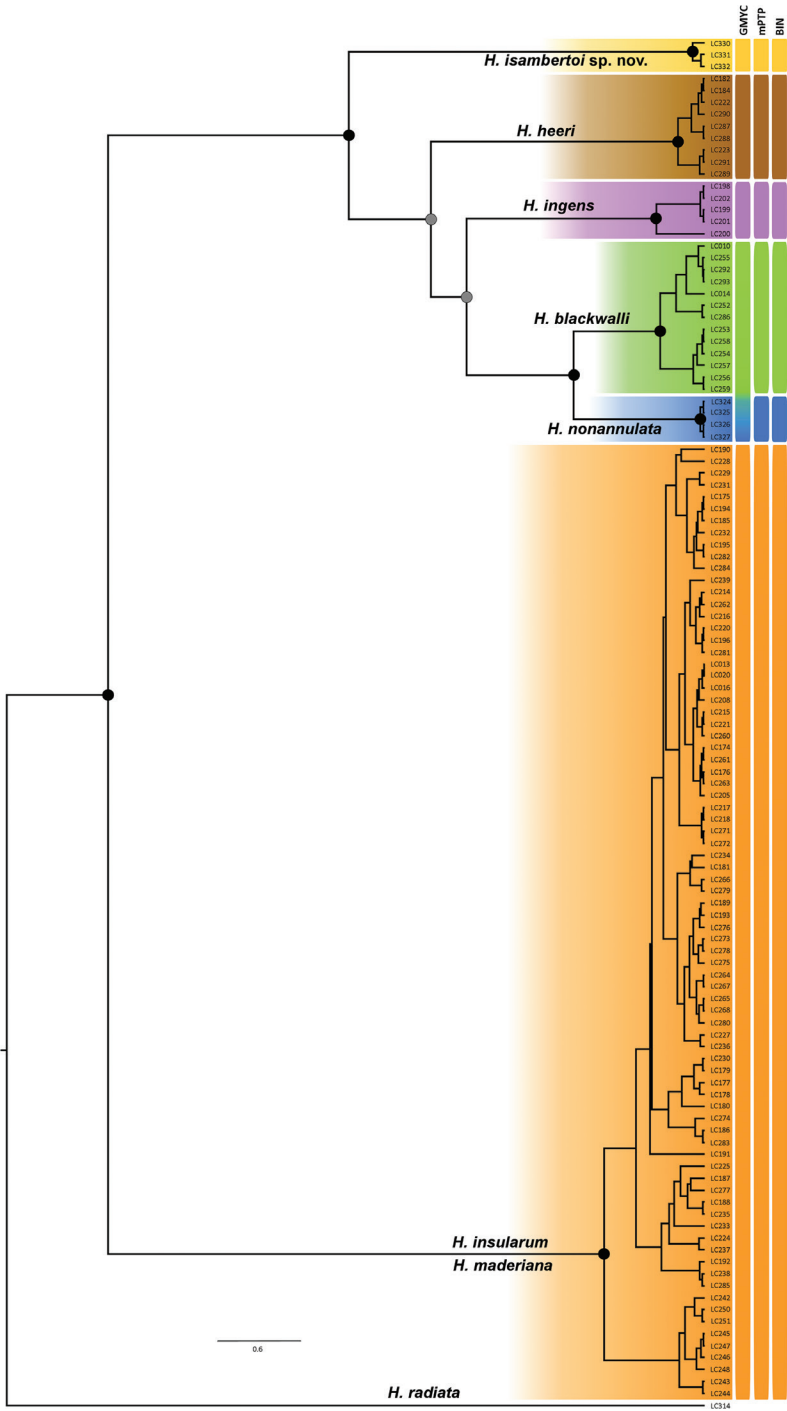


Figure 3. Ultrametric tree for the COI obtained with BEAST using a coalescent (constant population growth) prior to apply the GMYC model. Only unique sequences included. Support on nodes should be read as follows: black: BI posterior probability ≥ 0.95 ; grey: BI posterior probability < 0.95 . Species delimitations based on alternative approaches are indicated with boxes besides the terminal labels.

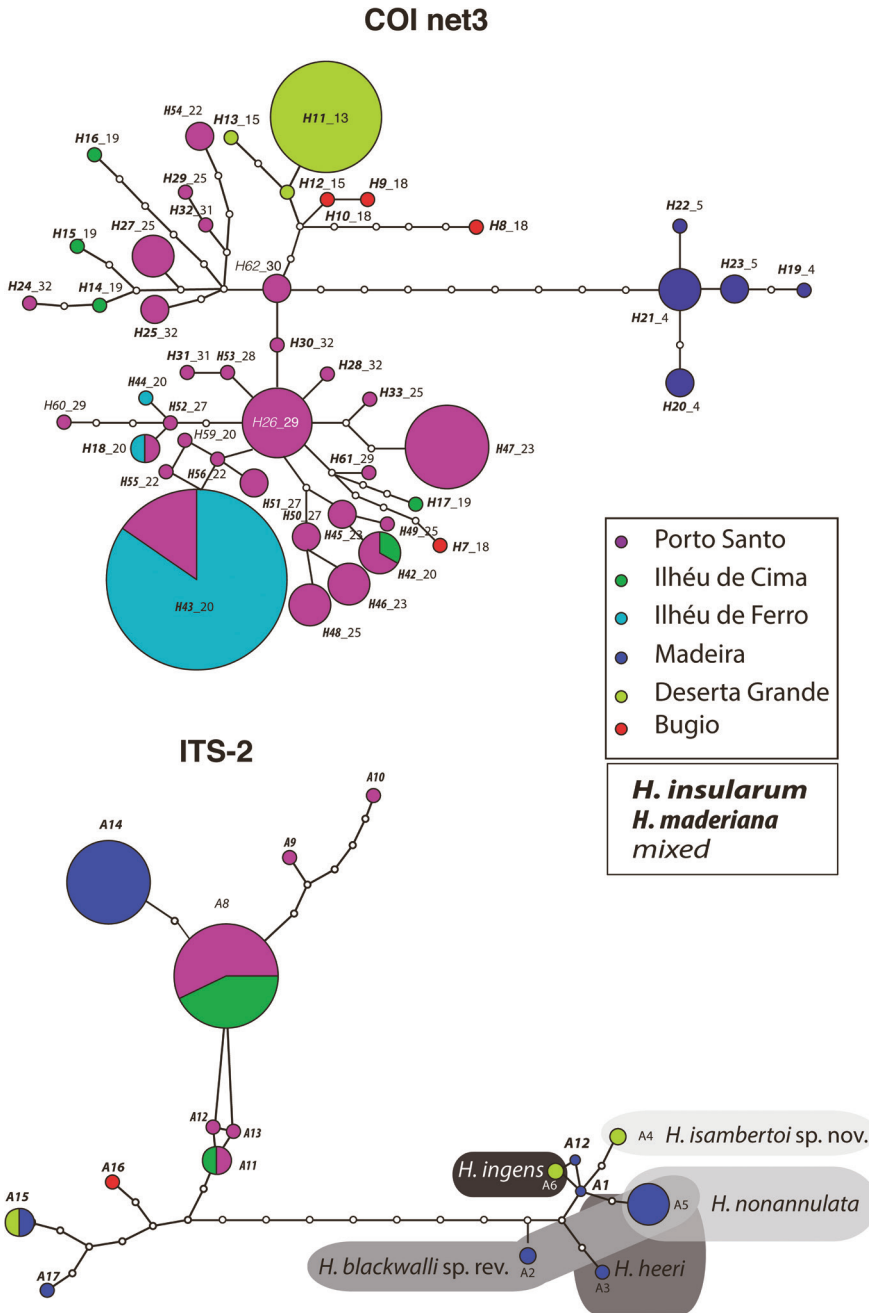


Figure 4. COI haplotype (upper) and ITS-2 allele (lower) networks inferred under statistical parsimony (0.95 probability). Pie size proportional to number of individuals which exhibited the same haplotype/alleles. White circles represent missing haplotypes/alleles. Colours correspond to islands (colour codes in upper box). For the COI haplotypes only the network (3) including *H. insularum* / *H. maderiana* haplotypes showed (each remaining nominal species were resolved as independent networks). ITS-2 alleles boxed per species, except for *H. insularum* / *H. maderiana*. Haplotype/allele labels for *H. insularum* in bold and italics, *H. maderiana* in condensed bold and italics, not assigned in light italics (see lower box legend).

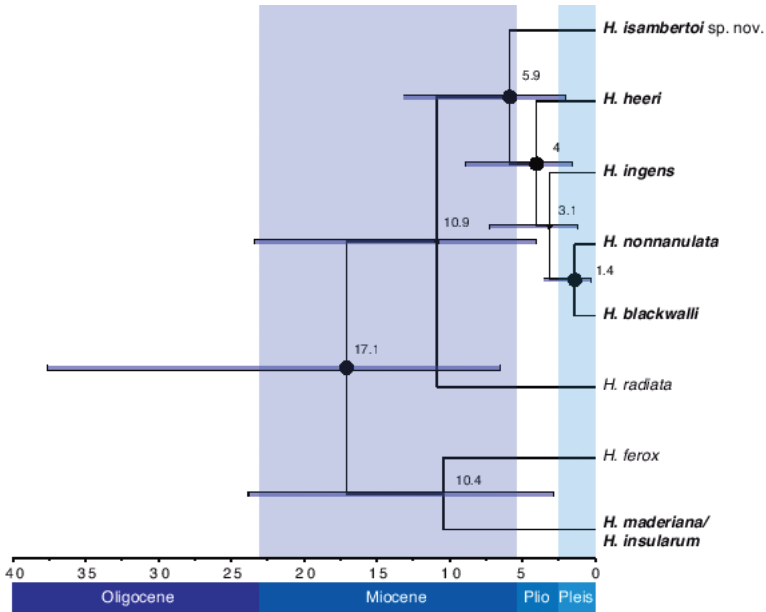


Figure 5. Species tree for the Madeiran *Hogna* including two outgroups. Values on nodes are estimated divergence times in millions of years (my). Dots on nodes indicate BI posterior probability >0.95. Bars correspond to the 95%HPD of the time estimates.

Taxonomy

Family Lycosidae Sundevall, 1833

Genus *Hogna* Simon, 1885

Type species. *Hogna radiata* (Latreille, 1817).

Diagnosis. We follow the diagnosis presented by Brady (2012).

Hogna blackwalli (Johnson, 1863)

Figures 6–8

Lycosa blackwalli Johnson, 1863: 152 (Dmf).

Trochosa maderiana Thorell, 1875: 167 (mf, misidentification).

Geolycosa blackwalli Roewer, 1955: 241.

Geolycosa blackwalli Roewer, 1960: 691, fig. 387a–d (mf).

Geolycosa ingens Denis, 1962: 96, f. 78 (f, misidentification).

Hogna maderiana Wunderlich, 1992: 461, fig. 720c–e (mf, S).

Hogna maderiana Wunderlich, 1995: 416, fig. 28 (f).

Types. Syntypes: MADEIRA • 2 ♀♀; Pico Ruivo, leg. Johnson, stored at OUMNH, collection number 1617. Examined.

Material examined. MADEIRA • between Pico do Areiro and Poiso, 1 ♀ (SMF65685), leg. K. Groh; Caramujo, 32.77161°N, 17.06205°W, 1 ♂ (CRBALC0010: LC010), 23.VIII.2016 (collected as subadult, reared in captivity to adult on 7.X.2016), hand collecting, leg. L. Crespo; “Funchal” [probably north of it because “600 to 2000 ft.” is written in label], 1 ♀ (NHM, mounted dry), V.1895, leg. O. Grant; Paúl da Serra, 1 ♀ (SMF65684), hand collecting, leg. I. Silva, 1 ♀ (CRBALC0496: LC254) and 3 juveniles (CRBALC0495: LC253, CRBALC0497: LC255, CRBALC0499: LC256), 32.78182°N, 17.09978°W, 28.III.2017, hand collecting, leg. L. Crespo & I. Silva; Paúl da Serra / Rabaçal, 5 ♀♀ (SMF65696); Pico do Areiro, 32.739067°N, 16.934448°W, 1 ♀ (CRBALC0516: LC270), 27.III.2017, hand collecting, leg. I. Silva; Pico do Cidrão, 32.74036°N, 16.93877°W, 1 ♀ (CRBALC0489: LC286), 27.III.2017, hand collecting, leg. L. Crespo; Rabaçal, 1 ♀ (MNHNP AR16185), IV.1957, leg. H. Coiffait, 1 ♀ (SMF65683), 18.VIII.1991, hand collecting, leg. I. Silva; Ribeiro Bonito, 32.79582°N, 16.93710°W, 1 juvenile (CRBALC0014: LC014), 4.VIII.2016, hand collecting, leg. L. Crespo; trail from Paúl da Serra to Montado dos Pessegueiros, 32.78837°N, 17.09857°W, 1 ♀ (CRBALC0271: LC252) and 2 juveniles (CRBALC0498: LC292, CRBALC0502: LC293), 28.III.2017, hand collecting, leg. L. Crespo & I. Silva, 2 ♀♀ (CRBALC0503: LC257, CRBALC0515: LC259) and 1 juvenile (CRBALC0514: LC258), 31.III.2017, hand collecting, leg. L. Crespo, M. Arnedo & P. Oromí, 1 ♂ (CRBALC0718), 2 ♀♀ (CRBALC0601, CRBALC0605) and 2 juveniles (CRBALC0603, CRBALC0698), 4.IV.2018, hand collecting, leg. L. Crespo & A. Bellvert; 1 ♀ (SMF9910750), 1 ♂, 2 ♀♀ and 4 juveniles (NHRS-JUST-000001114), 2 ♀♀ (NHM, mounted dry), [no collection data except for the data of collection of one of these females, IX.1963].

Diagnosis. *Hogna blackwalli* can be diagnosed from all other Madeiran *Hogna* by the aspect of its legs, with two small patches of yellow setae in the joints of anterior tibiae with metatarsi and of metatarsi with tarsi (Fig. 26A). In addition, by the genitalia: in males, the embolus with tip tilted retrolaterally and a tegular apophysis with a long, sharp ventral spur (Fig. 6A–C). In females, the epigynal anterior pocket shows a small indentation on the lateral border (white arrow in Fig. 6D).

Redescription. Male (CRBALC0718): (Fig. 6A–C). Total length: 18.9; carapace: 9.1 long, 6.8 wide.

Colour: carapace brown, with short black setae except anteriorly and laterally, where short white setae and long black setae are present; median cream longitudinal band present, covered with short white setae, anteriorly broadened, with suffused greyish brown patches covered by yellow setae; two yellow marginal bands, suffused with greyish brown patches, covered with short white setae; four black striae well visible on each flank. Chelicerae black, covered mostly in black setae but with sparse yellow setae. Gnathocoxae very dark orange-brown, labium blackish; sternum black, with a faint, thin longitudinal stripe extending to less than half of sternum length. Legs grey to greyish brown, with seven or eight patches of white setae (anterior legs with eight, posterior legs seven) except the patches in anterior metatarsi, both yellow. Pedipalpal femur as legs, patella, tibia and proximal cymbium with yellow to orange setae, apical cymbium covered

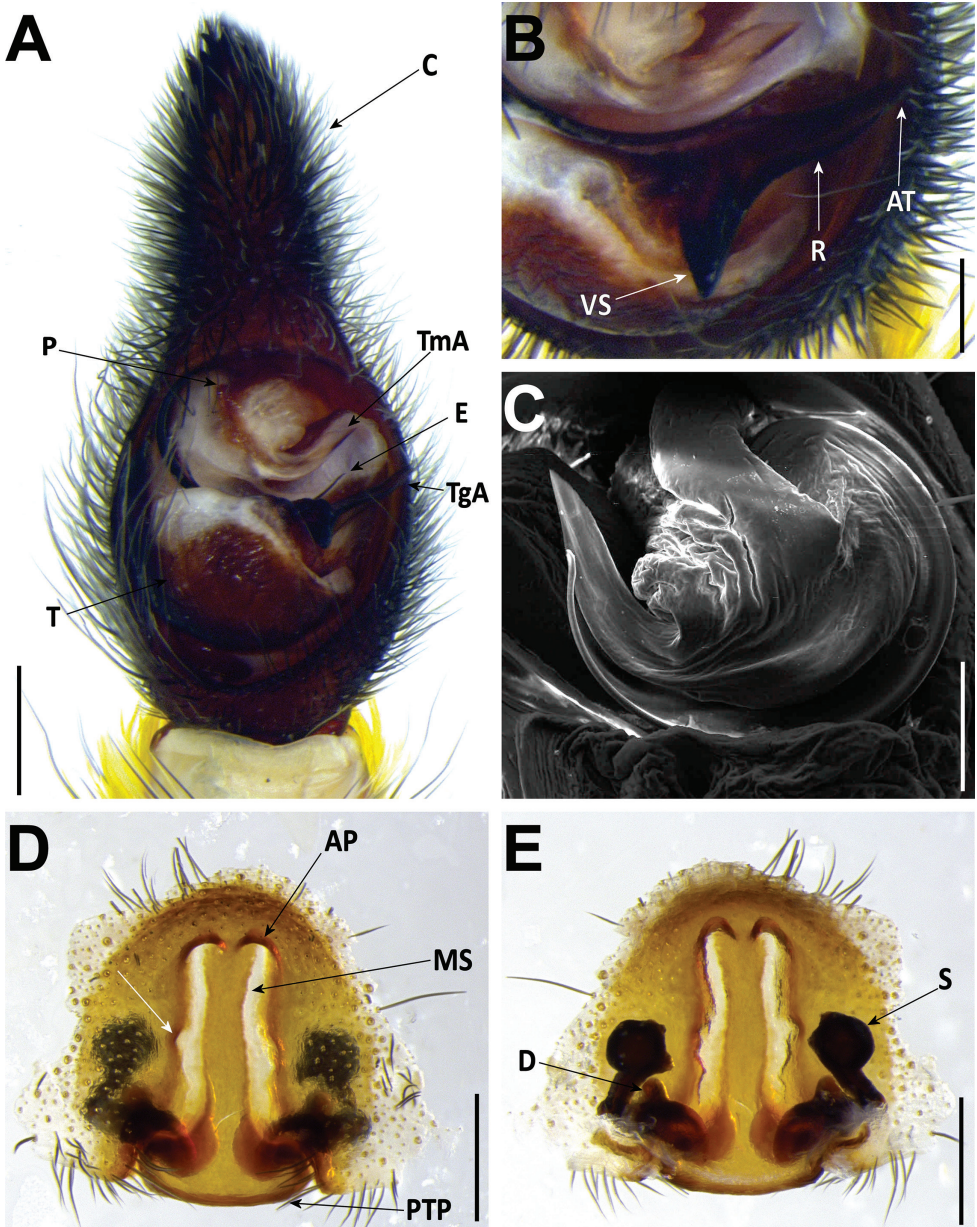


Figure 6. *Hogna blackwalli* **A–C** male (CRBALC0718): **A** left male pedipalp, ventral **B** detail of the median apophysis, anteroventral **C** SEM image, right male pedipalp, ventral **D, E** female (CRBALC0516): **D** epigyne, ventral (white arrow points to an indentation that may be helpful for diagnosis) **E** vulva, dorsal. Abbreviations, male pedipalp: AT – anterior point, C – cymbium, E – embolus, P – palea, R – ridge, T – tegulum, TA – terminal apophysis, TgA – tegular apophysis, VS – ventral spur. Abbreviations, female genitalia: D – diverticulum, H – epigynal hoods, MS – median septum, S – spermatheca. Scale bars: 0.5 mm (**A, D, E**); 0.2 mm (**B, C**).

in black setae. Abdomen with a pair of anterolateral black patches, extending laterally into grey to black flanks, interspersed with white patches; a median orange lanceolate patch is bordered by the aforementioned pattern, posteriorly also by dark chevrons; venter with a wide longitudinal black band, bordered by a mesh of white and black patches.

Eyes: MOQ: MW = 0.7 PW, MW = 1.1 LMP, MW = 1.1 AW; Cl = 0.5 DAME. Anterior eye row slightly procurved.

Legs: Measurements: Leg I: 27.3, Ti: 6.4; Leg IV: 29.7, Ti: 6.6; TiIL/D: 5.8. Spination of Leg I: Fe: d1.1.0, p0.0.2; Ti: p0.0.1, v2l.2l.2s; Mt: p0.0.1, r0.0.1, v2l.2l.1s. Mt with very dense scopulae.

Pedipalp: cymbium with eight dark, stout, macrosetae at tip, Fe with two dorsal and an apical row of four spines, Pa with one prolateral spine, Ti with one dorsal, one dorsoprolateral, and one prolateral spines. Tegular apophysis with ventral spur long, sharp, with a concave ridge leading to a thin apical point (Fig. 6A, B); terminal apophysis blade-shaped with sharp end (Fig. 6A–C); embolus short, with tip directed laterally (Fig. 6A–C); palea large (Fig. 6A).

Female (CRBALC0516): (Fig. 6D, E). Total length 29.9; carapace: 10.4 long, 8.0 wide.

Colour: overall as in male, but darker. Sternum entirely black. Yellow setae in pedipalp restricted to the joints of tibia with tarsus and patella with tibia.

Eyes: MOQ: MW = 0.7 PW, MW = 1.2 LMP, MW = 1.1 AW; Cl = 0.7 DAME. Anterior eye row slightly procurved.

Legs: Measurements: Leg I: 27.7, TiI: 6.3; Leg IV: 31.8, TiIV: 6.8; TiIL/D: 3.8. Spination of Leg I: FeI: d1.1.0, p0.0.2; TiI: p0.0.1, v2l.2l.2s; MtI: p0.0.1, r0.0.1, v2l.2l.1s. MtI with very dense scopulae.

Epigyne: anterior pockets almost touching, short, with lateral borders anteriorly parallel, medially slightly divergent after a small sinuosity (white arrow in Fig. 6D); anterior pocket cavities deep; median septum with narrow posterior transverse part (Fig. 6D); spermathecae globular (Fig. 6E); copulatory ducts with small, stout diverticulum ventrally (Fig. 6E); fertilisation ducts emerging at the base of copulatory duct (Fig. 6E).

Intraspecific variation. Carapace length, males: 7.4–9.1, females: 8.9–10.4. Suffused greyish brown patches in median yellow longitudinal band not necessarily covered with yellow setae. Epigyne can present two small depressions in the base of median septum, which can be of variable length, position and concavity of inflexion of the lateral hood walls can also be variable, either placed near hoods or medially, median septum can be swollen medially.

Distribution. This species is known from areas in or near the laurel forest patch in Madeira, in the north half of the island (Fig. 8).

Ecology. *Hogna blackwalli* can be found in montane grasslands surrounding laurel forest areas or *Erica* shrubland. Surprisingly, it can also be found in closed canopy laurel forest, where, at night, specimens can be found climbing tree trunks.

Conservation status. *Hogna blackwalli* was assessed according to the IUCN Red List criteria as *H. maderiana*, with the status of Least Concern (Cardoso et al. 2018a). The coastal records reported in the referred publication are probably of *H. nonannulata*.



Figure 7. Photograph of *H. blackwalli*. Female specimen, recently dead, in captivity. Photograph credit Emídio Machado.

Comments. There has been a great deal of confusion surrounding *H. blackwalli* and *H. maderiana*. Walckenaer’s original description of *H. maderiana* (Walckenaer 1837) based on material from Madeira island indicated that legs were “(...) reddish brown, suffused brown underneath (...)”. Subsequently, Blackwall described the alleged male of Walckenaer’s *H. maderiana* but mentioned a striking leg coloration: “(...) the femora, on the upper side, have a yellowish grey hue, that of the tibia, metatarsi and tarsi being bright orange-red, and the colour of the underside of all the joints is dark brown tinged with grey; (...)” (Blackwall 1857). Additionally, he reported the locality of origin of those specimens to be Porto Santo, not Madeira. Six years later, Johnson (1863) described *H. blackwalli* from Madeira island, indicating that “The metatarsus and tarsus of the two anterior pairs of legs are black, or very dark brown. At the distal extremities and on the upper sides of the femur and genua of the first two pairs of legs, as well as at the extremities of some of the joints of the two posterior pairs of legs, there is a patch of orange setae”. In the same publication, he also described and identified as *H. maderiana* specimens from Ilhéu de Ferro, near Porto Santo. It is unclear on how many specimens Johnson based his description, but we could locate a part of this material at the OUMNH, thus revalidating *H. blackwalli* Johnson, 1863.

The next author to make a taxonomic contribution on these spiders was Thorell (1875), who redescribed *H. maderiana* based on specimens from Madeira. However, his reference to the legs colouration that reads “palporum partibus pateliari et tibiali apice supra croceis, metatarsis tibiisque pedum anteriorum apice quoque croceis vel flavis” suggests that his redescription corresponds to *H. blackwalli* instead. We could locate 14 specimens labelled as *H. maderiana* in the NHRS, which most likely were the ones examined by Thorell, and we confirmed they correspond to *H. blackwalli*. Kulczynski (1899) followed Blackwall’s judgement to redescribe the large specimens from Porto

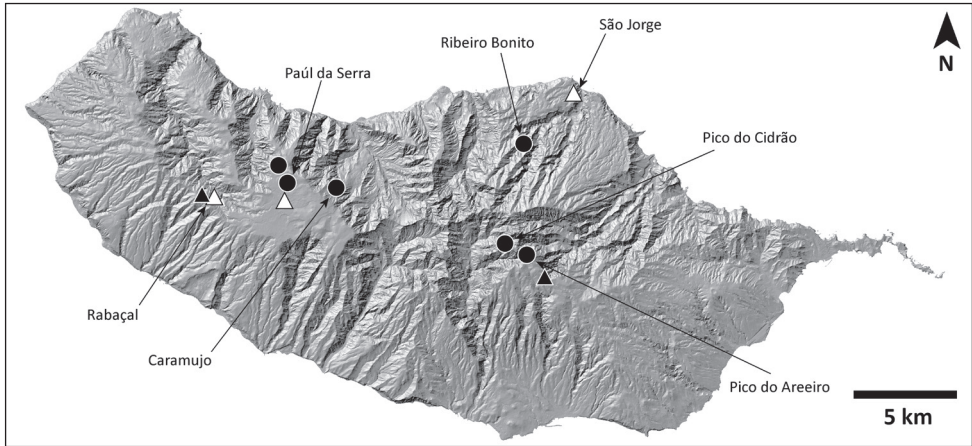


Figure 8. Distribution of *H. blackwalli*. Circles: present records; black triangles: revised records from literature; white triangles: unconfirmed records from literature.

Santo and Ilhéu de Ferro under the name *Trochosa maderiana*. Almost one century later, Roewer (1960) provided redescriptions of three Madeiran *Hogna*, but no reference was given to the leg coloration, which is the easiest way to distinguish these larger, aforementioned species. His epigyne drawings provided little additional information and were confusing. While the epigyne of *H. ingens* allows identification of this species (Roewer 1960: fig. 387e), the same is not true for the illustrations of *Isobogna maderiana* and *Geolycosa blackwalli* (Roewer 1960: figs 319a and 387a, respectively), which look rather the same. However, he reports that Thorell's *Trochosa maderiana* specimens are *H. blackwalli*, for which we assume Roewer's redescription of *Geolycosa blackwalli* to correspond to the same species we identify as *H. blackwalli*. Denis (1962) cited two females of *Geolycosa ingens* (Blackwall, 1857) and one male and two females of *H. insularum* from locations where *H. blackwalli* is usually found, Rabaçal and Paúl da Serra, on Madeira island. We could find the female identified as *H. insularum* (MNHNP AR16185), and confirm that this is *H. blackwalli*. We confidently attribute the remaining citations of *H. insularum* (specimens not found) to misidentified specimens of *H. blackwalli*. The last taxonomic works on Madeiran *Hogna* were by Wunderlich (1992, 1995). In the first of these (Wunderlich 1992), the species *H. maderiana* and *H. blackwalli* were wrongly synonymised and it was stated that “up to Denis (1962), most authors assumed that *H. maderiana* occurred both in Madeira and Porto Santo.” This is not accurate, since Johnson discriminated between *H. blackwalli* from Madeira and *H. maderiana* from Ilhéu de Ferro. In fact, this synonymy is even stranger because while revising the material present at the SMF, we found vial 9910750 of the Roewer collection, with an identification note by Wunderlich stating “*H. blackwalli* (Johnson)”. Finally, we have located only part of the type material described by Johnson at the OUMNH, because no males were found, even though his description mentioned males. Therefore, the whereabouts of the remaining specimens of the type series are unknown.

***Hogna ferox* (Lucas, 1838)**

Arctosa maderana Roewer, 1960: 604–605, fig. 334a (f), fig. 334 b (m). Syn. nov. (see WSC 2021 for a complete list of synonymies)

Types. Holotype: 1 ♀ (with 1 paratype ♂ in vial), leg. Roewer, stored at SMF, collection number 9903912. Examined.

Material examined. GRAN CANARIA • Gando, 1 ♂ (SMF25851), X.1961, leg. G. Schmidt; La Rosetas, 28.12196°N, 15.68662°W, 4 ♀♀ (CRBALC0586, CRBALC0602: LC329, CRBALC0706, CRBALC0719), 21.IV.2018, leg. L. Crespo & A. Bellvert; Playa del Inglés, 1 ♀ (SMF25422), 1970, leg. G. Schmidt; San Sebastian, 1 ♀ (SMF29107), IV.1974, leg. G. Schmidt. LA GOMERA • Lomada near San Sebastian, 1 ♀ (SMF29134), IV.1974, leg. Wild. TENERIFE • La Orotava, 28.36666°N, 16.51666°W, 1 ♂ (SMF2234), 1871, leg. Grenacher & Noll. TUNISIA • Jendouba, 1 ♀ (SMF63576), X.1995, leg. G. Eichler; (no sampling information), 1 ♀ (SMF37118). (No country or sampling information) • 2 ♂♂, 1 ♀ and 1 juvenile (SMF67996).

Justification of the synonymy. After its original description, the endemic species *Arctosa maderana* Roewer, 1960 was never again recorded in the archipelago of Madeira, despite extensive sampling through several biodiversity inventory projects (Crespo et al. 2014a; Boieiro et al. 2018; Malumbres-Olarte et al. 2020). We identified the type female and the paratype male as *H. ferox* (Lucas, 1838). *Hogna ferox* has a widespread distribution throughout the Mediterranean, being present in the Iberian Peninsula, North Africa, and the neighbouring archipelago of the Canary Islands. However, it has never been reported in Madeira, and after examination of specimens, we propose that *A. maderana* Roewer, 1960 is a junior synonym of *H. ferox* (Lucas, 1838) and should be removed from the Madeira archipelago fauna.

***Hogna heeri* (Thorell, 1875)**

Figures 9–11

Trochosa heeri Thorell, 1875: 166 (Df).

Trochosa heeri Kulczynski, 1899: 433, pl. 9, fig. 188 (f).

Hogna heeri Roewer, 1955: 248.

Hogna heeri Roewer, 1959: 411, fig. 221a–d (f, Dm).

Hogna heeri Wunderlich, 1992: 459, fig. 720, 720a (mf).

Types. Syntypes: MADEIRA • 2 ♀♀, leg. O. Heer, stored at NHRS, collection number JUST-000001113. Examined.

Material examined. BUGIO • Planalto Sul, 32.41228°N, 16.47466°W, 1 ♀ (LCPC), 3.XII.2012, hand collecting, leg. I. Silva. MADEIRA • between Eira do Serrado and Curral das Freiras, 1 ♀ (SMF69107); Paúl da Serra, 2 ♀♀ (MMUE

G7572.874), 25.IV.1973, leg. J. Murphy, 1 ♀ (CRBALC0492: LC289), 32.78182°N, 17.09978°W, 19.III.2017, hand collecting, leg. I. Silva, 1 ♀ (CRBALC0500: LC222) and 1 juvenile (CRBALC0494: LC291), 28.III.2017, leg. I. Silva; Pico do Cidrão, 32.74036°N, 16.93877°W, 1 ♀ (LCPC), 24.VI.2003, pitfall trapping, leg. M. Freitas, 2 ♀♀ (CRBALC0490: LC287, CRBALC0288: LC288), 27.III.2017, hand collecting, leg. L. Crespo & I. Silva; trail from Paúl da Serra to Montado dos Pessegueiros, 32.78837°N, 17.09857°W, 2 ♀♀ (CRBALC0270: LC184, CRBALC0501: LC223) and 1 juvenile (CRBALC0493: LC290), 28.III.2017, hand collecting, leg. L. Crespo & I. Silva; 1 ♀ (SMF37575).

Diagnosis. *Hogna heeri* can be diagnosed by the genitalia: the males, according to literature, by a straight embolus (Wunderlich 1992: 595, fig. 720); in females, by epigynal anterior pockets with widely divergent lateral border and median septum with a wide posterior transverse part (Fig. 9). Similar species include *H. insularum* and *H. isambertoii* sp. nov., from which it cannot be somatically differentiated.

Redescription. Male: We could not examine any male specimens.

Female (CRBALC0500): (Fig. 7 corresponds to specimen CRBALC0501). Total length 13.54; carapace: 5.63 long, 4.4 wide.

Colour: carapace greyish brown, covered with short black setae, with a median cream longitudinal band, anteriorly broadened, covered with short white setae, with suffused greyish brown patches; two yellow marginal bands, with roughly round grey patches, covered with short white setae; four black striae well visible on each flank. Chelicerae dark brown, covered in black and yellow setae. Gnathocoxae and labium overall brown, with posterior margin blackish; sternum yellow, with a faint V-shaped grey patch and grey lateral borders. Legs yellow, with irregular grey suffused patches, except metatarsi and tarsi, brown. Pedipalps yellow except tibia, brown, tarsus, blackish brown. Abdomen with a pair of anterolateral black patches, extending laterally into grey flanks, mottled with yellowish patches covered with white setae; a median dark

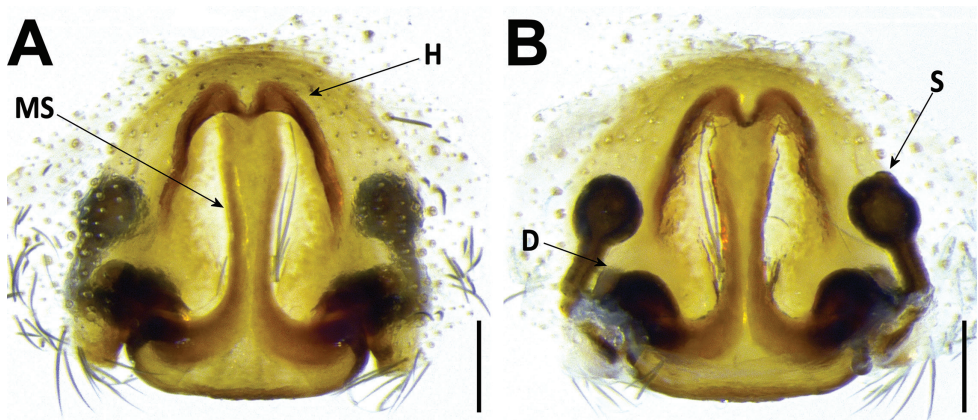


Figure 9. *Hogna heeri* female (CRBALC0501): **A** epigyne, ventral **B** vulva, dorsal. Abbreviations, female genitalia: D – diverticulum, H – epigynal hoods, MS – median septum, S – spermatheca. Scale bars: 0.2 mm.



Figure 10. Photograph of *H. heeri*. Female specimen in captivity. Photograph credit Emídio Machado.

lanceolate patch is bordered by two yellowish longitudinal bands interconnected in anterior half, posteriorly by means of dark chevrons; venter yellowish, with a median dark grey longitudinal band, bordered by yellowish and grey small patches.

Eyes: MOQ: MW = 0.7 PW, MW = 1.1 LMP, MW = 1.1 AW; CI = 0.9 DAME. Anterior eye row straight.

Legs: Measurements: Leg I: 13.0, TiI: 2.8; Leg IV: 16.10, TiIV: 3.22; TiIL/D: 3.7. Spination of Leg I: FeI: d1.1.1, p0.0.1; TiI: v2l.2l.2s; MtI: p0.0.1, r0.0.1, v2l.2l.1s. MtI with sparse scopulae in basal half and dense scopulae on distal half.

Epigyne: anterior pockets touching, short, with lateral borders widely divergent, converging solely at its posterior end (Fig. 9A); anterior pocket cavities deep; median septum with wide posterior transverse part (Fig. 9A); spermathecae globular (Fig. 9B); copulatory ducts basally with a laterally projected diverticulum (Fig. 9B); fertilisation ducts emerging at the base of copulatory duct (Fig. 9B).

Intraspecific variation. Carapace length, females: 5.6–5.8. In females, the ventral abdominal dark band may be entirely absent; the relative position of female epigynal anterior pockets may vary from touching to almost touching.

Distribution. This species is known from two distinct regions: high altitude localities in Madeira, always above 800 m, and the island of Bugio (Fig. 11).

Ecology. *Hogna heeri* occurs in montane grasslands or *Erica* shrubland in Madeira and the steep, semi-arid summit of Bugio.

Conservation status. *Hogna heeri* was assessed according to the IUCN Red List criteria, with the status of Least Concern (Cardoso et al 2018b).

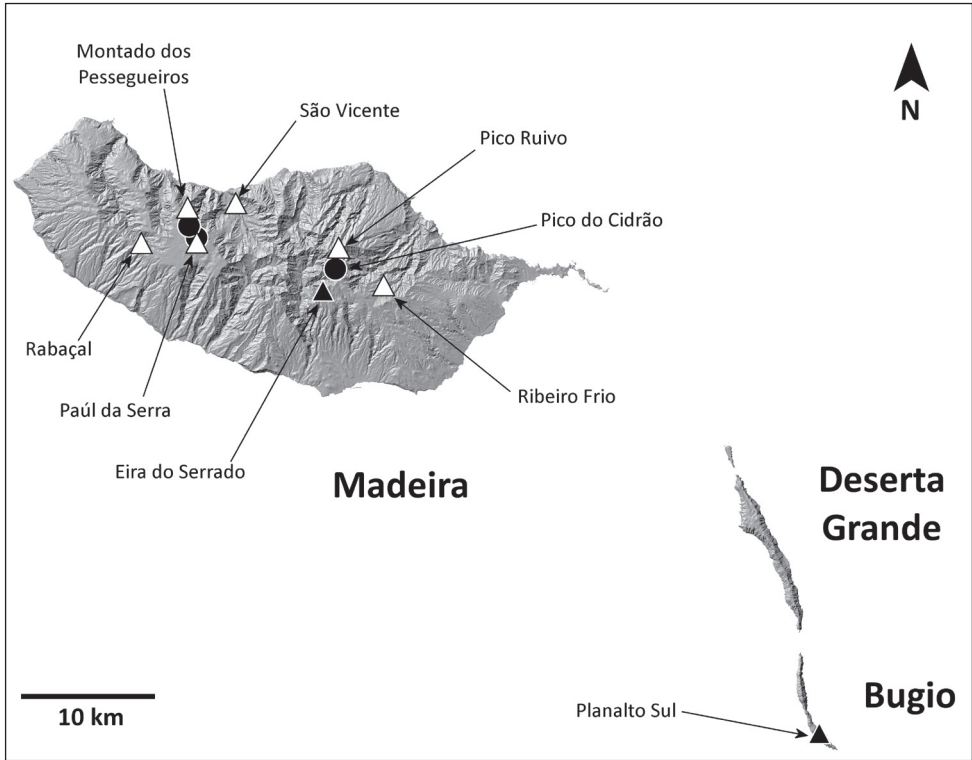


Figure 11. Distribution of *H. heeri*. Circles: present records; black triangles: revised records from literature; white triangles: unconfirmed records from literature.

Comments. The specific epithet of *H. heeri* has been one of the names re-named by Bonnet (1959), who changed all previously described spider species' names which were patronyms ending in "ii" to end in "i", as a way to correct spelling (Bonnet 1945). Although the ICZN argues for the maintenance of the original spelling, common usage dictates that these modified spellings continue to be used. The disjunct distribution of *H. heeri*, with populations in Madeira and Bugio, is somewhat baffling. The only known specimens from Bugio previously reported (Crespo et al. 2013) were examined: while the female matches *H. heeri*, the male pedipalp is the same as that of *H. isambertoii* sp. nov., with the tip of the embolus slightly tilted anteriorly (Fig. 18A). We would like to remark that Wunderlich reported an apophysis at the base of the embolus (indicated with an arrow in his figure) as a diagnostic feature to identify males of *H. heeri* (Wunderlich 1992: fig. 720), which appears to be either inconspicuous or missing altogether. To us it seems the arrow is pointing to the pars pendula membrane connecting the terminal apophysis with the embolus. Unfortunately, we could not gather molecular information from the Bugio specimens due to their poor preservation. Lastly, while revising Thorell's type series, we identified one of the three adult females in the original vial as *H. insularum*.

***Hogna ingens* (Blackwall, 1857)**

Figures 12–14

Lycosa ingens Blackwall, 1857: 284 (Df).*Lycosa ingens* Blackwalli, 1867: 203 (Dm).*Trochosa ingens* Kulczynski, 1899: 423, pl. 9, fig. 121 (mf).*Geolycosa ingens* Roewer, 1955: 241.*Geolycosa ingens* Roewer, 1960: 689, fig. 387e (f).*Hogna ingens* Wunderlich, 1992: 459, fig. 720b, fig. 724a.

Types. Holotype: no type materials from the Blackwall collection were found neither at the OUMNH nor the NHM.

Material examined. DESERTA GRANDE • Vale da Castanheira (N), 1 ♀ (SMF21994), 26.III.1967, 1 ♀ (CRBALC0591) and 4 juveniles (CRBALC0593, CRBALC0594, CRBALC0595, CRBALC0592), 32.56685°N, 16.53694°W, 25.III.2017, hand collecting, leg. L. Crespo; (unknown location), 3 ♀♀ (MNHNP AR16186).

Diagnosis. *Hogna ingens* can be diagnosed from all other Madeiran *Hogna* by the aspect of its legs, blackish with white patches (Figs 13, 26C), and additionally by its genitalia. In males, according to literature, by the inclined palea shield (Wunderlich 1992: 596, fig. 720f). In females, by short epigynal anterior pockets, with lateral borders divergent and anteriorly swollen median septum (Fig. 12A).

Redescription. Male: We could not examine any male specimens.

Female (CRBALC0591): (Fig. 12). Total length 25.1; carapace: 14.8 long, 11.0 wide.

Colour: carapace greyish brown, densely covered with short black setae, with a cream longitudinal band present from fovea to posterior margin of carapace; with two faint light grey marginal bands suffused with black patches, covered with white setae;

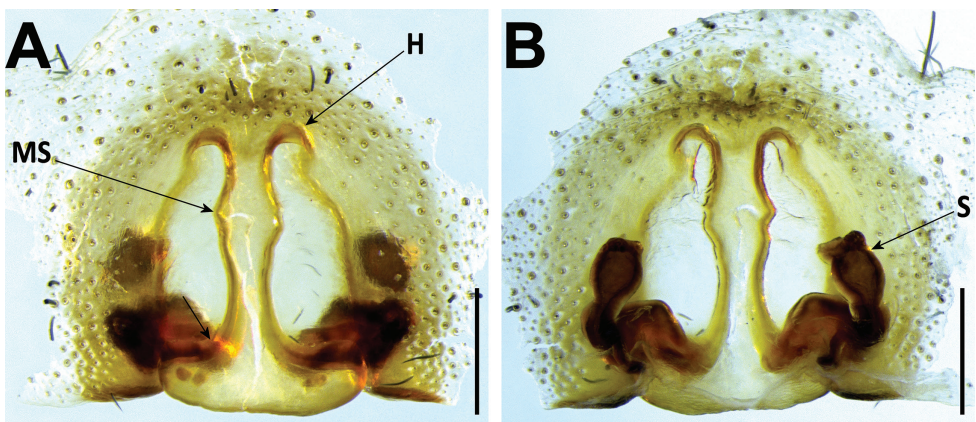


Figure 12. *Hogna ingens* female (CRBALC0591): **A** epigyne, ventral **B** vulva, dorsal. Abbreviations, female genitalia: H – epigynal hoods, MS – median septum, S – spermatheca. Scale bars: 0.5 mm.

four striae well visible on each flank. Chelicerae black except apically, reddish brown, covered in black setae. Gnathocoxae and labium overall orange-brown, densely covered with black setae; sternum greyish brown, densely covered with black setae. Legs greyish, with a variable number (6–8) of lightly coloured patches covered by white setae. Pedipalps greyish, densely covered in black setae. Abdomen densely covered in black setae, with only four very small white patches dorsally and a small anterolateral band of white setae; venter densely covered in black setae, with only two faint median bands of small white patches.

Eyes: MOQ: MW = 0.7 PW, MW = 1.2 LMP, MW = 1.1 AW; CI = 0.5 DAME. Anterior eye row slightly procurved.

Legs: Measurements: Leg I: 37.7, TiI: 8.9; Leg IV: 35.9, TiIV: 8.4; TiIL/D: 2.3. Spination of Leg I: FeI: d1.1.0, p0.0.2; TiI: p0.0.0, v2s.2s.2s; MtI: p0.0.1, r0.0.1, v2s.2s.1s. MtI an TiI with dense scopulae.

Epigyne: anterior pockets far apart, short, with lateral borders anteriorly convergent, then becoming divergent (Fig. 12A); anterior pocket cavities shallow; median septum anteriorly swollen, with wide posterior transverse part (Fig. 12A); spermathecae moderately swollen (Fig. 12B); copulatory ducts basally with a laterally projected bulbus (Fig. 12B); fertilisation ducts emerging at the base of copulatory duct (Fig. 12B).

Distribution. This species is known only from Vale da Castanheira, a 1 km² valley in the north end of Deserta Grande (Fig. 14).

Ecology. Vale da Castanheira is a semi-arid grassland area.



Figure 13. Photograph of *H. ingens*. Female specimen in the field. Photograph credit Pedro Cardoso.



Figure 14. Distribution of *H. ingens*. Black circles: present records; white triangle: unconfirmed record from literature.

Conservation status. *Hogna ingens* was declared Critically Endangered in previous works (Cardoso 2014; Crespo et al. 2014b). Its restricted habitat has been subject to biological invasions since humans set foot in Deserta Grande, with the introduction of herbivore vertebrates and, more recently, of the herb *Phalaris aquatica* L., which grows abundantly throughout the valley, limiting the access of *H. ingens* to shelter below rocks and fissures and displacing native flora. A recovery program of the valley's vegetation is being conducted, and recent data indicates the spider population is increasing. An ex-situ breeding program is currently being conducted by the Bristol Zoo to safekeep populational levels.

Hogna insularum (Kulczynski, 1899)

Figures 15–17

Trochosa insularum Kulczynski, 1899: 429, pl. 9, f. 122, 126 (Dmf).

Hogna insularum Roewer, 1959: 517, fig. 291c, d.

Hogna biscoitoi Wunderlich, 1992: 457, figs 708–709. Syn. nov.

Hogna insularum Wunderlich, 1995: 415, fig. 27 (m).

Types. *Hogna biscoitoi* Holotype ♂ without exact locality, Porto Santo; leg. Winkel-mayer, stored at MMF, collection number 24551. Not examined.

Syntypes: MADEIRA • 7 ♀♀ (MIZ217320–217326). PORTO SANTO • 2 ♂♂ and 14 ♀♀ and 1 juvenile (MIZ217327–217343), leg. Kulczynski, stored at MIZ, collection numbers indicated above. Examined 2 ♂♂ from Porto Santo, 1 ♀ from Madeira.

Material examined. BUGIO • Planalto Sul, 32.41228°N, 16.47466°W, 1 ♂ (CR-BALC0015) and 1 ♀ (CRBALC0017), 28.VI.2012, hand collecting, leg. I. Silva, 1 ♂ (CRBALC0316: LC229), 1 ♀ (CRBALC0301: LC190) and 2 juveniles (CR-BALC0315: LC228, CRBALC0318: LC231), 13.IV.2017, hand collecting, leg. L. Crespo. DESERTA GRANDE • Eira, 32.50993°N, 16.50240°W, 2 juveniles (CRBALC0312: LC282), CRBALC0319: LC232), 11.IV.2017, 1 ♀ (FMNH <http://id.luomus.fi/HLA.148894>), 17.IV.2011, hand collecting, leg. I. Silva; North end, 1 ♂ (MMUE G7508.51), 12.VIII.1981, under stone, leg. J. Murphy; Pedregal (E), 32.54613°N, 16.5234°W, 1 ♀ (CRBALC0308: LC197) and 1 juvenile (CRBALC0306: LC195), 8.IV.2017, hand collecting, leg. L. Crespo & I. Silva, 1 juvenile (CRBALC0285: LC185), 9.IV.2017, hand collecting, leg. L. Crespo; Planalto Sul, 32.50596°N, 16.49986°W, 1 juvenile (CRBALC0413: LC284), 11.IV.2017, hand collecting, leg. L. Crespo & I. Silva; Rocha do Barbusano (S), 32.53168°N, 16.51471°W, 1 juvenile (CRBALC0262: LC175), 10.IV.2017, hand collecting, leg. L. Crespo & I. Silva; Vale da Castanheira, 1 ♂ (FMNH <http://id.luomus.fi/HLA.148961>), 23.IV.2011, hand collecting, leg. I. Silva *et al.*, 1 ♂ (FMNH <http://id.luomus.fi/HLA.148976>), 5.V.2011, pitfall trapping, leg. I. Silva *et al.*, 1 ♀ (FMNH <http://id.luomus.fi/HLA.148982>), 2 ♀♀ (FMNH <http://id.luomus.fi/HLA.148986>), 22.IV.2011, hand collecting, leg. I. Silva; Vale da Castanheira (E), 32.5571°N, 16.52963°W, 1 ♂ (CRBALC0305: LC194), 9.IV.2017,

hand collecting, leg. I. Silva; Vale da Castanheira (SE), 32.55078°N, 16.52541°W, 2 ♂♂ (CRBALC0313: LC226, CRBALC0349: LC241) and 1 ♀ (CRBALC0348: LC240), 9.IV.2017, hand collecting, leg. I. Silva. ILHÉU DA CAL • 1 ♀ (SMF65693), leg. K. Groh. ILHÉU DE CIMA • top plateau, 33.05556°N, 16.28097°W, 1 ♀ (CRBALC0019), 9.IV.2012, hand collecting, leg. I. Silva, 1 ♂ (CRBALC0018), 22.V.2011, hand collecting, leg. I. Silva, 1 ♀ (CRBALC0302: LC191) and 4 juveniles (CRBALC0284: LC183, CRBALC0311: LC225, CRBALC0320: LC233, CRBALC0321: LC234), 19.IV.2017, hand collecting, leg. L. Crespo & I. Silva. ILHÉU DE FERRO • South tip, 33.03698°N, 16.40814°W, 1 ♀ (CRBALC0317: LC320) and 2 juveniles (CRBALC0265: LC178, CRBALC0266: LC179), 18.IV.2017, hand collecting, leg. L. Crespo & I. Silva. ILHÉU DO DESEMBARCADOURO • 2 ♀♀ (MMUE G7508.50), 28.VIII.1981, under stone, leg. J. Murphy. MADEIRA • Cais do Sardinha, 32.7419°N, 16.68317°W, 5 juveniles (CRBALC0504: LC242, CRBALC0505: LC243, CRBALC0506: LC244, CRBALC0507: LC245, CRBALC0508: LC246), 30.III.2017, hand collecting, leg. I. Silva; Caniçal, 1 ♀ (MMUE G7572.859), 24.IV.1973, leg. J. Murphy; Caniço, 1 ♀ (MMUE G7508.58), 11.VIII.1981, under stone, leg. J. Murphy; Ponta de São Lourenço, 1 ♂ (MMUE G7508.54), 29.VII.1981, 1 ♀ (MMUE G7508.57), 1.VIII.1981, under stone, leg. J. Murphy, 4 ♂♂ and 5 ♀♀ (FMNH <http://id.luomus.fi/HLA.156001>), 15.V.2011, pitfall trapping, leg. L. Crespo et al., 1 ♂ and 4 ♀♀ (FMNH <http://id.luomus.fi/HLA.156012>), 2.V.2011, hand collecting, leg. L. Crespo et al., 2 ♀♀ (FMNH <http://id.luomus.fi/HLA.156034>), 26.IX.2009, hand collecting, leg. L. Crespo, 1 ♀ (CRBALC0597) and 3 juveniles (CRBALC0599, CRBALC0600, CRBALC0651), 32.749965°N, 16.692817°W, 2.IV.2018, hand collecting, leg. L. Crespo; Ponta do Rosto, 1 ♀ (CRBALC0513: LC251) and 3 juveniles (CRBALC0509: LC247, CRBALC0510: LC248, CRBALC512: LC250), 32.75022°N, 16.70833°W, 30.III.2017, hand collecting, leg. I. Silva. PORTO SANTO • Rocha de Nossa Senhora, 33.07353°N, 16.3212°W, 1 ♂ (CRBALC0290: LC187) and 1 juvenile (CRBALC0291: LC188), 21.IV.2017, hand collecting, leg. L. Crespo & I. Silva; Pedras Vermelhas, 2 ♂♂ and 1 juvenile (SMF65689), 7.VII.1983, leg. K. Groh; Pico Ana Ferreira, 33.04728°N, 16.37171°W, 1 ♂ (CRBALC0310: LC224), 1 ♀ (CRBALC0327: LC239) and 5 juveniles (CRBALC0303: LC192, CRBALC0307: LC196, CRBALC0326: LC238, CRBALC0309: LC281, CRBALC0430: LC285), 20.IV.2017, hand collecting, leg. L. Crespo & I. Silva; Pico Branco, 33.09428°N, 16.30137°W, 1 ♂ (CRBALC0304: LC193), 21.IV.2017, hand collecting, leg. L. Crespo & I. Silva, 1 ♂ (CRBALC0314: LC227), 23.IV.2017, hand collecting, leg. L. Crespo; Pico da Juliana, 33.09270°N, 16.32186°W, 1 juvenile (CRBALC0286: LC186), 24.IV.2017, hand collecting, leg. L. Crespo; Pico do Castelo, 33.08196°N, 16.33277°W, 2 ♀♀ (CRBALC0300: LC189, CRBALC0322: LC235) and 2 juveniles (CRBALC0267: LC180, CRBALC0268: 181), 17.IV.2017, hand collecting, leg. L. Crespo & I. Silva, 1 ♂ (CRBALC0692), 8.IV.2018, hand collecting, leg. L. Crespo & A. Bellvert; Pico do Concelho, 1 ♀ (SMF65695), 29.VI.1983, leg. K. Groh; Pico do Espigão, 1 ♀ (SMF65692), 1.VII.1983, leg. K. Groh; Pico do Facho, 1 ♀ (SMF65694), 28.VI.1983, leg. K. Groh; Pico do Maçarico [the label reads “Pico dos Magaricos”, therefore we find it necessary

to present the correct locality name], 1 ♀ (SMF65691), 10.VII.1983, leg. K. Groh; Terra-Chá (Pico Branco), 33.09447°N, 16.29839°W, 1 ♂ (CRBALC0323: LC236) and 2 juveniles (CRBALC0324: LC327, CRBALC0396: LC283), 21.IV.2017, hand collecting, leg. L. Crespo & I. Silva, 4 juveniles (CRBALC0627, CRBALC0628, CRBALC0630, CRBALC0700), 10.IV.2018, hand collecting, leg. L. Crespo & A. Bellvert. Unknown location • 1 ♀ (NHRS-JUST-000001115), 1 ♂ (MMUE G7508.48), 28.VIII.1981, under stone, leg. J. Murphy, 1 ♂ 1 ♀ and 2 juveniles (SMF34577), 1983, leg. G. Schmidt, 1 ♂ and 1 ♀ (SMF65690), hand collecting, leg. I. Silva, 1 ♀ (NHM 1892.7.9.12.17), leg. W.R.O. Grant.

Diagnosis. *Hogna insularum* can be diagnosed from all other Madeiran *Hogna* by a combination of the following characters: the small to medium size (prosoma length < 10 mm), the aspect of its legs, brown, with black patches (Fig. 27C), male's embolus thin, with smoothly curved tip (Fig. 15), and female epigyne median septum roughly half as wide (at posterior transverse part) as long (Fig. 16A, C, E, G). It is most similar to *H. heeri* and *H. isambertoii* sp. nov., from which it cannot be somatically differentiated.

Redescription. Male (CRBALC0310): (Fig. 15A, E, F). Total length: 7.8; carapace: 4.6 long, 3.3 wide.

Colour: carapace greyish brown, covered with short black setae, with a median cream longitudinal band, anteriorly broadened, covered with short white setae, with suffused greyish brown patches; two yellow marginal bands, with roughly round grey patches, covered with short white setae; four black striae well visible on each flank. Chelicerae brownish orange, with blackish patches, covered in black and white setae. Gnathocoxae greyish yellow, labium overall blackish, with anterior margin greyish yellow; sternum yellow, with a V-shaped grey patch and suffused patches at lateral borders. Legs pale yellow to orange from femora to tibia, with irregular grey suffused patches, metatarsi and tarsi brown. Pedipalps pale yellow except tarsus, brown. Abdomen with a pair of anterolateral black patches, extending laterally into grey flanks, mottled with yellowish patches covered with white setae; a median dark lanceolate patch is bordered by two yellowish longitudinal bands interconnected in anterior half, posteriorly by means of dark chevrons; venter yellowish, with a median dark grey longitudinal band, bordered by small yellowish and grey patches.

Eyes: MOQ: MW = 0.8 PW, MW = 1.1 LMP, MW = 1.2 AW; CI = 0.3 DAME. Anterior eye row slightly procurved.

Legs: Measurements: Leg I: 13.6, TiI: 3.1; Leg IV: 14.9, TiIV: 3.1; TiIL/D: 5.5. Spination of Leg I: FeI: d1.1.0, p0.0.1–2; TiI: p1s.0.1s, r1s.0.1s, v2l.2l.2s; MtI: p0.1.1, r0.0.1, v2l.2l.1s. MtI with sparse scopulae in basal half and dense scopulae on distal half.

Pedipalp: cymbium with five dark, stout, macrosetae at tip, Fe with two dorsal and an apical row of four spines, Pa with one prolateral spine, Ti with one dorsal and one prolateral spines. Tegular apophysis with ventral spur short, blunt, with a straight ridge leading to a wide apical point (Fig. 15D); terminal apophysis blade-shaped with sharp end (Fig. 15A–C); embolus long and thin, with tip smoothly curved anteriorly (Fig. 15A–C); palea large (Fig. 15A–C).

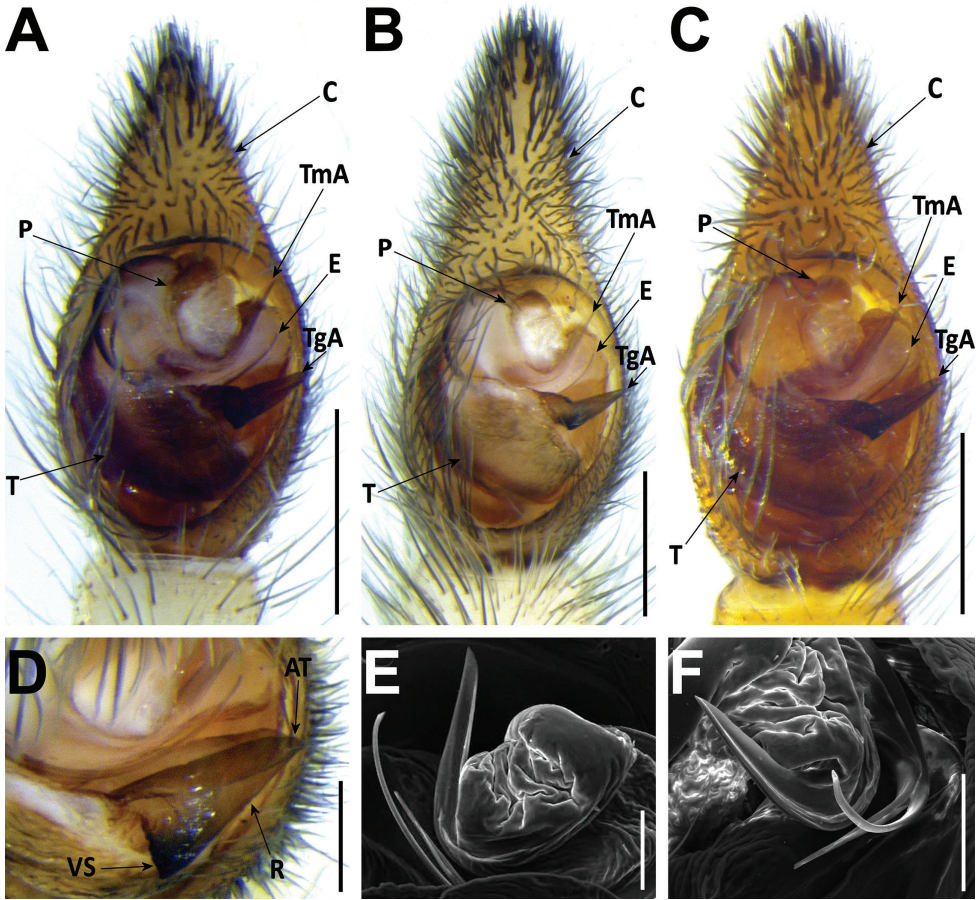


Figure 15. *Hogna insularum*, male pedipalps **A** male from Porto Santo (CRBALC0310), left pedipalp, ventral **B** male from Deserta Grande (CRBALC0305), left pedipalp, ventral **C** male from Bugio (CRBALC0015), left pedipalp, ventral **D** detail of the median apophysis of male from Deserta Grande (CRBALC0305), anteroventral **E** SEM image, right male pedipalp, male from Porto Santo (CRBALC0310), ventral **F** idem, retroventral. Abbreviations, male pedipalp: AT – anterior point, C – cymbium, E – embolus, P – palea, R – ridge, T – tegulum, TA – terminal apophysis, TgA – tegular apophysis, VS – ventral spur. Scale bars: 0.5 mm (**A, B, C**); 0.2 mm (**D**).

Female (CRBALC0308): (Fig. 16C–D). Total length 12.8; carapace: 5.4 long, 4.1 wide.

Colour: overall as in male, but darker in legs, chelicera and prosoma. Sternum with a faint V-shaped grey patch. Abdomen is lighter, with central chevrons and ventral longitudinal dark band faded.

Eyes: MOQ: MW = 0.8 PW, MW = 1.2 LMP, MW = 1.2 AW; Cl = 0.6 DAME. Anterior eye row slightly procurved.

Legs: Measurements: Leg I: 13.8, TiI: 3.1; Leg IV: 16.0, TiIV: 3.3; TiIL/D: 3.7. Spination of Leg I: FeI: d1.1.0, p0.0.2; TiI: p0.1s.0, v2l.2l.2s; MtI: p0.0.1, r0.0.1, v2l.2l.1s. MtI with sparse scopulae in basal half and dense scopulae on distal half.

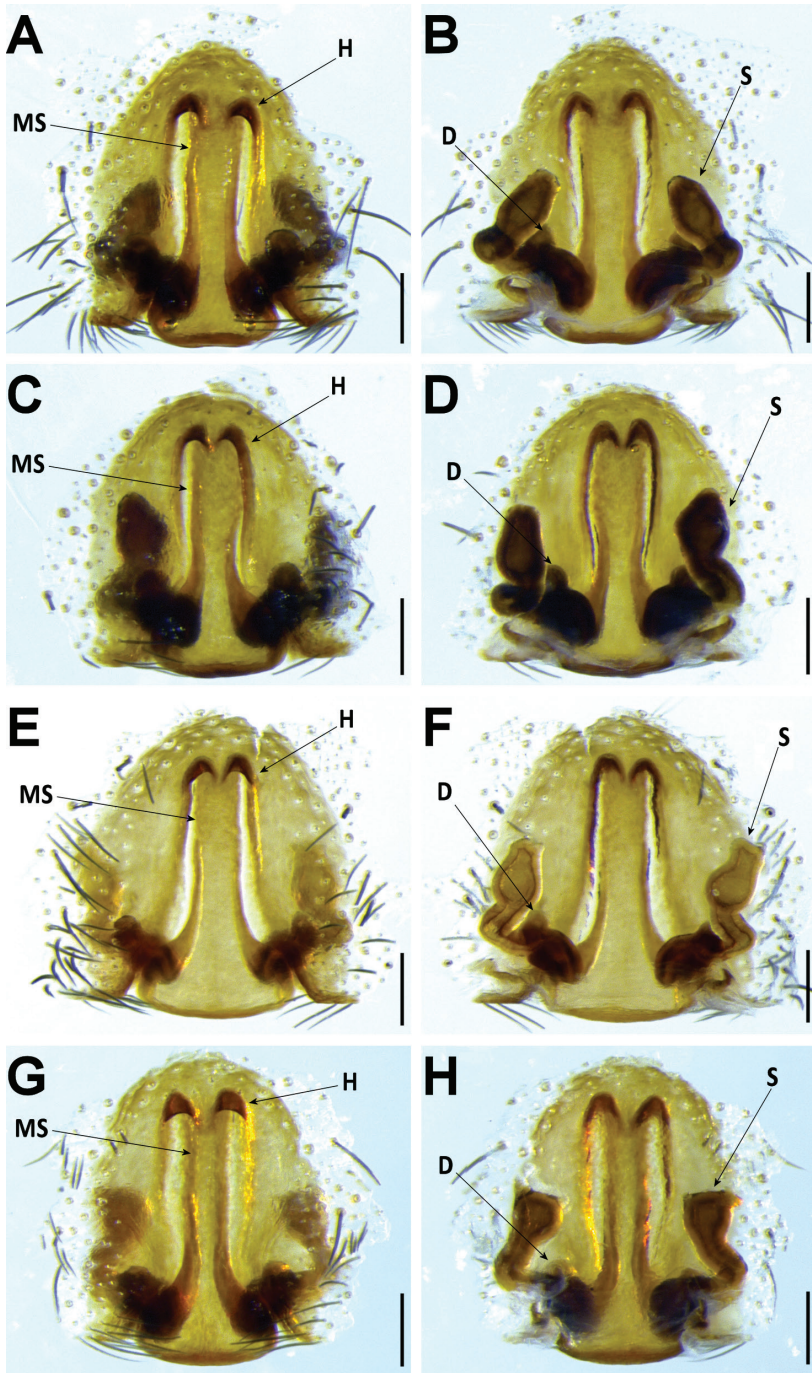


Figure 16. *Hogna insularum*, female genitalia **A, B** female from Bugio (CRBALC0301): **A** epigynum, ventral **B** vulva, dorsal **C, D** female from Deserta Grande (CRBALC0308): **C** epigynum, ventral **D** vulva, dorsal **E, F** female from Madeira (CRBALC0597): **E** epigynum, ventral **F** vulva, dorsal **G, H** female from Porto Santo (CRBALC0300): **G** epigynum, ventral **H** vulva, dorsal. Abbreviations, female genitalia: D – diverticulum, H – epigynal hoods, MS – median septum, S – spermatheca. Scale bars: 0.2 mm.

Epigyne: anterior pockets almost touching, short, with lateral borders parallel (Fig. 16C); anterior pocket cavities shallow; median septum with narrow posterior transverse part (Fig. 16C); spermathecae oval or piriform (Fig. 16D); copulatory ducts with small, stout diverticulum ventrally (Fig. 16D); fertilisation ducts emerging at the base of copulatory duct (Fig. 16D).

Intraspecific variation. Carapace length, males: 4.6–6.4, females: 5.1–7.4. Length of cymbium tip of male pedipalp can vary from shorter to longer than the bulbus. In the single available adult female from Madeira, the anterior pockets of the epigyne show slightly divergent lateral borders (posteriorly) (Fig. 16E), while specimens from the remaining islands show parallel lateral borders.

Distribution. This species is known from many locations on all islands of the archipelago except Madeira island, where it is only present at the southeast coastal region (Fig. 17).

Ecology. *Hogna insularum* occurs in a wide variety of habitats, from grasslands, *Erica* shrubland, to secondary forests (in the latter two cases, only in Porto Santo).

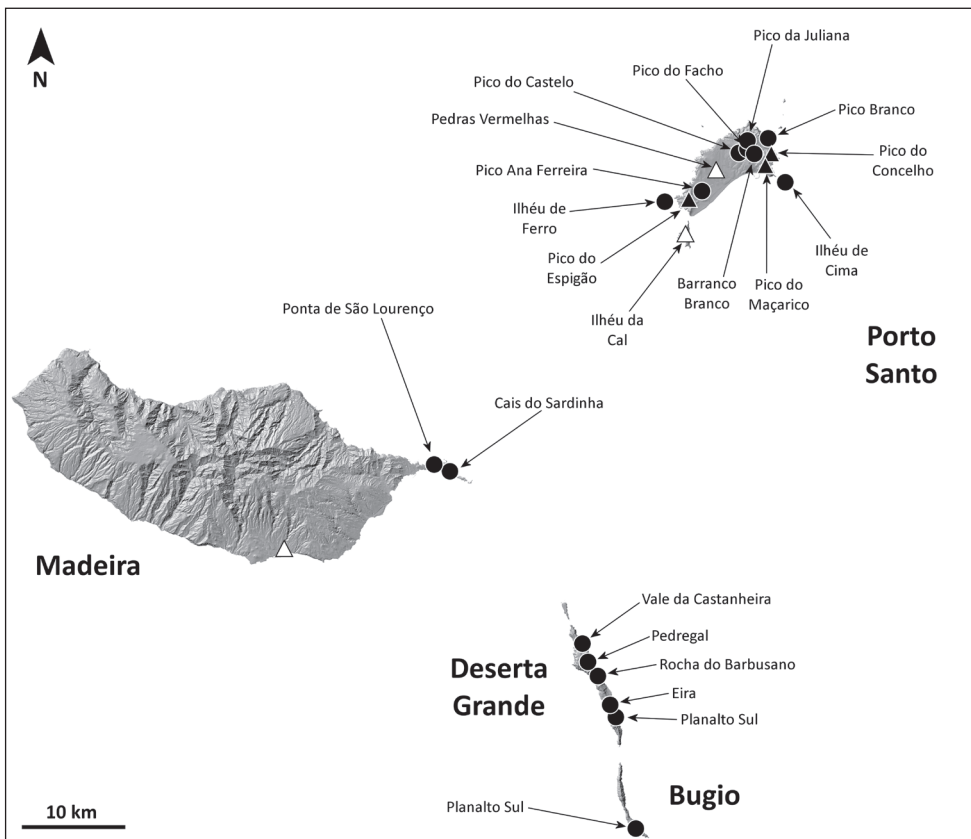


Figure 17. Distribution of *H. insularum*. Circles: present records; black triangles: revised records from literature; white triangles: unconfirmed records from literature.

Conservation status. *Hogna insularum* was assessed according to the IUCN Red List criteria, with the status of Least Concern (Cardoso et al. 2018c).

Comments. *Hogna insularum* displays remarkable intraspecific variation. In males, both the length of the cymbium tip and the position of the terminal apophysis relative to the embolus are variable (Fig. 15). In females, the epigyne usually presents anterior pockets with anteriorly parallel lateral borders, but a specimen from Madeira shows a posteriorly divergent lateral border. At the same time, the shape of spermathecae seem to vary from ovoid (Fig. 16A–D), to piriform (Fig. 16E, F), to rounded (Fig. 16G, H). Wunderlich (1992) described *H. biscoitoi* based on specimens from Porto Santo. To differentiate it from *H. insularum* he stated that in males “the sickle-shaped apophysis points more to the tip of the cymbium” while in the former species the same structure “(...) is directed more retrolaterally”. For females, although a diagnostic description was provided, the identification key directed to the same image when referring to the epigyne of both *H. insularum* and *H. biscoitoi*. We collected an array of specimens from different localities in Porto Santo (from Pico Ana Ferreira to Pico Branco) and surrounding islets. We did observe male pedipalps with different degrees of inclination of the terminal apophysis and with cymbium tip shorter than the length of the copulatory bulbus (Fig. 15A, C), but both characters were unlinked. We suspect that these traits may be affected by the time from the last moult (e.g., Fig. 15B was most likely a recently moulted individual, given its overall pale coloration). Furthermore, fixation in ethanol might sometimes cause a displacement of sclerites, even if small. Molecular data does not seem to provide any additional evidence regarding the possibility that the specimens from Porto Santo may belong to a different species than those reported from other islands. Unfortunately, we could not examine the type material of *H. biscoitoi* stored at the Funchal Municipal Museum, since it does not loan type material for study. Based on the variability in the supposedly diagnostic features and the lack of genetic divergence, we consider *H. biscoitoi* as a junior synonym of *H. insularum*.

***Hogna isamberto* Crespo, sp. nov.**

<http://zoobank.org/87BB2C30-D40D-4B5D-92F5-D7D23ED9A7BC>

Figures 18–20

Hogna heeri Crespo et al. 2013: 18 (m, misidentification).

Types. Holotype: DESERTA GRANDE • 1 ♂, Ponta Sul, 32.49562°N, 16.49562°W, coll. 4.XI.2017, leg. I. Silva, stored at SMF, collection number to be set after publication.

Paratypes: BUGIO • 1 ♂ (SMF), Planalto Sul, 3.XII.2012, hand collecting, leg. I. Silva. DESERTA GRANDE • Planalto Sul, 1 ♀ (SMF), 12.XI.2017, hand collecting, leg. I. Silva.

Material examined. DESERTA GRANDE • Planalto Sul, 1 juvenile (CRBALC0610: LC330), 12.XI.2017, hand collecting, leg. I. Silva.

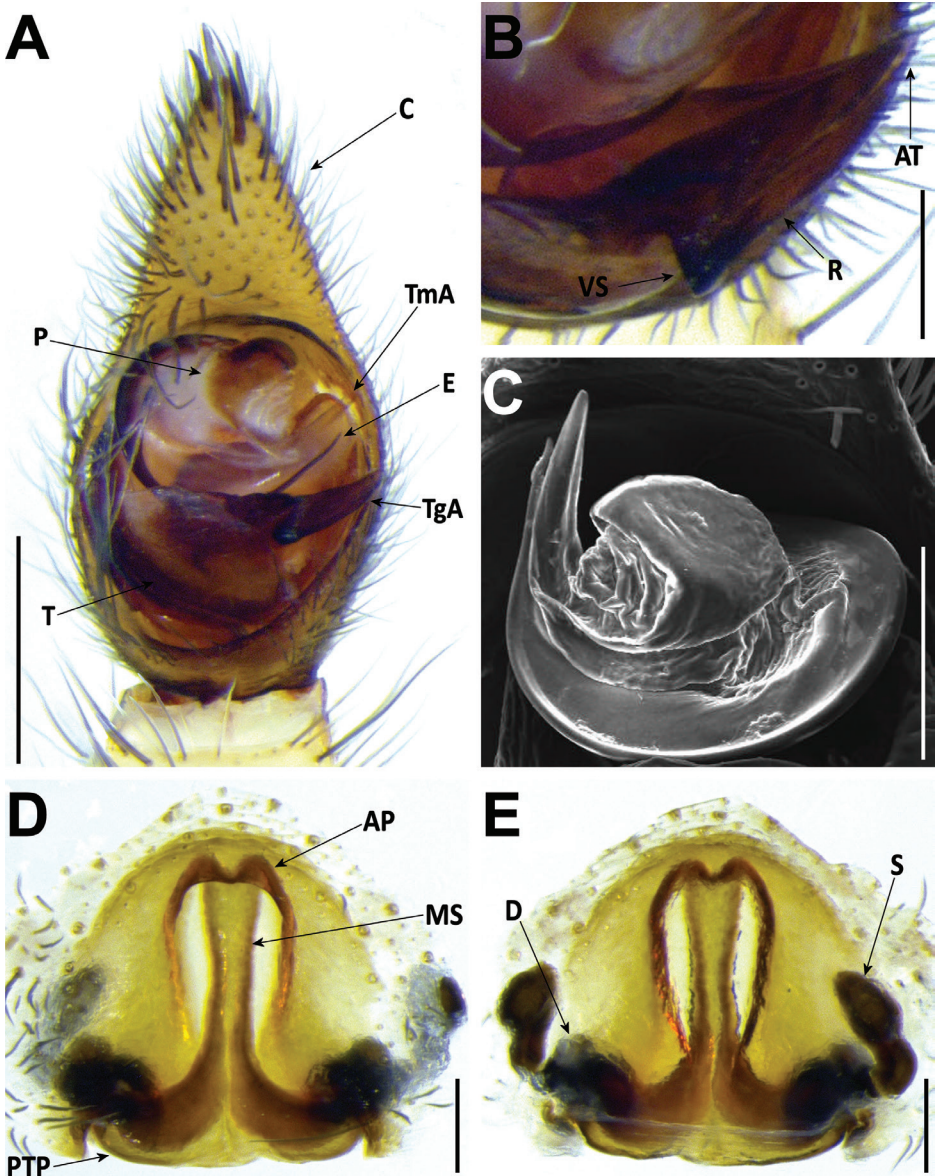


Figure 18. *Hogna isambertoi* sp. nov. **A–C** male (SMF): **A** left male palp, ventral **B** detail of the median apophysis, anteroventral **C** SEM image, right male palp, ventral **D, E** female (SMF): **D** epigynum, ventral **E** vulva, dorsal. Abbreviations, male palp: C – cymbium, E – embolus, MA – median apophysis, P – palea, T – tegulum, TA – terminal apophysis. Abbreviations, female genitalia: D – diverticulum, H – epigynal hoods, MS – median septum, S – spermatheca. Scale bars: 0.5 mm (**A**); 0.2 mm (**B–E**).

Diagnosis. *Hogna isambertoi* sp. nov. can be distinguished from all other Madeiran *Hogna* by its genitalia. In males, the embolus is thick and tilted anteriorly at the tip and a tegular apophysis with a very short ventral spur (Fig. 18A, C). In females, the epigynal anterior pockets show convergent lateral borders and the median septum has a wide

posterior transverse part (Fig. 18D). It is most similar to *H. heeri* and *H. insularum*, from which it cannot be somatically differentiated.

Description. Male holotype: (Figs 18A–C, 19A). Total length: 7.4; carapace: 4.6 long, 3.2 wide.

Colour: carapace greyish brown, covered with short black setae, with a median yellow longitudinal band, anteriorly broadened, covered with short white setae; two yellow marginal bands, suffused with grey patches, covered with short white setae; four black striae well visible on each flank. Chelicerae yellow, with grey suffused patches, covered in black and white setae. Gnathocoxae and labium overall pale yellow, with posterior margin with suffused grey patch; sternum pale yellow, with V-shaped grey patch. Legs pale yellow, with irregular grey suffused patches, except anterior metatarsi and tarsi, yellowish orange. Pedipalps yellow. Abdomen with a pair of anterolateral black patches, extending laterally into grey to black flanks; a median faint dark lanceolate patch is bordered by two yellowish longitudinal bands interconnected in anterior half, posteriorly by means of dark chevrons; venter yellowish, with large blackish patches near spinnerets and small patches medially.

Eyes: MOQ: MW = 0.8 PW, MW = 1.1 LMP, MW = 1.1 AW; CI = 0.5 DAME. Anterior eye row slightly procurved.

Legs: Measurements: Leg I: 11.7, TiI: 2.6; Leg IV: 13.8, TiIV: 2.8; TiIL/D: 6.6. Spination of Leg I: FeI: d1.1.1, p0.0.1; TiI: p1.0.1, v2l.2l.2s; MtI: p0.0.1, r0.0.1, v2l.2l.1s. MtI with sparse scopulae in basal half and dense scopulae on distal half.

Pedipalp: cymbium with one spine along prolateral rim and five dark, stout, macrosetae at tip, Fe with two dorsal and an apical row of four spines. Tegular apophysis

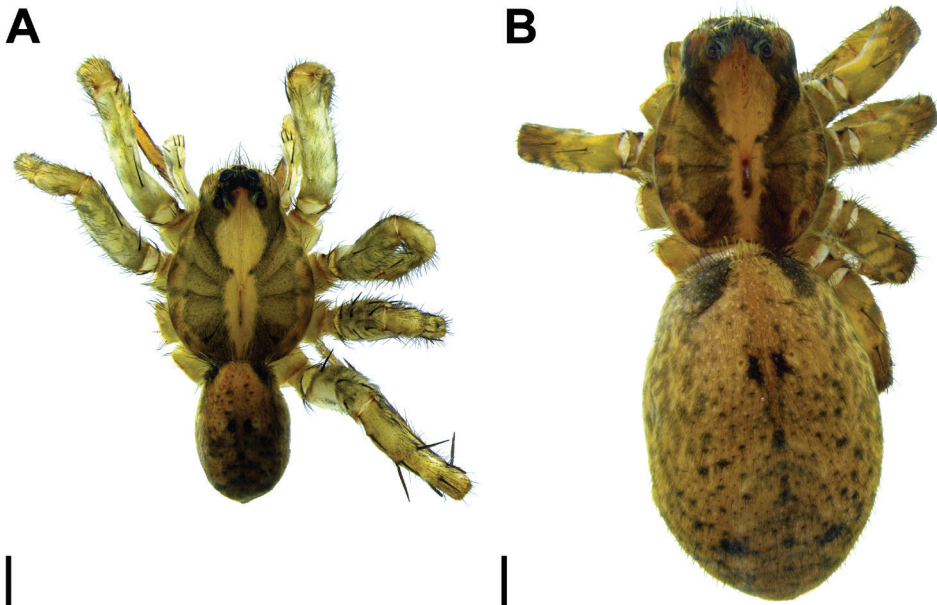


Figure 19. *Hogna isambertoi* sp. nov. **A** male habitus, dorsal (SMF) **B** female habitus, dorsal (SMF). Scale bars: 1 mm.

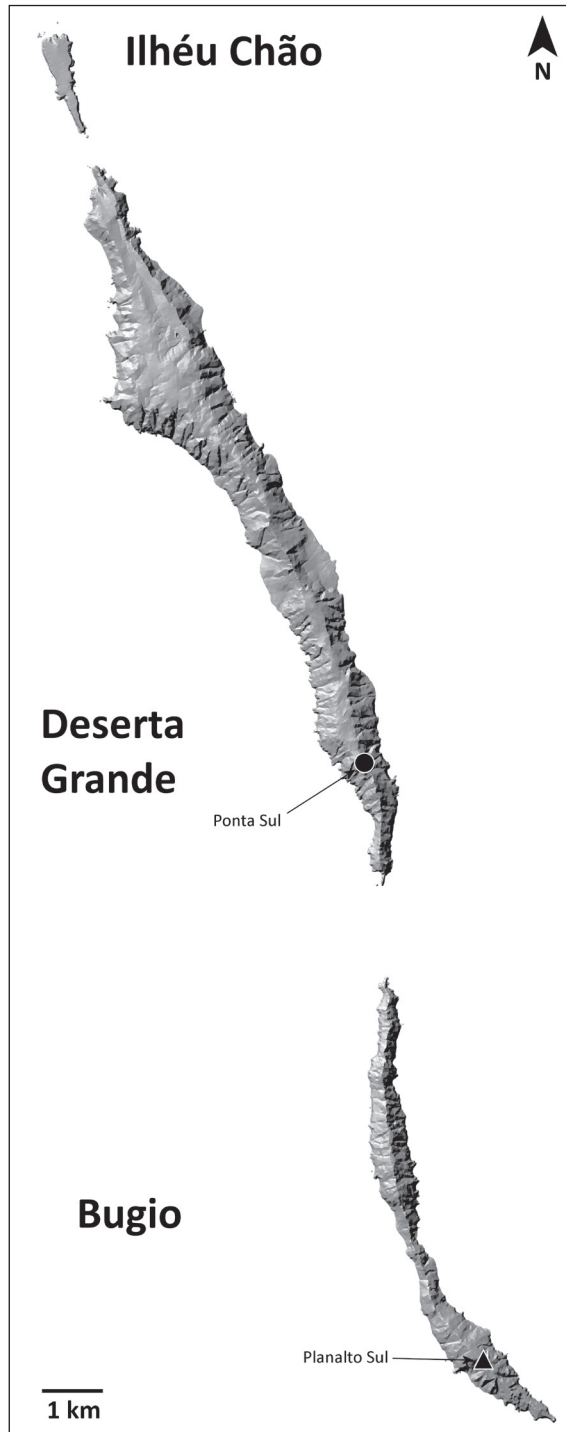


Figure 20. Distribution of *H. isambertoi* sp. nov. Circles: present records; black triangle: revised record from literature.

with ventral spur very short, blunt, with a concave ridge leading to a thin apical point (Fig. 18A, B); terminal apophysis in close apposition with subterminal apophysis, which is blade-shaped with blunt end (Fig. 18A, C); embolus long and thick, with tip tilted anteriorly (Fig. 18A); palea large (Fig. 18A).

Female paratype: (Figs 18D, E, 19B). Total length 12.1; carapace: 4.7 long, 3.6 wide.

Colour: overall as in male, but darker in legs, chelicera and prosoma, where additional faint striae are present. Abdomen is lighter, with central chevrons faded, possibly due to pregnancy and correspondent tegument extension.

Eyes: MOQ: MW = 0.8 PW, MW = 1.2 LMP, MW = 1.8 AW; CI = 0.4 DAME. Anterior eye row slightly procurved.

Legs: Measurements: Leg I: 9.9, TiI: 1.7; Leg IV: 13.0, TiIV: 2.6; TiIL/D: 3.2. Spination of Leg I: FeI: d1.1.0, p0.0.1–2; TiI: p0.0.0–1, v2l.2l.2s; MtI: p0.0.1, r0.0.1, v2l.2l.1s. MtI with sparse scopulae in basal half and dense scopulae on distal half.

Epigyne: anterior pockets touching, short, with lateral borders parallel (Fig. 18D); anterior pocket cavities deep; median septum with wide posterior transverse part (Fig. 18D); spermathecae oval (Fig. 18E); copulatory ducts simple (Fig. 18E); fertilisation ducts emerging at the base of copulatory duct (Fig. 18E).

Etymology. the specific epithet is a patronym in honour of Isamberto Silva, who not only collected the only known specimens of this species, but has provided invaluable support during field work.

Intraspecific variation. Carapace length, males: 4.1–4.3.

Distribution. This species is known only from the southernmost part of Deserta Grande and Bugio (Fig. 20).

Ecology. *Hogna isambertoii* sp. nov. occurs in arid, coastal scarps, with reduced vegetation cover.

Conservation status. the species seems to be restricted to a very small area, equivalent to an Extent of Occurrence and Area of Occupancy of 8 km² in two locations, both threatened by the effects of increasing aridification. The trends are unknown, but it is uncertain if the scarcity of specimens is due to rarity, or the fact that it seems to be a late autumn / early winter species, when collecting effort has been low. If the decline is confirmed the status might be Endangered, if not it might be Near Threatened.

Hogna maderiana (Walckenaer, 1837)

Figures 21–23

Lycosa tarentuloides maderiana Walckenaer, 1837: 291 (Df).

Lycosa tarentuloides maderiana Blackwall, 1857a: 282 (Dm).

Tarentula maderiana Simon, 1864: 350.

Lycosa maderiana Simon, 1898: 346.

Trochosa maderiana Kulczynski, 1899: 426, pl. 9, fig. 119–120 (mf).

Isobogna maderiana Roewer, 1955: 241.

Isobogna maderiana Roewer, 1960: 569, fig. 319a–c (mf).

Hogna schmitzi Wunderlich, 1992: 462, fig. 721–723 (Dmf). Holotype ♂ examined, Porto Santo, 8–11.VII.1983; leg. K. Groh, stored at SMF, collection number 37639. New synonymy.

Types. Holotype: Not examined, supposed lost.

Material examined. ILHÉU DE FERRO • 1 ♂ and 1 ♀ (SMF37637), 3.VII.1983, leg. K. Groh., 1 ♂ (CRBALC0013), 33.03698°N, 16.40814°W, 6.IV.2011, hand collecting, leg. I. Silva. PORTO SANTO • Pico Branco, 33.09366°N, 16.30776°W, 1 ♂ (CRBALC0734) and 2 ♀♀ (CRBALC0704, CRBALC0717), 10.IV.2018, hand collecting, leg. L. Crespo & A. Bellvert; Pico do Facho, 1 ♂ (SMF63869), 31.X.1972; (unknown location), 1 ♀ (MNHNP AR16184), 27.III.1959, leg. A. Vandel, 2 ♀♀ and 2 juveniles (FMNH <http://id.luomus.fi/KN.23945>), 4.X.1959, 1 ♀ (SMF34482), VII.1983, 1 ♀ (SMF36760), 26.X.1985, leg. G. Schmidt, 1 ♀ (SMF37636) and 2 juveniles (SMF37638), leg. K. Groh, 8 ♂♂ and 11 ♀♀ (NHM, in ethanol), VI.1962, leg. S.W. Bristowe, 1 ♀ (NHM), VII.1963, leg. B.M. Clifton, 2 ♂♂ and 2 ♀♀ (NHM 1892.7.9.12.17), leg. W.R.O. Grant, 1 ♀ (NHM), 12.VI.1964, 1 ♂ and 1 ♀ (NHM, mounted dry).

Diagnosis. *Hogna maderiana* can be distinguished from all other Madeiran *Hogna* by a combination of the following characters: the large size (prosoma length > 10 mm), the presence of conspicuous orange setae (Fig. 27A), and its genitalia. In males by a combination of a smoothly curved tip of the embolus, a long, blunt ventral spur, and a deeper tegular concavity (Fig. 21A–D). In females by epigyne with median septum more than twice as long as wide (at posterior transverse part) (Fig. 21E, F).

Redescription. Male (CRBALC0734): (Fig. 21D, E). Total length: 19.5; carapace: 11.9 long, 8.9 wide.

Colour: carapace brown, with short black setae covering flanks, short white setae present posteriorly, anteriorly and laterally, long black setae are present anteriorly or scattered around median band; median yellow longitudinal band present but faint, covered with short white setae and scattered long black setae, anteriorly broadened; marginal bands indistinct, made apparent only by the cover of short white setae, long black setae also present laterally; four darker lateral bands visible, but without striae. Chelicerae black, apically dark brown, covered in black and yellow setae. Gnathocoxae very dark orange-brown, labium blackish; sternum brown, medially lighter, but without any stripe. Legs yellow to orange-brown, without annulations, with anterior tibiae, all metatarsi and tarsi dark brown, and covered dorsally with yellow setae (probably orange in living or fresh specimen). Pedipalpal femur, patella, and tibia as legs, cymbium darker, yellow setae present in all segments except femur. Abdomen with a pair of anterolateral black patches, extending laterally into grey flanks; a median yellow lanceolate patch is bordered by few whitish patches; venter greyish, darker near spinnerets.

Eyes: MOQ: MW = 0.7 PW, MW = 1.2 LMP, MW = 1.2 AW; CI = 0.5 DAME. Anterior eye row slightly procurved.

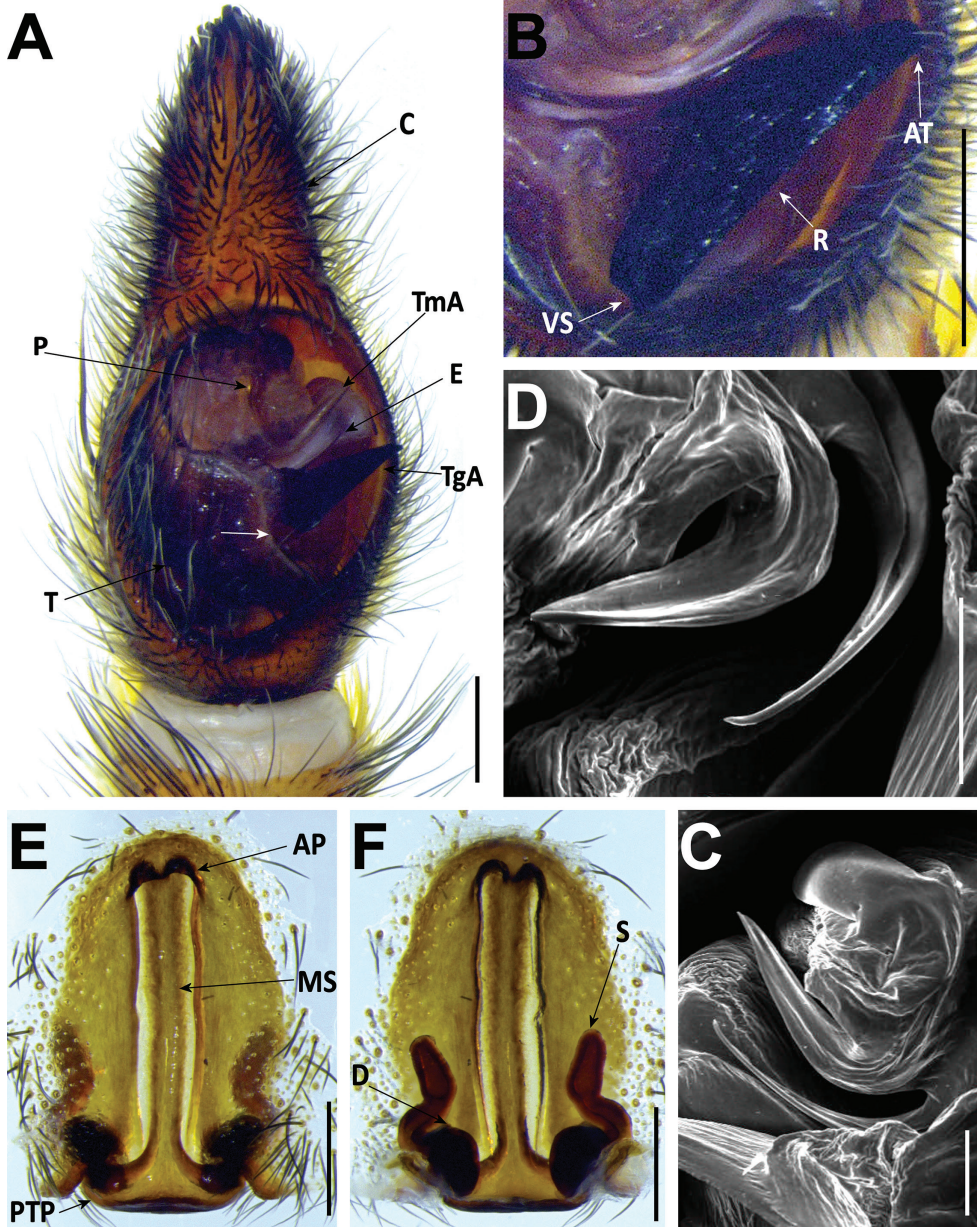


Figure 21. *Hogna maderiana* **A–D** male (CRBALC0734): **A** left male palp, ventral (white arrow points to a tegular concavity that may be helpful for diagnosis) **B** detail of the median apophysis, anteroventral **C** SEM image, right male palp, ventral **D** idem, retroventral **E, F** female (CRBALC0717): **E** epigynum, ventral **F** vulva, dorsal. Abbreviations, male pedipalp: AT – apical point, C – cymbium, E – embolus, P – palea, R – ridge, T – tegulum, TA – terminal apophysis, TgA – tegular apophysis, VS – ventral spur. Abbreviations, female genitalia: D – diverticulum, H – epigynal hoods, MS – median septum, S – spermatheca. Scale bars: 0.5 mm (**A, B, E, F**); 0.2 mm (**C, D**).



Figure 22. Photograph of *H. maderiana*. Female specimen in the field. Photograph credit Pedro Cardoso.

Legs: Measurements: Leg I: 36.7, TiI: 8.85; Leg IV: 37.3, TiIV: 8.1; TiIL/D: 4.4. Spination of Leg I: FeI: d1.1.0, p0.0.2; TiI: p1.0.1, r1.0.0, v2s.2s.2s; MtI: p0.0.1, r0.0.1, v2s.2s.1s. MtI with very dense scopulae.

Pedipalp: cymbium with one prolateral spine and six dark, stout, macrosetae at tip, Fe with two dorsal and an apical row of four spines, Pa with one prolateral spine, Ti with one dorsoprolateral and one prolateral spines. Tegular apophysis with ventral spur long, blunt, with a straight ridge leading to a wide apical point (Fig. 21A, B); terminal apophysis blade-shaped with sharp end (Fig. 21A–D); embolus long, with tip directed anterolaterally (Fig. 21A–D); palea small (Fig. 21A).

Female (CRBALC0717): (Fig. 21E, F). Total length 23.5; carapace: 11.3 long, 8.3 wide.

Colour: overall as in male, with the following differences: median yellow longitudinal band in prosoma clear. Cheliceral setae black. Legs with few faint greyish patches in femora. Abdominal pattern overall greyish, darker near spinnerets, with patches unapparent.

Eyes: MOQ: MW = 0.7 PW, MW = 1.1 LMP, MW = 1.2 AW; CI = 0.4 DAME. Anterior eye row slightly procurved.

Legs: Measurements: Leg I: 30.3, TiI: 7.2; Leg IV: 33.9, TiIV: 7.4; TiIL/D: 3.5. Spination of Leg I: FeI: d1.1.0, p0.0.2; TiI: 0.1s.0, v2s.2s.2s; MtI: p0.0.1, r0.0.1, v2l.2s.1s. MtI with very dense scopulae.

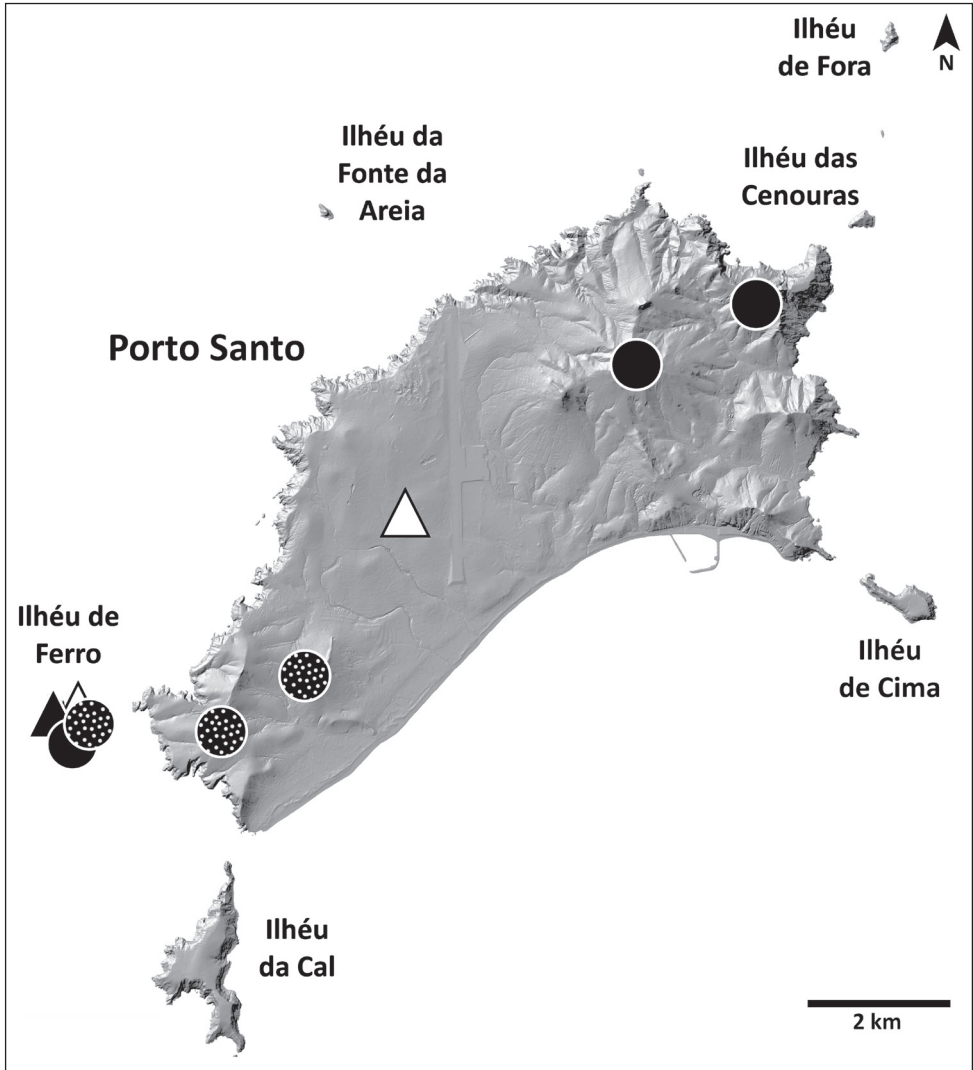


Figure 23. Distribution of *H. maderiana*. Black circles: present records; dotted circles: records from only leg samples; black triangles: revised records from literature; white triangles: unconfirmed records from literature.

Epigyne: anterior pockets touching, short, with lateral borders parallel (Fig. 21E); anterior pocket cavities deep; median septum with narrow posterior transverse part (Fig. 21E); spermathecae elongated (Fig. 21F); copulatory ducts with very small diverticulum ventrally (Fig. 21F); fertilisation ducts emerging at the base of copulatory duct (Fig. 21F).

Intraspecific variation. Carapace length, males: 11.9–14.4, females: 11.0–11.5.

Distribution. This species is known from the island of Porto Santo and one of its surrounding islets, Ilhéu de Ferro (Fig. 23).

Ecology. *Hogna maderiana* can be found in open habitats, such as grasslands, shrubland or sand banks. Very common even in relatively disturbed habitats across Porto Santo.

Conservation status. *Hogna maderiana* was assessed according to the IUCN Red List criteria as *H. schmitzi* (Cardoso et al. 2018d), with the status of Least Concern.

Comments. As mentioned above (see remarks on *H. blackwalli*), the large specimens with striking orange coloration in legs from Porto Santo island and its neighbouring islet Ilhéu de Ferro were known to pioneer arachnologists. The original, somewhat obscure, description by Walckenaer described a 2.5 cm spider (“1 pouce”) with reddish brown legs (“Pattes rouges, lavées de brun en dessus (...)”), from the island of Madeira (“Ile de Madère”). After this, Blackwall was the first to provide a clear description of this taxon, while at the same time stating that it was collected in the island of Porto Santo, not Madeira. Subsequent authors reported additional material from either Porto Santo or Ilhéu de Ferro (Johnson 1863; Kulczynski 1899). Wunderlich considered *H. blackwalli* a junior synonymy of *H. maderiana* based on the wrong assumption that previous authors repeatedly misidentified *H. maderiana* from Porto Santo, assigning *H. maderiana* to the large species with annulated legs from Madeira island. Following synonymy, Wunderlich himself named the large species from Porto Santo as *H. schmitzi*. As a matter of fact, the only indication of the presence of a large spider with reddish leg coloration in Madeira island is Walckenaer’s original description. Unfortunately, Walckenaer’s type seems to be lost. However, Simon most likely examined it because he stated that “*L. maderiana* Walck. est, en grande partie, revêtu, en dessus, de pubescence courte d’un beau rouge orange.” (Simon 1898: 332). The two large species are easy to distinguish, the only misidentification between them being made by Thorell, who identified *H. blackwalli* from Madeira as *Trochosa maderiana* (Thorell 1875). We argue that the presence of *H. maderiana* in the island of Madeira reported in Walckenaer’s original description was likely a labelling mistake or a misinterpretation, and probably referred to the archipelago.

***Hogna nonannulata* Wunderlich, 1995**

Figures 24, 25

Types. Holotype: MADEIRA • 1 ♂, coll. 25–30.IV.1957, leg. Roewer, stored at SMF, collection number 10754. Examined.

Material examined. MADEIRA • Câmara de Lobos, 32.6525°N, 16.96683°W, 1 ♂ (CRBALC0703: LC326), 27.V.2018, hand collecting, leg. É. Pereira, 1 ♂ (CRBALC0701: LC325, CRBALC0702: LC324), 29.V.2018, hand collecting, leg. I. Silva & É. Pereira, 1 ♂ (CRBALC0608: LC328), 21.VI.2017, hand collecting, leg. I. Silva, 1 ♂ (CRBALC0607: LC327), 11.VIII.2017, hand collecting, leg. I. Silva.

Diagnosis. *Hogna nonannulata* can be distinguished from all other Madeiran *Hogna* by the aspect of its legs, without annulations or bright yellow or orange setae (Fig. 24D). In addition, males have an elongate cymbium tip, clearly longer than the

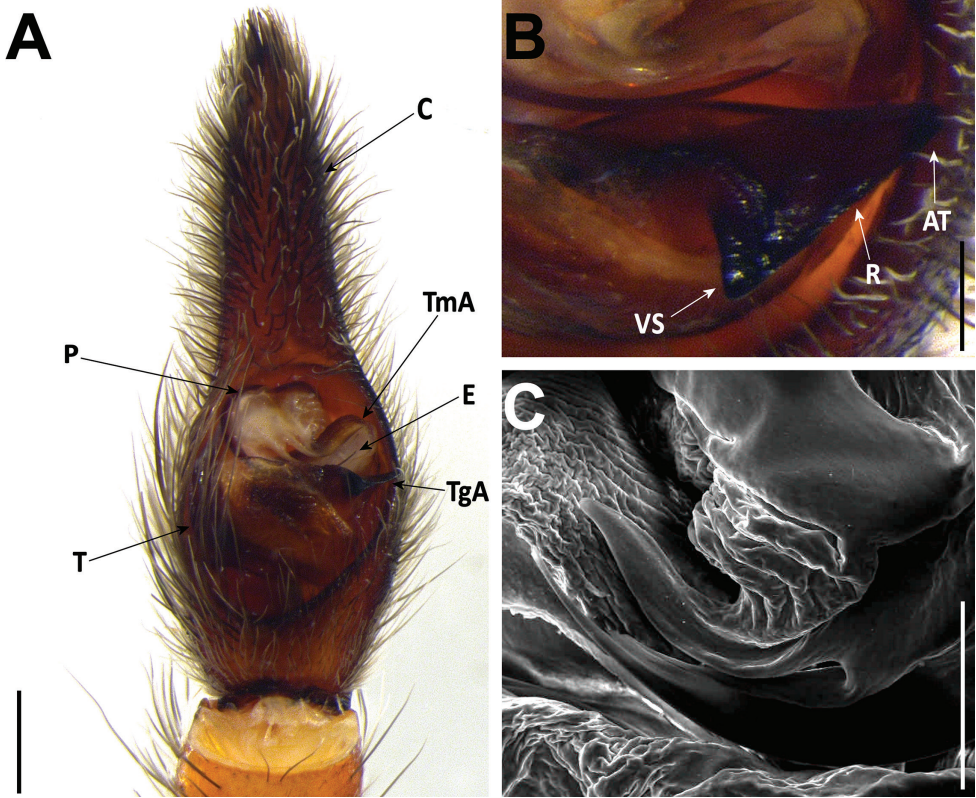


Figure 24. *Hogna nonannulata* male (CRBALC0701): **A** left male pedipalp, ventral **B** detail of the median apophysis, anteroventral **C** SEM image, right male pedipalp, ventral. Abbreviations, male pedipalp: AT – apical point, C – cymbium, E – embolus, P – palea, R – ridge, T – tegulum, TA – terminal apophysis, TgA – tegular apophysis, VS – ventral spur. Scale bars: 0.5 mm (**A**); 0.2 mm (**B, C**).

length of the alveolus of the bulb (Fig. 24A). We could not revise any female materials, for which we propose that the leg aspect can be used to diagnose females.

Redescription. Male (CRBALC0701): (Fig. 24). Total length: 18.6; carapace: 10.3 long, 8.2 wide.

Colour: carapace greyish brown with transverse yellowish bands, generally covered with short black setae, except anteriorly and laterally, provided with short white setae and long black setae; median yellow longitudinal band present, anteriorly broadened, with suffused greyish brown patches; two yellow marginal bands, suffused with greyish brown patches; ca. seven faint blackish striae on each flank. Chelicerae blackish to dark brown, mostly covered with black and white setae. Gnathocoxae very dark orange-brown, labium blackish; sternum yellowish grey, with a faint, longitudinal yellow stripe extending to less than half of sternum length. Legs yellow to brown, without any clearly coloured patch, just scattered areas suffused with grey, grey setae present in tibia, metatarsus and tarsus. Pedipalpal femur, patella, and tibia yellow, except cym-

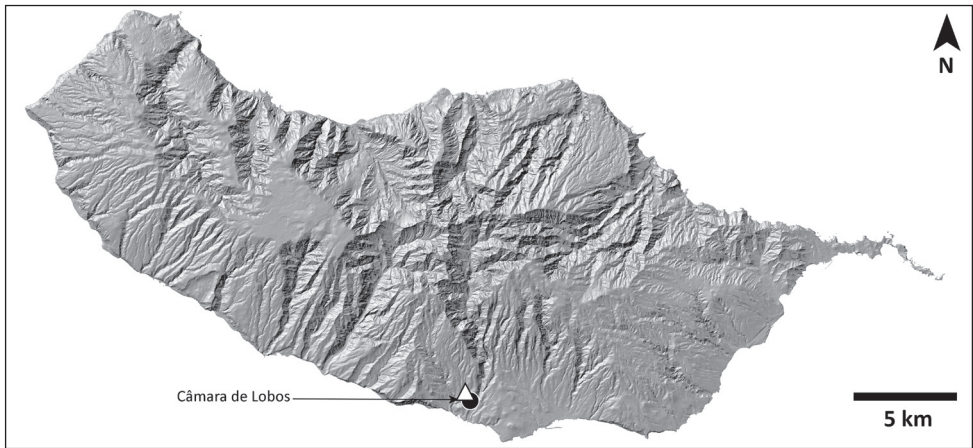


Figure 25. Distribution of *H. nonannulata*. Black circle: present record; white triangle: unconfirmed record from literature.

bium, brown. Abdomen with both short and long black setae, additionally with short greyish white setae; with a pair of anterolateral faint blackish patches, extending laterally into grey flanks, interspersed with greyish white patches; a median greyish lanceolate patch is bordered by two yellowish longitudinal bands interconnected in anterior half, posteriorly by means of faint dark chevrons; venter yellowish except around spinnerets, dark grey, with small blackish patches scattered laterally.

Eyes: MOQ: MW = 0.8 PW, MW = 1.2 LMP, MW = 1.3 AW; CI = 0.7 DAME. Anterior eye row slightly procurved.

Legs: Measurements: Leg I: 40.9, TiI: 10.8; Leg IV: 43.0, TiIV: 9.8; TiIL/D: 8.8. Spination of Leg I: FeI: d1.1.0, p0.0.2; TiI: p1.0.1, v2s.2s.2s; MtI: p1.0.1, r1.0.1, v2s.2s.1s. MtI with very dense scopulae.

Pedipalp: cymbium with two prolateral spines, one basal, the other at rim, apically with four dark macrosetae, Fe with two dorsal and an apical row of four spines, Pa with one prolateral spine, Ti with one dorsal, one dorsoprolateral, and one prolateral spines. Tegular apophysis with ventral spur short, blunt, with a short straight ridge leading to a wide apical point; terminal apophysis separated from subterminal apophysis due to a clearly visible excavation, blade-shaped with sharp end; embolus moderately elongated, with tip directed anteriorly; palea small.

Female: We could not revise any female material.

Intraspecific variation. Carapace length, males: 7.2–11.3. Smaller males have proportionally longer tibial spines than longer males.

Distribution. This species is known from the southern coastal area of Câmara de Lobos in the island of Madeira (Fig. 25).

Ecology. *Hogna nonannulata* can be found in coastal shrub- or grassland and rocky areas.

Conservation status. It was not previously possible to assess *H. nonannulata* according to the IUCN Red List criteria given the scarcity of past information,

hence a status of Data Deficient was suggested (Cardoso et al. 2018e). Its known distribution is now limited to the area of Camara de Lobos in the southern coast of Madeira Island, an area with no remaining natural habitat beyond the rocky areas. With an EOO and AOO of 4 km² and a single location threatened by urban and agricultural pressure, if the trend of the species is negative its status might be Critically Endangered.

Key to the *Hogna* species endemic to the Madeira Archipelago

- 1 Species from Porto Santo. **2**
- Species from Madeira or Desertas. **3**
- 2 Large species (prosoma length > 10 mm), legs furnished with orange setae (Fig. 27A). *H. maderiana*
- Small to medium species (prosoma length < 10 mm), legs with whitish setae (Fig. 27C). *H. insularum*
- 3 Species from Madeira. **4**
- Species from Desertas. **7**
- 4 Legs with a small, bright yellow patch of setae at joints of anterior metatarsus and pedipalp (Fig. 26A). *H. blackwalli*
- Species without bright yellow patches of setae in anterior legs. **5**
- 5 Legs without any reticulated or annulated pattern (Fig. 26D) *H. nonannulata*
- Legs with reticulated or annulated pattern. **6**
- 6 Male with straight embolus (Wunderlich 1992: 595, fig. 720). Female epigynal anterior pockets with highly divergent lateral borders (Fig. 9A). Species from montane habitats. *H. heeri*
- Male with embolus smoothly curved (Fig. 15). Female epigynal anterior pockets with parallel lateral borders (Fig. 16C). Species from southeastern coastal grassland habitats. *H. insularum*
- 7 Very large species (prosoma length > 14 mm). Black legs with white patches (Fig. 26C). *H. ingens*
- Smaller species (prosoma length < 10 mm). **8**
- 8 Male pedipalp with embolus smoothly curved (Fig. 15). Female epigyne with median septum roughly half as wide (at posterior transverse part) as long (Fig. 16A, C, E, G). *H. insularum*
- Male pedipalp with embolus straight or with only tilted tip. Female epigyne with median septum almost as wide (at posterior transverse part) as long (Figs 9A, B, 18D, E). **9**
- 9 Male pedipalp with embolus with tip tilted anteriorly (Fig. 18A, C). Female epigynal anterior pockets with convergent lateral borders (Fig. 18D) *H. isambertoi* sp. nov.
- Male pedipalp with straight embolus (Wunderlich 1992: 595, fig. 720). Female epigynal anterior pockets with highly divergent lateral borders (Fig. 9A) *H. heeri*

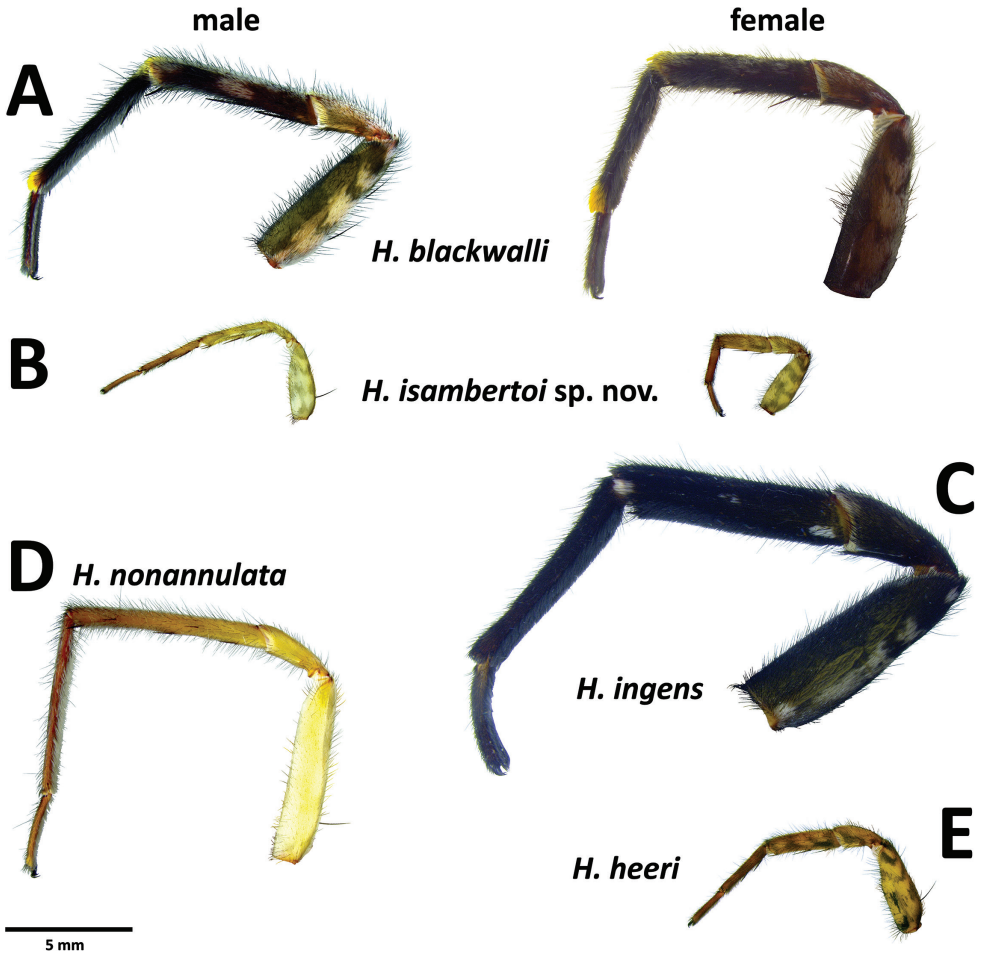


Figure 26. Plate with photographs of the lateral view of the leg I for easily diagnosable species.

Discussion

Origins of Madeiran *Hogna*

Our analyses support the long-standing view that the genus *Hogna* is a paraphyletic assemblage in much need of a thorough taxonomic revision that could establish its limits and diagnosis. Unfortunately, only 18 species of *Hogna* were represented by at least one DNA sequence in public repositories, out of the 228 currently valid species and subspecies, excluding Madeiran ones (World Spider Catalog 2021). Albeit with low support, our results suggested a strong geographic component in the phylogenetic relationship of *Hogna* species, recovering mixed genera clades from the same region (e.g., North America, South America or Australia). Madeiran species were consistently recovered by all analyses as closely related to the type species of the genus, *H. radiata*, represented in the analyses by specimens from the Iberian Peninsula, yet both the

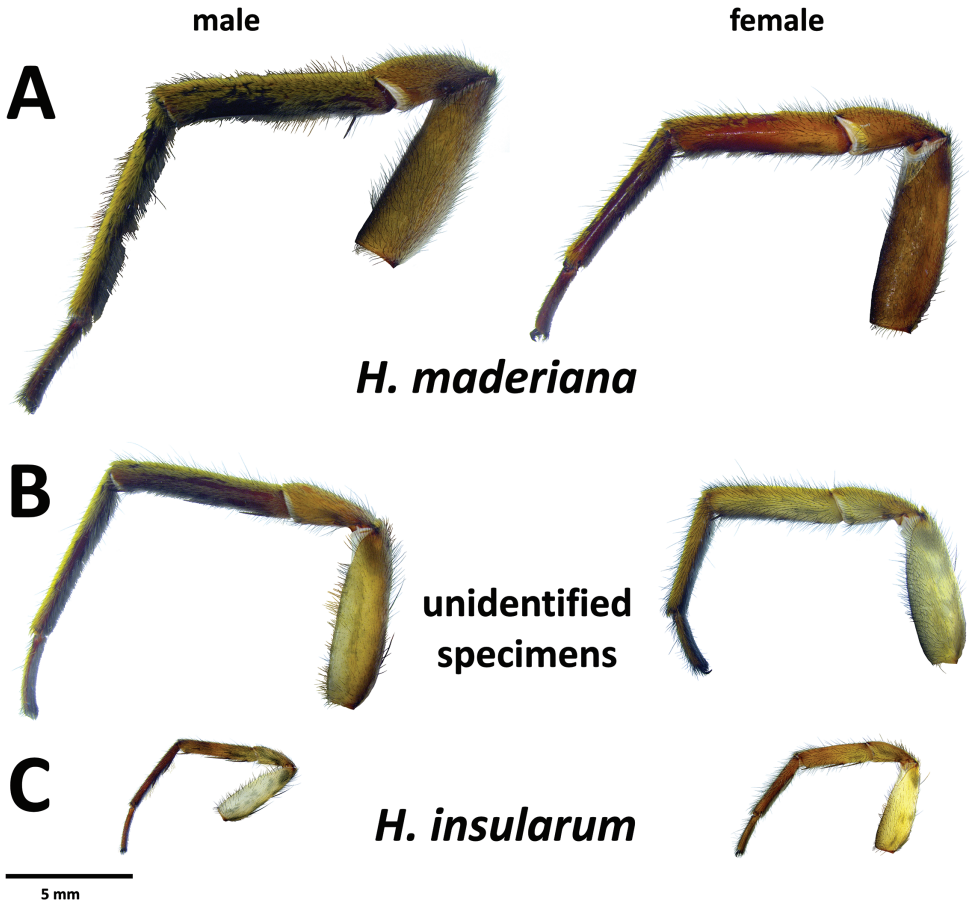


Figure 27. Plate with photographs of the lateral view of the leg I for the complex of *H. maderiana*, *H. insularum* and their intermediate forms.

monophyly of the Madeiran species and their relation with *H. radiata* are poorly supported. Although our sampling is far from being representative of the *Hogna* diversity in the western palearctic (only two species of 45 described were included), the results are congruent with the Iberian Peninsula as a colonisation source of Madeiran species. This biogeographic connection has been recently confirmed for the endemic Madeiran species of the spider genus *Dysdera*, and was most likely favoured by the predominant aerial and marine currents in the region (Crespo et al. 2021).

Our time estimates suggest a colonisation of the archipelago by the late Miocene (but note the large confidence intervals recovered). Interestingly, this sub-epoch coincides with an episode of major global cooling that brought about dramatic changes in the ecosystems, which included the expansion of grasslands and the associated fauna (see Herbert et al. 2016 and references therein). The increase in the amount of habitat types preferred by many wolf spider species may have facilitated the expansion and diversification of lycosids into the Mediterranean region and eventually the colonisation of the Madeiran Archipelago. In this regard, it is worth mentioning that the origin

of the western Mediterranean species of the other genus of large wolf spiders, *Lycosa* Latreille, 1804, seems also to trace back to the late Miocene (Planas et al. 2013).

Model-based analyses recovered the monophyly of all Madeiran endemics, which would suggest a single colonisation event of the archipelago. This result was disputed by parsimony analysis, which suggested at least two different events by placing the Iberian *H. radiata* as sister to the *ingens* clade. None of these alternative arrangements, however, received high support. Conversely, the existence of two well-defined lineages, the *ingens* and *maderiana* clades, were supported in all analyses. Interestingly, our analyses also signalled multiple colonisations of another volcanic archipelago, the Galapagos Islands. Up to seven endemics species are known from this Pacific archipelago, which include species adapted to habitats at different altitudes (Baert et al. 2008). All our analyses supported the independent colonisation of the Galapagos by at least two or even three different ancestors, one of which resulted in local diversification. Multiple island colonisation should not be unexpected in wolf spiders, given their good dispersal ability and frequent use of ballooning by many species (Richter 1970; Greenstone 1982; Bonte and Maelfait 2001; Bonte et al. 2006), although it was never assessed in *Hogna*.

Regardless of the actual number of colonisations, *Hogna* underwent processes of local diversification, as illustrated by the *ingens* clade. Similarly, to what has been observed in endemic *Hogna* from the Galapagos (Busschere et al. 2010), Madeiran endemics show a certain ecological differentiation associated to elevation, some species are found in montane habitats (*H. heeri*, *H. blackwalli* sp. rev. and *H. ingens*), while other are mostly found in coastal areas (*H. isambertoii* sp. nov. and *H. nonannulata*). Body size is another functional trait with a noticeable variation across Madeiran *Hogna*, *H. ingens* and *H. maderiana* can be considered giant species for *Hogna* standards (> 10 mm of carapace length), while *H. blackwalli* (7.3–10.4 mm) and *H. nonannulata* (7.2–11.2 mm) are medium-large, and *H. insularum* (4.1–4.7 mm), *H. heeri* (5.2–5.8 mm), and *H. isambertoii* sp. nov. (4.1–4.7 mm) are small. Often sympatric species have disparate sizes, as is the case in Porto Santo with *H. maderiana* and *H. insularum*, or in Deserta Grande with *H. ingens* and *H. insularum*, or even in Madeira with *H. blackwalli*, and *H. heeri*. Yet, it also happens that in Deserta Grande (only in the southern end) two very similar species, *H. insularum* and *H. isambertoii* sp. nov., share the same habitat. And in Bugio island, an even smaller and steeper island than Deserta Grande, the three small species of the archipelago, *H. heeri*, *H. insularum*, and *H. isambertoii* sp. nov., are found together. The few specimens available of *H. isambertoii* sp. nov. and the single specimen of *H. heeri* from Bugio were all collected in late autumn, which, hypothetically, might suggest phenological displacement against the spring-dominant *H. insularum*.

Within the *ingens* clade, the only well-supported sister group relationship is between *H. blackwalli* and *H. nonannulata*, which can represent an example of ecological shift within the same island, from the ancestral open habitat represented by the coastal species *H. nonannulata*, to the laurel forest habitats inhabited by *H. blackwalli*. This is a more plausible scenario than its opposite, but more detailed natural history and ecological information will be required to rigorously test the role of habitat shifts in the diversification of *Hogna* in Madeira, as well as to determine instances of parallel

evolution in habitat and functional traits, as has been reported in *Hogna* in the Galapagos Is. (Busschere et al. 2010; De Busschere et al. 2012).

Hogna insularum and *H. maderiana*: one or two species?

The species pair *H. insularum* and *H. maderiana* poses a taxonomic and evolutionary conundrum. Our molecular data were unable to establish boundaries between the large specimens of *Hogna* from the island of Porto Santo showing orange pilosity, identified using traditional diagnoses as *H. maderiana*, and the smaller specimens, without such pilosity, identified as *H. insularum*. Re-examination of morphological data suggested the existence of a continuum of phenotypic traits between the two extremes represented by specimens univocally referred to as either *H. maderiana* or *H. insularum*. Several specimens of intermediate size in Porto Santo (Figs 28, 29) showed clear yellowish to orange pilosity in anterior legs (colour fades to yellow after depositing specimen in ethanol), but not as dense as in the larger specimens. Furthermore, we were able to spot the usual dark reticulate pattern on the legs of these specimens, unlike in the large specimens, which are dark, bearing no traces of reticulated patterns (Fig. 27). We considered these specimens tentatively as “unidentified” (sp.). At the other extreme, the smaller specimens from Porto

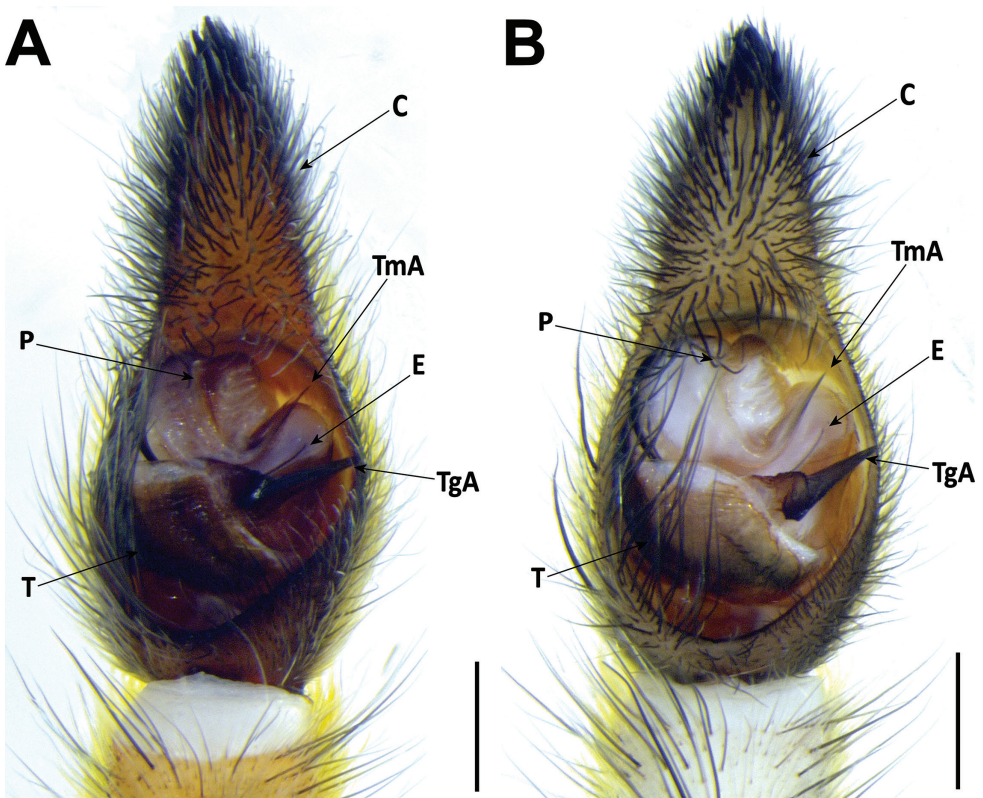


Figure 28. Unidentified male specimens belonging to the *H. maderiana* / *H. insularum* complex from Porto Santo. Left male pedipalps, ventral **A** CRBALC0328 **B** CRBALC0345. Scale bar: 0.5 mm (**A**).

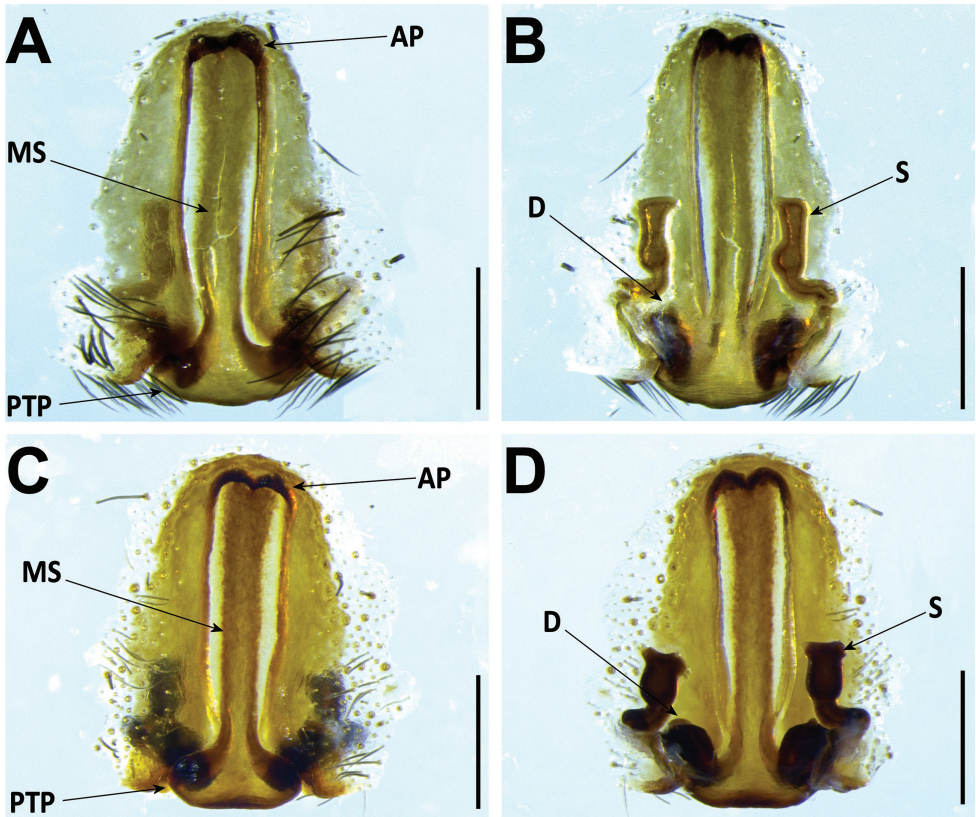


Figure 29. Unidentified female specimens belonging to the *H. maderiana* / *H. insularum* complex from Porto Santo. Female genitalia **A,B** CRBALC0329 **A** epigyne, ventral **B** vulva, dorsal **C,D** CRBALC0346 **C** epigyne, ventral **D** vulva, dorsal. Scale bar: 0.5 mm (**A**).

Santo, putatively identified as *H. insularum*, lacked orange setae, but showed yellowish to whitish setae. Certainly, although a remarkable size difference stands between the smallest specimens identified as *H. insularum* and the largest specimens identified as *H. maderiana*, similar wide intraspecific variation in size has been observed in other *Hogna* species, for example the Mediterranean species *H. radiata* (Latreille, 1817), which may range in size from 10 to 25 mm (Moya-Laraño, pers. comm.). Regarding male genitalic characters, Wunderlich (1992) proposed that the presence of a concavity in the tegulum as a diagnostic trait for *H. maderiana*. This trait is readily apparent in the large specimen we photographed (Fig. 21A, white arrow), but not in the unidentified specimens of intermediate size (Fig. 28). This feature, however, could be the result of a mechanical constraint associated to the role of the tegulum in supporting the tegular apophysis in large specimens. Similarly, although the embolus is usually smoothly curved in both *H. maderiana* and *H. insularum*, the actual degree of curvature may also vary across specimens (e.g., specimen CRBALC0328 bears a straighter embolus compared to other specimens, Fig. 28A). On the other hand, the SEM imaging revealed the presence in the embolic area of *H. insularum* (specimen CRBALC0310, from Porto Santo, Fig. 15E, F) of the loose membranous

subterminal apophysis, indistinct under the microscope, which is not present in *H. maderiana* (Fig. 21D). However, caution should be taken as this might be an artifact of suboptimal drying process of the former specimen, which could have detached the pars pendula from the apposition with the embolus. Also, by looking at Fig. 15F, we can see that the subterminal apophysis is folded in a way that could plausibly accompany the embolus over a larger length. A similar pattern of intermediate forms can also be recognised among female specimens. Although *H. maderiana* specimens may be diagnosed by long median septum of the epigyne, the longest among Madeiran *Hogna* (Fig. 21E, F), a significant correlation exists between epigyne size (length/width at base) and body size (Pearson's $R = 0.71$, $p < 0.05$, from a sample of 12 females), as revealed by the unidentified specimens from Porto Santo and females identified as *H. insularum*. Regardless of the actual length, the overall shape of the lateral borders of the anterior pockets is very similar across both taxa, showing parallel borders. Interestingly, the single adult *H. insularum* female available from Madeira, a population with distinct and exclusive mtDNA haplotypes, showed a slightly different epigynal shape (Fig. 16C). A similar relationship with body size is also observed in the shape of the spermathecae, which are pear-shaped in larger specimens (Fig. 21F), but from ovoid, to pear-shaped and rounded in smaller *H. insularum* specimens (Fig. 16B, D, F, H). Finally, regarding habitats, the largest specimens identified as *H. maderiana* are usually found in open, grassy meadows, while smaller specimens identified as *H. insularum* can be found both in the former habitat but also in shady (secondary) forest.

With the data at hand, it may seem advisable to merge both names into the same species. However, by doing so we might be concealing some interesting biological processes. For instance, hybridisation among close relatives have been uncovered between closely related *Hogna* species from the Galapagos islands (De Busschere et al. 2015). Hypothetically, introgression of adaptive genes among populations on different Galapagos islands may have contributed to the parallel evolution of similar ecological preferences. The ability of *Hogna* endemic species in Madeira to disperse between islands, which could promote introgression, is evident by the surprising finding of immature specimens originally identified as *H. insularum*, but that both mitochondrial and nuclear DNA suggested they belong to *H. ingens*, supposedly endemic to Desertas. Similar conflicting signals between different sources of evidence, namely morphology and molecules, may also arise in recently diverged species or species with large ancestral population sizes, as exemplified by wolf spiders in the genus *Pardosa* (Ivanov et al. 2021). Discerning alternative scenarios will require the future integration of large-scale population sampling with novel genome wide screening (e.g., ddRADSeq) methods.

Conservation status

As for other taxa in the archipelago (Crespo et al. 2014, 2021; Cardoso et al. 2018e), the combination of restricted range and degrading habitat has led several species of endemic *Hogna* to be considered as threatened. While many seem to be relatively widely distributed and abundant, three species are of concern.

Hogna ingens, the Desertas wolf spider, is limited to a single valley in the northern tip of Deserta Grande and was recently subjected to a reduction of 80% of its range in

a few years (Crespo et al. 2014b), leading to a classification of Critically Endangered. A habitat recovery program is underway and several ex-situ populations are now guaranteeing its future survival. Recent data suggest that the habitat recovery is resulting in the recovery of the spider population to previously affected areas. If this is confirmed the status might improve and the status should be revised in the near future.

Hogna nonannulata seems to be restricted to a small range in the south coast of the island of Madeira. With increasing urban pressure, it is possible that the status of Critically Endangered is warranted for the species. More information should be collected however, as contrary to most other regions in the archipelago, the area was never subject to extensive sampling.

Hogna isambertoi sp. nov. is the third species of conservation concern, given its small range and possible threat from aridification of the two locations from where it is known. The scarce available data of its life cycle, with adults emerging during November and December, warrant a monitoring program to confirm a possible status of Endangered.

We strongly recommend the rapid collection of data that can confirm or not the status of *H. nonannulata* and *H. isambertoi*, by focusing on monitoring programs of the southern coast of the Island of Madeira and overwintering in the southern tip of Deserta Grande and Bugio. If confirmed, these species would benefit from both habitat recovery programs and ex-situ conservation as is proving successful for *H. ingens*.

Conclusions

Our study underlines the importance of the integration of different lines of evidence to fully understand the origin and diversification of species endemic to oceanic islands. Madeiran *Hogna* colonised the archipelago at a time of global expansion of grasslands and subsequently diversified throughout the archipelago into a variety of forms and sizes. Yet, the boundaries of some species are ill-defined and there are cases where both morphological and molecular suggest complex underlying evolutionary processes.

We tackled nomenclatural issues by revising old types and descriptions, describing a new species, and providing the first molecular data for Madeiran *Hogna*. The newly collected data confirmed the localised distribution and narrow range of some species. Our study sets the stage for the urgent implementation of conservation measures for the protection of these remarkable endemic species.

Acknowledgements

We thank the IFCN of the Madeira Regional Secretariat of Environment, Natural Resources and Climate Change for coordinating the logistical arrangements, providing collection and transport permits, and field work support at Desertas, namely to C. Santos, D. Menezes, and the team of rangers, respectively. Additional field work support was provided by A. Bellvert and M. Domènech. The museum curators that loaned or sent photographs of material are hereby acknowledged: J. Beccaloni (MNH),

B. Caballero (MZB), R. Crowther (OUMNH), E.-A. Leguin, D. Logunov (MMUE), C. Rollard, J. Stigenberg (NHRS) and W. Wawer (MIZ). Peter Jäger and J. Altmann are thanked for their hospitality and support during a short stay of LC at the SMF to revise the material in the Wunderlich and Roewer collections, as well as to deposit the type of *H. isambertoi* sp. nov. Daphne Niehoff at the De Bastei museum (Nijmegen, The Netherlands) is thanked for kindly acting as a proxy to the shipment of loans destined to LC. Original distribution maps from Madeira were provided under copyright agreement by DROTA. Live photographs of *H. blackwalli* and *H. heeri* were provided by courtesy of E. Machado. Finally, we thank J. Moya-Laraño for a fruitful discussion about intraspecific variation on *H. radiata*. For comments on earlier drafts that greatly improved the manuscript we thank Ingi Agnarsson (editor), Volker Framenau, Dmitri Logunov, Luis Piacentini, and two anonymous reviewers.

LC was funded by an individual PhD grant SFRH/BD/110280/2015 from the Foundation for Science and Technology (FCT, Portugal). This work was supported by project CGL2016-80651-P from the Spanish Ministry of Economy and Competitiveness (MA). Additional funds were provided by the project 2017SGR83 from the Catalan Government (MA).

References

- Aktas C (2015) R Package haplotypes: Haplotype Inference and Statistical Analysis of Genetic Variation.
- Baert BL, Maelfait J, Hendrickx F (2008) The Wolf Spiders (Araneae, Lycosidae) from the Galápagos Archipelago. *Bulletin de l'Institut Royal des Sciences Naturelles de Belgique, Entomologie* 78: 5–37.
- Bell JR, Bohan D, Shaw EM, Weyman G (2005) Ballooning dispersal using silk: World fauna, phylogenies, genetics and models. *Bulletin of entomological research* 95: 69–114. <https://doi.org/10.1079/BER2004350>
- Bidegaray-Batista L, Arnedo M (2011) Gone with the plate: The opening of the Western Mediterranean basin drove the diversification of ground-dweller spiders. *BMC Evolutionary Biology* 11: e317. <https://doi.org/10.1186/1471-2148-11-317>
- Blackwall J (1857) Description of the male of *Lycosa tarentuloides Maderiana* Walck., and of three newly discovered species of the genus *Lycosa*. *Annals and Magazine of Natural History* 20: 282–287. <https://doi.org/10.1080/00222935709487920>
- Boieiro M, Matthews TJ, Rego C, Crespo L, Aguiar CAS, Cardoso P, Rigal F, Silva I, Pereira F, Borges PAV, Serrano ARM (2018) A comparative analysis of terrestrial arthropod assemblages from a relict forest unveils historical extinctions and colonization differences between two oceanic islands. *PLoS ONE* 13: 1–22. <https://doi.org/10.1371/journal.pone.0195492>
- Bonnet P (1945) *Bibliographia araneorum. Analyse méthodique de toute la littérature aranéologique jusqu'en 1939. Tome I.* Douladoure, Toulouse, 832 pp.
- Bonnet P (1959) *Bibliographia araneorum. Analyse méthodique de toute la littérature aranéologique jusqu'en 1939. Tome II. Systématique des araignées (Étude par ordre alphabétique) (5^{ème} partie: T-Z).* Douladoure, Toulouse, 4231–5058.

- Bonte D, Maelfait J (2001) Life history, habitat use and dispersal of a dune wolf spider (*Pardosa monticola* (Clerck, 1757) Lycosidae, Araneae) in the Flemish coastal dunes (Belgium). *Belgian Journal of Zoology* 131: 145–157.
- Bonte D, Borre J Vanden, Lens L, Jean-Pierre Maelfait (2006) Geographical variation in wolf spider dispersal behaviour is related to landscape structure. *Animal Behaviour* 72: 655–662. <https://doi.org/10.1016/j.anbehav.2005.11.026>
- Brady AR (2012) Nearctic species of the new genus *Tigrosa* (Araneae: Lycosidae). *Journal of Arachnology* 40: 182–208. <https://doi.org/10.1636/K11-77.1>
- De Busschere C, Van Belleghem SM, Hendrickx F (2015) Inter and intra island introgression in a wolf spider radiation from the Galápagos, and its implications for parallel evolution. *Molecular Phylogenetics and Evolution* 84: 73–84. <https://doi.org/10.1016/j.ympev.2014.11.004>
- De Busschere C, Baert L, Van Belleghem SM, Dekoninck W, Hendrickx F (2012) Parallel phenotypic evolution in a wolf spider radiation on Galápagos. *Biological Journal of the Linnean Society* 106: 123–136. <https://doi.org/10.1111/j.1095-8312.2011.01848.x>
- Busschere C De, Hendrickx F, Van Belleghem SM, Backeljau T, Lens L, Baert L (2010) Parallel habitat specialization within the wolf spider genus *Hogna* from the Galápagos. *Molecular Ecology* 19: 4029–4045. <https://doi.org/10.1111/j.1365-294X.2010.04758.x>
- Cardoso P, Crespo L, Silva I, Borges P, Boieiro M (2018a) *Hogna maderiana*. The IUCN Red List of Threatened Species 2018. <https://doi.org/10.2305/IUCN.UK.2018-2.RLTS.T58048618A58061017.en>
- Cardoso P, Crespo LC, Silva I, Borges P, Boieiro M (2018b) *Hogna beeri*. The IUCN Red List of Threatened Species 2018: 8. <https://doi.org/10.2305/IUCN.UK.2018-2.RLTS.T58048559A58061002.en>
- Cardoso P, Crespo LC, Silva I, Borges P, Boieiro M (2018c) *Hogna insularum*. The IUCN Red List of Threatened Species 2018. <https://doi.org/10.2305/IUCN.UK.2018-2.RLTS.T58048609A58061012.en>
- Cardoso P, Crespo LC, Silva I, Borges P, Boieiro M (2018d) *Hogna schmitzi*. The IUCN Red List of Threatened Species 2018. <https://doi.org/10.2305/IUCN.UK.2018-2.RLTS.T58048645A58061027.en>
- Cardoso P, Crespo LC, Silva I, Borges P, Boieiro M (2018e) *Hogna nonannulata*. The IUCN Red List of Threatened Species 2018. <https://doi.org/10.2305/IUCN.UK.2018-2.RLTS.T58048634A58061022.en>
- Cardoso P (2014) *Hogna ingens*. The IUCN Red List of Threatened Species 2014. <https://doi.org/10.2305/IUCN.UK.2014-2.RLTS.T58048571A58061007.en>
- Cardoso P, Bushell M, Stanley-Price M (2016) The Desertas Wolf Spider – A Strategy for its Conservation 2016–2022.
- Clement M, Posada D, Crandall K (2000) Clement MD, Posada D, Crandall KA. TCS: a computer program to estimate gene genealogies. *Molecular Ecology* 9: 1657–1659. <https://doi.org/10.1046/j.1365-294x.2000.01020.x>
- Crespo L, Boieiro M, Cardoso P, Aguiar C, Amorim I, Barrinha C, Borges P, Menezes D, Pereira F, Rego C, Ribeiro S, Silva I, Serrano A (2014a) Spatial distribution of Madeira Island Laurisilva endemic spiders (Arachnida: Araneae). *Biodiversity Data Journal* 2: e1051. <https://doi.org/10.3897/BDJ.2.e1051>

- Crespo L, Silva I, Borges P, Cardoso P (2013) Rapid biodiversity assessment, faunistics and description of a new spider species (Araneae) from Desertas Islands and Madeira (Portugal). *Revista Iberica de Aracnología* 23: 11–23.
- Crespo L, Silva I, Borges P, Cardoso P (2014b) Assessing the conservation status of the strict endemic Desertas wolf spider, *Hogna ingens* (Araneae, Lycosidae). *Journal for Nature Conservation* 22: 516–524. <https://doi.org/10.1016/j.jnc.2014.08.005>
- Crespo L, Silva I, Enguídanos A, Cardoso P, Arnedo M (2021) Integrative taxonomic revision of the woodlouse-hunter spider genus *Dysdera* (Araneae: Dysderidae) in the Madeira archipelago with notes on its conservation status. *Zoological Journal of the Linnean Society* 192: 356–415. <https://doi.org/10.1093/zoolinnean/zlaa089>
- Crespo LC, Silva I, Borges PAV, Cardoso P (2014c) Assessing the conservation status of the strict endemic Desertas wolf spider, *Hogna ingens* (Araneae, Lycosidae). *Journal for Nature Conservation* 22: 516–524. <https://doi.org/10.1016/j.jnc.2014.08.005>
- Denis J (1962) Les araignées de l'archipel de Madère (Mission du Professeur Vandel). *Publicações do Instituto Zoologia Doutor Augusto Nobre* 79: 1–118.
- Dondale C, Redner J (1990) The insects and arachnids of Canada, Part 17. The wolf spiders, nurseryweb spiders, and lynx spiders of Canada and Alaska, Araneae: Lycosidae, Pisauridae, and Oxyopidae. *Research Branch Agriculture Canada Publication* 1856: 383.
- Ezard T, Fujisawa T, Barraclough T (2017) splits: SPecies' LImits by Threshold Statistics. <https://r-forge.r-project.org/projects/splits/>
- Fujisawa T, Aswad A, Barraclough TG (2016) A rapid and scalable method for multilocus species delimitation using bayesian model comparison and rooted triplets. *Systematic Biology* 65: 759–771. <https://doi.org/10.1093/sysbio/syw028>
- Geldmacher J, Hoernle K (2000) The 72 Ma geochemical evolution of the Madeira hotspot (eastern North Atlantic): Recycling of Paleozoic (≤ 500 Ma) oceanic lithosphere. *Earth and Planetary Science Letters* 183: 73–92. [https://doi.org/10.1016/S0012-821X\(00\)00266-1](https://doi.org/10.1016/S0012-821X(00)00266-1)
- Goloboff PA, Catalano SA (2016) TNT version 1.5, including a full implementation of phylogenetic morphometrics. *Cladistics* 32: 221–238. <https://doi.org/10.1111/cla.12160>
- Greenstone MH (1982) Ballooning Frequency and Habitat Predictability in Two Wolf Spider Species (Lycosidae: *Pardosa*). *The Florida Entomologist* 65: 83–89. <https://doi.org/10.2307/3494147>
- Hebert PDN, Cywinska A, Ball SL, DeWaard JR (2003) Biological identifications through DNA barcodes. *Proceedings of the Royal Society B: Biological Sciences* 270(1512): 313–321. <https://doi.org/10.1098/rspb.2002.2218>
- Herbert TD, Lawrence KT, Tzanova A, Peterson LC, Caballero-Gill R, Kelly CS (2016) Late Miocene global cooling and the rise of modern ecosystems. *Nature Geoscience* 9: 843–847. <https://doi.org/10.1038/ngeo2813>
- Hoang DT, Chernomor O, von Haeseler A, Minh BQ, Vinh LS (2018) UFBoot2: Improving the Ultrafast Bootstrap Approximation. *Molecular biology and evolution. Molecular Biology and Evolution* 35: 518–522. <https://doi.org/10.1093/molbev/msx281>
- Ivanov V, Marusik Y, Pétillon J, Mutanen M (2021) Relevance of ddRADseq method for species and population delimitation of closely related and widely distributed wolf spiders (Araneae, Lycosidae). *Scientific Reports* 11: 1–14. <https://doi.org/10.1038/s41598-021-81788-2>

- Jocqué R, Alderweireldt M (2005) Lycosidae: the grassland spiders. *Acta Zoologica Bulgarica* 2005: 125–130. http://www.european-arachnology.org/proceedings/22nd/15_Jocque.pdf
- Johnson J (1863) Description of a new species of *Lycosa* living in the island of Madeira; with some remarks on the *Lycosa tarentuloides maderiana* Walckenaer. *Annals and Magazine of Natural History* 12: 152–155. <https://doi.org/10.1080/00222936308681494>
- Kalyaanamoorthy S, Minh BQ, Wong TKE, Von Haeseler A, Jermiin LS (2017) ModelFinder: Fast model selection for accurate phylogenetic estimates. *Nature Methods* 14: 587–589. <https://doi.org/10.1038/nmeth.4285>
- Kapli P, Lutteropp S, Zhang J, Kobert K, Pavlidis P, Stamatakis A, Flouri T (2017) Multi-rate Poisson tree processes for single-locus species delimitation under maximum likelihood and Markov chain Monte Carlo. *Bioinformatics* 33: 1630–1638. <https://doi.org/10.1093/bioinformatics/btx025>
- Katoh K, Standley DM (2013) MAFFT multiple sequence alignment software version 7: Improvements in performance and usability. *Molecular Biology and Evolution* 30: 772–780. <https://doi.org/10.1093/molbev/mst010>
- Kulczynski W (1899) Arachnoidea opera Rev. E. Schmitz collecta in insulis Maderianis et in insulis Selvages dictis. *Rozprawy i Sprawozdania z Posiedzen Wydzialu Matematyczno Przyrodniczego Akademji Umiejetnosci, Krakow* 36: 319–461.
- Kumar S, Stecher G, Li M, Knyaz C, Tamura K (2018) MEGA X: Molecular Evolutionary Genetics Analysis across Computing Platforms. *Molecular biology and evolution* 35: 1547–1549. <https://doi.org/10.1093/molbev/msy096>
- Lanfear R, Frandsen PB, Wright AM, Senfeld T, Calcott B (2017) Partitionfinder 2: New methods for selecting partitioned models of evolution for molecular and morphological phylogenetic analyses. *Molecular Biology and Evolution* 34: 772–773. <https://doi.org/10.1093/molbev/msw260>
- Langlands PR, Framenau VW (2010) Systematic revision of *Hoggicosa* Roewer, 1960, the Australian “*bicolor*” group of wolf spiders (Araneae: Lycosidae). *Zoological Journal of the Linnean Society* 158: 83–123. <https://doi.org/10.1111/j.1096-3642.2009.00545.x>
- Logunov DV (2020) On three species of *Hogna* Simon, 1885 (Aranei: Lycosidae) from the near East and Central Asia. *Arthropoda Selecta* 29: 349–360. <https://doi.org/10.15298/arthsel.29.3.08>
- Löytynoja A, Goldman N (2010) webPRANK: a phylogeny-aware multiple sequence aligner with interactive alignment browser. *BMC Bioinformatics* 11: e579. <https://doi.org/10.1186/1471-2105-11-579>
- Malumbres-Olarte J, Boeiro M, Cardoso P, Carvalho R, Crespo LCF, Gabriel R, Hernández NM, Paulo OS, Pereira F, Rego C, Ros-Prieto A, Silva I, Vieira A, Rigal F, Borges PAV (2020) Standardised inventories of spiders (arachnida, araneae) of Macaronesia ii: The native forests and dry habitats of madeira archipelago (Madeira and Porto Santo islands). *Biodiversity Data Journal* 8: e47502. <https://doi.org/10.3897/BDJ.8.e47502>
- Miller M, Pfeiffer W, Schwartz T (2010) Creating the CIPRES Science Gateway for inference of large phylogenetic trees. In: *Proceedings of the Gateway Computing Environments Workshop (GCE)*, 1–8. <https://doi.org/10.1109/GCE.2010.5676129>
- Minh BQ, Schmidt HA, Chernomor O, Schrempf D, Woodhams MD, von Haeseler A, Lanfear R (2020) IQ-TREE 2: New Models and Efficient Methods for Phylogenetic Infer-

- ence in the Genomic Era. *Molecular Biology and Evolution* 37: 1530–1534. <https://doi.org/10.1093/molbev/msaa015>
- Monaghan MT, Wild R, Elliot M, Fujisawa T, Balke M, Inward DJG, Lees DC, Ranaivosolo R, Eggleton P, Barraclough TG, Vogler AP (2009) Accelerated Species Inventory on Madagascar Using Coalescent-Based Models of Species Delineation. *Systematic Biology* 58: 298–311. <https://doi.org/10.1093/sysbio/syp027>
- Müller K (2005) SEQSTATE – primer design and sequence statistics for phylogenetic DNA data sets. *Applied bioinformatics* 4: 65–69. <https://doi.org/10.2165/00822942-200504010-00008>
- Ogilvie HA, Bouckaert RR, Drummond AJ (2017) StarBEAST2 Brings Faster Species Tree Inference and Accurate Estimates of Substitution Rates. *Molecular Biology and Evolution* 34: 2101–2114. <https://doi.org/10.1093/molbev/msx126>
- Piacentini LN, Ramírez MJ (2019) Hunting the wolf: A molecular phylogeny of the wolf spiders (Araneae, Lycosidae). *Molecular Phylogenetics and Evolution* 136: 227–240. <https://doi.org/10.1016/j.ympev.2019.04.004>
- Planas E, Fernández-Montraveta C, Ribera C (2013) Molecular systematics of the wolf spider genus *Lycosa* (Araneae: Lycosidae) in the Western Mediterranean Basin. *Molecular Phylogenetics and Evolution* 67: 414–428. <https://doi.org/10.1016/j.ympev.2013.02.006>
- Ramalho RS, Brum Da Silveira A, Fonseca PE, Madeira J, Cosca M, Cachão M, Fonseca MM, Prada SN (2015) The emergence of volcanic oceanic islands on a slow-moving plate: The example of Madeira Island, NE Atlantic. *Geochemistry, Geophysics, Geosystems* 16: 522–537. <https://doi.org/10.1002/2014GC005657>
- Rambaut A, Drummond AJ, Xie D, Baele G, Suchard MA (2018) Posterior summarization in Bayesian phylogenetics using Tracer 1.7. *Systematic Biology* 67: 901–904. <https://doi.org/10.1093/sysbio/syy032>
- Ratnasingham S, Hebert PDN (2007) bold: The Barcode of Life Data System (<http://www.barcodinglife.org>). *Molecular Ecology Notes* 7: 355–364. <https://doi.org/10.1111/j.1471-8286.2007.01678.x>
- Ratnasingham S, Hebert PDN (2013) A DNA-Based Registry for All Animal Species: The Barcode Index Number (BIN) System. *PLoS ONE* 8: e66213. <https://doi.org/10.1371/journal.pone.0066213>
- Richter CJJ (1970) Aerial dispersal in relation to habitat in eight wolf spider species (*Pardosa*, Araneae, Lycosidae). *Oecologia* 5: 200–214. <https://doi.org/10.1007/BF00344884>
- Roewer C (1960) Araneae Lycosaeformia II (Lycosidae) (Fortsetzung und Schluss). *Exploration du Parc National de l'Upemba, Mission G. F. de Witte* 55: 519–1040.
- Ronquist F, Teslenko M, Van Der Mark P, Ayres DL, Darling A, Höhna S, Larget B, Liu L, Suchard MA, Huelsenbeck JP (2012) Mrbayes 3.2: Efficient bayesian phylogenetic inference and model choice across a large model space. *Systematic Biology* 61: 539–542. <https://doi.org/10.1093/sysbio/sys029>
- Schwarz S, Klügel A, van den Bogaard P, Geldmacher J (2005) Internal structure and evolution of a volcanic rift system in the eastern North Atlantic: The Desertas rift zone, Madeira archipelago. *Journal of Volcanology and Geothermal Research* 141: 123–155. <https://doi.org/10.1016/j.jvolgeores.2004.10.002>

- Simmons M, Ochoterena H (2000) Gaps as Characters in Sequence-Based Phylogenetic Analyses. *Systematic Biology* 49: 369–381. <https://doi.org/10.1093/sysbio/49.2.369>
- Simon E (1898) Histoire naturelle des araignées. Deuxième édition, tome second. Roret (Ed.), Paris, 193–380.
- Soto EM, Labarque FM, Ceccarelli FS, Arnedo MA, Pizarro-Araya J, Ramírez MJ (2017) The life and adventures of an eight-legged castaway: Colonization and diversification of *Philisca* ghost spiders on Robinson Crusoe Island (Araneae, Anyphaenidae). *Molecular Phylogenetics and Evolution* 107: 132–141. <https://doi.org/10.1016/j.ympev.2016.10.017>
- Suman TW (1964) Spiders of the Hawaiian Islands: catalog and bibliography. *Pacific Insects* 6: 665–687.
- Templeton AR, Crandall KA, Sing CF (1992) A cladistic analysis of phenotypic associations with haplotypes inferred from restriction endonuclease mapping and DNA sequence data. III. Cladogram estimation. *Genetics* 132: 619–633. <https://doi.org/10.1093/genetics/132.2.619>
- Thorell T (1875) Descriptions of several European and North African spiders. *Kongliga Svenska Vetenskaps-Akademiens Handlingar* 13: 1–204.
- Tongiorgi P (1977) Fam. Lycosidae. In La faune terrestre de l'île de Sainte-Hélène. IV. Annales, Musée Royal de l'Afrique Centrale, Sciences zoologiques (Zool.-Ser. 8°) 220: 105–125.
- Vaidya G, Lohman DJ, Meier R (2011) SequenceMatrix: concatenation software for the fast assembly of multi-gene datasets with character set and codon information. *Cladistics* 27: 171–180. <https://doi.org/10.1111/j.1096-0031.2010.00329.x>
- Walckenaer CA (1837) Histoire naturelle des insectes. Aptères. Histoire naturelle des insectes. Aptères, 682 pp. <https://doi.org/10.5962/bhl.title.61095>
- World Spider Catalog (2021) World Spider Catalog. Natural History Museum Bern. Online at <http://wsc.nmbe.ch>, version 22.0. <https://doi.org/10.24436/2> [accessed on 21.04.2021]
- Wunderlich J (1992) Die Spinnen-Fauna der Makaronesischen Inseln: Taxonomie, Ökologie, Biogeographie und Evolution. *Beiträge zur Araneologie* 1: 1–619.
- Wunderlich J (1995) Zu Ökologie, Biogeographie, Evolution und Taxonomie einiger Spinnen der Makaronesischen Inseln (Arachnida: Araneae). *Beiträge zur Araneologie* 4: 385–439.

Supplementary material I

Table S1. Primers used for amplification

Authors: Luís C. Crespo, Isamberto Silva, Alba Enguídanos, Pedro Cardoso, Miquel Arnedo

Data type: docx. file

Explanation note: Primers used for amplification.

Copyright notice: This dataset is made available under the Open Database License (<http://opendatacommons.org/licenses/odbl/1.0/>). The Open Database License (ODbL) is a license agreement intended to allow users to freely share, modify, and use this Dataset while maintaining this same freedom for others, provided that the original source and author(s) are credited.

Link: <https://doi.org/10.3897/zookeys.1086.68015.suppl1>

Supplementary material 2

Tables S2, S3

Authors: Miquel Arnedo

Data type: Materials

Explanation note: Spreadsheet containing all the studied specimens, their collection data and the checklist of amplified genes, as well as the outgroup taxa accession numbers.

Copyright notice: This dataset is made available under the Open Database License (<http://opendatacommons.org/licenses/odbl/1.0/>). The Open Database License (ODbL) is a license agreement intended to allow users to freely share, modify, and use this Dataset while maintaining this same freedom for others, provided that the original source and author(s) are credited.

Link: <https://doi.org/10.3897/zookeys.1086.68015.suppl2>

Supplementary material 3

Figure S1

Authors: Miquel Arnedo, Luís C. Crespo

Data type: Phylogenetic (tiff. image)

Explanation note: Full best Maximum Likelihood tree of Lycosoidea, inferred with IQTREE2 after selecting the best partition scheme and evolutionary models. Nodes are split in three sections, representing the different methods. Support on nodes should be read as follows: black: ML ultrafast bootstrap and BI posterior probability ≥ 0.95 , MP Jackknife ≥ 0.7 ; grey: ML Ultrafast Bootstrap and BI posterior probability < 0.95 , MP Jackknife < 0.7 ; white: unrecovered node.

Copyright notice: This dataset is made available under the Open Database License (<http://opendatacommons.org/licenses/odbl/1.0/>). The Open Database License (ODbL) is a license agreement intended to allow users to freely share, modify, and use this Dataset while maintaining this same freedom for others, provided that the original source and author(s) are credited.

Link: <https://doi.org/10.3897/zookeys.1086.68015.suppl3>

Iguana insularis (Iguanidae) from the southern Lesser Antilles: An endemic lineage endangered by hybridization

Michel Breuil¹, David Schikorski², Barbara Vuillaume², Ulrike Krauss³, Jennifer C. Daltry^{4,5}, Glenroy Gaymes⁶, Joanne Gaymes⁶, Olivier Lepais⁷, Nicolas Bech⁸, Mišel Jelić⁹, Thomas Becking⁸, Frédéric Grandjean⁸

1 Muséum national d'Histoire naturelle, Laboratoire des Reptiles et Amphibiens, Bâtiment 30, 57, rue Cuvier, CP n° 30, 75231 Paris cedex 05, France **2** Laboratoire Labofarm-Genindexe, 4 rue Théodore Botrel, 22600 Loudéac, France **3** Maison du Soleil, Dauphin Road, La Borne, PO Box GM 1109, Saint Lucia, West Indies **4** Fauna & Flora International, David Attenborough Building, Pembroke Street, Cambridge CB2 3QZ, UK **5** Re:wild, PO Box 129, Austin, TX 78767, USA **6** Science Initiative for Environmental Conservation and Education, Kingstown, St Vincent & the Grenadines **7** INRAE, Univ. Bordeaux, BIOGECO, 69 route d'Arcachon, 33612 Cestas Cedex, France **8** Laboratoire Écologie et Biologie des Interactions, équipe EES, UMR CNRS 7267, Université de Poitiers, 5 rue Albert Turpin, 86073 Poitiers Cedex 9, France **9** Department of Natural Sciences, Varaždin City Museum, Šetalište Josipa Jurja Strossmayera 3, 42000 Varaždin, Croatia

Corresponding author: Frédéric Grandjean (frederic.grandjean@univ-poitiers.fr)

Academic editor: Aaron Bauer | Received 3 October 2021 | Accepted 7 January 2022 | Published 17 February 2022

<http://zoobank.org/54704B1A-65D0-4AE0-9F29-5524A60F3EF9>

Citation: Breuil M, Schikorski D, Vuillaume B, Krauss U, Daltry JC, Gaymes G, Gaymes J, Lepais O, Bech N, Jelić M, Becking T, Grandjean F (2022) *Iguana insularis* (Iguanidae) from the southern Lesser Antilles: An endemic lineage endangered by hybridization. ZooKeys 1086: 137–161. <https://doi.org/10.3897/zookeys.1086.76079>

Abstract

The newly described horned iguana *Iguana insularis* from the southern Lesser Antilles is separated in two easily recognized subspecies: *I. insularis sanctaluciae* from St. Lucia and *I. insularis insularis* from the Grenadines. Its former description is completed by the use of 38 new samples for genetic and morphological analysis. Seventeen microsatellites were used to estimate genetic diversity, population structure and the level of introgression with other *Iguana* species over nearly the whole range of the species. ND4 and PAC sequences were also used to better characterize hybridization and to complete the description of this lineage. The *I. insularis* population of St. Vincent shows a high level of introgression from *I. iguana* whereas in the Grenadines, most islands present pure *insularis* populations but several show evidence of introgressions. Of the two remaining populations of *I. insularis sanctaluciae*, only one is still purebred. The

recent identification of this and other distinct insular species and subspecies in the eastern Caribbean, and evaluation of where hybridization has occurred, are timely and important because the native iguanas are in urgent need of conservation action. Among the greatest threats is the ongoing human-mediated spread of invasive iguanas from Central and South America, which are destroying the endemic insular lineages through multiple diachronic introgression events.

Keywords

Caribbean, *Iguana insularis insularis*, *Iguana insularis sanctaluciae*, introgression, invasive alien species, microsatellites, ND4, PAC

Introduction

Resolving taxonomic or phylogenetic uncertainties and delineating management units according to the genetic characteristics of populations are important in conservation biology (Groom et al. 2006; Pasachnik et al. 2009, 2020; Malone et al. 2017). This is particularly challenging when reproductive barriers are absent between native and alien species and interspecific hybridization occurs; sometimes leading to the extinction of rare taxa through genetic swamping. A good example concerns the genus *Iguana* which was long thought to be represented by only two species (Lazell 1973): the Lesser Antillean iguana *I. delicatissima* (Laurenti 1768), endemic to the Lesser Antilles, and the invasive common or green iguana (*Iguana iguana*) [Linnaeus 1758], with a large distribution range encompassing Central America and some offshore islands, the north of South America and offshore islands (e.g., the ABC Islands, Los Roques and Margarita). Recently, Vuillaume et al. (2015) reported that *I. delicatissima* hybridizes with invasive *I. iguana* in the Lesser Antilles, resulting in the progressive elimination of *I. delicatissima* by genetic swamping.

The range of the *Iguana iguana* complex sensu van den Burg et al. (2021) covers approximately 5 million km² (Breuil 2013) and contains independent lineages identified by Stephen et al. (2013). Thus, obtaining sufficient numbers of individuals over the entire geographic range for comprehensive phylogenetic and taxonomic studies covering the entire range is difficult. However, Buckley et al. (2016) acknowledged that Breuil (2013) found significant morphological differences between the Saba, St. Lucia, and South American populations. Taxonomic interpretation across the global range may be much more complicated than the conclusions drawn from our Lesser Antilles samples (Breuil et al. 2019, 2020) as suggested by recent research on the ABC Islands and Colombia (van den Burg and Malone 2018). In addition, numerous iguana translocations have occurred in the Lesser Antilles since the Caribbean period (Bochaton et al. 2015; Vuillaume et al. 2015; De Jesús Villanueva et al. 2021) and have altered the original endemic populations.

The iguanas used by Breuil et al. (2019, 2020) to differentiate Lesser Antillean taxa from continental iguanas originate from northern South America (French Guiana), representing only 1% of the global range. Furthermore, van den Burg et al. (2021)

showed that these French Guiana iguanas do belong to the same genetic group as those from Surinam, Trinidad, Venezuela (Bolívar Rio Caroni) and Brazil (Alter do Chao), a conclusion previously reached by Stephen et al. (2013) using three nuclear genes and one mitochondrial gene. We therefore considered that these French Guiana iguanas correspond to the species *Iguana iguana* (Breuil 2013, 2016; Breuil et al. 2019, 2020) described by Linnaeus (1758) based on the type locality assigned to this species by Hoogmoed (1973) “confluence of the Cottica River and Perica Creek, Surinam” and Duellman (2012) “vicinity of Paramaribo, Surinam”. Thus, the common iguanas of northern South America do belong to the species *Iguana iguana* described by Linnaeus without prejudging the taxonomic status of populations in the rest of South America. This is also the position taken by Buckley et al. (2016) if it is considered that those from Central America belong to the species *Iguana rhinolopha* (Wiegemann 1834).

Based on both genetic and morphological data, five species are now recognized (Breuil 2013, 2016; Breuil et al. 2020; Breuil 2021; van den Burg et al. 2021; Caribherp 2021) without considering some regions for which we had no data for these studies (east Ecuador and Columbia, NW Venezuela and ABC Islands, South Brazil): *I. iguana* endemic to north South America, east of the Andes, *I. rhinolopha* endemic to Central America, and, in the eastern Caribbean, *I. delicatissima* in the northern Lesser Antilles, *I. melanoderma* endemic to Saba and Montserrat, and *I. insularis* (Breuil et al. 2020) endemic to the southern Lesser Antilles (Fig. 1). Van den Burg and Malone (2018) argued for a revision of the taxonomy of the *Iguana iguana* complex and our proposals are in total accordance with published data. However, the Reptile Database (2021) prefers to consider *insularis*, *sanctaluciae* and *melanoderma* as subspecies of *Iguana iguana* and follows the opinion of Lazell (1973) by not recognizing *rhinolopha* as a subspecies of *Iguana iguana* nor as a species on a morphological basis. This work was impacted by the low number of samples, their low geographic coverage and the long overlooked hybridization between *Iguana iguana* and *Iguana delicatissima* that has blurred the morphological distinctions between the different lineages. Given that *I. delicatissima* and *I. iguana* readily interbreed and produce fertile hybrids, interspecific hybridizations could be widespread in the genus *Iguana*. To inform conservation management, it is important identify which populations of endemic lineages are still purebred and which show evidence of hybridization. This can be done only if the different lineages are well characterized by means of genetic and morphological data.

The newly described horned insular iguana *Iguana insularis* from the southern Lesser Antilles is separated in two subspecies, *I. insularis sanctaluciae* from St. Lucia and *I. insularis insularis* from the Grenadines. The first descriptions of these taxa were supported by, morphology, including scales and color, and genetic criteria (Breuil et al. 2019). For example, the dewlap of adult iguanas from St. Lucia (*I. insularis sanctaluciae*) becomes totally black with age and the body barred with broad black bands, whereas the dewlap of the Grenadines pink rhino iguana (*I. insularis insularis*) is typically light cream to cream, its bands are narrower, and, in old individuals, markings fade until the animal is almost uniform light cream to nearly white. The genetic analysis was based

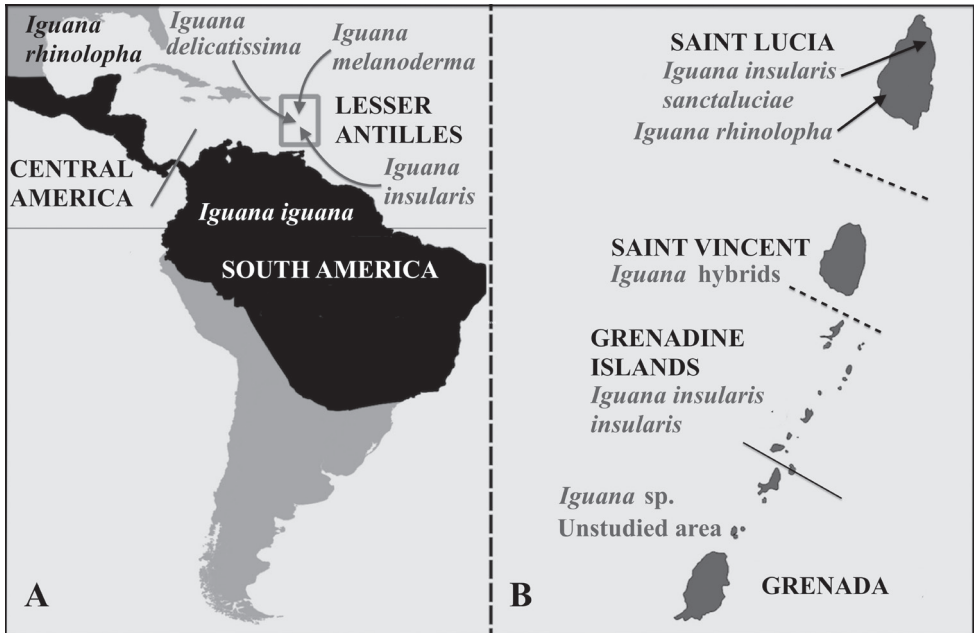


Figure 1. **A** distribution of the five *Iguana* species recognized by Breuil et al. (2020). The Lesser Antilles contain three endemic species (*I. delicatissima*, *I. insularis*, *I. melanoderma*) and the invasive aliens *I. iguana* and *I. rhinolopha*, which hybridize with the endemic insular taxa. The grey line between Central and South America indicates the approximate limit between the two recognized continental species, but the taxonomy and distribution of iguanas in this area warrants further investigation **B** the three geological banks referred to in this paper are separated by two horizontal dash black lines. The black line indicates the political boundary between the country of St. Vincent and the Grenadines to the north and Grenada to the south. The iguanas are named according to the results of this study and Breuil et al. (2020).

on a relatively large number of individuals from St. Lucia but only four individuals from two islands in the Grenadines (Breuil et al. 2019) and none from St. Vincent. This limited genetic sampling made it difficult to draw firm conclusions about the distribution of *I. insularis insularis* and its relationship to *sanctaluciae*.

The present paper adds distribution and genetic data from a further 34 individuals sampled from 20 Grenadine Islands and, for the first time, four specimens from St. Vincent. Seventeen microsatellites were used to estimate genetic diversity, population structure and differentiation between the two subspecies as well as the level of introgression with other *Iguana* species. In addition, both the mitochondrial ND4 and nuclear gene PAC sequences were obtained to gain valuable additional information on genetic variation and hybridization within *Iguana insularis*. This work aims to inform conservation strategies to preserve the genetic integrity of purebred populations of both subspecies, *I. insularis insularis* and *I. insularis sanctaluciae*.

Materials and methods

Field methods

A total of 24 islands and islets were surveyed in St. Vincent and the Grenadines, of which 19 were confirmed to have iguanas. In the Grenadines, the islands surveyed by JD, GG, JG, and colleagues were Union, Tobago Cays, Petit St. Vincent, Canouan and adjacent islands from 5–8 August 2018; Bequia, Battowia Group and adjacent islands from 15–16 August 2018; Bequia alone on 30 August 2018; and Mustique and its adjacent islands on 20 and 21 August 2018. Petit Canouan, Petit Nevis, Isle à Quatre, Pigeon (Ramier) and Mustique were visited between 10–15 September 2019 (Fig. 2). No surveys were conducted on Grenadines islands within Grenada's borders. St. Vincent was also visited by GG and JG, but sampling was confined to Kingstown Botanical Garden.

The iguanas were captured by hand or with a noose. Measurements (snout-vent length and total length) and photographs were taken. Tissue samples (tail tip or shed skin) were collected and preserved in 70% ethanol. The procedure was done as quickly as possible, and the iguanas were released back in their habitat. Photographs were also taken of individuals that evaded capture. Iguanas observed and/or caught in St. Vincent and the Grenadines were identified by using the suite of morphological traits recognized as diagnostic by Breuil (2013, 2016) and Breuil et al. (2019, 2020).

Genetic samples and genetic diversity: microsatellites

For this genetic study, we took biopsies from 34 iguanas from 15 Grenadine Islands and four iguanas from St. Vincent. These 38 samples were genotyped using 17 microsatellite markers amplified as described by Valette et al. (2013) and Vuillaume et al. (2015) (whereas only 15 were used in Breuil et al. 2019) (Tables 1, 2). Subsequently, amplification products were resolved by electrophoresis on an ABI PRISM 3130 Genetic Analyzer. Product sizes were determined using the GeneMapper software (Applied Biosystems, Saint Aubin, France), followed by verification by eye.

These individuals were considered to belong to one group according to the description of Lazell (1973) (St. Vincent and the Grenadines) and compared to other groups identified by Breuil et al. (2019, 2020) (Table 1). We tested all these groups of individuals for departures from Hardy-Weinberg expectations using the software GenAlEx (Peakall and Smouse 2006). Linkage disequilibrium was assessed for each specific microsatellite marker as implemented in FSTAT ver. 2.9.3.2 (Goudet 2001) (with 1,200 permutations). We adjusted the levels of significance for multiple tests using the standard Bonferroni correction (Rice 1989). Further, we assessed genetic polymorphism with the Allelic richness (A_r), expected heterozygosity (H_e) and F_{is} using FSTAT ver. 2.9.3.2 (Goudet 2001) with 1,200 permutations.

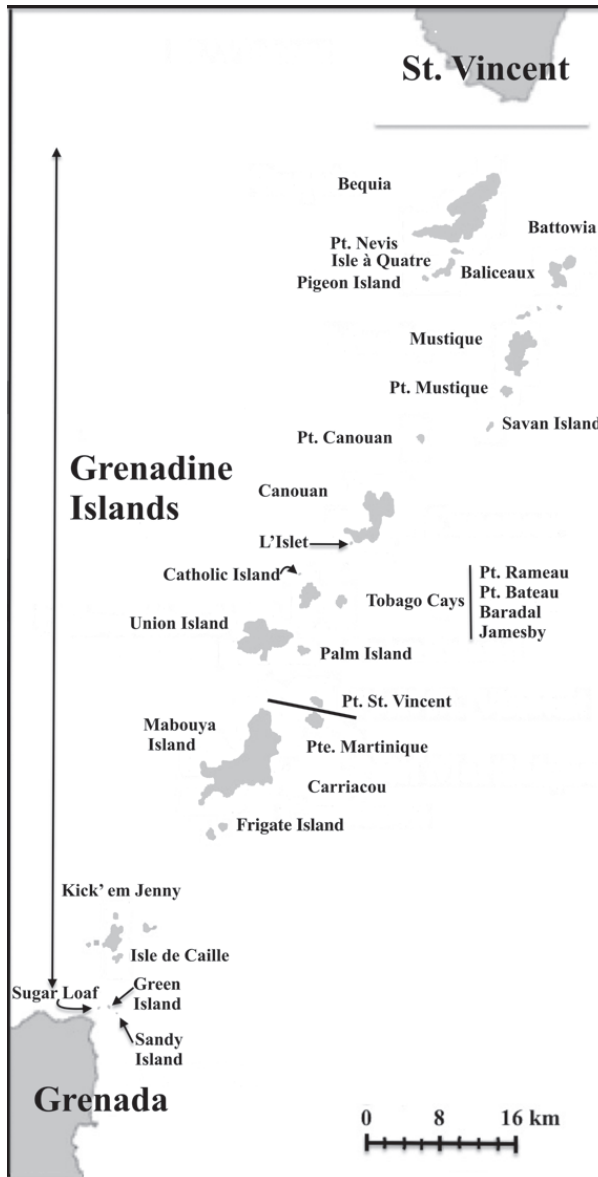


Figure 2. Distribution of iguanas in the Grenadine Islands (modified from Henderson and Powell 2018; Breuil et al. 2019). Note there are alien iguanas on some islands and not all of the island clusters shown here have purebred populations of *I. insularis insularis*. The grey line south of St. Vincent marks the break between the Saint Vincent Bank to the north and the Grenada Bank to the south. The black line between Petit St. Vincent and Petit(e) Martinique shows the political boundary between St. Vincent and the Grenadines to the north and Grenada to the south. The Grenadine Islands form an archipelago from the south of St. Vincent to the north of Grenada. Almost all the Grenadine Islands in St. Vincent and the Grenadines were surveyed during this work and, with the exception of Savan Island, had iguanas at the time of our visits. Petit Mustique was inaccessible during our survey. The islets of Sugar Loaf, Green Island, and Sandy Island (all in Grenada) are reported to no longer have iguanas (Henderson and Powell 2018) but iguanas fitting the morphology of *I. insularis insularis* have been observed on Carriacou and Mabouya Islands (see text).

Table 1. Iguanas sampled for genetic analysis.

Localities	Taxa	Sample size
French Guiana	<i>iguana</i>	7
St. Lucia (South West)	<i>rhinolopha</i>	7
St. Lucia (Grand Anse)	hybrid [#]	4
St. Lucia (Louvet)	<i>sanctaluciaie</i>	13
St. Vincent (Kingstown)	hybrid [#]	4
Grenadines (Battowia)	<i>insularis</i>	3*
Grenadines (Balliceaux)	<i>insularis</i>	1*
Grenadines (Petit Nevis)	<i>insularis</i>	1*
Grenadines (Pigeon)	<i>insularis</i>	2*
Grenadines (Mustique)	<i>insularis</i>	4*
Grenadines (Petit Canouan)	<i>insularis</i>	3*
Grenadines (Canouan)	<i>insularis</i>	1*
Grenadines (L'Islet)	<i>insularis</i>	2*
Grenadines (Tobago Cays: Baradal)	<i>insularis</i>	4*
Grenadines (Tobago Cays: Jamesby)	<i>insularis</i>	4*
Grenadines (Tobago Cays: Petit Bateau)	<i>insularis</i>	2*
Grenadines (Tobago Cays: Petit Rameau)	<i>insularis</i>	2*
Grenadines (Union Island)	<i>insularis</i>	(3* + 1)
Grenadines (Palm Island)	<i>insularis</i>	3
Grenadines (Petit St. Vincent)	<i>insularis</i>	2*
Montserrat	<i>melanoderma</i>	11
Saba	<i>melanoderma</i>	6

* denotes individuals that were new to this study and not presented in previous publications.

[#] hybrid indicates introgressed populations that were identified by a previous study for St. Lucia (Breuil et al. 2019) and by morphology and genetic analysis for St. Vincent.

Genetic structure and introgression

For these analyses, we used microsatellite data from the first four iguanas captured in the Grenadines (*I. insularis insularis* from Union and Palm Islands) in 2018, 17 iguanas from northeast St. Lucia corresponding to *I. insularis sanctaluciaie*, seven *I. rhinolopha* collected from southwest St. Lucia (where this species is an invasive alien), seven *I. iguana* from French Guiana (see Breuil et al. 2019) and 17 *I. melanoderma* from Saba and Montserrat (Breuil et al. 2020) to obtain information about introgression and genetic structure (Table 1). All these analyses were made using 17 microsatellite markers (Table 2).

We computed pairwise fixation index (F_{st}) values between groups of individuals (Weir and Cockerham 1984) using FSTAT v. 2.9.3.2 (Goudet 2001). We adjusted the levels of significance for multiple tests using the standard Bonferroni correction as implemented in FSTAT v. 2.9.3.2 (Goudet 2001).

We conducted a Discriminant Analysis of Principal Components (DAPC) in the *adeget* package (Jombart 2008; Jombart et al. 2010) for R version 3.5.0 to investigate population genetic structure at the individual level. We first performed a Principal Component Analysis (PCA) to transform the raw genetic data retaining all principal components to maximize the variation of the original data. The best number of clusters K was estimated using the function *find.clusters* that implemented a K-means clustering minimizing the variation within clusters and a Bayesian Information Criterion (BIC) approach. We assumed a maximum number of 10 clusters and ran the K-means

Table 2. Summary of the genetic diversity parameters for each locus and each locality.

Loci	Parameters	Groups of individuals							All
		<i>iguana</i> French Guiana	<i>rhinolopha</i> St. Lucia	Hybrid St. Lucia Grand Anse	<i>sanctaluciae</i> St. Lucia Louvet	<i>insularis</i> St. Vincent and the Grenadines	<i>melanoderma</i> (Montserrat)	<i>melanoderma</i> (Saba)	
		<i>n</i> = 7	<i>n</i> = 7	<i>n</i> = 4	<i>n</i> = 13	<i>n</i> = 42	<i>n</i> = 11	<i>n</i> = 6	90
L2	<i>He</i>	0.262	0.476	0.583	0.000	0.587	0.245	0.000	0.320
	<i>Ar</i>	1.505	1.789	1.929	1.000	2.195	1.470	1.000	2.318
	<i>Fis</i>	-0.091	1.000	0.571	NA	0.716	-0.111	NA	0.428
L3	<i>He</i>	0	0.000	0.000	0.000	0.000	0.000	0.000	0.000
	<i>Ar</i>	1.000	1.000	1.000	1.000	1.000	1.000	1.000	1.29
	<i>Fis</i>	NA	NA	NA	NA	NA	NA	NA	NA
L5	<i>He</i>	0.524	0.690	0.750	0.000	0.000	0.364	0.333	0.380
	<i>Ar</i>	1.915	2.538	2.643	1.000	1.000	1.674	1.576	1.666
	<i>Fis</i>	-0.091	-0.448	0.000	NA	NA	-0.250	1.000	0.042
L6	<i>He</i>	0.524	0.429	0.583	0.000	0.260	0.564	0.2	0.366
	<i>Ar</i>	1.869	1.789	1.971	1.000	1.522	2.154	1.400	2.218
	<i>Fis</i>	0.727	-0.333	0.143	NA	0.634	0.355	0.000	0.254
L8	<i>He</i>	0.262	0.5	0	0	0	0	0	0.109
	<i>Ar</i>	1.505	2.000	1.000	1.000	1.000	1.000	1.000	1.117
	<i>Fis</i>	-0.091	0.000	NA	NA	NA	NA	NA	-0.046
L9	<i>He</i>	0.607	0.619	0.583	0.000	0.675	0.672	0.717	0.553
	<i>Ar</i>	2.326	2.181	1.971	1.000	2.478	2.507	2.461	2.652
	<i>Fis</i>	-0.412	0.308	0.143	NA	0.577	0.256	0.535	0.235
L13	<i>He</i>	0.000	0.000	0.583	0.000	0.266	0.000	0.000	0.121
	<i>Ar</i>	1.000	1.000	1.971	1.000	1.496	1.000	1.000	1.866
	<i>Fis</i>	NA	NA	0.143	NA	0.373	NA	NA	0.258
L14	<i>He</i>	0.143	0.000	0.250	0.091	0.157	0.467	0.683	0.256
	<i>Ar</i>	1.286	1.000	1.500	1.182	1.308	1.845	2.434	1.995
	<i>Fis</i>	0	NA	0	0	0.546	-0.5	0.024	0.012
L15	<i>He</i>	0.679	0.357	0.250	0.000	0.092	0.091	0.000	0.210
	<i>Ar</i>	2.426	1.670	1.500	1.000	1.180	1.182	1.000	1.806
	<i>Fis</i>	0.158	-0.200	0.000	NA	0.484	0.000	NA	0.088
L16	<i>He</i>	0.143	0.733	0.000	0.000	0.175	0.000	0.000	0.150
	<i>Ar</i>	1.286	2.461	1.000	1.000	1.335	1.000	1.000	1.452
	<i>Fis</i>	0.000	0.773	NA	NA	0.457	NA	NA	0.410
L17	<i>He</i>	0.488	0.548	0.750	0.000	0.184	0.000	0.000	0.281
	<i>Ar</i>	1.955	1.915	2.557	1.000	1.367	1.000	1.000	2.236
	<i>Fis</i>	0.415	0.478	0.333	NA	0.736	NA	NA	0.491
L18	<i>He</i>	0.533	0.381	0.000	0.000	0.177	0.403	0.000	0.213
	<i>Ar</i>	1.939	1.670	1.000	1.000	1.335	1.810	1	1.978
	<i>Fis</i>	-0.250	0.625	NA	NA	1.000	0.448	NA	0.456
L19	<i>He</i>	0.524	0.000	0.750	0.000	0.218	0.650	0.533	0.382
	<i>Ar</i>	1.930	1.000	2.643	1.000	1.428	2.381	1.919	2.172
	<i>Fis</i>	-0.364	NA	0.000	NA	0.344	-0.119	0.063	-0.015
L20	<i>He</i>	0.655	0.524	0.750	0.000	0.198	0.445	0.000	0.367
	<i>Ar</i>	2.411	1.915	2.557	1.000	1.383	1.809	1.000	2.422
	<i>Fis</i>	-0.091	-0.091	0.333	NA	0.759	-0.429	NA	0.096
L23	<i>He</i>	0.821	0.350	0.750	0.000	0.296	0.000	0.200	0.345
	<i>Ar</i>	2.921	1.667	2.643	1.000	1.616	1.000	1.400	2.454
	<i>Fis</i>	0.304	-0.143	0	NA	0.239	NA	0.000	0.080
L24	<i>He</i>	0.000	0.000	0.000	0.000	0.000	0.000	0.000	0.000
	<i>Ar</i>	1.000	1.000	1.000	1.000	1.000	1.000	1.000	1.000
	<i>Fis</i>	NA	NA	NA	NA	NA	NA	NA	NA
L25	<i>He</i>	0.000	0.000	0.750	0.520	0.000	0.000	0.303	0.315
	<i>Ar</i>	1.000	1.000	2.643	1.904	1.000	1.000	1.576	2.089
	<i>Fis</i>	NA	NA	0.000	-1.000	NA	NA	1.000	-0.152
All	<i>He</i>	0.363	0.330	0.431	0.036	0.193	0.229	0.174	0.257
	<i>Ar</i>	1.722	1.623	1.855	1.063	1.391	1.461	1.339	1.925
	<i>Fis</i>	0.038	0.198	0.118	-0.846	0.583	-0.017	0.432	0.288

N: number of analyzed samples; He: expected heterozygosity, Ar: allelic richness and Fis: inbreeding coefficient. In italics and bold: the Fis value with significant departures from Hardy-Weinberg expectations (i.e., significantly different from 0; $P < 0.0005$ after Bonferroni adjustment). NA = not available. The iguanas of St. Vincent were included in the group *insularis* according to their geographical origin.

algorithm with 1,000 random starting values and 10^8 iterations to ensure convergence. A Discriminant Analysis (DA) was then applied with the DAPC function using 30 principal components explaining more than 95% of the total variance of the data and retaining two discriminant functions that carried most information.

At the individual level, we also accessed the genetic structure using the Bayesian approach implemented by the software STRUCTURE (Pritchard et al. 2000). This clustering approach estimated both the number (K) of genetic cluster(s) and the admixture coefficient of individuals to be assigned to the inferred clusters. We selected the admixture model and the option of correlated allele frequencies among populations. As recommended by Evanno et al. (2005), we replicated 20 independent runs for each value of K (with K varying from 1 to 10) with a total of 100,000 burn-in and 100,000 recorded iterations. To determine the number of genetic clusters from structure analyses, we used the STRUCTURE HARVESTER program (Earl and VonHoldt, 2011) to compare the mean likelihood computed from the 20 independent runs.

The best number of clusters was determined using the hierarchical approach delta K method (Evanno et al. 2005). In a first stage, the uppermost hierarchical structure was determined by determining the best number of clusters using delta K on the entire dataset. In a second stage, independent analyses were performed with individual belonging to each genetic cluster identified in the first stage to identify more refined population genetic structure within main genetic clusters. The total number of clusters was then determined by summing up the number of clusters in analyses of the subset of the data. The final result was obtained by selecting the most likely run from the entire dataset analysis (i.e., showing the highest likelihood) within repeated runs at optimal K value. The R package ape (Paradis et al. 2019) was used to build a genetic distance tree based on the allele frequency divergence among genetic clusters computed by STRUCTURE.

Mitochondrial and nuclear genes

ND4 sequences were obtained from 14 individuals from St. Vincent and the Grenadines following the methods of Breuil et al. (2019), and the PAC region was sequenced from five individuals from St. Lucia, three from St. Vincent, and 10 from the Grenadine Islands according to the protocol of Stephen et al. (2013). These were used to gain a more complete insight into introgression because these two genes are diagnostic of *Iguana insularis sanctaluciae* in St. Lucia (Stephen et al. 2013) and, as discovered in this work, also of *I. insularis insularis* in St. Vincent and the Grenadines.

Results

Geographical distribution of iguanas in St. Vincent and the Grenadines

This analysis confirms the presence of Grenadines pink rhino iguanas (*I. insularis insularis*) on the following Grenadine Islands (listed from north to south): Bequia, Petit

Nevis, Isle à Quatre, Pigeon Island, Battowia, Baliceaux, Mustique, Petit Canouan, Canouan, L'Islet, Catholic Island, Mayreau, Baradal, Jamesby, Petit Bateau, Petit Rameau, Union Island, Palm Island, Frigate Rock, and Petit Saint Vincent (Fig. 2). No iguanas were observed on Petit Tabac, Church Cay, West Cay, the Pillories (small cays between Battowia and Baliceaux) or Savan Island. All the aforementioned islands are within the political boundary of St. Vincent and the Grenadines: no genetic data were obtained from islands belonging to Grenada.

All the iguanas captured and/or photographed from the Grenadines showed characteristics consistent with *I. insularis insularis* (Breuil et al. 2019). For example, 12 iguanas from the Tobago Cays (Baradal, Jamesby, Petit Bateau, and Petit Rameau, Fig. 3) were adults that had lost their juvenile green coloration (Fig. 4), 11 of which had black stripes of variable intensity and width on a pale body, often with a pinkish hue (hence their trade name “zebra iguanas” or “Grenadines pink rhino iguanas”). Some iguanas had lost their black stripes, with only a few dark scales remaining. These iguanas were typically the largest and presumably oldest ones encountered. The largest individual (136 cm total length) was captured on Petit Bateau.

Three out of the four iguanas captured on St. Vincent (Kingstown Botanical Garden) were photographed (Fig. 5) and did not present any of the diagnostic characteristics of *I. insularis* described by Breuil et al. (2019). IGU139 (Fig. 5) is an old male with an elongated head, no nasal horns, a light eye with no white visible, a huge sub-tympanic plate, a mosaic of small scales anterior to this plate and a green body with light grey dorsal spines. This phenotype can be interpreted as an intermediate between *I. iguana* from French Guiana and *I. rhinolopha* with no apparent morphological traits of *I. insularis* apart from a low number of small to medium-sized tubercles on the neck. IGU140 was a young individual without horns, but other diagnostic characters could not be checked because of its age. IGU141 (Fig. 5) was a female that did not present any morphological characteristics of *I. insularis*. The very small nasal horns cannot be interpreted on this picture as typical of *rhinolopha* or *insularis* or intermediate between them. This individual possessed black scales between the eye and the tympanum that forms a kind of discontinuous spot (not dissimilar to the black spot of *I. melanoderma*: Breuil et al. 2020). Overall, these three iguanas had a phenotype most similar to *I. iguana* from French Guiana.

Genetic diversity

No linkage disequilibrium was detected after applying a Bonferroni correction (p-value threshold after Bonferroni adjustment, $P = 0.0005$). Only eight of the 105 groups of individuals/locus combinations deviated significantly from Hardy-Weinberg expectations (adjusted p-value threshold after Bonferroni adjustment, $P = 0.0004$). These deviations occurred only for populations of *I. insularis* and likely resulted from a Wahlund effect because the individuals came from different Grenadine islands and likely displayed different genetic signatures. All microsatellite loci were polymorphic with an allelic richness (A_r) ranging from 1 to 2.921 and a genetic diversity (H_e) ranging from 0 to 0.821 across groups of individuals (Table 2).

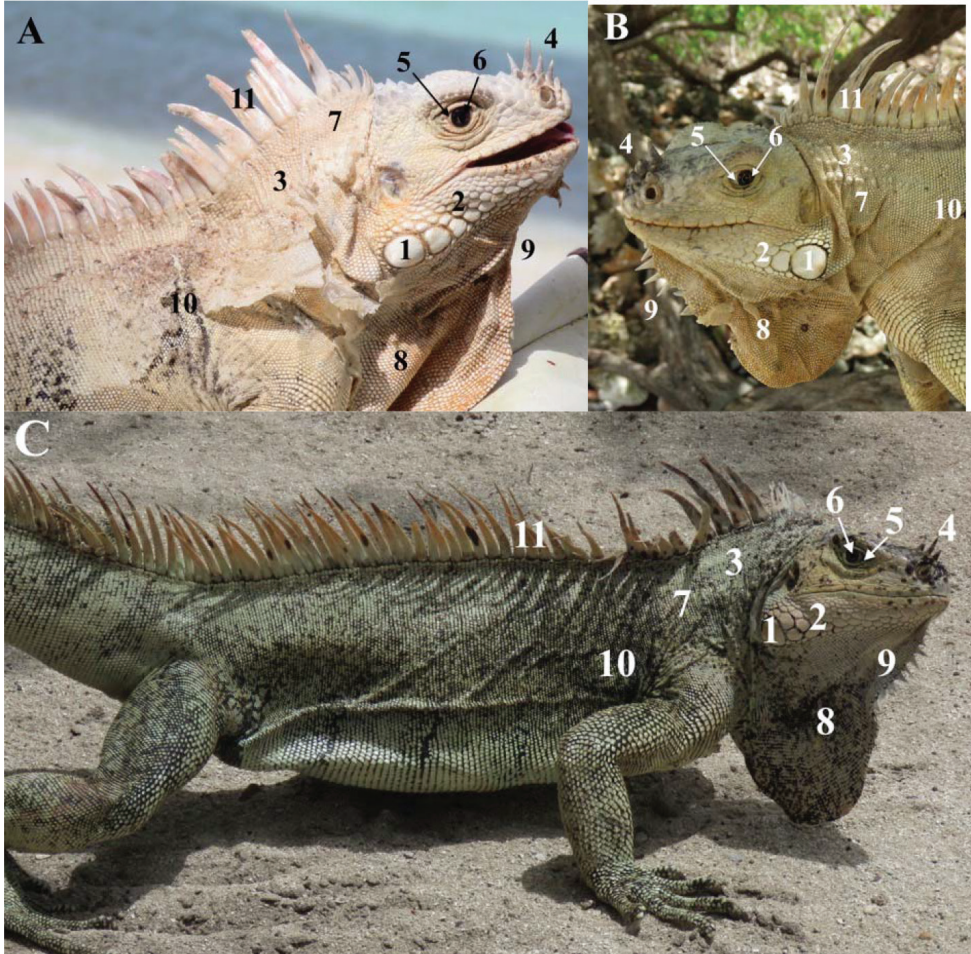


Figure 3. Photographs of three adult male *Iguana insularis insularis* on the Tobago Cays (Grenadine Islands). **A** IGU105 (Baradal). This male has the typical coloration of *I. insularis insularis* with faint black banding, eye with visible white area, nasal horns, small subtympanic plate and very few and small tubercles on the neck, but also presents atypical sublabbial scales and conical scales on the nape **B** IGU112 (Petit Rameau) is a typical older male *I. insularis insularis*, with no black bands on the body (not shown in this photograph) **C** IGU110 (Petit Bateau) has a body with small and narrow ventral black bands and numerous black scales on the body. 1. relatively small subtympanic plate 2. mosaic of small scales 3. very low to low number of small neck tubercles 4. lateral and median horns 5. white visible in the eye. 6. brown eye 7. light cream coloration in old adults; green in juveniles and younger adults 8. light dewlap with some black scales (**C**) 9. small number of small gular spikes (not always visible on the photographs) 10. light body with different degrees of persistence of black stripes 11. light and high dorsal spikes with a pink or orange hue.

Population structure

Results revealed significant genetic differentiation between groups of individuals (mean F_{st} value = 0.55) (Table 3). DAPC (Fig. 6) clearly suggested a strong genetic differentiation between five groups: alien individuals from St. Lucia (*I. rhinolopha*),

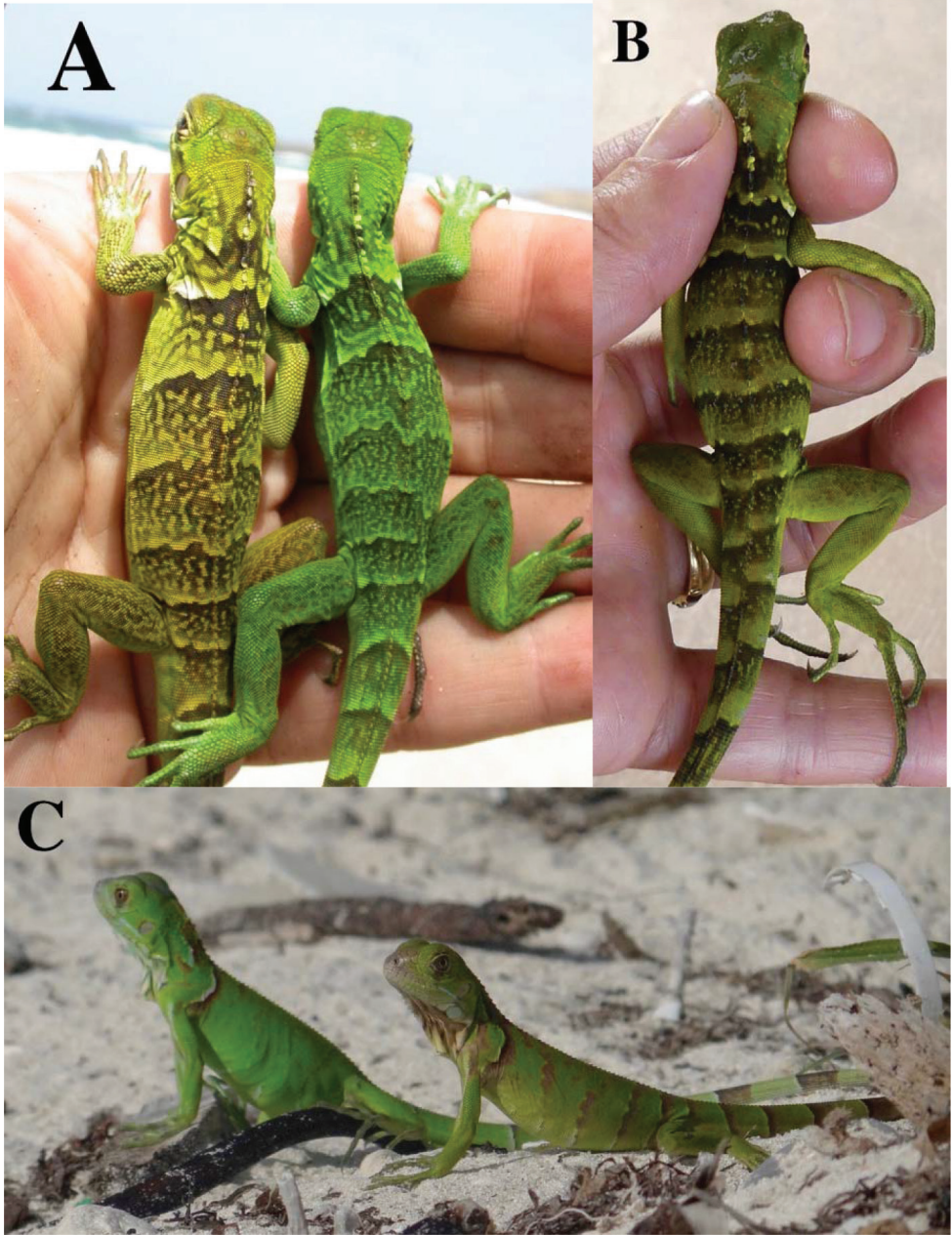


Figure 4. **A** *Iguana insularis sanctaluciae* hatchlings (northeast Saint Lucia) **B** hatchling *I. insularis insularis* (IGU143, Union Island, Grenadines). The *I. insularis* hatchlings in both **A** and **B** show strong dark green to light green banding on the body and the tail, with a white mark at the scapular level **C** hatchlings alien *I. rhinolopha* in Florida. These iguanas have a nearly uniform green body with only some brown narrow banding on the body.

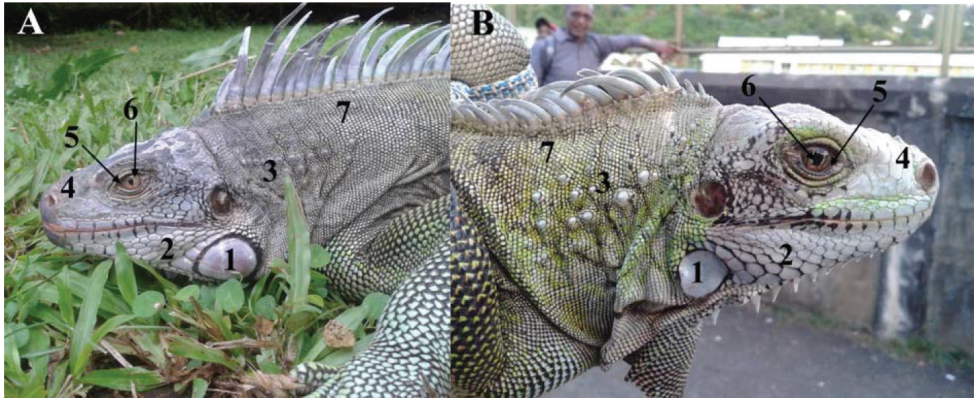


Figure 5. Hybrid iguanas IGU139 **A** and IGU141 **B** from the island of St. Vincent. (see text for more information) 1. medium (**B**) to large subtympnic plate (**A**) 2. mosaic of small scales 3. low number of small neck tubercles 4. no horn (**A**) or very short horns (**B**) 5. no white visible in the eye 6. yellowish-brown eye (**A**) or light brown eye (**B**) 7. grey-green coloration (**A, B**) or green-black coloration (**B**). None of these morphological features conform with the characteristics of *I. insularis insularis*.

Table 3. Comparison of *Fst* values for each pairwise group of individuals (below diagonal) and their significance (above diagonal). P-value threshold after Bonferroni adjustment, P = 0.0024. NS = not significant; * = significant. Mean *Fst* values: 0.55. The iguanas of St. Vincent were included in the group *insularis* according to their geographical origin but are hybrids as this was discovered by this work.

	1	2	3	4	5	6	7
1 <i>Iguana iguana</i> French Guiana	–	NS	NS	*	*	*	NS
2 <i>I. rhinolopha</i> St Lucia	0.53	–	NS	NS	*	NS	NS
3 Hybrid St Lucia Grand Anse	0.26	0.45	–	NS	*	*	NS
4 <i>I. insularis sanctaluciaae</i> St Lucia Louvet	0.74	0.82	0.54	–	*	*	*
5 <i>I. insularis insularis</i> St Vincent and the Grenadines	0.53	0.72	0.38	0.34	–	*	*
6 <i>I. melanoderma</i> Montserrat	0.38	0.63	0.45	0.81	0.64	–	*
7 <i>I. melanoderma</i> Saba	0.46	0.66	0.50	0.87	0.71	0.11	–

native individuals from both Montserrat and Saba (endemic *I. melanoderma*), individuals from St. Lucia (endemic *I. insularis sanctaluciaae*), individuals from the Grenadines (endemic *I. insularis insularis*), and French Guiana (*I. iguana*). It confirmed there is clear genetic differentiation between *I. insularis insularis* from the Grenadines and *I. insularis sanctaluciaae* from St. Lucia. Moreover, the populations of St. Vincent and Grand Anse (St. Lucia) show mostly hybrids (*I. insularis* admixed with alleles from *I. iguana* and *I. rhinolopha*; Fig. 7).

Moreover, the twenty independent runs implemented in the STRUCTURE and STRUCTURE HARVESTER software revealed the highest mean likelihood for *K* = 2 genetic clusters (Fig. 7). Indeed, the main genetic structure we found clearly distin-

guished individuals of both *I. insularis insularis* and *I. insularis sanctaluciae* (from the Grenadines and St. Lucia, respectively) from other taxa (i.e., *I. rhinolopha*, *I. iguana*, *I. melanoderma*). The results also highlighted individuals showing intermediate admixture coefficients on both St. Lucia and St. Vincent, suggesting hybridization (Figs 5, 7). With $K = 5$, the STRUCTURE software also clearly separated genetic clusters that fit well with the five taxa (Figs 6, 7).

Mitochondrial and Nuclear Genes

Of 14 individuals from St. Vincent ($n = 3$) and the Grenadine Islands ($n = 11$) sequenced for ND4 for this study, the haplotype of St. Lucia AF217782 identified by Stephen et al. (2013) was found on St. Vincent ($n = 3$), Battowia ($n = 3$), Tobago Cays ($n = 3$), Pigeon Island ($n = 1$), Union Island ($n = 1$) and Petit St. Vincent ($n = 1$). Moreover, an *insularis* haplotype (MK687402-3) previously identified by Breuil et al. (2019) on Palm Island was also found on Jamesby (MN590142) and Mustique (MN590150).

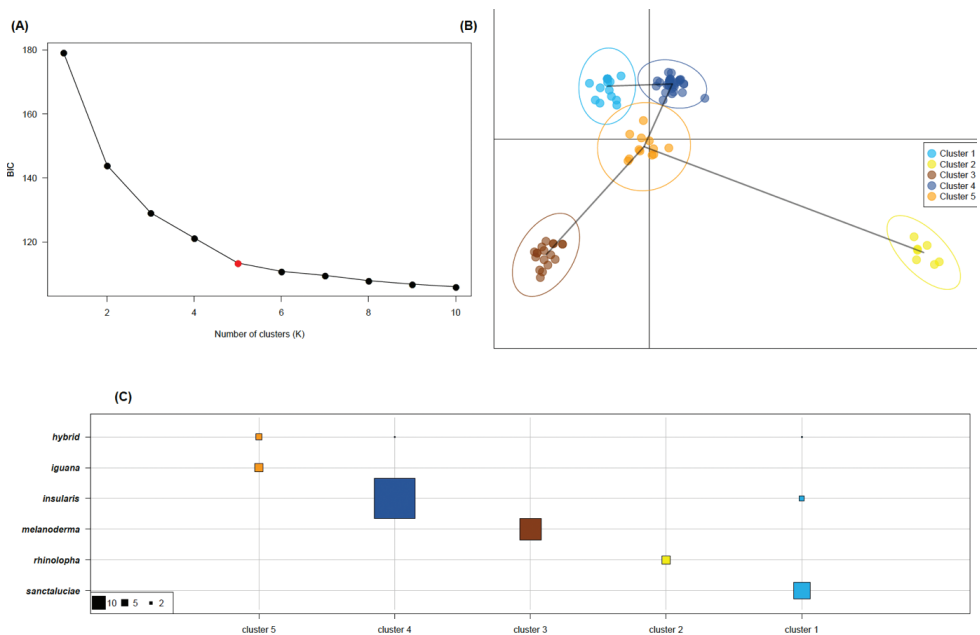


Figure 6. Discriminant Analysis of Principal Components (DAPC). **A** variation of the Bayesian Information Criterion (BIC) as a function of the assumed number of genetic clusters (K) **B** scatterplot representing individual (dots) and clusters (inertia ellipse) location in the principal component space **C** correspondence between species determination (in line) and genetic cluster (in column). The taxa names refer to species level for all them except for *insularis* and *sanctaluciae* which are the two subspecies of *Iguana insularis*. Hybrid refers to the population of St. Vincent.

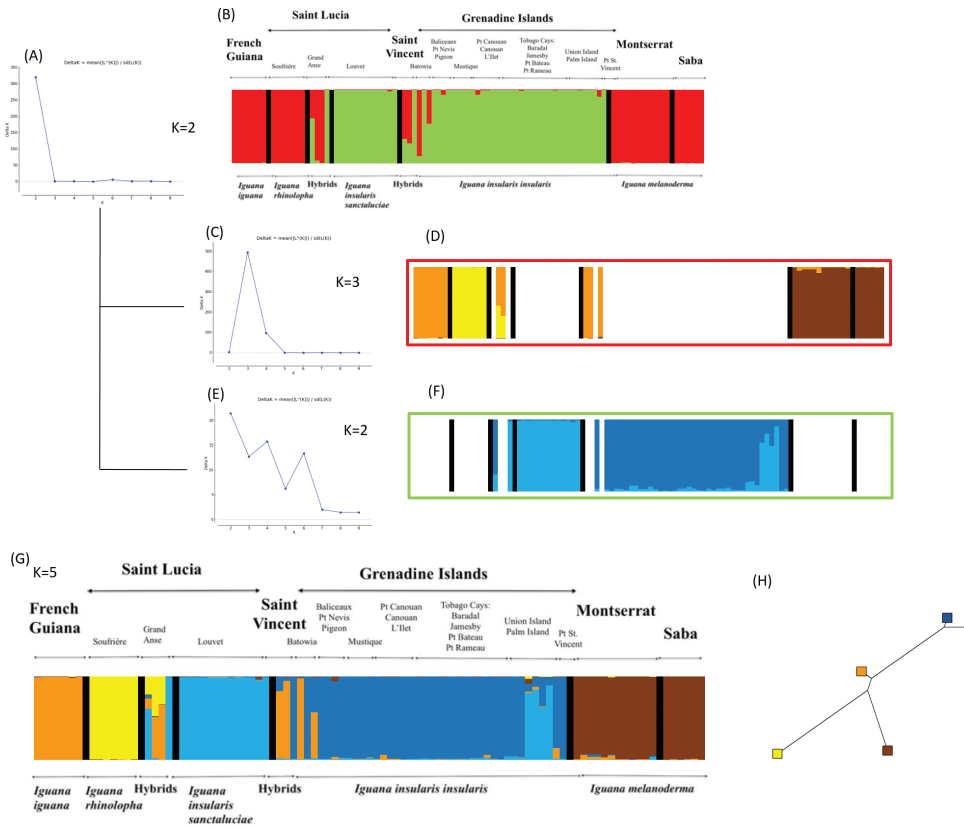


Figure 7. Hierarchical Structure analysis: **A** delta K method estimating that the uppermost hierarchical structure is composed of two main genetic clusters **B** corresponding barplot showing each individual as a vertical bar where each color corresponds to the admixture coefficient of the inferred genetic clusters; additional analyses within each of these two genetic clusters **C-F** showed that the first genetic cluster is composed of three genetic clusters (**C, D**) and the second one of two genetic clusters (**E, F**) totaling an overall number of five genetic clusters across the whole dataset **G** genetic distance tree between genetic clusters based on the allele frequencies divergence among clusters **H**.

The ND4 haplotype AF217782 identified by Stephen et al (2013) in St. Lucia is also present in *I. insularis insularis*: the three hybrids from St. Vincent, the three from Battowia, in three of four individuals from the Tobago Cays (Baradal, Petit Bateau, Petit Rameau), in the one from Petit St. Vincent, and in one of the two iguanas from Union Island. Palm Island has three different haplotypes, but we did not find AF217782 here. Jamesby (Tobago Cays) and Mustique have another haplotype. Thus of the 28 sequences available for *Iguana insularis* (Stephen et al. 2013; Breuil et al. 2019, this study) none of the haplotypes of this species were observed among the 201 sequences studied (Stephen et al. 2013: $n = 73$; Breuil et al. 2019, 2020: $n = 19$; De Jesús Villanueva: $n = 109$). Breuil et al. (2019, 2020) published two median-joining

haplotype networks for ND4 showing the independent position of these *insularis* haplotypes at the end of a branch.

All the sequenced iguanas from the Grenadines ($n = 10$) had the same endemic haplotype of the PAC gene (JN811117) as the one found in Louvet (St. Lucia) by Stephen et al. (2013) with $n = 6$. This haplotype differs by a G instead of a A at site 323. Moreover, we also found this haplotype in three hybrids from St. Vincent that were homozygous for this gene. Conversely, the population of Grand Anse (St. Lucia) had two iguanas (IGU53, IGU57) with this endemic JN811117 haplotype, whereas two others (IGU55, IGU56) are homozygous for a widespread Central American haplotype (JN811107).

The haplotype (JN811117) of the PAC gene identified by Stephen et al. (2013) in six individuals from St. Lucia was also found in all individuals of *I. insularis*: three from St. Lucia (Louvet), ten from the Grenadines and three hybrid individuals from St. Vincent. Two iguanas from the Grand Anse (St. Lucia) hybrid population out of the four sampled are homozygous for this haplotype while the other two recognized as hybrids (Breuil et al. 2019) are homozygous for a haplotype (JN811107) present in iguanas from Belize, El Salvador, Honduras, Guatemala, and Nicaragua. For example, the 70 PAC gene sequences obtained by Stephen et al. (2013), the 86 sequences from invasive exotic iguanas (De Jesús Villanueva et al. 2021) and the 19 from this study reveal 25 different haplotypes for this gene. Of 175 iguanas sequenced for this gene, haplotype JN811117, found nowhere else, unambiguously identifies *Iguana insularis* among all other lineages and thus confirms the complex hybridization history of some populations.

Discussion

Distribution of *Iguana insularis* on the St. Vincent and Grenada/Grenadines banks

All 34 iguanas sampled on 15 islands across the Grenadines during the present survey were identified as *I. insularis insularis* and their morphology reinforced the assertion by Breuil et al. (2019) that the subspecies *insularis* and *sanctaluciae* can be reliably distinguished as adults from their coloration: Adult *I. insularis insularis* are characterized by a beige, cream or even dirty white dewlap with relatively narrow black body stripes that tend to fade with age, whereas *I. insularis sanctaluciae* typically develops a black dewlap and has relatively wide black body stripes that become even more pronounced with age.

Results from microsatellites from the 34 new samples from the Grenadines were found to be in accordance with morphological data. This study confirms the presence of *Iguana insularis insularis* on multiple Grenadine Islands based on genetic data. Both STRUCTURE and DAPC genetic analyses confirmed there is a clear differentiation between *I. insularis insularis* and *I. insularis sanctaluciae* (which was reported by Breuil et al. 2019 but based only on four genetic samples from the Grenadines). The *F_{st}* value was around 0.32, which supported a strong genetic difference between the two subspecies.

While *I. insularis sanctaluciae* is restricted to St. Lucia (Breuil et al. 2019), the new genetic evidence from the Grenadines shows *I. insularis insularis* extends from Bequia (North) to at least as far south as Petit St. Vincent. Gaymes and Justo-Gaymes (2018) observed iguanas with this phenotype on 19 of the 24 islands surveyed within the national boundary of St. Vincent and the Grenadines. Photographs of iguanas nesting in April 2020 on Anse la Roche, Carriacou, and iguanas in December 2020 on Mabouya Island, two of the Grenadine Islands in Grenada, were also consistent with *I. insularis insularis* (Juliana Coffey in litt. to JD). Indeed, the native range of this taxon might extend as far south as the main island of Grenada, as suggested by the pioneering work of Lazell (1973), which shares the same geological bank as the Grenadines. Photographs of Grenadian iguanas published in Henderson and Powell (2018: 43, 267), however, show a combination of morphological characteristics that indicates the presence of hybrids with *I. iguana* and *I. rhinolopha*.

One of the challenges to elucidating the natural ranges of iguanas in this region is that they are often transported by people. For example, it is common practice for hunters to collect live iguanas from the Grenadines to sell as bushmeat on St. Vincent and Grenada during the hunting season from October through January (GG, pers. obs.). Daudin and de Silva (2011) reported that hunting is frequent on the uninhabited island of Baliceaux, from which hunters from Bequia and St. Vincent “carry away dozens of iguanas”. Some years ago, 30 iguanas from Palm Island were translocated to Petit St. Vincent, and in 2005 the St. Vincent & the Grenadines Forestry Department relocated 260 iguanas from Palm Island to the nearby Tobago Cays (also in the Grenadines) and to the Kingstown Botanical Garden on St. Vincent (Daudin and de Silva 2011). In 2020, 20 iguanas from Palm Island were translocated to Union Island by the Forestry Department, again in response to complaints from the Palm Island Resort. These translocations show the impact of human on the distribution and genetic structure of iguana populations in this region and thus it might be supposed that no population has remained untouched. Natural dispersal between nearby islands may also serve to homogenize these populations.

Spread and impacts from alien iguanas: introgression of *Iguana insularis*

Our samples from Battowia, Baliceaux, and Petit Canouan (Grenadine Islands) showed evidence of introgression of *I. insularis insularis* by South American *I. iguana*. Similar observations were reported by Breuil et al. (2019) in one specimen of *I. insularis insularis* on Union Island that harbored a South American mitochondrial haplotype (based on the analyze of the ND4 *loci* MK687401). Introgression is already a well-known phenomenon in iguana populations, notably between *I. iguana* and *I. delicatissima* in Guadeloupe and Anguilla and between *I. rhinolopha* and *I. delicatissima* in St. Barthélemy (Breuil 2013, 2016; Vuillaume et al. 2015; Pounder et al. 2020) and St. Eustatius (van den Burg et al. 2018). *Iguana rhinolopha* is an invasive alien species in the Lesser Antilles and is inferred to have originated from breeding farms in Central America (Costa Rica, Nicaragua, Honduras, Guatemala, El Salvador), which supply the pet trade (Stephen et al. 2011). *Iguana iguana* is also invasive in the Lesser

Antilles and may have arrived in St. Vincent and in the Grenadine Islands from the allochthonous *I. iguana* population of Martinique, where the species was introduced from Les Saintes and thus from French Guiana (Breuil 2009). In the light of both genetic and morphological results, the islands where *I. insularis insularis* specimens showed no or very low introgression with continental alien iguanas were Baliceaux, Petit Nevis, Mustique, Pigeon (Ramier), Petit Canouan, L'Islet, and the Tobago Cays (Baradal, Jamesby, Petit Rameau, Petit Bateau). On Battowia, Union Island, Palm Island, and Petit St. Vincent, on the other hand, the situation is more complex with some individuals being admixed with continental iguana alleles and, on Union and Palm islands, *I. insularis sanctaluciae* alleles.

While *I. insularis insularis* is considered endemic to the Grenada Bank (which includes the Grenadines) and *I. insularis sanctaluciae* is endemic to St. Lucia, Breuil et al. (2019) were unable to identify the taxon indigenous to the St. Vincent Bank, which lies between the two (Fig. 1B). The present study was unfortunately unable to answer this question definitively because all four iguanas sampled on St. Vincent during the present survey were found to belong to a hybrid population. All three that were photographed had a phenotype closely resembling French Guiana *I. iguana* whereas their PAC and ND4 sequences are *insularis* and their microsatellites are a combination of *Iguana iguana*, *I. rhinolopha*, and *I. insularis insularis*. We have no data on the morphology of the fourth specimen, IGU132, but its microsatellite genotype corresponded with *I. insularis insularis*. It is, however, impossible to establish whether this last specimen represents an endemic iguana from the original population of St. Vincent or is the descendant of released or escaped iguanas from the Grenadines (e.g., Daudin and de Silva 2011). The ND4 haplotype of these three St. Vincent iguanas shows that the maternal lineage is *I. insularis* and this haplotype is the most common found in this species (MN590151-53). The homozygous PAC diagnostic locus (JN811117) shows that there have been at least backcrosses with *I. insularis*. The microsatellites also indicate that this population is deeply introgressed. We see on St. Vincent an important discrepancy between the genetic analysis of this hybrid population and its morphology, which seems to indicate a nearly pure *Iguana iguana* population.

We have not found any genetic or morphological signs of *I. delicatissima* in the iguanas from St. Vincent and the Grenadines. Conversely, in one population sampled on St. Lucia (Grand Anse, $n = 4$), Breuil et al. (2019) found two *I. insularis sanctaluciae* with a *delicatissima* mitochondrial haplotype (MK687394-95). Moreover, these two individuals are homozygous for a PAC Central American haplotype (JN811107) and present microsatellites typical from *I. iguana* and *I. rhinolopha*. The third individual has a *delicatissima* ND4 like haplotype (MK687392) and is homozygous for the PAC *insularis* diagnostic haplotype (JN811117), while its microsatellites show introgression with both *I. iguana* and *I. rhinolopha*. The fourth individual from this population has ND4 and PAC haplotypes and microsatellites typical from *I. insularis sanctaluciae*. Thus, this St. Lucian population demonstrates the complexity of hybridization in the genus *Iguana*, where some individuals possess genetic sequences belonging to four phylogenetic species that all have the ability to breed and produce fertile offspring,

as demonstrated by the backcrosses. One of us (JD) was told in May 2021 that the Forestry Department of St. Lucia used to take iguanas handed in by the public to release at Grand Anse. This was done at a time where the morphological differences between iguanas were not well understood and these unfortunate translocations may well explain the alien genes in that population.

Implications of these findings for the conservation of *Iguana insularis*

As a result of both deliberate and accidental transportation, invasive alien iguanas (*I. iguana* and *I. rhinolopha*) and their fertile hybrids are now widely scattered across the Eastern Caribbean and pose a serious threat to all remaining indigenous populations of *I. insularis*, *I. melanoderma* and *I. delicatissima* (Breuil et al. 2019, 2020; Pounder et al. 2020; van den Burg et al. 2018; Breuil 2021). Indeed, a number of populations have already been lost following incursions by invasive alien *Iguana* species, e.g., *I. delicatissima* from most of Guadeloupe after the arrival of *I. iguana* (Vuillaume et al. 2015). The spread of alien lineages is likely to accelerate, with increasing traffic between islands and the projected increase in the frequency and severity of hurricanes due to climate change. Shortly after Hurricane Maria struck Dominica in September 2017, conservationists on the island discovered an incursion of alien iguanas that were inferred to have arrived on cargo boats with relief supplies, posing a major threat to the indigenous *I. delicatissima* population (van den Burg et al. 2020, 2021). At the time of writing, St. Vincent, reeling from a series of volcanic eruptions that began in April 2021, is receiving humanitarian aid on boats from Martinique and other islands whose harbors are infested with hybrid iguanas. Further arrivals of alien iguanas could eventually result in the progressive genetic absorption of *I. insularis*. The available evidence, mainly photographs, suggests that this may have already been the fate of the native iguanas on the main islands of St. Vincent and Grenada. Further surveys are urgently needed on both islands to determine whether any intact populations of their native iguanas remain.

These findings have important implications for conserving *I. insularis*. Most of the known populations are small, fragmented and exposed to multiple anthropogenic threats in addition to the alien iguanas. St. Lucia's native population (subsp. *sanctaluciae*) is severely depleted and restricted to northeast St. Lucia, where it is under immense pressure from habitat loss, illegal poaching for bushmeat and the international pet trade, and feral and invasive alien mammals. Furthermore it faces a rising population of invasive alien *I. rhinolopha* that is spreading from southwest St. Lucia (Krauss et al. 2014). This subspecies clearly meets the IUCN criteria for Critically Endangered (Breuil et al. 2019), meaning it is at high risk of extinction. As shown in this paper, there is already clear evidence of hybridization in Grand Anse, an area that was erroneously believed to contain only purebred St. Lucia iguanas.

The situation looks somewhat brighter in the Grenadines, where the native iguanas (subsp. *insularis*) still occupy at least 21 of the 35 named islands. Unfortunately, most of these sites are very small and unprotected, and there is little to prevent incursions of

alien iguanas from St. Vincent or Grenada, especially during the hunting season when live iguanas are openly transported between islands. Evidence of past hybridization with *I. iguana* was detected on several islands. Other threats observed during our field surveys included invasive alien cats, dogs, and rats (which prey on iguanas and eggs), domestic goats (which destroy vegetation), and bushfires (including the near-annual fires on Petit Canouan lit by seabird egg-collectors) (Gaymes and Justo-Gaymes 2018; Daltry and Steele 2020). Iguanas are hunted across the Grenadines for meat and, increasingly, for the international pet trade. A recent study found the “Grenadines pink rhino iguana” among the top three reptiles traded from the Eastern Caribbean (Noseworthy 2017). By recognizing the new species and two subspecies, we realize that the demand from reptile collectors could increase (Auliya et al. 2016) and this must be countered by increased protection both locally and internationally. We therefore uphold the recommendation in Breuil et al. (2019) to upgrade *Iguana insularis* from CITES Appendix II to Appendix I. We also call for tighter controls on the movements of iguanas between islands, even within national borders, to avoid unsustainable hunting and reduce the spread of alien iguanas.

Differentiation of *Iguana insularis*

The microsatellites used in this study clearly show the uniqueness of the *insularis* lineage compared to other representative populations in the *Iguana iguana* complex. Furthermore, comparison of the two subspecies of *insularis*, in a broader geographic context (van den Burg et al. 2021) including individuals from the different clades identified by Stephen et al. (2013), supports the originality of this species and its separation into two subspecies.

All of these genetic data (unique PAC and ND4 haplotypes) also confirm the uniqueness of the iguana populations of the southern Lesser Antilles, which were first identified by Lazell (1973). The combination of different morphological characteristics (scales, color) gives them a unique phenotype found nowhere else. These distinctive features have been acquired through an independent evolutionary history and are arguments for the recognition of the southern Lesser Antilles populations as a species with two easily identified subspecies which share morphological and genetic synapomorphies. However it would be similarly reasonable to hypothesize that *insularis* and *sanctaluciae* are subspecies of *Iguana iguana* along with *melanoderma* and *rhinolopha*. Based on our data (morphology, genetic), we lean towards splitting this complex into several species, but we know well that further research is needed, especially in South America, to get a consensus for the taxonomy of this iconic lizard.

Conclusion

The current range of the southern Antilles horned iguana *Iguana insularis* includes St. Lucia (subsp. *sanctaluciae*) and at least 21 islands in the Grenadines (subsp. *insularis*).

The first descriptions of these taxa were informed by genetic analysis of a relatively large number of individuals from St. Lucia but only four from the Grenadines (Breuil et al. 2019). The present paper adds genetic data from a further 34 individuals in the Grenadines and, for the first time, four from St. Vincent. Seventeen microsatellites, PAC and ND4 genes were used to estimate genetic diversity, population structure, and differentiation between the two subspecies as well as the level of introgression with other *Iguana* species. The results support recognition of *Iguana insularis* as an independent lineage and also confirms there is a clear genetic differentiation between *I. insularis insularis* and *I. insularis sanctaluciae*. Because gene flow with introgression exists between all these five species, these recognized taxa do not fit the biological species concept and thus could be considered as subspecies of *Iguana iguana* (as suggested by the Reptile Database, 2021). However, this gene flow is a recent phenomenon due to human activities. These anthropogenic movements of iguanas have disrupted the normal and independent evolution of these different island populations.

Despite having only recently been described, *Iguana insularis* faces multiple threats, including unsustainable hunting, habitat loss and invasive alien species, including alien iguanas. While purebred *I. insularis insularis* populations survive on several islands in the Grenadines, our results reveal evidence of hybridization with *I. iguana*, an invasive alien species from South America, and *I. rhinolopha* from Central America. The *I. insularis* population of St. Vincent shows a high level of introgression from *I. iguana*, while on St. Lucia, a growing population of invasive Central American *I. rhinolopha* endangers the remnant population of *I. insularis sanctaluciae*. Experiences from other islands suggest that both invasive alien species are capable of driving native iguana to extinction through competition and introgression. Stronger protection of *I. insularis* is required throughout its range, coupled with concerted efforts to curb the spread of alien iguanas, *I. iguana* and *I. rhinolopha*.

Acknowledgements

Fieldwork in St. Vincent and the Grenadines in 2018 and 2019 was conducted by staff from the St. Vincent and the Grenadines Forestry Department (G. Gaymes, Bradford Latham, Ian Christopher, Victor Primus, and J. Justo-Gaymes) and Fauna & Flora International (J. Daltry, Sophia Steele, and Isabel Vique) with local residents including Nielsen Williams, Roseman Adams, Kayroy Baptiste, Esrome Durant, Joshua Harvey, and Orsen Ollivierre. JD, GG, and JG thank the Forestry Department, Fauna & Flora International, the Species Fund, Disney Conservation Fund, the SVG Environment Fund and US Fish & Wildlife Service (#F18AP00796) for funding and in-kind support, and are grateful for the kind cooperation of the Tobago Cays Marine Park, Union Island Environmental Attackers, the Mustique Company Ltd., Canouan Coast Guard, Canouan Police, Tamarind Beach Hotel, Louise Mitchell-Joseph, Kenneth Williams, Javan Lewis, Nakita Poon Kong, Mr. Martin, and the boat captains and crew. Computer time for the STRUCTURE analysis was provided by the computing

facilities MCIA (Mésocentre de Calcul Intensif Aquitain) of the Université de Bordeaux and of the Université de Pau et des Pays de l'Adour.

References

- Auliya M, Altherr S, Ariano-Sanchez D, Baard EH, Brown C, Brown RM, Cantu JC, Gentile G, Gildenhuis P, Henningheim E, Hintzmann J, Kanari K, Krvavac M, Lettink M, Lippert J, Luiselli L, Nilson G, Nguyen TQ, Nijman V, Parham JF, Pasachnik SA, Pedrono M, Rauhaus A, Rueda Córdova D, Sanchez ME, Schepp U, van Schingen M, Schneeweiss N, Segniagbeto GH, Somaweera R, Sy EY, Türkozan O, Vinke S, Vinke T, Vyas R, Williamson S, Ziegler T (2016) Trade in live reptiles, its impact on wild populations, and the role of the European market. *Biological Conservation* 204: 103–119. <https://doi.org/10.1016/j.biocon.2016.05.017>
- Bochaton C, Grouard S, Cornette R, Ineich I, Tresset A, Bailon S (2015) Fossil and subfossil herpetofauna from Cadet 2 Cave (Marie-Galante, Guadeloupe Islands, F.W.I.): Evolution of an insular herpetofauna since the Late Pleistocene. *Comptes Rendus Paléontologie Evolution* 14: 101–110. <https://doi.org/10.1016/j.crpv.2014.10.005>
- Breuil M (2009) The terrestrial herpetofauna of Martinique: Past, present, future. *Applied Herpetology* 6: 123–149. <https://doi.org/10.1163/157075408X386114>
- Breuil M (2013) Caractérisation morphologique de l'iguane commun *Iguana iguana* (Linnaeus, 1758), de l'iguane des Petites Antilles *Iguana delicatissima* Laurenti, 1768 et de leurs hybrides. *Bulletin Société herpétologique France* 147: 309–346.
- Breuil M (2016) Morphological characterization of the common iguana *Iguana iguana* (Linnaeus, 1758), of the Lesser Antillean iguana *Iguana delicatissima* Laurenti, 1768 and of their hybrids. (Same paper as Breuil 2013, translated into English, by the International Reptile Conservation Foundation, IRCF), 1–13.
- Breuil M (2021) Les iguanes des Petites Antilles. Les espèces endémiques sur le déclin. *Le Courrier de la Nature* 326: 27–33.
- Breuil M, Vuillaume B, Schikorski D, Krauss U, Morton M, Haynes P, Daltry Corry EJ, Gaymes G, Gaymes J, Bech N, Jelić M, Grandjean F (2019) A story of nasal horns: A new species of *Iguana* Laurenti, 1768 (Squamata, Iguanidae) in Saint Lucia, St Vincent and the Grenadines, and Grenada (Southern Lesser Antilles) and its implications for the taxonomy of the genus *Iguana*. *Zootaxa* 4608(2): 201–232. <https://doi.org/10.11646/zootaxa.4608.2.1>
- Breuil M, Schikorski D, Vuillaume B, Krauss U, Morton M, Corry E, Bech N, Jelić M, Grandjean F (2020) Painted black: *Iguana melanoderma* (Reptilia, Squamata, Iguanidae) a new melanistic endemic species from Saba and Montserrat islands (Lesser Antilles). *Zookeys* 926: 95–131. <https://doi.org/10.3897/zookeys.926.48679>
- Buckley LJ, De Queiroz K, Grant TD, Hollingsworth BD, Iverson JB, Pasachnik SA, Stephen CL (2016) A checklist of the iguanas of the World. In: Iverson JB, Knapp CR & Pasachnik SA (Eds.) *Iguanas: Biology, Systematics, and Conservation*. *Herpetological Conservation and Biology* 11: 4–46. [Monograph 6]

- Caribherp website (2021) <http://www.caribbeanherpetology.org/> [Accessed on 09/05/2021]
- Daltry JC, Steele S (2020) The Grenadines pink rhino iguana: Recent findings, with special reference to Mustique. Unpublished report from Fauna & Flora International to The Mustique Company Ltd.
- Daudin J, de Silva M (2011) An annotated checklist of the amphibians and terrestrial reptiles of the Grenadines with notes on their local natural history and conservation. In: Hailey A, Wilson BS, Horrocks JA (eds) Conservation of Caribbean Island Herpetofaunas, Vol. 2 Regional Accounts of the West Indies: Conservation Biology and the Wider Caribbean, p. 259–271. Leiden, The Netherlands: Brill. Reprinted from Applied Herpetology 4: 163–175. <https://doi.org/10.1163/ej.9789004194083.i-439.105>
- De Jesús Villanueva CN, Falcon W, Velez-Zuazo X, Papa R, Malone CL (2021) Origin of the green iguana (*Iguana iguana*) invasion in the greater Caribbean Region and Fiji. Biological Invasions 23: 2591–2610. <https://doi.org/10.1007/s10530-021-02524-5>
- Duellman WE (2012) Linnaean Names in South American Herpetology Bibliotheca Herpetologica 9 : 87–97.
- Earl DA, VonHoldt BM (2012) STRUCTURE HARVESTER: a website and program for visualizing STRUCTURE output and implementing the Evanno method. Conservation Genetic Resource 4: 359–361. <https://doi.org/10.1007/s12686-011-9548-7>
- Evanno G, Regnaut S, Goudet J (2005) Detecting the number of clusters of individuals using the software STRUCTURE: a simulation study. Molecular Ecology 14: 2611–2620. [10.1111/j.1365-294X.2005.02553.x](https://doi.org/10.1111/j.1365-294X.2005.02553.x)
- Gaymes G, Justo-Gaymes, J (2018) Preliminary study on the distribution range of the pink rhino iguana. Unpublished report to Fauna & Flora International and the St Vincent and the Grenadines Forestry Department, 1–10.
- Goudet J (2001) FSTAT, a program to estimate and test gene diversities and fixation indices (version 2.9.3). <http://www2.unil.ch/popgen/softwares/fstat.html>.
- Groom MJ, Meffe GK, Carroll CR (2006) Principles of Conservation Biology, 3rd Ed. Sinauer Associates. Sunderland, MA, 780 pp.
- Henderson RW, Breuil M (2012) Island lists of West Indian amphibians and reptiles: Lesser Antilles. Bulletin of the Florida Museum of Natural History 51: 148–159.
- Henderson RW, Powell R (2018) Amphibians and Reptiles of the St. Vincent and Grenada Banks, West Indies. Edition Chimaera: Frankfurt, Germany, 448 pp.
- Hoogmoed MS (1973) Notes on the herpetofauna of Surinam IV. The lizards and amphisbaenians of Surinam. Dr. W. Junk, The Hague, 419 pp. <https://doi.org/10.1007/978-94-010-2706-9>
- Jombart T (2008) ADEGENET: a R package for multivariate analysis of genetic markers. Bioinformatics 24: 1403–1405. <https://doi.org/10.1093/bioinformatics/btn129>
- Jombart T, Devillard S, Balloux F (2010) Discriminant analysis of principal components: a new method for the analysis of genetically structured populations. BMC Genetics 11: e94. <https://doi.org/10.1186/1471-2156-11-94>
- Krauss U, Isidore L, Mitchel N, Seely L, Prospere A, Ramessar A, Johnny A, Joseph B, James M, Dornelly A, Breuil M, Vuillaume B, Morton M, John L, Bobb M (2014) Assessment of control methods for invasive alien iguanas in Saint Lucia. Closing Symposium for GEF

- project “Mitigating the Threat of Invasive Alien Species in the Insular Caribbean”, Port of Spain, Trinidad, 30 March–3 April 2014, 1–36.
- Lazell JD (1973) The lizard genus *Iguana* in the Lesser Antilles. Bulletin of the Museum of Comparative Zoology at Harvard College 145: 1–28.
- Linnaeus C (1758) Systema Naturæ per Regna tria Naturæ, Secundum Classes, Ordines, Genera, Species, cum Characteribus, Differentiis, Synonymis, Locis. Ed. 10. Vol. 1. Stockholm: Laurentii Salvii, 4 + 824 pp. <https://doi.org/10.5962/bhl.title.542>
- Malone CL, Reynoso VH, Buckley L (2017) Never judge an iguana by its spines: Systematics of the Yucatan spiny tailed iguana, *Ctenosaura defensor* (Cope, 1866). Molecular Phylogenetics and Evolution 115: 27–39. <https://doi.org/10.1016/j.ympev.2017.07.010>
- Noseworthy J (2017) Cold-blooded conflict: tackling the illegal trade in endemic Caribbean island reptiles. MPhil thesis, University of Cambridge, UK.
- Paradis E, Blomberg S, Bolker B, Brown J, Claude J, Cuong HS, Desper R. (2015) Package ‘ape’. Analyses of phylogenetics and evolution, version 2. 4–1, 1–296.
- Pasachnik SA, Fitzpatrick BM, Near TJ, Echthornacht AC (2009) Gene flow between an endangered endemic iguana, and its wide spread relative on the island of Utila, Honduras: when is hybridization a threat? Conservation Genetics 10: 1247–1254. <https://doi.org/10.1007/s10592-008-9692-0>
- Paschnik SA, Colosimo G, Carreras-De Leon, Gerber G (2020) Genetic structure of rhinoceros rock Iguanas, *Cyclura cornuta*, in the Dominican Republic, with insights into the impact of captive facilities and the taxonomic status of *Cyclura* on Mona Island. Conservation Genetics 21: 837–851 <https://doi.org/10.1007/s10592-020-01290-6>
- Peakall R, Smouse PE (2006) GenAlEx 6: genetic analysis in Excel. Population genetic software for teaching and research. Molecular Ecology Notes 2006: 288–295. <https://doi.org/10.1111/j.1471-8286.2005.01155.x>
- Pounder KC, Mukhida F, Brown RP, Carter D, Daltry JC, Fleming T, Goetz M, Hughes G, Questel K, Saccheri IJ, Williams R, Soanes LM (2020) Testing for hybridisation of the Critically Endangered *Iguana delicatissima* on Anguilla to inform conservation efforts. Conservation Genetics 21: 405–420. <https://doi.org/10.1007/s10592-020-01258-6>
- Pritchard JK, Stephens M, Donnelly P (2000) Inference of population structure using multi-locus genotype data. Genetics 155: 945–959. <https://doi.org/10.1093/genetics/155.2.945>
- Rice WR (1989) Analyzing tables of statistical tests. Evolution 43: 223–225. <https://doi.org/10.1111/j.1558-5646.1989.tb04220.x>
- Reptile Database (2021) <http://reptile-database.org/> [Accessed on 09/05/2021]
- Stephen C, Pasachnik S, Reuter A, Mosig P, Ruyle L, Fitzgerald L (2011) Survey of status, trade, and exploitation of Central American Iguanas. Report, Department of Interior, United States Fish and Wildlife Service, Washington, DC, USA, 1–53.
- Stephen CL, Reynoso VH, Collett WS, Hasbun, CR, Breinholt JW (2013) Geographical structure and cryptic lineages within common green iguanas, *Iguana iguana*. Journal of Biogeography 40: 50–62. <https://doi.org/10.1111/j.1365-2699.2012.02780.x>
- Valette V, Filipova L, Vuillaume B, Cherbonnel, C, Risterucci AM, Delaunay, C, Breuil M, Grandjean F (2013) Isolation and characterization of microsatellite loci from *Iguana delicatissima* (Reptilia: Iguanidae), new perspectives for investigation of hybridization

- events with *Iguana iguana*. Conservation Genetic Resource 5: 173–175. <https://doi.org/10.1007/s12686-012-9761-z>
- van den Burg MP, Malone CL (2018) Common Green Iguana (*Iguana iguana*). Assessing the Taxonomic status of the *Iguana iguana* population on Curaçao and the threat of hybridization with already present non-native *I. iguana* Lineages. ISG Newsletter 18: 12–15.
- van den Burg MP, Meirmans PG, van Wagenveld TP, Kluskens B, Madden H, Welch ME, Breeuwer JAJ (2018) The Lesser Antillean iguana (*Iguana delicatissima*) on St. Eustatius: genetically depauperate and threatened by ongoing hybridization. Journal of Heredity 109: 426–437. <https://doi.org/10.2305/IUCN.UK.2018-1.RLTS.T10800A122936983.en>
- van den Burg MP, Brisbane JLK, Knapp CR (2020) Post-hurricane relief facilitates invasion and establishment of two invasive alien vertebrate species in the Commonwealth of Dominica, West Indies. Biological Invasions 22: 195–203. <https://doi.org/10.1007/s10530-019-02107-5>
- van den Burg MP, Daltry JC, Angin B, Boman E, Brisbane JLK, Collins K, Haakonsson JE, Hill A, Horrocks JA, Mukhida F, Providence F, Questel K, Ramnanan N, Steele S, Vique Bosquet IM, Knapp CR (2021) Biosecurity for humanitarian aid. Science 372: 581–582. <https://doi.org/10.1126/science.abj0449>
- van den Burg MP, Grandjean F, Schikorski D, Breuil M, Malone CL (2021) A genus-wide analysis of genetic variation to guide population management, hybrid identification, and monitoring of invasions and illegal trade in Iguana (Reptilia: Iguanidae). Conservation Genetic Resource 13: 435–445 <https://doi.org/10.1007/s12686-021-01216-5>
- Vuillaume B, Valette V, Lepais O, Grandjean F, Breuil M (2015) Genetic evidence of hybridization between the Endangered native species *Iguana delicatissima* and the invasive *Iguana iguana* (Reptilia, Iguanidae) in the Lesser Antilles: Management implications. PLoS ONE 10(6): e0127575. <https://doi.org/10.1371/journal.pone.0127575>
- Weir BS, Cockerham CC (1984) Estimating F-statistics for the analysis of populations structure. Evolution 38: 1358–1370. <https://doi.org/10.1111/j.1558-5646.1984.tb05657.x>

Phylogenomics of paleoendemic lampshade spiders (Araneae, Hypochilidae, *Hypochilus*), with the description of a new species from montane California

Erik Ciaccio^{1,2}, Andrew Debray^{1,3}, Marshal Hedin¹

1 Department of Biology, San Diego State University, San Diego, California, USA **2** Department of Entomology, Plant Pathology and Nematology, University of Idaho, Idaho, USA **3** Nano PharmaSolutions Inc., San Diego, California, USA

Corresponding author: Marshal Hedin (mhedin@sdsu.edu)

Academic editor: Cristina Rheims | Received 27 October 2021 | Accepted 18 January 2022 | Published 17 February 2022

<http://zoobank.org/943CD2EE-BCD6-4F8A-8C7A-B7690408B785>

Citation: Ciaccio E, Debray A, Hedin M (2022) Phylogenomics of paleoendemic lampshade spiders (Araneae, Hypochilidae, *Hypochilus*), with the description of a new species from montane California. ZooKeys 1086: 163–204. <https://doi.org/10.3897/zookeys.1086.77190>

Abstract

Hypochilus is a relictual lineage of Nearctic spiders distributed disjunctly across the United States in three montane regions (California, southern Rocky Mountains, southern Appalachia). Phylogenetic resolution of species relationships in *Hypochilus* has been challenging, and conserved morphology coupled with extreme genetic divergence has led to uncertain species limits in some complexes. Here, *Hypochilus* interspecies relationships have been reconstructed and cryptic speciation more critically evaluated using a combination of ultraconserved elements, mitochondrial CO1 by-catch, and morphology. Phylogenomic data strongly support the monophyly of regional clades and support a ((California, Appalachia), southern Rocky Mountains) topology. In Appalachia, five species are resolved as four lineages (*H. thorelli* Marx, 1888 and *H. coylei* Platnick, 1987 are clearly sister taxa), but the interrelationships of these four lineages remain unresolved. The Appalachian species *H. pococki* Platnick, 1987 is recovered as monophyletic but is highly genetically structured at the nuclear level. While algorithmic analyses of nuclear data indicate many species (e.g., all *H. pococki* populations as species), male morphology instead reveals striking stasis. Within the California clade, nuclear and mitochondrial lineages of *H. petrunkevitchi* Gertsch, 1958 correspond directly to drainage basins of the southern Sierra Nevada, with *H. bernardino* Catley, 1994 nested within *H. petrunkevitchi* and sister to the southernmost basin populations. Combining nuclear, mitochondrial, geographical, and morphological evidence a new species from the Tule River and Cedar Creek drainages is described, *Hypochilus xomote* sp. nov. We also emphasize the conservation issues that face several micro-endemic, habitat-specialized species in this remarkable genus.

Keywords

Conservation, mountains, multispecies coalescent, short-range endemism, Sierra Nevada, southern Appalachians, taxonomic over-splitting, ultraconserved elements

Introduction

Discovering and delimiting cryptic species boundaries is, almost by definition, challenging. When the multispecies coalescent (**MSC**) is applied to species delimitation, species boundaries are explored by estimating gene trees and accounting for species tree/gene tree discordance using MSC models. Critical to this approach is discerning the boundary between population-level versus species-level divergence, as a core assumption of most MSC models is that species are panmictic and without population structure (Degnan and Rosenberg 2009). It is now well-established that, in systems with high natural population genetic structuring, MSC-based delimitation methods can conflate structure at the population level with divergence at the species level (Carstens et al. 2013; Sukumaran and Knowles 2017; Chambers and Hillis 2019; Mason et al. 2020). Many empirical studies indicate that, used alone, MSC methods can drastically over-split taxa (e.g., Niemiller et al. 2012; Satler et al. 2013; Hedin et al. 2015; Derkarabetian et al. 2019; Hundsdoerfer et al. 2019).

Population genetic structuring is rather ubiquitous in nature. Species with strict or semi-strict habitat or microhabitat preferences will naturally occur discontinuously over a landscape. Combine this natural habitat fragmentation with limited dispersal ability, and populations will evolve to be genetically different, to various degrees (Templeton et al. 1990; Coates et al. 2018; Marshall et al. 2021). Under some circumstances, arrays of parapatric or allopatric populations which are diverging genetically might remain morphologically quite similar, particularly when microhabitat preferences are strong (Stockman and Bond 2007; Bernardo 2011; Fišer et al. 2018). This combined suite of circumstances corresponds to what we refer to as a “no gene flow” or “non-adaptive radiation” speciation model (Gittenberger 1991; Kozak et al. 2006). Non-adaptive speciation is quite common in nature (e.g., Reilly and Wake 2005; Leavitt et al. 2007; Emata and Hedin 2016; Singhal et al. 2018; Derkarabetian et al. 2022), and challenges species delimitation. This species delimitation problem lies at one end of a *spectrum* of difficult scenarios for species delimitation (a high gene flow model representing an opposite, but equally challenging, scenario). Non-adaptive speciation represents a conundrum for species delimitation, as genetic data combined with many currently available models will likely over-split taxa, while other lines of evidence needed to confirm or reject this over-splitting (e.g., morphological evidence, etc.) is difficult to uncover in these same taxa (Derkarabetian et al. 2022).

The spider genus *Hypochilus* Marx, 1888 represents a challenging system for species delimitation, combining allopatric geographic distributions, morphological conservatism, and high genetic structuring. *Hypochilus* is a Nearctic genus representing one of two described genera in the family Hypochilidae, a family of true spiders which retain

many interesting plesiomorphic traits (Forster et al. 1987; Alberti and Coyle 1991; Catley 1994). Commonly known as lampshade spiders, *Hypochilus* spiders are microhabitat specialists occurring in shaded, mesic, rock outcrop habitats (Catley 1994; Hedin and Wood 2002; Keith and Hedin 2012). *Hypochilus* includes ten described species from three disjunct montane regions: the southern Appalachians, the southern Rocky Mountains, and the California mountains (Fig. 1). Described species are mostly exclusively allopatric, and within montane regions where species are in close geographic proximity, occur in parapatric patchworks. These spiders are textbook examples of so-called short-range endemic (SRE) taxa, including species with naturally small geographic distributions (often defined as less than 10,000 km²; Harvey 2002, Harvey et al. 2011). Several *Hypochilus* species occupy severely limited geographic distributions; for example, *H. bernardino* Catley, 1994 is only known from a handful of locations in a single mountain range (San Bernardino mountains of southern California). Multiple restricted-distribution species also warrant conservation attention, particularly in the face of climate change; this conservation focus also highlights the need for rigorous species delimitation (e.g., Hedin 2015).

As spiders with extraordinarily low vagility, one would expect deeper phylogenetic relationships in *Hypochilus* to closely mirror geography, with phylogenetic predictions following geography. However, previous studies have suggested that this may be an oversimplification. Both morphological and mitochondrial data suggest that the geographically separated California and Appalachian mountain faunas are sister lineages (Catley 1994; Hedin 2001), although this inferred relationship is sensitive to varying combinations of data and analyses (Hedin 2001). Also, monophyly of the California fauna has been questioned, as both morphological and mitochondrial tree topologies sometimes recover an Appalachian clade within a larger paraphyletic Californian group (Hoffman 1963; Hedin 2001). Given the impressive geographic disjunction between these faunas (Fig. 1), such a pattern would be biogeographically compelling, if verified. Regional non-monophyly has been well-established in other north-temperate, habitat-specialized arthropods (e.g., *Brachycybe* millipedes – Brewer et al. 2012; *Sabacon* harvesters – Schönhofer et al. 2013; travunioid harvesters – Derkarabetian et al. 2018; leptonetid spiders – Ledford et al. 2021), so this biogeographic pattern is certainly possible.

As commonly found in SRE taxa, prior intraspecific genetic research in *Hypochilus* has revealed ubiquitous and extensive genetic structuring. In Appalachia, extreme mitochondrial genetic divergence occurs within and among five described species over small geographic distances (Hedin 2001; Hedin and Wood 2002; Keith and Hedin 2012). Within *H. pococki* Platnick, 1987, recovered as paraphyletic on mitochondrial gene trees, highly divergent, geographically cohesive “microclades” have been discovered (Keith and Hedin 2012). In California, mitochondrial CO1 sequences for *H. petrunkevitchi* Gertsch, 1958 from the Merced versus Kaweah River basins reveal extreme intraspecific genetic divergences (> 15% divergent; Hedin 2001). Past mitochondrial studies have attributed extensive genetic structuring to limited female-biased gene flow (Hedin and Wood 2002; Keith and Hedin 2012), but whether such genetic

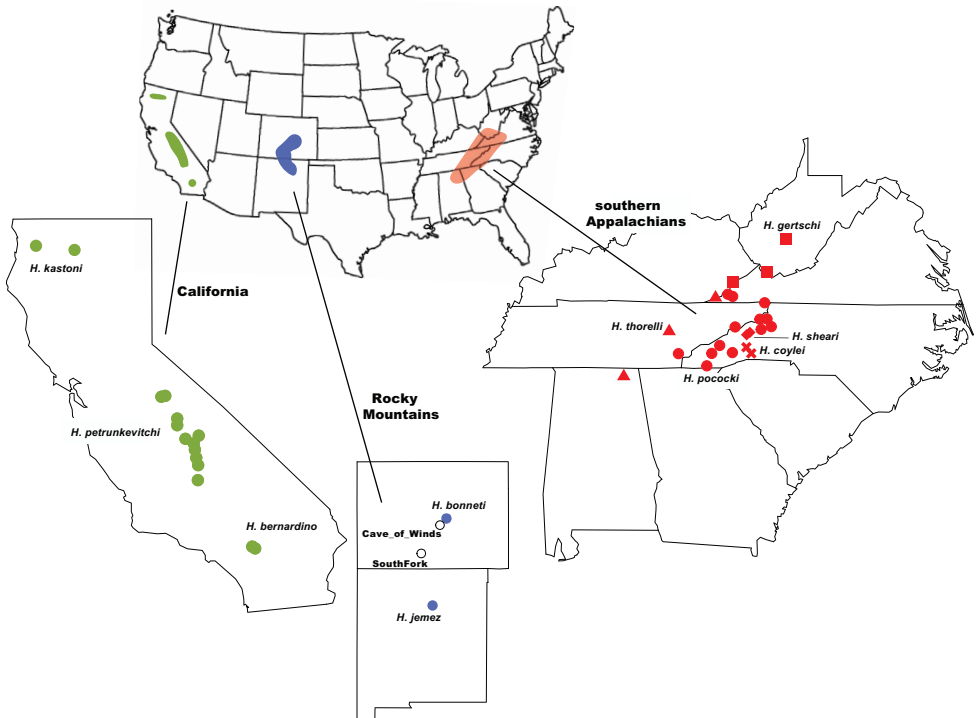


Figure 1. Distribution of the three geographic groups of *Hypochilus* in the mountains of California, the Rocky Mountains, and the southern Appalachians. Regional insets show the sampling locations of forty-three *Hypochilus* specimens used in genetic analyses; Appalachian species represented by different symbols.

patterns extend to the nuclear genome and are less pronounced because of male-based gene flow remains unknown.

In this research we used phylogenomic data to resolve *Hypochilus* species relationships within and among montane regions. We also explored putative cryptic diversification within Appalachian *H. pococki* and Californian *H. petrunkevitchi*. In Appalachia, previous mitochondrial-based species delimitation using a Generalized Mixed Yule Coalescent (GMYC) model (Fujisawa and Barraclough 2013) appears to severely over-split species (Keith and Hedin 2012), likely due to strong genetic structuring. We asked whether similar results applied to nuclear single nucleotide polymorphism (SNP) datasets derived from ultraconserved elements (UCEs), using additional MSC methods (Bayes Factor Delimitation and TR2 rooted triplet analysis). We combine these molecular data and analyses with SEM images of the male pedipalp for large samples of *H. pococki* and *H. petrunkevitchi*, and gather UCE CO1 mitochondrial “by-catch” data for *H. petrunkevitchi*. Based on evidence derived from a combination of nuclear phylogenomic and mitochondrial data, geography, and adult male and female morphology, we describe a new SRE species from the southern Sierra Nevada of California.

Materials and methods

Molecular sampling

Specimens representing the genus *Ectatosticta* Simon, 1892 from China, the sister genus to *Hypochilus* (and the only other hypochilid genus described), were used to root all phylogenies (UCE data from Ramírez et al. 2021). The monophyly of the family, and two constituent genera, is strongly supported by both morphology (Forster et al. 1987; Alberti and Coyle 1991; Catley 1994; Li et al. 2021) and phylogenomics (Fernández et al. 2018; Ramírez et al. 2021). Phylogenomic data were gathered for forty-three *Hypochilus* specimens, representing all ten described species (see Suppl. material 1; Fig. 1). A priori species identifications were based on male morphology in combination with geography (Forster et al. 1987; Catley 1994), and we included many samples from prior genetic research (Keith and Hedin 2012). Multiple specimens per species were sampled, chosen to maximize the breadth of geographic coverage within species (Fig. 1). Our southern Rocky Mountain samples included collections from near the respective type localities (Gertsch 1964; Catley 1994) of both *H. bonneti* Gertsch, 1964 and *H. jemez* Catley, 1994, plus two geographically intermediate populations from southern Colorado of uncertain species identity. For species delimitation focal taxa (*H. pococki* and *H. petrunkevitchi*), larger sample sizes were used to obtain more fine-scale genetic data on potentially cryptic species (Fig. 1). For *H. pococki*, sampling included representatives of the five mitochondrial haplogroups identified in Keith and Hedin (2012). For *H. petrunkevitchi*, specimens were sampled from multiple drainage basins, including the Merced River (**YOSE**), San Joaquin River (**SAN**), Kings River (**KING**), Kaweah River (**KAW**), Tule River (**TULE**), and Cedar Creek (**CEDAR**) drainages.

UCE data collection

For almost all specimens (with tissues stored at -80 °C), DNA extraction was performed using a Qiagen DNEasy kit from leg tissues. Sequence capture libraries were prepared using an ultraconserved elements capture protocol for arachnids (Starrett et al. 2017; Hedin et al. 2019), with arachnid probes designed by Faircloth (2017). Sequencing was done at the Brigham Young University DNA Sequencing Center on an Illumina HiSeq 2500 150 cycle paired-end sequencing platform. Published data for two *H. pococki* specimens (H595 and H232, from Starrett et al. 2017), one *H. kastoni* Platnick, 1987 (G2519, Hedin et al. 2019), and *Ectatosticta* (Ramírez et al. 2021) were used from prior studies. Raw reads were filtered using the illumiprocessor wrapper (Faircloth 2013) within PHYLUCE v1.6 (Faircloth 2016), after which cleaned reads were assembled using Trinity v2.0.6 (Grabherr et al. 2011) and Velvet v1.0.19 (Zerbino and Birney 2008) on the HPC Cluster at UC Riverside. These assemblies were combined and resulting contigs were matched to probes with minimum identity and minimum coverage values of 80 (--min-identity 80 --min-coverage 80). UCE loci were aligned and trimmed within PHYLUCE using MAFFT (Katoh and Standley

2013) and Gblocks (Castresana 2000; Talavera and Castresana 2007) with relatively liberal settings for GBLOCKS (--b1 0.5 --b2 0.5 --b3 10 --b4 8).

A 50 percent occupancy matrix (623 loci) was generated from the pipeline above (here called the “unfiltered” matrix). A second matrix was further filtered to remove duplicate and potentially non-homologous sequences. Previous work has shown that arthropod UCEs are mostly located within exonic regions (Bossert and Danforth 2018), and the arachnid probe set is no exception (Hedin et al. 2019). In fact, the arachnid probe set can target separate exons from the same protein as separate loci (Hedin et al. 2019), perhaps violating assumptions such as independence and linkage of loci. An annotated list of the arachnid UCEs from Hedin et al. (2019) was used to identify duplicate loci. A total of 73 duplicate loci was found, with the longest locus in each instance retained while the rest were discarded. Using the annotated list, those loci identified by Hedin et al. (2019) as including potential paralogs were also identified and discarded ($n = 2$), leaving a matrix containing a total of 550 loci. Finally, this filtered dataset was trimmed again with more stringent Gblocks settings (--b1 0.5 --b2 0.85 --b3 4 --b4 8), resulting in a “filtered and trimmed” matrix. This last step was conducted to isolate as much of the purely exonic region as possible for each locus.

Generic-level phylogenomics

Interspecific relationships were reconstructed using all three UCE data matrices (“unfiltered”, “filtered”, and “filtered and trimmed”), utilizing both concatenation and coalescent-model approaches. Data were partitioned by locus, with optimal models selected using PartitionFinder2 (Lanfear et al. 2012) on the CIPRES portal HPC Cluster. Concatenated maximum likelihood trees were reconstructed using RAxML v8.2.12 (Stamatakis 2014) and IQ-TREE v1.5.0 (Nguyen et al. 2015). Using IQ-TREE 2 we also calculated gene (gCF) and site concordance (sCF) factors. For every node of a reference tree, gCF can be defined as the percentage of “decisive” gene trees containing that node, while sCF can be defined as the percentage of decisive sites (in an alignment) supporting a node (Minh et al. 2018). The latter support metric is particularly useful when individual gene trees are uncertain, perhaps because individual alignments are short. Concordance factor calculations were performed using the topology from IQ-TREE which has an identical topology to the RAxML tree and mostly agrees with the SVDquartets reconstruction (see Results). The latter is a coalescent-model topology reconstructed using SVDquartets v1.0 (Chifman and Kubatko 2014) implemented in PAUP* (Swofford 2003), set for 1M quartets with 500 bootstrap replicates for all runs.

Nuclear species delimitation

Nuclear single nucleotide polymorphism (SNP) data were extracted from UCE loci following the methods of Harvey et al. (2016) and a combination of tools and methods from vcf tools (Danecek et al. 2011) and a modified version of the best practices approach for variant isolation with GATK v4.0.0.0 (Van der Auwera et al. 2013).

Separate datasets were created for Californian *H. petrunkevitchi* plus *H. bernardino* specimens, and for samples of *H. pococki*. These matrices started with cleaned read data containing only relevant samples and used a highest coverage reference specimen (H_petrunkevitchi_G2543, H_pococki_H551). Genetic structure and sample clustering were explored using k-means clustering in STRUCTURE v2.3.4 (Pritchard et al. 2000), with unlinked SNPs. Multiple K values (K = 1–10) were run for 100,000 generations with each K value replicated 10 times. Optimal K values were determined following Pritchard et al. (2000) and Evanno et al. (2005), using the online resource CLUMPAK (Kopelman et al. 2015).

Using multiple data sources (phylogenomic results, STRUCTURE results, geography for *H. petrunkevitchi*, and mitochondrial haplogroup membership for *H. pococki*), alternative species models were generated and compared using nuclear SNP datasets in the program SNAPP (Tables 1, 2; Bryant et al. 2012). These analyses also included outgroup data (other *Hypochilus* species), allowing us to test hypotheses of *H. pococki* as a single species (current taxonomy) and *H. petrunkevitchi* lumped with *H. bernardino* (see Tables 1, 2). The averaged marginal likelihoods of duplicate runs were compared for alternative species models using Bayes Factor Delimitation for genomic data (*BFD) (Leaché et al. 2014); we followed the recommendations of Kass and Raftery (1995) in interpreting Bayes factor values.

A rooted triplet species delimitation approach was also implemented using the Python2 compatible version of the program TR2 (Fujisawa et al. 2016). Here, nuclear

Table 1. Alternative species model comparison results for *H. petrunkevitchi*, from SNAPP. Alternative models were compared to current taxonomy and ranked with 1 as the most favorable and 5 as the least. Bayes factors were calculated as (BF = 2 × (model 1 – model 2)) where negative values represent support for model 2 (alternative model) and positive values are support for the null model (current taxonomy).

Model	Species	Partitioning	MLE	MLE 2	BF	Rank
Every Tip	16	Every specimen as a species	-105	-105.2	-7056	1
Basins	8	<i>H. kastoni</i> , <i>H. bernardino</i> , CEDAR, TULE, KAW, KING, SAN, YOSE	-1781	-1781	-3704	2
STRUCTURE	6	<i>H. kastoni</i> , <i>H. bernardino</i> , TULE+CEDAR, KAW+KING, SAN, YOSE	-1939	-1939	-3388	3
Current Taxonomy	3	<i>H. kastoni</i> , <i>H. petrunkevitchi</i> , <i>H. bernardino</i>	-3633	-3633	-	4
Collapse	2	<i>H. kastoni</i> , <i>H. petrunkevitchi</i> + <i>H. bernardino</i>	-4223	-4223	1180	5

Table 2. SNAPP results for *H. pococki*. Models were compared to current taxonomy and ranked with 1 as the most favorable and 4 as the least.

Model	Species	Partitioning	MLE	MLE 2	BF	Rank
Every Tip	16	Every specimen as a species	-62.9	-62.8	-5030	1
Mitochondrial	6	<i>H. thorelli</i> , WEST+bone+alark, CENT, VA, ELK, NE	-3917	-3917	-4462	2
STRUCTURE	5	<i>H. thorelli</i> , WEST+bone+alark, CENT, ELK+NE, VA	-4338	-4340	-3620	3
Current Taxonomy	2	<i>H. thorelli</i> , <i>H. pococki</i>	-6148.9	-6148	-	4

gene trees are decomposed into partially rooted triplets and congruence is assessed among triplet topologies using a likelihood model testing framework. Input gene trees were constructed in RAxML using rapid bootstrap analysis (-f a) with 200 bootstrap replicates for each gene tree with 550 UCE loci from the “filtered and trimmed” dataset. With the intent to detect patterns of increasing support for increasing species number (i.e., over-splitting), models in which every tip was categorized as a species were included in both SNAPP and TR2 runs.

COI phylogeny, distances, and GMYC

Mitochondrial Cytochrome c oxidase subunit I (COI) data for the California taxa were captured from UCE “by-catch” for purposes of phylogenetic and distance analyses, particularly considering the extreme COI distances observed in Hedin (2001). A consensus reference sequence was created from specimens of *H. petrunkevitchi* and *H. bernardino* (from Hedin 2001), which was then used as a custom database for a BLASTN search for extracting COI sequences from UCE contigs. The BLASTN search and subsequent alignment was performed using Geneious Prime (2020.2). Sequence alignments were partitioned by codon position using MODELFINDER (Kalyaanamoorthy et al. 2017) and a phylogeny was constructed using IQ-TREE with 1000 ultrafast bootstrap replicates. A pairwise mitochondrial distance matrix was generated in PAUP* (Swofford 2003) using a Kimura two-parameter model of nucleotide substitution (Kimura 1980).

A Generalized Mixed Yule Coalescent (**GMYC**) model was used to algorithmically delimit Californian species using COI data, in a manner similar to the approach of Keith and Hedin (2012) for Appalachian *H. pococki*. A GMYC model assumes a difference in intra and inter-specific branching patterns under maximum likelihood and estimates a threshold for the transition from intraspecific (a coalescent process) to interspecific (speciation) branching on an ultrametric tree. Both a single threshold and multiple thresholds can be estimated in different approaches with the model. To this end, an ultrametric COI tree was generated using the *chronopl* function from the APE library in R version 4.0. 2 (Paradis and Schliep 2019), with both single and multiple threshold models performed on the GMYC web server (<https://species.h-its.org/gmyc/>; Fujisawa and Barraclough 2013).

Morphological study

Although *Hypochilus* is a strongly morphologically conserved genus, current species were described and are diagnosed using subtle morphological variation, mostly in male genitalia (Hoffman 1963; Forster et al. 1987; Catley 1994). Using SEM we examined male palpal morphology for California taxa (*H. kastoni*, *H. bernardino*, multiple lineages of *H. petrunkevitchi*), and for all primary lineages of *H. pococki*. We lacked adult males for the southern Rocky Mountain populations of uncertain species identity, so could not study them at this time. Male pedipalps preserved in 80% EtOH were

transferred to pure EtOH (200 PF, $\geq 99.5\%$) for at least 10 min. Following EtOH dehydration, samples were placed in a multilayered sample holder and dried to the critical point using a Tousimis SAMDRI790. Transitional and intermediate fluids used were CO₂(l) and pure EtOH, respectively. Dried palps were mounted on aluminum stubs fitted with sticky carbon conductive spectro-grade tabs. Following mounting, samples were run through an EMS Quorum Q150T sputter coater and covered with 6 nm platinum nanoparticles. SEM micrographs of retrolateral and prolateral views were taken using a vertical stage on an FEI Quanta 450 FEG. Female spermathecal organs were imaged using a Visionary Digital Imaging System, comprising a Canon EOS 5D Mk II DSLR mounted to an Infinity Optics microscope tube. Spermathecal organs were dissected from specimens using fine forceps, immersed for 2–5 minutes in BioQuip specimen clearing fluid (<http://www.bioquip.com>), then imaged in this fluid on depression slides.

For taxonomic descriptions, morphological measurement details follow Catley (1994: figs 1–4):

PTW/PTL	maximum width of male pedipalpal tibia in retrolateral view/length of tibia in retrolateral view;
CdL	male palp conductor length in retrolateral view;
AME	diameter of anterior median eye pupil;
PTaL	length of male palpal tarsus in retrolateral view;
CTpr	number of promarginal cheliceral teeth;
CTre	number of retromarginal cheliceral teeth.

Measurements were taken from alcohol-preserved specimens using an Olympus SZ40 dissecting microscope fitted with an ocular micrometer, and converted to millimeters; raw measurements are provided in Suppl. material 2, and summarized in Table 5.

Results

UCE processing and generic-level phylogenomics

Original UCE raw reads have been submitted to the SRA (PRJNA760946), with summary statistics presented in the Suppl. material 1. Data matrices and resulting .tre files are deposited at Dryad (<https://doi.org/10.5061/dryad.g1jwstqsd>). The “unfiltered” matrix included 623 UCE loci with an average length of 783 base pairs (**bp**) and a concatenated length of 734,881 bp (189,387 parsimony informative (**PI**) sites). The “filtered” matrix included 550 loci with an average length 921 bp and concatenated length of 506,689 bp (145,037 PI sites), while the “filtered and trimmed” matrix contained 550 loci with an average length of 591 bp and concatenated length of 325,452 bp (81,911 PI).

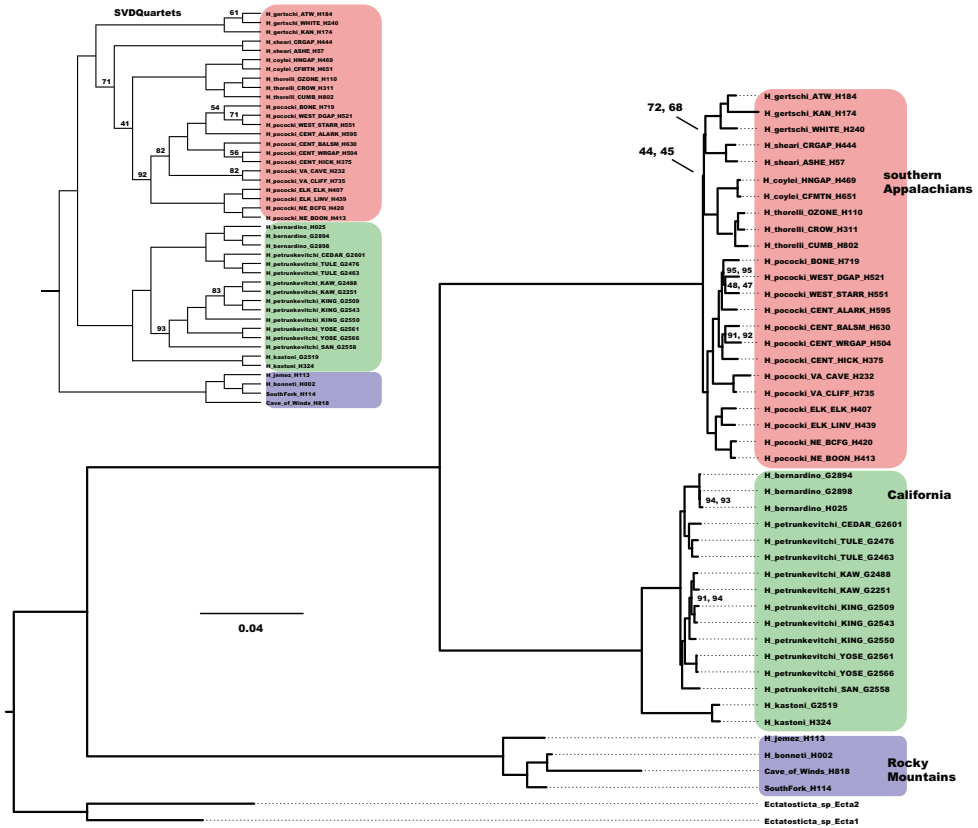


Figure 2. UCE phylogeny. Phylogeny reconstructed from partitioned RAXML analysis of “filtered and trimmed” UCE matrix. Bootstrap support values are 100 for all nodes unless otherwise indicated; second support values from IQ-TREE. Inset – SVDquartets UCE tree with bootstrap support values less than 95 shown.

Concatenated ML and SVDquartets analyses of the above three matrices recover nearly identical *Hypochilus* relationships, except for some nodes in the Appalachian and Rocky Mountain clades (Figs 2, 3; <https://doi.org/10.5061/dryad.g1jwstqsd>). These analyses confirm regional faunas as monophyletic, rejecting CA parphyly, and recover Appalachia and California clades as sister taxa. Within Appalachia, a sister species relationship between the geographically disjunct *H. thorelli* Marx, 1888 and *H. coylei* Platnick, 1987 is strongly supported across all analyses, consistent with mitochondrial evidence (Hedin 2001; Keith and Hedin 2012), but contrary to morphological evidence which groups *H. coylei* with the geographically adjacent *H. sheari* Platnick, 1987 (Huff and Coyle 1992; Catley 1994). The monophyly of all currently recognized Appalachian species is supported, contradicting mitochondrial results which had previously suggested *H. pococki* parphyly. Certain parts of the Appalachian topology include low bootstrap values, low gene and site concordance values, and discordant topologies among analyses. Whereas ML analyses place *H. pococki* as sister to other Appalachian species, SVDquartets nests *H. pococki* well within the clade with *H. gertschi* Hoffman,

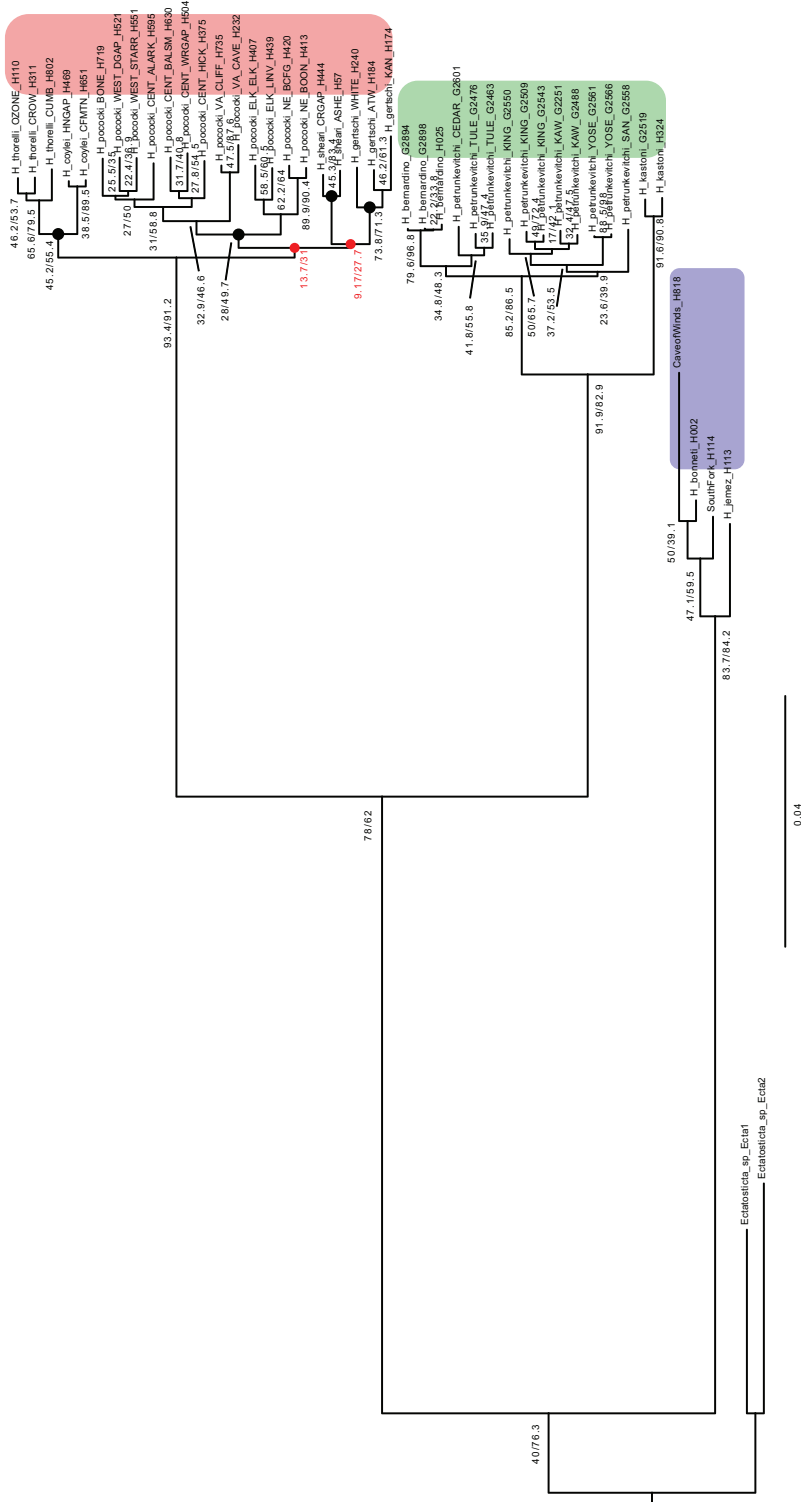


Figure 3. Concordance Factor values. Phylogeny reconstructed from partitioned RAxML analysis of “filtered and trimmed” UCE matrix, with gCF / sCF values. The lowest gCF and sCF values, for two unresolved nodes which collapse to a four lineage polytomy within the Appalachian clade, are highlighted by red text.

1963 as sister to other Appalachian species (Fig. 2). A California clade is consistently recovered, with *H. kastoni* sister to remaining lineages. *Hypochilus bernardino* is nested prominently within *H. petrunkevitchi*, and for this reason analyses examining species boundaries included samples of all three species (see below).

Nuclear species delimitation

Nuclear SNP datasets included 670 unlinked SNPs for the California sample (allowing 20% missing data) and 655 unlinked SNPs for the Appalachian sample (19% missing data). Overall, STRUCTURE analyses reveal strong population structure for both samples, with inferred genetic clusters congruent with phylogenomic clades (Fig. 4). Within California there is little evidence for mixed ancestry, with genetic populations of *H. petrunkevitchi* also appearing to be structured by river basin (Fig. 4). Best K as determined by the Pritchard et al. (2000) method is decisive for K = 5 while the Evanno method is less conclusive, supporting a scenario of K = 2 with almost equal but slightly lower support for K = 4 (<https://doi.org/10.5061/dryad.g1jwstqsd>). When *H. kastoni* samples were included

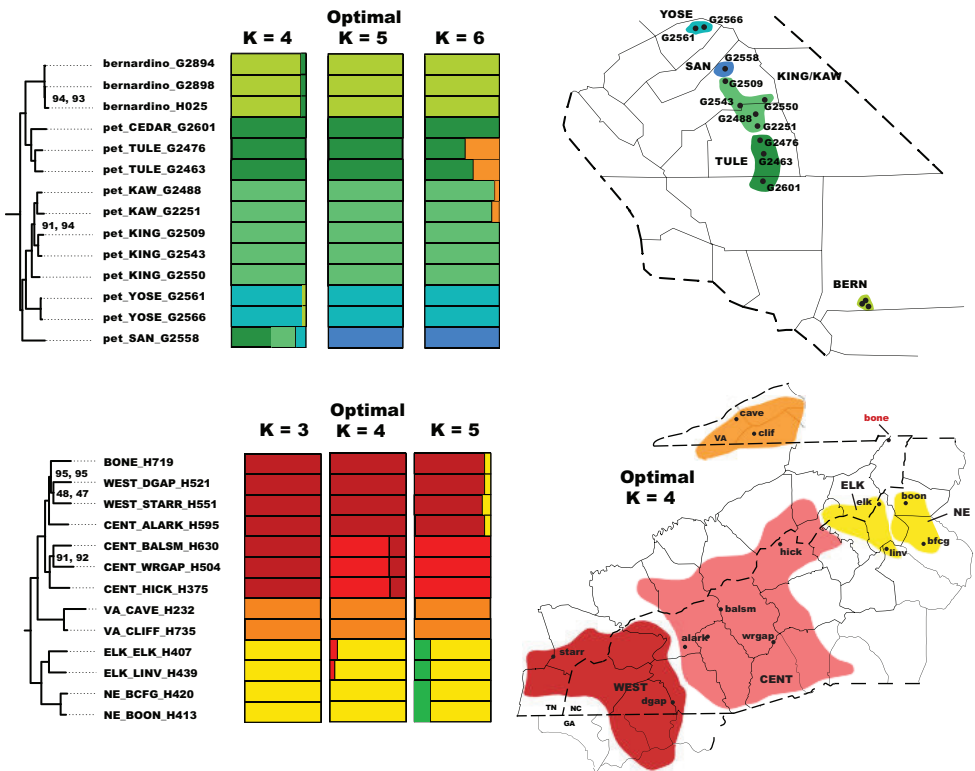


Figure 4. UCE STRUCTURE results, with optimal and suboptimal K clusters shown in relation to UCE RAxML phylogeny and geography. For *H. pococki*, the distribution of mitochondrial “microclades” follows Keith and Hedin (2012).

in STRUCTURE runs, the Pritchard method recovered the same population structure scheme with the addition of a separate *H. kastoni* “population”, while the Evanno method recovered stronger support for $K = 2$ in which *H. kastoni* and *H. bernardino* comprised a single genetic population. Because we viewed this latter $K = 2$ result as spurious (see Janes et al. 2017), we generally preferred optimal K values as inferred by the Pritchard method.

There is more evidence for mixed ancestry in *H. pococki* STRUCTURE analyses, using a best K from both Pritchard ($K = 4$) and Evanno ($K = 3$) methods. The Elk and Northeast “microclades” (ELK and NE) are lumped as a single genetic population, while one member from the mitochondrial Central (CENT) group clusters with the WEST population (Fig. 4), discordant with previously delineated mitochondrial groups (Keith and Hedin 2012). The geographically isolated BONE population, not sampled in previous mitochondrial studies, clusters with disjunct WEST specimens (Fig. 4).

Alternative species hypothesis models were generated and compared using SNAPP and TR2 for both *H. petrunkevitchi* (five models) and *H. pococki* (four models). Pritchard-based best K schemes were used for the STRUCTURE derived species models. The most-favored SNAPP model for *H. petrunkevitchi* (Table 1) is one where every tip represents a species; the next best supported model is the “Basins”, 8-taxon model. SNAPP results for *H. pococki* were similar and favored every tip as a species as the best model, with a pattern of more speciose models being more favored (Table 2). The rooted triplet TR2 approach also found this pattern of favoring more species-rich models over current taxonomy with the most species-rich model, every tip as a distinct taxon, being the most favored (Tables 3, 4).

Table 3. TR2 results for *H. petrunkevitchi*; ranking of the models with 1 being the most favored and 6 being the least favored.

Model	Species	Partitioning	Score	Rank
Every Tip	16	Every specimen as a species	171.62	1
Basins	8	<i>H. kastoni</i> , <i>H. bernardino</i> , TULE, CEDAR, KAW, KING, SAN, YOSE	213.95	2
STRUCTURE	6	<i>H. kastoni</i> , <i>H. bernardino</i> , TULE+CEDAR, KAW+KING, YOSE, SAN	348.23	3
Current Taxonomy	3	<i>H. kastoni</i> , <i>H. petrunkevitchi</i> , <i>H. bernardino</i>	9334.94	4
Collapse	2	<i>H. kastoni</i> , <i>H. petrunkevitchi</i> + <i>H. bernardino</i>	25926.79	5
One species	1	<i>H. kastoni</i> + <i>H. petrunkevitchi</i> + <i>H. bernardino</i>	30938.48	6

Table 4. TR2 results for *H. pococki*; ranking of the models with 1 being the most favored and 5 being the least favored.

Model	Species	Partitioning	score	Rank
Every Tip	16	Every specimen as a species	344.10	1
Mitochondrial	7 (*includes BONE as separate lineage)	<i>H. thorelli</i> , WEST, CENT, ELK, NE, VA, BONE	366.66	2
STRUCTURE	5	<i>H. thorelli</i> , WEST+Bone+Alark, CENT, ELK+NE, VA	819.85	3
Current	2	<i>H. thorelli</i> , <i>H. pococki</i>	9930.73	4
Collapse	1	<i>H. thorelli</i> + <i>H. pococki</i>	17961.09	5

COI phylogeny, distances, and GMYC

The COI by-catch phylogeny, using *H. kastoni* and *H. bernardino* as possible out-groups, shows strong support (BP = 100) for a clade including *H. bernardino* and *H. petrunkevitchi* together (Fig. 5). Within this clade, recovered mitochondrial lineages are consistent with UCE optimal K = 5 STRUCTURE lineages, but the interrelationships of these mitochondrial lineages are not resolved. Considering this phylogenetic uncertainty (i.e., collapsing poorly-resolved nodes), the mitochondrial results are not strictly inconsistent with nuclear results. Pairwise mitochondrial distance values are extremely high among primary lineages (Fig. 5 inset), ranging from 12%–15%. Divergence values within lineages are lower, except for the combined SAN + KING + KAW lineage (> 12% divergence); this obviously reflects significant mitochondrial divergence across drainage basins within this more broadly-distributed lineage. Similarly, there is evidence for structuring across drainage basins within the combined TULE + CEDAR lineage (Fig. 5 inset). As shown previously for Appalachian *H. pococki* (Keith and Hedin 2012), implementation of a GMYC model using COI data appears to

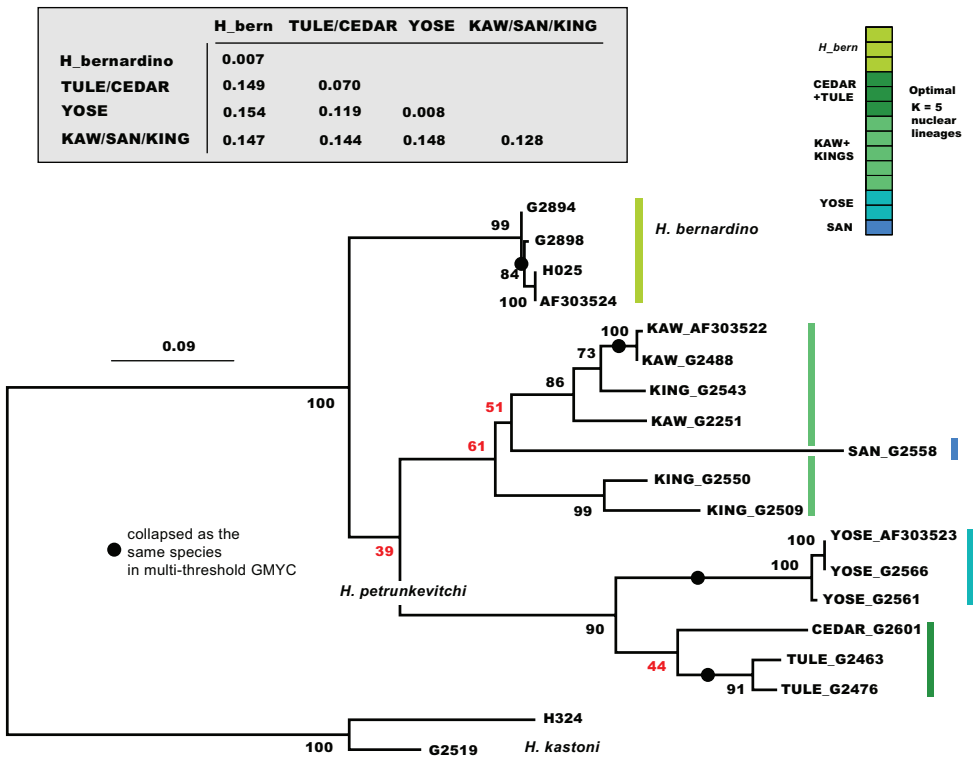


Figure 5. Maximum likelihood mitochondrial tree. Black circles designate clusters of sequences collapsed as the *same* species in multi-threshold GMYC analyses; all other branches supported as separate species (e.g., n = 13 for multi-threshold model). **Inset** – K2P distances within and among primary mitochondrial lineages.

severely over-split species. Specimens from the same geographic location are collapsed as the same species, but all unique geographic locations are delimited as distinct species (multi = 13, single = 14; Fig. 5 inset).

Morphology

Morphological data for *H. pococki* and California taxa are presented below in the Discussion and Taxonomy sections, respectively.

Discussion

Broad-scale phylogenomics and biogeography

Our results confirm the Catley (1994) hypothesis of a sister relationship between highly disjunct California and Appalachian faunas, sister to a more geographically central Rocky Mountain clade. Support was unequivocal for this topology, recovered in all analyses from all UCE matrices (Figs 2, 3; <https://doi.org/10.5061/dryad.g1jwstqsd>). These regional relationships in *Hypochilus* are contrary to patterns seen in the salamander genus *Aneides*, a taxon which also includes montane-associated species from California, the southern Rocky Mountains, and Appalachia. Molecular phylogenetic research in *Aneides* has recovered a sister relationship between California and southern Rocky Mountain species, sister to Appalachian taxa (Vieites et al. 2007). Inter-regional divergences in *Aneides* are estimated to have occurred roughly in the timeframe spanning the Eocene to the Oligocene, perhaps coincident with periods of global warming allowing for intercontinental dispersal events (Vieites et al. 2007).

We hypothesize that *Hypochilus* has a more ancient history, and that this timing difference might also explain the unique phylogenetic topology seen in *Hypochilus*. Divergence time estimates for *Hypochilus* are hindered by a lack of direct fossil evidence, with current age estimates for the genus derived from broader examinations of diversification dates for spiders. For example, using published transcriptome data, Magalhaes et al. (2020) estimated divergence between *H. gertschi* and *H. pococki* (both Appalachian taxa) during the early Paleogene, with a very large confidence interval. Given approximately polytomous relationships within Appalachia (see below), this point estimate would correspond to a crown group age for the Appalachian radiation, and thus implies older divergences at the base of *Hypochilus*, perhaps during the Cretaceous. We note here that many other non-entelegyne araneomorph spider lineages are at least this ancient (both within extant families and sometimes within extant genera), as estimated from molecular clock analyses (e.g., sicariids – Magalhaes et al. 2019; leptonetids – Ledford et al. 2021), but also known directly from Upper Cretaceous Burmese amber fossils (e.g., psilodercids – Magalhaes et al. 2021). Also, the combination of Cretaceous fossil evidence in the context of living spider families suggests that non-entelegyne araneomorph lineages (akin to *Hypochilus* and

Hypochilidae) dominated spider diversity at this time (Wunderlich 2008; Magalhaes et al. 2020).

Hypothesized Cretaceous-age divergences for *Hypochilus* are complicated by the presence of the Western Interior Seaway of North America, a major transcontinental marine barrier in place from ~ 105–65 mya (Blakey and Ranney 2017). Although an east / west vicariance hypothesis associated with the Western Interior Seaway seems attractive, the Rocky Mountain orogeny took place after the withdrawal of the Western Interior Seaway (Blakey and Ranney 2017). We speculate that *Hypochilus* is either much older than imagined (ages exceeding 105 mya), or that diversification (and dispersal) was spurred soon after the withdrawal of the Western Interior Seaway. Lacking the discovery of relevant fossils, future work could aim to more precisely estimate rates of nuclear gene molecular evolution in *Hypochilus*, in order to better understand the origin and timing of *Hypochilus* diversification events. Also, inclusion of a transcriptome representing the Rocky Mountain clade could be incorporated into the well-calibrated Magalhaes et al. (2020) dataset, allowing for a crown group age estimate for the entire genus.

Appalachian diversification and potential cryptic species

Within Appalachia, nuclear UCE data strongly support a monophyletic *H. pococki*, contra mitochondrial paraphyly as in Keith and Hedin (2012). Although all currently described species in Appalachia are recovered as monophyletic, and the geographically disjunct *H. thorelli* and *H. coylei* are strongly supported as sister species (see also Hedin 2001; Keith and Hedin 2012), our nuclear datasets otherwise do not resolve species relationships, with an overall topology consistent with a four-lineage polytomy. Gene and site concordance factor values at two key unresolved interspecific nodes take lower values than seen anywhere else in *Hypochilus*, including all nodes within species (Fig. 3). Gene CF values are 9–13 for these nodes, meaning that only ~ 10% of the UCE alignments support these nodes. Site CF values that hover around minimum values (30%) illustrate that the data are essentially equivocal regarding three possible resolutions of a quartet for both of these unresolved nodes (Lanfear 2018). This incongruence and lack of resolution possibly points to a non-adaptive radiation where lineages became rapidly isolated from one another due to environmental factors, but the nature of incongruence requires more study.

Nuclear STRUCTURE results confirm distinct genetic groups within *H. pococki* (Fig. 4); however, these genetic groups do not correspond exactly to the previously described mitochondrial “microclades”. In particular, the Alarka Mountain specimen from the mitochondrial Central (CENT) clade of Keith and Hedin (2012) instead groups with the nuclear WEST genetic cluster (Fig. 4). This is important because the geographic boundaries of previously defined mitochondrial clades were hypothesized to coincide with riverine barriers (e.g., the Little Tennessee River separating the CENT versus WEST mitochondrial clades, etc.; see Keith and Hedin 2012: fig. 2). In fact, most phylogeographic studies in the southern Appalachians have primarily relied upon mitochondrial evidence to define geographic groupings (e.g., references in Keith and

Hedin 2012). Future studies that include dense geographic sampling of nuclear lineages will be important here, with *H. pococki* representing a prime candidate. More generally, if gene flow across cryptic lineages is promoting mitonuclear discordance, this system might provide interesting insight into how cryptic lineages interact at areas of contact. Also, areas of parapatric contact can be used to understand the degree to which gene flow is restricted across cryptic lineage boundaries, providing strong and direct tests of species status (see Singhal et al. 2018).

Although SNAPP and TR2 show higher support for increasing species numbers within *H. pococki* (i.e., a many species hypothesis), nuclear STRUCTURE results and consideration of male pedipalp morphology suggest more conservative species numbers. In their diagnosis, Forster et al. (1987) stated that *H. pococki* males “*can be recognized by the flaplike tip of the palpal conductor*”. We thus focused particular attention on this structure when searching for morphological differences that might distinguish primary genomic lineages (e.g., VA, ELK + NE, CENT, WEST), and included representatives of all such lineages in our SEM surveys. We did not examine female variation (e.g., in spermathecal morphology), but this is another character system to search for morphological differentiation. We observed minimal differences in male palpal morphology across *H. pococki* populations and genomic lineages (Figs 6–8). One possible difference is the shorter secondary coil of the conductor tip observed in ELK specimens (Fig. 6), but we note that ELK itself is well nested within the primary $K = 4$ lineages (Fig. 4). The discord between nuclear genomic data (and analytical results) which suggest many species, versus morphology which suggests few to one species, is a conspicuous example of the cryptic species challenge, and also focuses attention on patterns of morphological stasis. Despite high genomic divergences and ample evolutionary time, morphological change in *Hypochilus* remains conservative. We might expect conserved *Hypochilus* somatic morphology because of selective constraints on both niche evolution and morphological differentiation, under a model of phylogenetic niche conservatism (Keith and Hedin 2012; Fišer et al. 2018). The fact that we also observe similar conservatism in genitalia, where at least genetic drift in isolated populations is expected, is compelling.

A new *Hypochilus* species from montane California

Both nuclear and mitochondrial genetic structuring is very prominent in the California region, and our analyses show that this structure generally follows a pattern of relatedness by drainage basin (Figs 4, 5, 9). The observed divergence within *H. petrunkevitchi* was not surprising as it has previously been noted as having high levels of intraspecific mitochondrial variation (Hedin 2001). As also found for Appalachian samples, both SNAPP and TR2 show a trend of increasing support for models with increasing numbers of species (Tables 1, 3). GMYC analysis of CO1 data similarly delimits all unique geographic locations as distinct species (Fig. 5 inset). We contend that not all local populations can represent unique species, and instead view this as another example of algorithmic over-splitting.

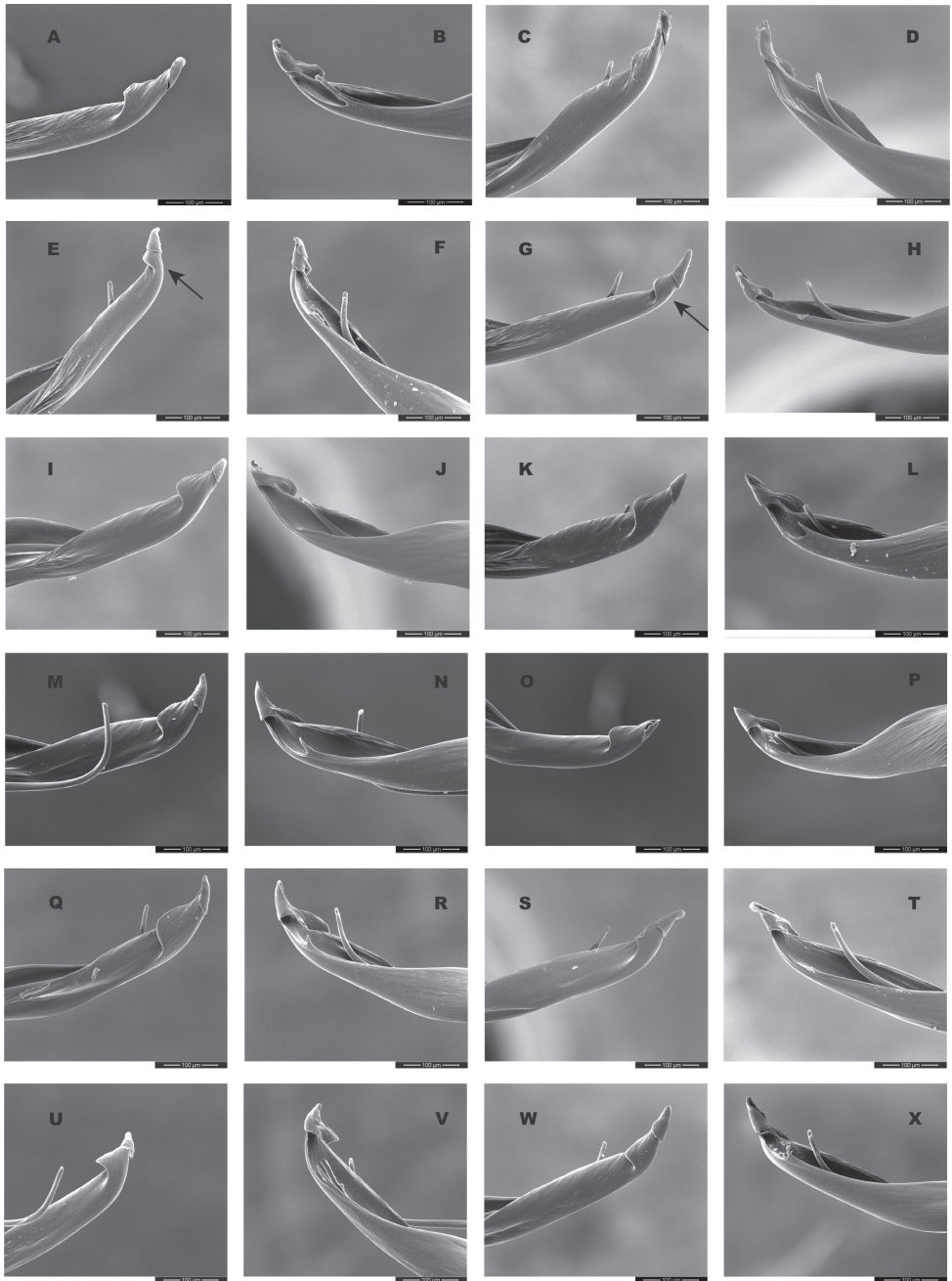


Figure 6. *H. pococki* male palp (conductor) comparison. For each specimen, left panel = prolateral view, right panel = retrolateral view. *NE lineage* **A, B** Green Mtn (MCH 01_162) **C, D** Boone Fork (MCH 01_159); *ELK lineage* **E, F** Elk River (MCH 01_155) **G, H** Linville Gorge (MCH 01_165). Shorter secondary coil for ELK specimens highlighted by arrows; *VA lineage* **I, J** Cliff Mtn (MCH 04_028) **K, L** Guest River (MCH 04_027); *CENT lineage* **M, N** Hickory (MCH 01_144) **O, P** Wagon Road Gap (MCH 01_181); *WEST lineage* **Q, R** Alarka (MCH 02_168) **S, T** Starr Mtn (MCH 02_156) **U, V** Backbone Rock (MCH 04_025) **W, X** Chunky Gal Mtn (MCH 02_142). Detailed specimen information provided in Suppl. material 2.

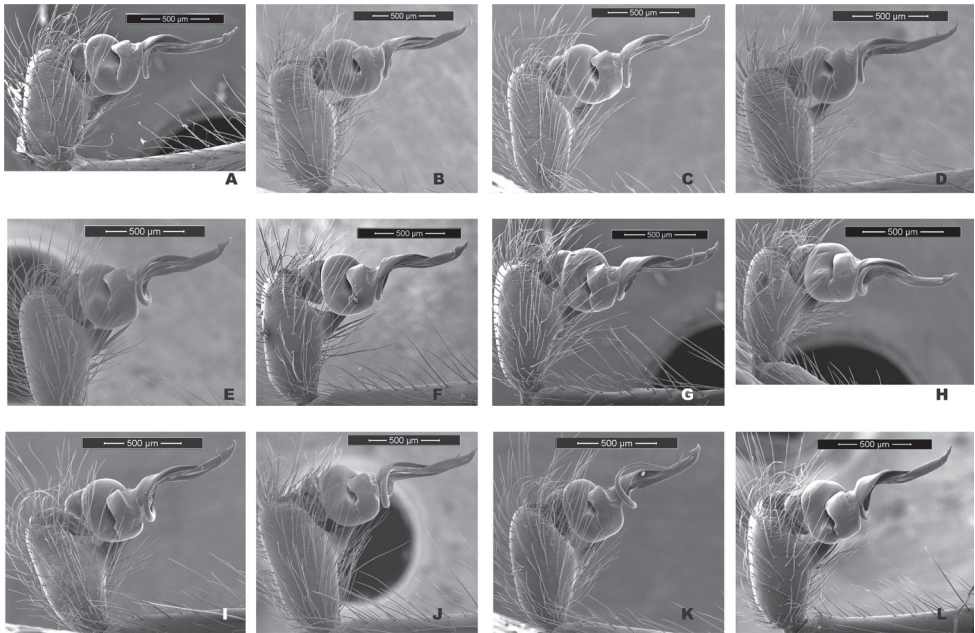


Figure 7. *H. pococki* male palp comparison, prolateral views. *NE lineage* **A** Green Mtn (MCH 01_162) **B** Boone Fork (MCH 01_159); *ELK lineage* **C** Elk River (MCH 01_155) **D** Linville Gorge (MCH 01_165); *VA lineage* **E** Cliff Mtn (MCH 04_028) **F** Guest River (MCH 04_027); *CENT lineage* **G** Hickory (MCH 01_144) **H** Wagon Road Gap (MCH 01_181); *WEST lineage* **I** Alarka (MCH 02_168) **J** Starr Mtn (MCH 02_156) **K** Backbone Rock (MCH 04_025) **L** Chunky Gal Mtn (MCH 02_142). Detailed specimen information provided in Suppl. material 2.

Based on bootstrap values, nuclear data strongly support the hypothesis that *H. bernardino* is phylogenetically nested within *H. petrunkevitchi* (bootstrap = 100 for all matrices across all analyses; Figs 2, 3; <https://doi.org/10.5061/dryad.g1jwstqsd>). Acknowledging that bootstrap values can provide an inflated view of support (Lanfear 2018; Minh et al. 2018), we considered several other concordance factor values for this node (gCF = 34.8, sCF = 48.3, Fig. 3). From a gene (individual UCE locus) perspective, of 155 alignments that could have included the branch of interest (gN = 155), 34.84% or ~ 50 alignments (= gCF) showed the Fig. 3 topology, with very few alignments supporting an alternative topology at high frequency (gDF1 = 3.23, gDF2 = 8.39). Similarly, from a site perspective, of ~ 200 decisive sites for the quartet of interest (sN = 199.42), approximately half support the Fig. 3 topology (sCF = 48.28), with fewer supporting alternative resolutions (sDF1 = 18.33, sDF2 = 29.4). Overall, we view these values (see Lanfear 2018), in concert with bootstrap values, as strongly supporting the paraphyly of *H. petrunkevitchi* with respect to *H. bernardino*.

Based on this phylogenomic pattern we see two obvious taxonomic alternatives. The first is to sink *H. bernardino* into a broadly distributed, highly genetically-structured *H. petrunkevitchi*. The second is to elevate and formally describe the distinct genetic lineage that is sister to *H. bernardino*. We prefer and argue for the latter approach, for

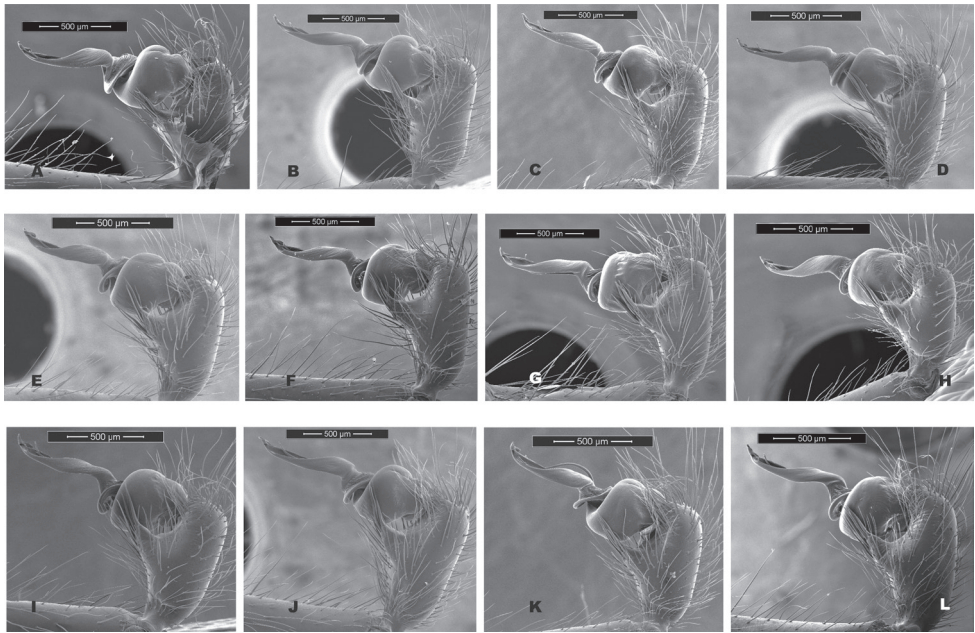


Figure 8. *H. pococki* male palp comparison, retrolateral views. *NE lineage* **A** Green Mtn (MCH 01_162) **B** Boone Fork (MCH 01_159); *ELK lineage* **C** Elk River (MCH 01_155) **D** Linville Gorge (MCH 01_165); *VA lineage* **E** Cliff Mtn (MCH 04_028) **F** Guest River (MCH 04_027); *CENT lineage* **G** Hickory (MCH 01_144) **H** Wagon Road Gap (MCH 01_181); *WEST lineage* **I** Alarka (MCH 02_168) **J** Starr Mtn (MCH 02_156) **K** Backbone Rock (MCH 04_025) **L** Chunky Gal Mtn (MCH 02_142). Detailed specimen information provided in Suppl. material 2.

reasons concisely summarized as follows: 1) *H. bernardino* is already described based on a diagnostic morphology (Catley 1994, and revised diagnosis below), 2) *H. bernardino* is geographically-localized, known only from a single mountain range in southern California, highly disjunct from more northern populations (Fig. 9), and 3) *H. bernardino* is supported both as a distinct nuclear and mitochondrial genetic lineage (Figs 2–5). By these multiple measures of genetic, morphological, and geographic distinctiveness, we view *H. bernardino* as an evolutionary lineage on a unique and independent trajectory. Catley (1994) described *H. bernardino* from the southern section of the San Bernardino mountains of southern California. The few known populations are separated from the southern Sierra Nevada by hundreds of kilometers of mostly inappropriate habitat (lower elevations, fewer granite outcrops), where these spiders (or their distinctive webs) have never been found (Fig. 9). This lack of records includes not only our own extensive field work in the intervening region, but also that of the many arachnologists that have conducted research in California, as well as modern-day tools such as iNaturalist. This sort of geographic disjunction has been found in some other taxa, for example, the iconic *Ensatina* salamander complex, where the geographic disjunction is known as “Bob’s Gaps” (Jackman and Wake 1994). In this instance, separated populations have been described as separate subspecies (*E. eschscholtzii klauberi* in the Tehachapi mountains distinct from *E. eschscholtzii croceator* in the San Bernardino

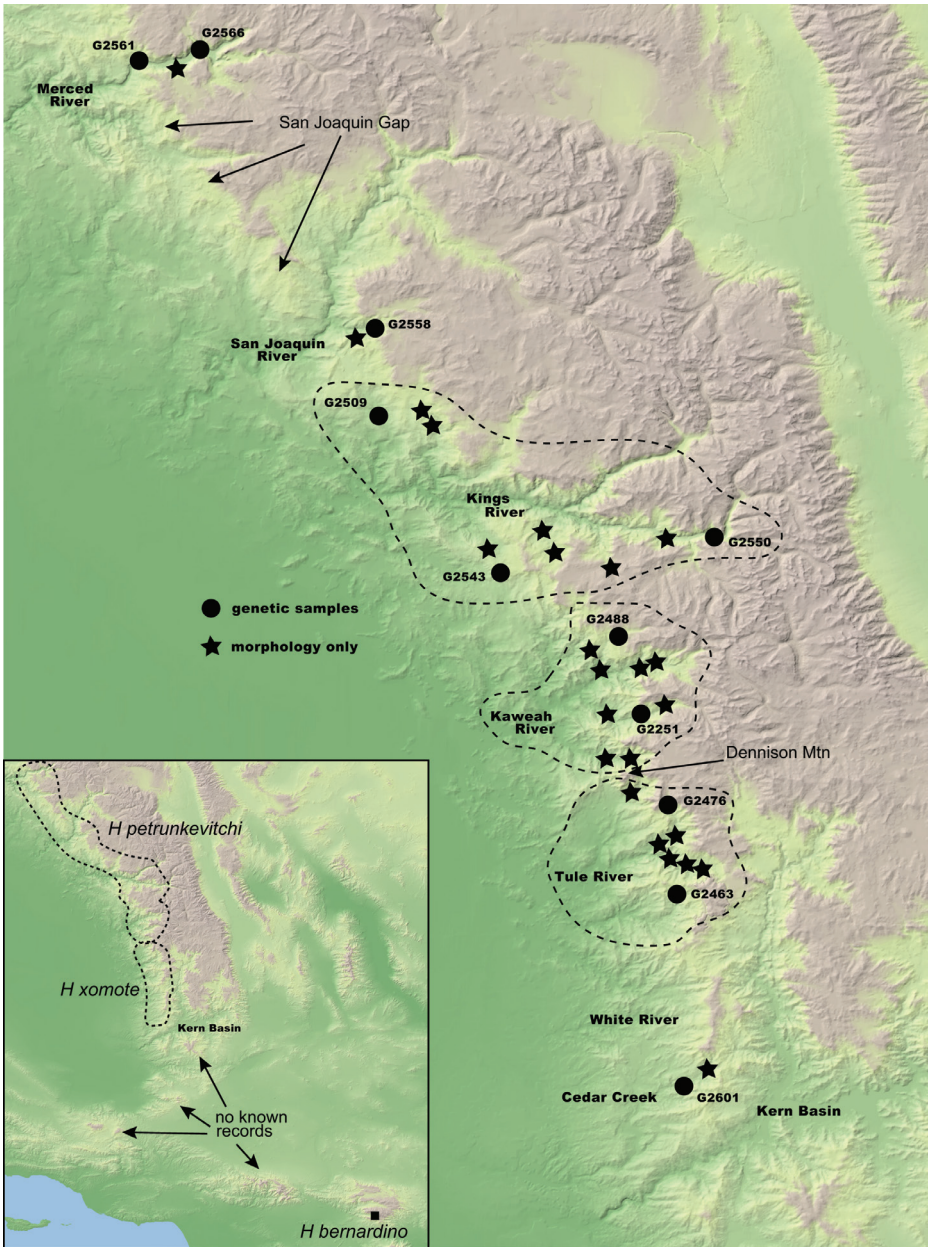


Figure 9. Southern Sierra Nevada topography map with genetic and morphological sample locations (see Suppl. material 1 and Suppl. material 2). Geographic gaps and other notable geographic features mentioned in the text are highlighted.

mountains; Jackman and Wake 1994), but *Ensatina* taxonomy is generally regarded as being fairly conservative.

Accepting *H. bernardino* as an independently evolving lineage, the current taxonomy must be updated to reflect unique lineages discovered within *H. petrunkevitchi*.

Conservatively, we retain the northern lineages that include the type locality (male holotype of *H. petrunkevitchi* from Cedar Grove, Fresno County = KINGS lineage) as *H. petrunkevitchi*. This lineage is distributed across the Merced, San Joaquin, Kings and Kaweah River basins (Fig. 9). Again, accepting *H. bernardino* as a unique species, our data indicate that populations from the Tule River and Cedar Creek drainage basins need to be recognized as a new species, which we formally describe below. Specimens from these drainage basins represent new locality records and the southern-most known observations of *Hypochilus* spiders in the Sierra Nevada (Fig. 9). More generally, this part of the southern Sierra Nevada is a well-known area of active speciation, with many short-range endemic arthropods and vertebrates (Bond 2012; Jockusch et al. 2012; Papenfuss and Parham 2013; Satler et al. 2013; Leavitt et al. 2015; Emata and Hedin 2016; Starrett et al. 2018; Bennett et al. 2021; Weng et al. 2021). In this regard, discovering a new species in the southern Sierra Nevada is not surprising.

Cryptic species concept

We define species as evolutionary lineages on a “unique and independent trajectory”. Following Davis et al. (2021), we consider species to be cryptic “*if they depend on additional sources of data to formulate the delineation hypothesis prior to establishing diagnostic morphological characters*”. This definition applies well to the new species description below, which is motivated by a combination of genetic divergence and uniqueness, phylogenetic pattern (paraphyly w.r.t. *H. bernardino*) and geographic allopatry, which has prompted us to take a closer look at morphology. Additionally, the definition allows for an initial hypothesis of morphological crypsis that does not preclude future downstream studies that in fact find morphological (or other) differences, making the species no longer technically “cryptic”. In many instances, species are morphologically cryptic because of their youth, where morphological divergence has not yet caught up with molecular divergence. But as noted above, the measured mitochondrial differences in *Hypochilus* are among the highest known in spiders (a clade with ~ 50,000 described species), and we hypothesize relatively ancient divergences in the genus. These data and arguments are inconsistent with recent evolutionary divergence, and we instead favor a model of long-term phylogenetic niche conservatism constraining morphological evolution (Fišer et al. 2018), as argued above.

Overall, we view our new cryptic species hypotheses as conservative, consistent with perspectives that genomic data should be interpreted conservatively when describing new species (Coates et al. 2018). In *Hypochilus*, this is particularly true since genomic diagnosability is ubiquitous, and extends to the level of localized populations, as reflected in nuclear and mitochondrial algorithmic delimitations. Our hypotheses below do not recognize all genetically divergent lineages as species and allow for varying degrees of population divergence within described species (e.g., *H. petrunkevitchi*, new species below). In particular, there is evidence that the Yosemite Valley (Merced River) population is on a unique evolutionary trajectory due to its disjunct distribution and because samples from the isolated valley floor routinely fall out as a divergent

group in both nuclear and mitochondrial analyses (Figs 2–5). The single sampled population from the San Joaquin drainage is similarly genetically divergent and geographically isolated. This disjunction might be natural, as spiders have never been collected in the apparently suitable granite outcrop habitats between San Joaquin locations and the Yosemite Valley, despite concerted collecting efforts (Fig. 9). In the context of an integrative taxonomic framework, we weigh conservation considerations, extreme geographic allopatry, and well-supported paraphyly as particularly important. Genomic diagnosability is important but not decisive, with morphological diagnosability as least important, again reflecting phylogenetic niche conservatism. Regarding conservation value, we argue that sinking *H. bernardino* into a broadly distributed, highly genetically-structured *H. petrunkevitchi* would immediately decrease the conservation value and importance of the former.

Taxonomy

Hypochilus Marx, 1888

Diagnosis. following Forster et al. (1987).

Hypochilus bernardino Catley 1994

Figs 9–13

Hypochilus petrunkevitchi Gertsch 1958: Forster et al. 1987: 22 (San Bernardino county records).

Hypochilus bernardino Catley 1994: 10, figs 7, 11, 25, 33, 36–39.

Material examined. F from Forsee Creek (SDSU_G2893), Ms from East Fork Mountain Home Creek (SDSU_G2929–2932), see Suppl. material 2.

Diagnosis. Following from the original diagnosis of Catley (1994), we paid closest attention to the length of the PTaL (should be shorter in *H. bernardino*), and the PTW/PTL (should be shorter and more thickened proximally in *H. bernardino*). We found that PTaL overlaps with northern populations (Table 5), and is therefore not diagnostic. The PTW/PTL ratio is generally smaller in *H. bernardino*, but there is some overlap with northern populations, again calling into question the diagnostic value of this character. We did find that the male CdL is consistently shorter in *H. bernardino* (Table 5), and hypothesize this as a new morphological character diagnostic for the species. Again, consistent with a hypothesis of phylogenetic niche conservatism imparting morphological stasis, the species is only weakly morphologically diagnoseable. The disjunct geographic distribution (Fig. 9) and hundreds of diagnostic nucleotide changes (alignments at <https://doi.org/10.5061/dryad.g1jwstqsd>) can also be used to recognize this species.

Table 5. Morphological measurements. PTW/PTL (maximum width of male pedipalpal tibia in retrolateral view/length of tibia in retrolateral view), CdL (male palpal conductor length in retrolateral view), AME (diameter of anterior median eye pupil), PTaL (length of male palpal tarsus in retrolateral view), CTpr (number of promarginal cheliceral teeth), CTre (number of retromarginal cheliceral teeth). Raw measurements provided in Suppl. material 2.

	PTW/PTL	CdL	AME	PTaL	CTpr	CTre
<i>H. bernardino</i>	0.253–0.267	0.475–0.50	0.1–0.125	0.82–1.0	4–5	2–3
<i>H. petrunkevitchi</i> YOSE lineage	0.259–0.292	0.625	0.10–0.125	0.925–1.0	5	2
<i>H. petrunkevitchi</i> KING lineage	0.278	0.60	0.10	0.875	5	2
<i>H. petrunkevitchi</i> KAW lineage	0.274–0.307	0.575–0.675	0.10–0.125	0.925–1.15	4–5	2
<i>H. xomote</i> sp. nov.	0.256–0.338	0.525–0.575	0.10–0.125	0.775–1.075	4–5	1–2

Genetic data. SRA Accession numbers: SAMN21239435–SAMN21239437.

New records. California, San Bernardino County, San Bernardino Mountains, Camp Creek east of Forest Falls, 34.0760, -116.8876, coll. M. Hedin, 10 July 1993 (SDSU_H0025–0027, 3I). San Bernardino County, San Bernardino Mountains, Hwy 38, tributary into East Fork Mountain Home Creek, in culvert and tunnel under highway, 34.1198, -116.9768, coll. E. Ciaccio, 4 August 2018 (SDSU_G2897–2899, 3I). San Bernardino County, San Bernardino Mountains, Hwy 38, tributary into East Fork Mountain Home Creek, in culvert and tunnel under highway, 34.1198, -116.9768, coll. E. Ciaccio, 27 Sept 2018 (SDSU_G2929–2932, 4M). San Bernardino County, San Bernardino Mountains, Hwy 38, Forsee Creek, along stream and tunnel under highway, 34.1574, -116.9315, coll. E. Ciaccio, 4 August 2018 (SDSU_G2893–2896, F, 3I). See also Suppl. material 2 for locality (including elevation) and natural history information for specimens examined.

Remarks. Catley (1994) hypothesized the following diagnostic features, based on comparisons to near-type locality *H. petrunkevitchi*:

“*The species most closely resembles its sister species Hypochilus petrunkevitchi in general coloration, eye dimensions, and male pedipalpal morphology. Males can be recognized by the apex of the conductor which is more loosely whorled (fig. 24) than in H. petrunkevitchi, the shorter pedipalpal tarsus, a greatly reduced distal palpal (conductor) apophysis (fig. 25), and a median palpal apophysis that is significantly smaller than H. petrunkevitchi, with no notch (fig. 7). The short palpal tibia is strongly incrassate proximally. Females ... are particularly difficult to separate from H. petrunkevitchi females, the former possessing similar but smaller convoluted spermathecal ducts (fig. 11).*”

Our comparisons of near-type *H. bernardino* to larger samples (Suppl. material 2) of more northern populations in California (not including the distinctive *H. kastoni*) suggests the following character trends. Regarding the shape of the apex of the conductor, we find no consistent difference in tightness of the whorls (Fig. 10), a feature that we also found difficult to characterize. The small distal conductor apophysis is likewise inconsistently absent or barely present across populations (Fig. 10). We also could not discern a consistent difference in the shape of the median palpal apophysis (Figs 11, 12), with our SEM imaged *H. bernardino* specimens appearing much like the

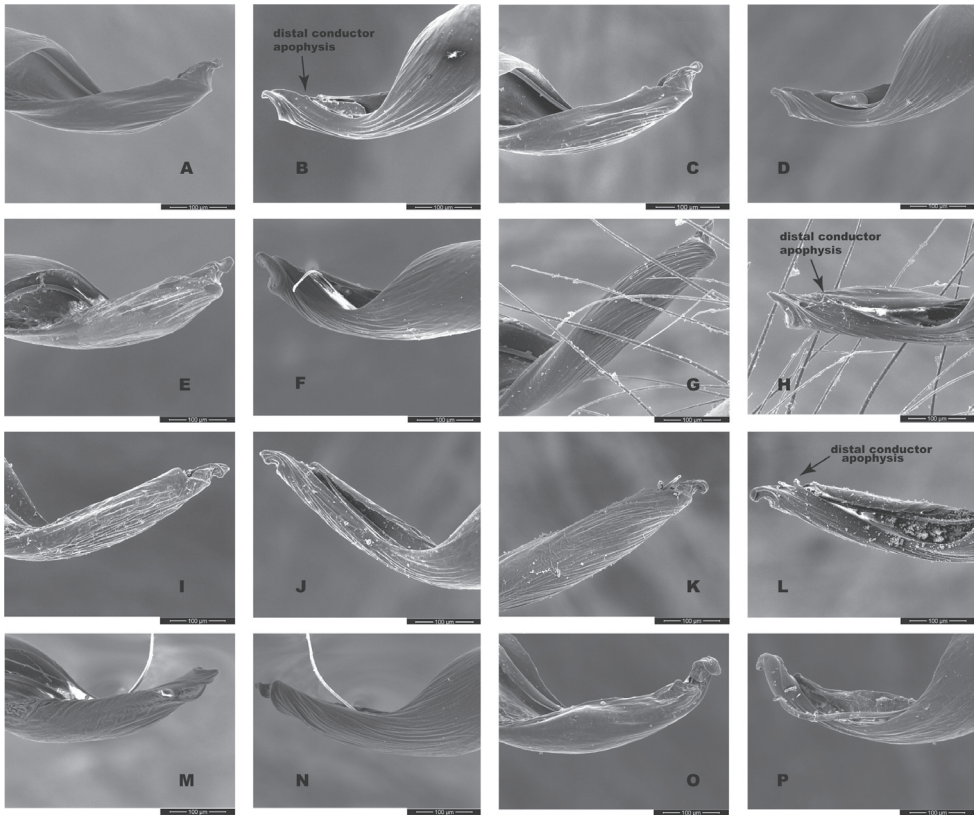


Figure 10. California taxa male palp (conductor) comparison. For each specimen, left panel = prolateral view, right panel = retrolateral view. *H. bernardino* **A, B** Mtn Home (SDSU_G2931) **C, D** Mtn Home (SDSU_G2932); *H. xomote* **E, F** Alder Creek (SDSU_G2600) **G, H** Tule River (SDSU_G2289); *H. petrunkevitchi* KINGS lineage **I, J** Mill Flat (SDSU_G2554); *H. petrunkevitchi* KAW lineage **K, L** Mineral King Road (SDSU_TAC000192); *H. petrunkevitchi* YOSE lineage **M, N** Yosemite (SDSU_G2568); *H. kastoni* **O, P** Ney Springs (SDSU_TAC000191). Distal conductor apophysis highlighted by arrows. Detailed specimen information provided in Suppl. material 2.

original drawings of *H. petrunkevitchi* (Catley 1994: fig. 8). Differences in the degree of sclerotization at the base of this apophysis also makes the narrowness somewhat subjective to score, at least in some specimens. Finally, we found female spermathecal morphology to be highly conserved (Fig. 13); it is possible that the median ducts are more convoluted in *H. bernardino* than in northern populations, but this difference is subtle given our sampling.

Distribution and habitat. Known only from two primary forks of a single drainage basin (headwaters of Santa Ana River, and Mill Creek, a large tributary of the Santa Ana), south side of the San Bernardino Mountains of southern California (Fig. 9). The Forsee Creek population, near the headwaters of the Santa Ana River, represents a new record for this species. We suspect that additional populations likely exist in the narrow

canyons that lead into the Santa Ana River, for example, Bear Creek, Warm Springs Canyon, etc. In our recent collections we have found spiders in webs on large, sheltered granite boulders near streams, and in stream culverts beneath a primary highway.

Conservation. We view *H. bernardino* as a short-range endemic taxon with a precarious future, deserving of special conservation attention and monitoring efforts. Over 25 years ago, Catley (1994) discussed how populations may have been negatively affected by drought. More recently, large fires have burned the forests of the Mountain Home Creek drainage (e.g., 2018 Valley fire). The loss of forest canopy cover is expected to result in fundamental changes in microhabitat conditions, and in concert with increasing global temperatures, calls for continued close monitoring of *H. bernardino* populations.

Hypochilus petrunkevitchi Gertsch, 1958

Figs 9–13

Hypochilus petrunkevitchi Gertsch 1958: 11, figs. 5, 7, 15, 17, 21; Lehtinen 1967: 431, fig. 14; Forster et al. 1987: 21, figs 68–72; Catley 1994: 7, figs. 8, 13, 24.

Material examined. Fs from Ladybug Trail (SDSU_G2275), Mineral King Road (SDSU_G2485), Providence Creek (SDSU_G2508), Mill Creek (SDSU_G2543), Huntington Lake Road (SDSU_G2514, SDSU_G2557), Yosemite Falls (SDSU_G2564); Ms from Atwell-Hockett Trail (SDSU_G2260), Big Fern Springs (SDSU_G2262), Ladybug Trail (SDSU_G2274), Mehrten Creek (SDSU_G2285), Mineral King Road (SDSU_TAC000192), South Fork Kaweah River (SDSU_G2279), Mill Flat (SDSU_G2254), and Yosemite Falls (SDSU_G2568, SDSU_G2569); see Suppl. material 2.

Diagnosis. We found that the male palpal conductor (CdL) is consistently longer in *H. petrunkevitchi* than in both *H. bernardino* and the new species below, although barely for the latter (Table 5), and larger sample sizes might negate this difference. It is clear that all southern Sierran populations retain a very similar morphology, with minor morphological divergence associated with evolution in the southern Transverse ranges (*H. bernardino*).

Genetic data. SRA Accession numbers: SAMN21239424–SAMN21239431.

New records. Merced River drainage (YOSE): California, Mariposa County, Yosemite NP, Big Oak Flat Rd., bridge over Tamarack Creek, 37.7278, -119.7143, coll. E. Ciaccio, M. Hedin, A. Rivera, 29 Sept 2017 (SDSU_G2561–2563, 3I). Mariposa County, Yosemite NP, vic Bridalveil Falls, 37.7167, -119.6519, coll. E. Ciaccio, 3 August 2017 (SDSU_G2515–2518, 4I). Mariposa County, Yosemite NP, near Yosemite Falls, 37.7491, -119.5965, coll. E. Ciaccio, M. Hedin, A. Rivera, 29 Sept 2017 (SDSU_G2564–2566, 2I, 2F, 2M). Mariposa County, Yosemite NP, near Yosemite Falls, 37.7491, -119.5965, coll. M. Hedin, K. Crandall, 27 June 1992 (SDSU_H0015–H0016, 2I). San Joaquin River drainage (SAN): Fresno County, Sierra NF,

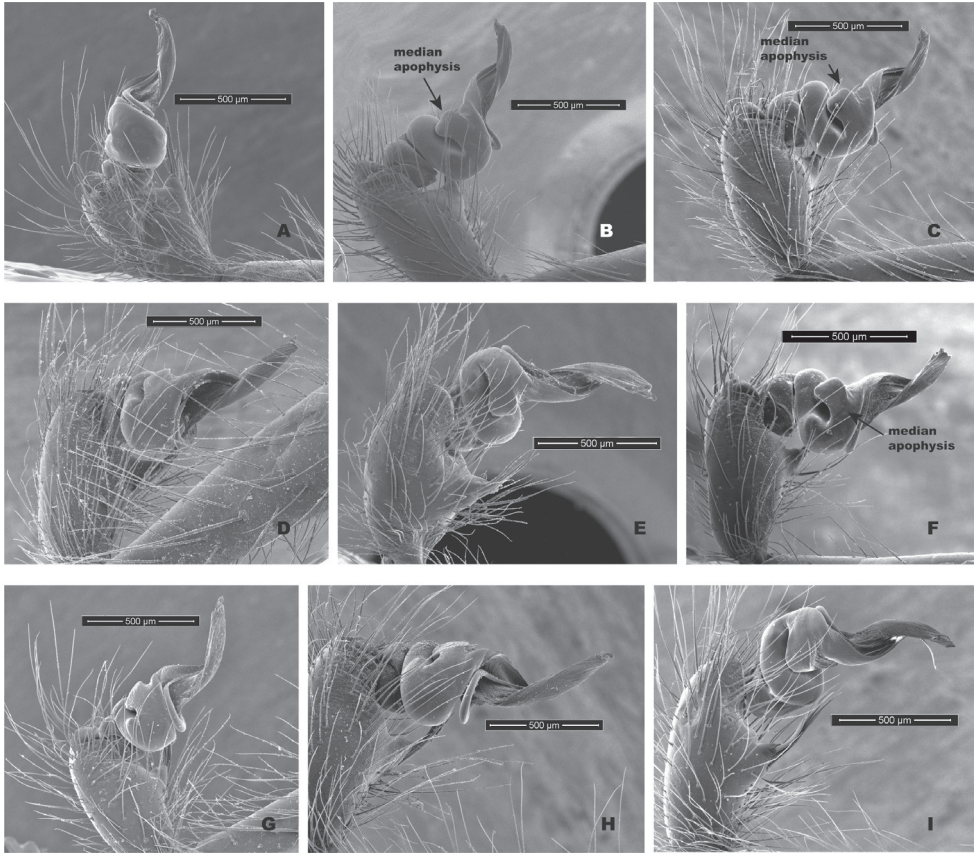


Figure 11. California taxa male palp comparison, prolateral views. *H. kastoni* **A** Ney Springs (SDSU_TAC000191); *H. bernardino* **B** Mtn Home (SDSU_G2931) **C** Mtn Home (SDSU_G2932); *H. xomote* **D** Tule River (SDSU_G2289) **E** Alder Creek (SDSU_G2600) **F** Belknap Springs (SDSU_G2300); *H. petrunkevitchi* KINGS lineage **G** Mill Flat (SDSU_G2554); *H. petrunkevitchi* KAW lineage **H** Mineral King Road (SDSU_TAC000192); *H. petrunkevitchi* YOSE lineage **I** Yosemite (SDSU_G2568). Median apophysis highlighted by arrows. For specimens E and I the bulb has rotated during specimen prep; these two images are retrrolateral views, subsequently flipped in Photoshop. Detailed specimen information provided in Suppl. material 2.

Huntington Lake Rd., Balsam Creek turnout, 37.1884, -119.2591, coll. E. Ciaccio, 31 July 2017 (SDSU_G2510–2514, 1I, 4F). Fresno County, Sierra NF, Snowslide Creek on Huntington Lake road, 37.2029, -119.2367, coll. E. Ciaccio, 10 Sept 2017 (SDSU_G2557–2560, 1I, 3F). Kings River drainage (KING): California, Fresno County, Sierra NF, McKinley Grove Rd., Bear Creek turnout, 37.0411, -119.1202, coll. E. Ciaccio, B. Hernandez, S. Torres, J. Waters, 24 July 2017 (SDSU_G2557–2560, 4I, 1M). Fresno County, Sierra NF, McKinley Grove Big Trees Area, 37.0224, -119.1066, coll. E. Ciaccio, 10 Sept 2017 (SDSU_G2555, G2556, 1I, 1F). Fresno County, Bretz Mill, Providence Creek, 37.0427, -119.2371, coll. E. Ciaccio, 31 July

2017 (SDSU_G2505–2509, 2M, 3F). Fresno County, Kings Canyon NP, dam at Sheep Creek on Don Cecil Trail, 36.7840, -118.6784, coll. E. Ciaccio, 9 Sept 2017 (SDSU_G2551, 1I). Fresno County, Kings Canyon NP, Road's end permit station, Bubbs Creek/Zumwalt Meadow trail jct, 36.7918, -118.5871, coll. E. Ciaccio, 9 Sept 2017 (SDSU_G2549–2550, 1I, 1F). Fresno County, Mill Flat OHV staging area, Mill Flat Creek, 36.7452, -119.0047, coll. E. Ciaccio, 30 July 2017 (SDSU_G2502–2504, 3I). Fresno County, Sequoia NF, Mill Flat OHV Staging Area, 36.7471, -119.0046, coll. E. Ciaccio, 9 Sept 2017 (SDSU_G2552–2554, M, 2F). Fresno County, Sequoia NF, Ten Mile Rd., at bridge N of Hume Lake, 36.7838, -118.9006, coll. E. Ciaccio, 8 Sept 2017 (SDSU_G2546–2548, I, 2F). Fresno County, Sequoia NF, Ten Mile Rd., Landslide Creek turnout, 36.7625, -118.8801, coll. E. Ciaccio, 29 July 2017 (SDSU_G2497–2501, 1I, 2M, 2F). Fresno County, Sequoia NF, Hwy 245 at Mill Creek, ~1 mi S of Hwy 180 Jct, 36.7145, -118.9879, coll. E. Ciaccio, 30 July 2017 (SDSU_G2542–2545, 2I, 2F). Kaweah River drainage (KAW): Tulare County, Sequoia NP, Hwy 198, Big Fern Springs, 36.5382, -118.7751, coll. M. Hedin, 12 July 1993 (SDSU_H0020–H0022, 3I). Tulare County, Sequoia NP Hwy 198, Big Fern Springs, 36.5382, -118.7751, coll. E. Ciaccio, 17 August 2016 (SDSU_G2261–G2265, 1M, 3F, 1I). Tulare County, Sequoia NF, Forest Rte 14S11, Boulder Creek turnout, 36.7342, -118.7736, coll. E. Ciaccio, 29 July 2017 (SDSU_G2492–G2496, 1M, 4F). Tulare County, Sequoia NP, Hwy 198 near Lodgepole CG, Marble Fork Kaweah River, 36.6037, -118.7392, coll. E. Ciaccio, 29 July 2017 (SDSU_G2487–G2491, 4M, 1F). Tulare County, Sequoia NP, Mineral King Rd., Squirrel Creek pullout, 36.4428, -118.7694, coll. E. Ciaccio, 28 July 2017 (SDSU_G2482–G2486, 3M, 1F, 1I). Tulare County, Sequoia NP, Atwell-Hockett Trail, bridge on trail, 36.4584, -118.6564, coll. E. Ciaccio, 16 August 2016 (SDSU_G2256–G2260, 3M, 1F, 1I). Tulare County, Sequoia NP, bridge over Marble Fork on road to Crystal Cave, 36.5759, -118.7860, coll. E. Ciaccio, 17 August 2016 (SDSU_G2266–G2270, 4F, 1I). Tulare County, Sequoia NP, Ladybug Trail, upstream from bridge at start of trail, 36.35005, -118.76238, coll. E. Ciaccio, B. Hernandez, S. Torres, 3 Sept 2016 (SDSU_G2273–G2278, 2M, 3F, 1I). Tulare County, Sequoia NP, Middle Fork Trail, 36.5416, -118.7074, coll. E. Ciaccio, 18 August 2016 (SDSU_G2271, 1I). Tulare County, Sequoia NP, Middle Fork Trail, Mehrten Creek, 36.5457, -118.6920, coll. E. Ciaccio, B. Hernandez, S. Torres, 4 Sept 2016 (SDSU_G2284–G2288, 2M, 2F, 1I). Tulare County, Sequoia NP, Middle Fork Trail, near Mehrten Creek, 36.5456, -118.7036, coll. E. Ciaccio, 16 August 2016 (SDSU_G2272, 1I). Tulare County, Sequoia NP, Mineral King Road, turnout on the road, 36.45346, -118.6923, coll. E. Ciaccio, 18 August 2016 (SDSU_G2251–2255, 5F). Tulare County, Sequoia NP, Mineral King Road, crossing of Redwood Creek, W of Atwell Mill CG, 36.4533, -118.7036, coll. M. Hedin, 24 August 2009 (SDSU_TAC000192–TAC000193, 1F, 1M). Tulare County, Sequoia NP, South Fork Kaweah River, jct of Cedar Creek and South Fork Kaweah River, 36.3551, -118.7335, coll. E. Ciaccio, B. Hernandez, S. Torres, 4 Sept 2016 (SDSU_G2279–G2283, 1M, 3F, 1I). Tulare County, Sequoia NP, below Atwell Mill CG, along Kaweah River, 36.4584, -118.6561, coll. M. Hedin, 23 August 2009 (SDSU_H0842–H0844, 1F, 1M, 1I). See

also Suppl. material 2 for locality (including elevation) and natural history information for specimens examined.

Remarks. Catley (1994) provided no formal diagnosis for *H. petrunkevitchi* (and original diagnoses only compared *H. petrunkevitchi* to the easily distinguishable *H. kastoni*), but offered the following differences from *H. bernardino* in his keys to males and females - length of male PTaL relatively long (0.99–1.10 mm); index of shape of male palpal median apophysis (= vertical height of distal edge of apophysis \times length of ventral border of apophysis) large (0.02–0.03) and strongly notched at proximal edge; apex of the conductor in tight whorl with large inwardly directed distal apophysis. Spermathecal bulbs large, diameter of largest not less than 0.11 mm; median ducts of greater length than lateral ducts. We have commented above on the shape of the apex of the male conductor (Fig. 10), the shape of the male palpal median apophysis (Figs 11, 12), and a PTaL which overlaps in length (Table 5). Similarly, we view the relative size of spermathecal bulbs, and relative length of median versus lateral ducts as qualitatively similar (Fig. 13).

Distribution and habitat. *H. petrunkevitchi* was previously known from a handful of locations in the west-central Sierra Nevada, and our work has greatly expanded our distributional knowledge for this species (Fig. 9). All previous taxonomic publications involving this species examined only northern specimens (Kaweah River drainage and northwards), which here retain the name *H. petrunkevitchi*.

Conservation. Of all the basins in the southern Sierra Nevada, the Kaweah and Kings populations appear to occupy the most contiguous habitat, as reflected in both nuclear phylogenies and STRUCTURE results (Figs 2–5, 9). The Yosemite and San Joaquin populations, which are geographically isolated and particularly genetically divergent, deserve close monitoring. While all Yosemite populations lie within the boundaries of Yosemite National Park, this does not strictly assure future persistence. Populations in Yosemite Valley occur only in deep breakdown “caves”, and in our experience spiders are not abundant. Both known San Joaquin populations occur in habitats that have recently burned as part of the devastating 2020 Creek Fire, again likely changing the nature of the canopy structure (and thus microclimatic conditions) in this area.

***Hypochilus xomote* Hedin & Ciaccio, sp. nov.**

<http://zoobank.org/7AF45D16-59AC-4E3D-B846-3DD14D4B8BBE>

Figs 9–14

Type material. *Holotype* male (SDSU_TAC000658) from California, Kern County, upstream of Cedar Creek campground, off Hwy 155, Sequoia National Forest, 35.7508, -118.5807, elevation ~ 1520 meters, coll. M. Hedin, 4 October 2021 (MCH 21_091). Deposited at the University of California Davis Bohart Museum of Entomology. *Paratype* females (SDSU_TAC000659, TAC000660) and paratype male (SDSU_TAC000661) from same collecting event (MCH 21_091). Deposited at the Denver Museum of Nature and Science.

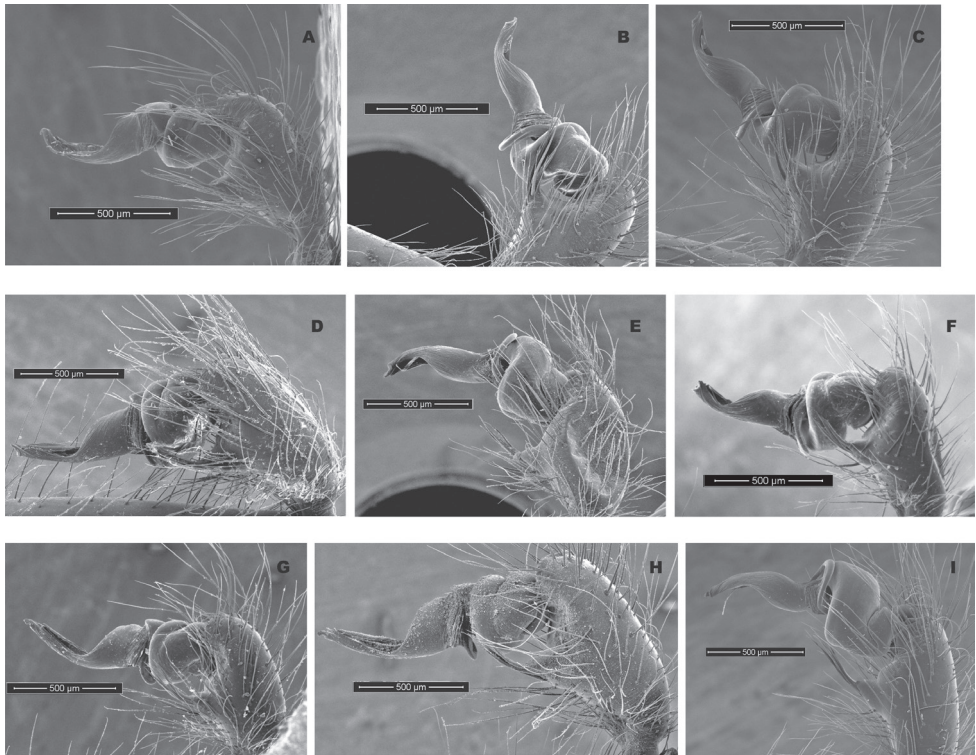


Figure 12. California taxa male palp comparison, retrolateral views. *H. kastoni* **A** Ney Springs (SDSU_TAC000191); *H. bernardino* **B** Mtn Home (SDSU_G2931) **C** Mtn Home (SDSU_G2932); *H. xomote* **D** Tule River (SDSU_G2289) **E** Alder Creek (SDSU_G2600) **F** Belknap Creek (SDSU_G2300); *H. petrunkevitchi* KINGS lineage **G** Mill Flat (SDSU_G2554); *H. petrunkevitchi* KAW lineage **H** Mineral King Road (SDSU_TAC000192); *H. petrunkevitchi* YOSE lineage **I** Yosemite (SDSU_G2568). For specimens E and I the bulb has rotated during specimen prep; these two images are prolatateral views, subsequently flipped in Photoshop. Detailed specimen information provided in Suppl. material 2.

Etymology. *xomote*, from the Native American Yowlumni tribal word for south, providing a name for the southern-most known *Hypochilus* populations in the California Sierra Nevada. The X of *xomote* is pronounced as a “breathy, hissy sort-of H” (Vera and Clark 2002). Language translation from the Tule River Yokuts Language Project (Vera and Clark 2002), representing the language of the Yowlumni Yokuts. Members of the larger Yokuts people historically occupied the southern San Joaquin Valley and adjacent Sierran foothills, including the Tule River basin; the Yowlumni occupied a smaller region near the valley outlet of the Kern River (see Fig. 9).

Diagnosis. CdL of intermediate length (Table 5), longer than *H. bernardino* but shorter than *H. petrunkevitchi*, although barely so for geographically adjacent KAW populations of *H. petrunkevitchi*.

Genetic data. SRA Accession numbers: SAMN21239432–SAMN21239434.

Description. Male holotype – Total length 7.5. Cephalothorax 3.0 long, 2.4 wide; clypeus 0.10. Eye diameters: AME 0.125, ALE 0.225, PME 0.175, PLE 0.20.

Chelicerae pale yellow to white, dusky markings at base; promarginal cheliceral teeth 5, cheliceral formula 52314, retromarginal cheliceral teeth two; one distal, one proximal, both very small. Endites and labium white to pale yellow; sternum with dusky pigmentation, small unpigmented patches circling sparse weak setae; coxae whitish; trochanters with proximal and distal pigmented patches; all legs yellow tan with broken dark annulations on femora and tibiae; prolateral proximal aspect of femur 1 with ~ 20 unpigmented weak setae; leg 1 > 20 × length of cephalothorax. Abdomen dorsally pale yellow-white with darker maculations over the entire surface, clothed with sparse hairs, with multiple transverse rows of small weak setae. Palpal tarsus (left) (0.875), palpal tibia short (1.875), thickened proximally (width 0.5), PTW/PTL = 0.267. Conductor length (0.55), conductor tip loosely whorled with very small distal apophysis in retrolateral view. Leg formula 1243; spination (only surfaces bearing spines listed): pedipalpal femur: none; tibia: many dorsal, many prolateral, few to none retrolateral; tarsus: setose with five closely appressed black spines on retrolateral surface of apical spur. Femur I-many prolateral/dorsal; legs II–IV one dorsal proximally. Trichobothrial distribution: all legs with one trichobothria distally on tibia and metatarsus.

Female paratype (SDSU_TAC000659): Total length 11.8, cephalothorax 3.8 long, 3.1 wide; clypeus 0.20. Eye diameters: AME 0.175, ALE 0.275, PME 0.225, PLE 0.20. Clypeal area, lateral aspects of head, and foveal area with dusty maculations. Pedipalp pale yellow-white, legs pale yellow-white with femora and tibiae of all legs with broken dark rings and conspicuous dark spots, first leg > 9 × length of cephalothorax. Chelicerae pale yellow, dusky on front proximal surface. Spermathecae with convoluted ducts and relatively large receptacula (e.g., Fig. 13F). Leg formula 1243; spination (only surfaces bearing spines listed): pedipalpal femur: few distal and dorsal; tibia: few dorsal and prolateral, few to none retrolateral; metatarsus: stronger and denser than other pedipalp elements. Femur I-many prolateral/dorsal; legs II–IV one dorsal proximally. Trichobothrial distribution: pedipalpal tibia with a series of dorsal trichobothria; all legs with one trichobothria distally on tibia and metatarsus.

Other material examined. Tule River drainage: California, Tulare County, Sequoia NF, Balch Park Road, Jenny Creek, 36.2843, -118.7335, coll. E. Ciaccio, 28 July 2017 (SDSU G2477–2481, 5F). Tulare County, Sequoia NF, Hwy 190 turnout, Belknap Creek, 36.1534, -118.5977, coll. E. Ciaccio, 23 Sept 2016 (SDSU G2296–G2300, 4F, M). Tulare County, Mountain Home State Forest, Hidden Falls campground, 36.2585, -118.6631, coll. E. Ciaccio, 28 July 2017 (SDSU G2472–G2476, 2F, 3I). Tulare County, Sequoia NF, Hwy 190, McIntyre Creek turnout, 36.1509, -118.5831, coll. E. Ciaccio, 27 July 2017 (SDSU G2467–2471, 3F, 2I). Tulare County, Sequoia NF, North Fork Middle Fork Tule River, 36.2082, -118.6488, coll. E. Ciaccio, 24 Sept 2016 (SDSU G2307–G2311, 4F, M). Tulare County, Sequoia NF, Road 208, North Fork Middle Fork Tule River, 36.1879, -118.6775, coll. E. Ciaccio, 23 Sept 2016 (SDSU G2301–2306, 5F, 1I). Tulare County, Sequoia NF, Hwy 190, Middle Fork Tule River, 36.1556, -118.6688, coll. E. Ciaccio, 23 Sept 2016 (SDSU G2289–2295, 1I, 1M, 5F). Tulare County, Sequoia NF, Forest Route 21S94, Windy Creek turnout, 36.0810, -118.6055, coll. E. Ciaccio, 27 July 2017 (SDSU G2462–2466, 4F, 1I). Cedar Creek drainage: Kern County, Sequoia NF, Alder Creek campground, north

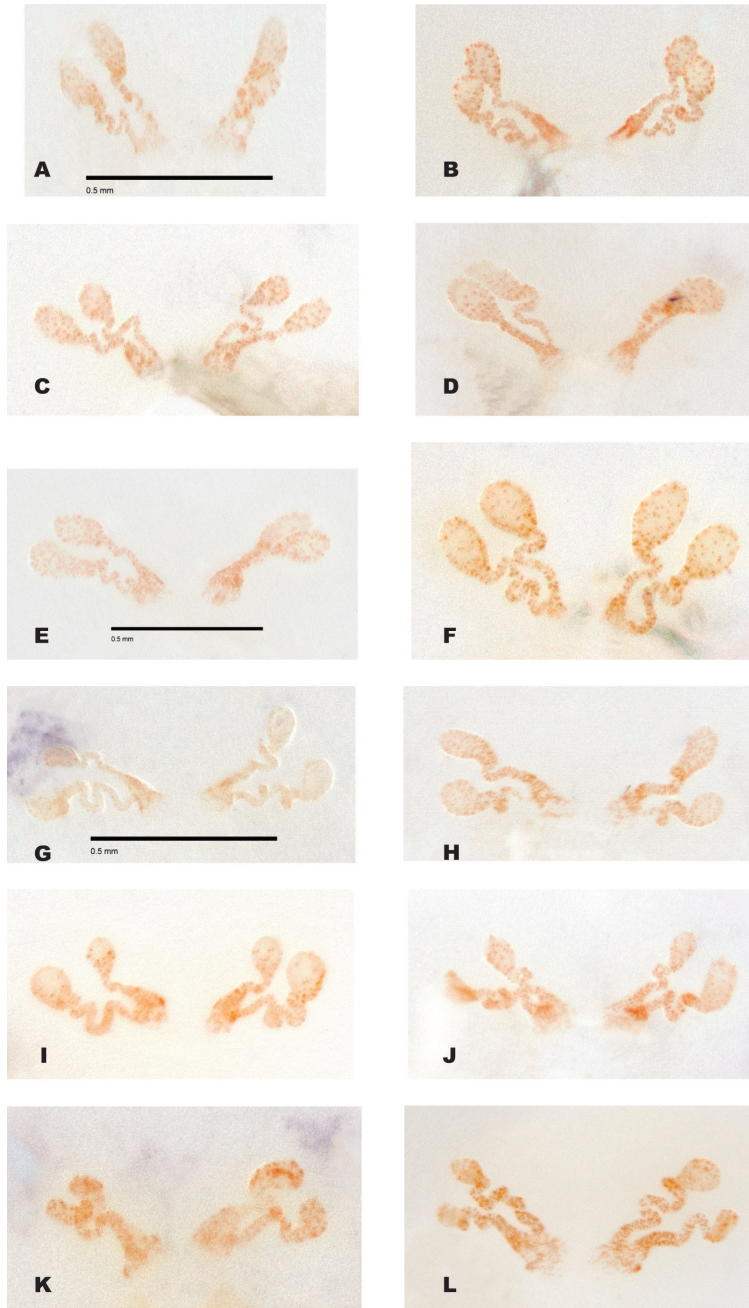


Figure 13. Comparative female spermathecal morphology for California taxa. *H. bernardino* **A** Foresee Creek (SDSU_G2893); *H. petrunkevitchi* YOSE lineage **B** Yosemite (SDSU_G2564); *H. xomote* **C** Jenny Creek (SDSU_G2477) **D** Windy Creek (SDSU_G2465) **E** Belknap Creek (SDSU_G2296) **F** Alder Creek (SDSU_G2601); *H. petrunkevitchi* KAW lineage **G** Ladybug Trail (SDSU_G2275) **H** Mineral King Road (SDSU_G2485); *H. petrunkevitchi* KINGS lineage **I** Mill Creek (SDSU_G2543) **J** Providence Creek (SDSU_G2508); *H. petrunkevitchi* SAN lineage **K** Snowslide Creek (SDSU_G2557) **L** Balsam Creek (SDSU_G2415). Scale bars shown for select specimens. Detailed specimen information provided in Suppl. material 2.

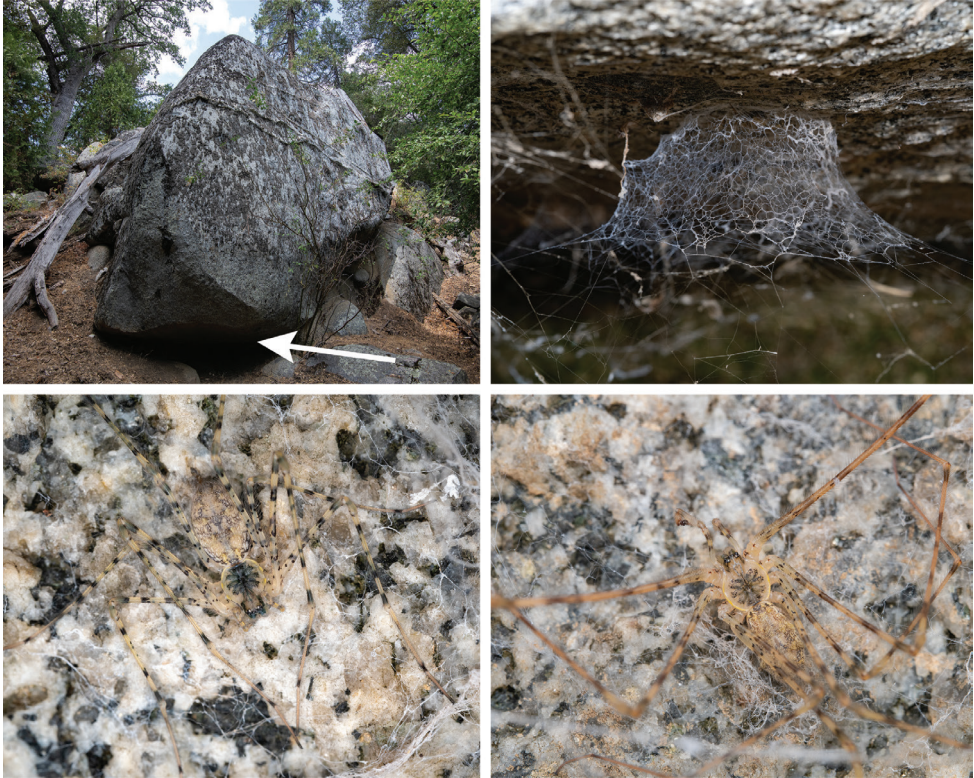


Figure 14. Habitat, web, and live specimen digital images for *H. xomote*. From Kern County, vicinity Alder Creek campground, along Cedar Creek, 5–6 Sept 2020 (see Suppl. material 2) **A** large S-facing granite boulder, on the north side of Cedar Creek. Spider aggregations found in shaded areas, at white arrow **B** web of an adult female **C** image of live adult female **D** image of live adult male.

side of campground along Cedar Creek, 35.7201, -118.6138, coll. E. Ciaccio & T. Bougie, 26 March 2018 (SDSU G2600–2602, 1M, 2F). Kern County, Sequoia NF, Alder Creek campground, north side of campground along Cedar Creek, 35.7201, -118.6125, coll. M Hedin & O. Hedin, 5 Sept 2020 (SDSU_TAC000657, 2M). Kern County, Hwy 155, Cedar Creek campground, Hwy 155, 35.7500, -118.5810, coll. E. Ciaccio & T. Bougie, 25 March 2018 (SDSU G2596–2599, 4I). Kern County, upstream of Cedar Creek campground, off Hwy 155, Sequoia National Forest, 35.7508, -118.5807, elevation ~ 1520 meters, coll. M. Hedin, 4 October 2021 (MCH 21_091, 1M, 4F).

Distribution and habitat. Known only from the upper Tule River and upper Cedar Creek drainages, at the southern end of the California Sierra Nevada mountains (Fig. 9). We hypothesize that higher elevation xeric ridges (Dennison Mountain ridge in particular) separate the distribution of this species from Kaweah River drainage populations of *H. petrunkevitchi*. Populations of *H. xomote* sp. nov. are predicted to be present in the White River drainage that lies between the Tule and Cedar Creek drainages (Fig. 9), although collecting efforts in this drainage have failed thus far. We

have collected these spiders on shaded granite boulders, in mineshafts, and in stream culverts, generally near water along rivers or streams, in conifer or mixed oak/conifer forests (Fig. 14; Suppl. material 2). See also Suppl. material 2 for locality (including elevation) and natural history information for specimens examined.

Conservation. Specimens are more abundant and populations appear more secure in the densely forested and higher elevation / higher latitude Tule River drainage. Specimens are less abundant and populations appear more fragmented in the lower elevation and more southerly Cedar Creek drainage. Recent large fires have occurred in both drainages.

Acknowledgements

We dedicate this work to Dr. David Wake, a brilliant and generous herpetologist and evolutionary biologist from the Museum of Vertebrate Zoology and UC Berkeley, who passed away in early 2021. Dr. Wake's work on California biodiversity and the speciation processes of this landscape, and his open-mindedness and appreciation for both vertebrate and invertebrates, have long served to inspire the senior author.

California specimens were collected under permit from Yosemite National Park (YOSE-2017-SCI-0039) and Sequoia/Kings Canyon National Park (SEKI-2017-SCI-0026). Several people helped to collect spiders, including Tierney Bougie, Keith Crandall, Ole Hedin, Bradley Hernandez, Andrew Rivera, Cristina Torres, and Jennifer Waters. See prior acknowledgements of Keith and Hedin (2012) for Appalachian collection support. Ingrid Niesman from the SDSU Electron Microscopy Facility provided excellent technical support. Guilherme Azevedo and Rodrigo Monjaraz Ruedas provided advice regarding patterns of morphological variation. Sean Kelly and Jasmine Llamas imaged spermathecal organs. EC was funded by the American Arachnological Society's Vincent Roth Fund for Systematics Research, which funded multiple field trips to the Sierra Nevada. Comments by Guilherme Azevedo, Karina Silvestre Bringas, Chris Hamilton, Ivan Magalhaes, Michael Rix, and Rodrigo Monjaraz Ruedas greatly helped to improve the manuscript.

References

- Alberti G, Coyle FA (1991) Ultrastructure of the primary male genital system, spermatozoa, and spermiogenesis of *Hypochilus pococki* (Araneae, Hypochilidae). *Journal of Arachnology* 19: 136–149.
- Bennett R, Copley C, Copley D (2021) *Cybaeus* (Araneae: Cybaeidae): the *aspenicolens* species group of the Californian clade. *Zootaxa* 4926(2): 224–244. <https://doi.org/10.11646/zootaxa.4926.2.4>
- Bernardo J (2011) A critical appraisal of the meaning and diagnosability of cryptic evolutionary diversity, and its implications for conservation in the face of climate change. In: Hodkinson

- TR, Jones MB, Waldren S, Parnell JAN (Eds) Climate change, ecology and systematics. Cambridge University Press, Cambridge, UK, 380–438. <https://doi.org/10.1017/CBO9780511974540.019>
- Bickford D, Lohman DJ, Sodhi NS, Ng PK, Meier R, Bickford D, Lohman DJ, Sodhi NS, Ng PK, Meier R, Winker K, Ingram KK, Das I (2007) Cryptic species as a window on diversity and conservation. *Trends in Ecology & Evolution* 22(3): 148–155. <https://doi.org/10.1016/j.tree.2006.11.004>
- Blakey RC, Ranney WD (2017) Ancient landscapes of western North America: A geologic history with paleogeographic maps. Springer, Switzerland, 228 pp. <https://doi.org/10.1007/978-3-319-59636-5>
- Bond JE (2012) Phylogenetic treatment and taxonomic revision of the trapdoor spider genus *Aptostichus* Simon (Araneae, Mygalomorphae, Euctenizidae). *ZooKeys* 252: 1–209. <https://doi.org/10.3897/zookeys.252.3588>
- Bossert S, Danforth BN (2018) On the universality of target-enrichment baits for phylogenomic research. *Methods in Ecology and Evolution* 9(6): 1453–1460. <https://doi.org/10.1111/2041-210X.12988>
- Brewer MS, Spruill CL, Rao NS, Bond JE (2012) Phylogenetics of the millipede genus *Brachycybe* Wood, 1864 (Diplopoda: Platydesmida: Andrognathidae): Patterns of deep evolutionary history and recent speciation. *Molecular Phylogenetics and Evolution* 64(1): 232–242. <https://doi.org/10.1016/j.ympev.2012.04.003>
- Bryant D, Bouckaert R, Felsenstein J, Rosenberg NA, RoyChoudhury A (2012) Inferring species trees directly from biallelic genetic markers: bypassing gene trees in a full coalescent analysis. *Molecular Biology and Evolution* 29(8): 1917–1932. <https://doi.org/10.1093/molbev/mss086>
- Carstens BC, Pelletier TA, Reid NM, Satler JD (2013) How to fail at species delimitation. *Molecular Ecology* 22(17): 4369–4383. <https://doi.org/10.1111/mec.12413>
- Castresana J (2000) Selection of conserved blocks from multiple alignments for their use in phylogenetic analysis. *Molecular Biology and Evolution* 17: 540–552. <https://doi.org/10.1093/oxfordjournals.molbev.a026334>
- Catley KM (1994) Descriptions of new *Hypochilus* species from New Mexico and California with a cladistic analysis of the Hypochilidae (Araneae). *American Museum Novitates* 3088: 1–27.
- Chambers EA, Hillis DM (2019) The multispecies coalescent over-splits species in the case of geographically widespread taxa. *Systematic Biology* 69(1): 184–193. <https://doi.org/10.1093/sysbio/syz042>
- Chifman J, Kubatko L (2014) Quartet inference from SNP data under the coalescent model. *Bioinformatics* 30(23): 3317–3324. <https://doi.org/10.1093/bioinformatics/btu530>
- Coates DJ, Byrne M, Moritz C (2018) Genetic diversity and conservation units: dealing with the species-population continuum in the age of genomics. *Frontiers in Ecology and Evolution* 6: 1–13. <https://doi.org/10.3389/fevo.2018.00165>
- Danecek P, Auton A, Abecasis G, Albers CA, Banks E, DePristo MA, Handsaker RE, Lunter G, Marth GT, Sherry ST, McVean G (2011) The variant call format and VCFtools. *Bioinformatics* 27(15): 2156–2158. <https://doi.org/10.1093/bioinformatics/btr330>

- Davis HR, Das I, Leaché AD, Karin BR, Brennan IG, Jackman TR, Nashriq I, Onn Chan K, Bauer AM (2021) Genetically diverse yet morphologically conserved: Hidden diversity revealed among Bornean geckos (Gekkonidae: *Cyrtodactylus*). *Journal of Zoological Systematics and Evolutionary Research* 59: 1113–1135. <https://doi.org/10.1111/jzs.12470>
- Degnan JH, Rosenberg NA (2009) Gene tree discordance, phylogenetic inference and the multispecies coalescent. *Trends in Ecology & Evolution* 24(6): 332–340. <https://doi.org/10.1016/j.tree.2009.01.009>
- Derkarabetian S, Starrett J, Tsurusaki N, Ubick D, Castillo S, Hedin M (2018) A stable phylogenomic classification of Travunioidea (Arachnida, Opiliones, Laniatores) based on sequence capture of ultraconserved elements. *ZooKeys* (760): 1–36. <https://doi.org/10.3897/zookeys.760.24937>
- Derkarabetian S, Castillo S, Koo PK, Ovchinnikov S, Hedin M (2019) A demonstration of unsupervised machine learning in species delimitation. *Molecular Phylogenetics and Evolution* 139: 106562. <https://doi.org/10.1016/j.ympev.2019.106562>
- Derkarabetian S, Starrett J, Hedin M (2022) Using natural history to guide supervised machine learning for cryptic species delimitation with genetic data. *Frontiers in Zoology*. <https://doi.org/10.1186/s12983-022-00453-0>
- Emata KN, Hedin M (2016) From the mountains to the coast and back again: Ancient biogeography in a radiation of short-range endemic harvestmen from California. *Molecular Phylogenetics and Evolution* 98: 233–243. <https://doi.org/10.1016/j.ympev.2016.02.002>
- Evanno G, Regnaut S, Goudet J (2005) Detecting the number of clusters of individuals using the software STRUCTURE: a simulation study. *Molecular Ecology* 14(8): 2611–2620. <https://doi.org/10.1111/j.1365-294X.2005.02553.x>
- Faircloth BC (2013) illumiprocessor: a trimmomatic wrapper for parallel adapter and quality trimming. <http://dx.doi.org/10.6079/J9ILL>
- Faircloth BC (2016) PHYLUCE is a software package for the analysis of conserved genomic loci. *Bioinformatics* 32: 786–788. <https://doi.org/10.1093/bioinformatics/btv646>
- Faircloth BC (2017) Identifying conserved genomic elements and designing universal bait sets to enrich them. *Methods in Ecology and Evolution* 8(9): 1103–1112. <https://doi.org/10.1111/2041-210X.12754>
- Fernández R, Kallal RJ, Dimitrov D, Ballesteros JA, Arnedo MA, Giribet G, Hormiga G (2018) Phylogenomics, diversification dynamics, and comparative transcriptomics across the spider tree of life. *Current Biology* 28(9): 1489–1497. <https://doi.org/10.1016/j.cub.2018.03.064>
- Fišer C, Robinson CT, Malard F (2018) Cryptic species as a window into the paradigm shift of the species concept. *Molecular Ecology* 27(3): 613–635. <https://doi.org/10.1111/mec.14486>
- Forster RR, Platnick NI, Gray MR (1987) A review of the spider superfamilies Hypochiloidea and Austrochiloidea (Araneae, Araneomorphae). *Bulletin of the American Museum Natural History* 185(1): 1–116. <https://digitallibrary.amnh.org/handle/2246/969?show=full>
- Fujisawa T, Barraclough TG (2013) Delimiting species using single-locus data and the Generalized Mixed Yule Coalescent approach: a revised method and evaluation on simulated data sets. *Systematic Biology* 62(5): 707–724. <https://doi.org/10.1093/sysbio/syt033>

- Fujisawa T, Aswad A, Barraclough TG (2016) A rapid and scalable method for multilocus species delimitation using Bayesian model comparison and rooted triplets. *Systematic Biology* 65(5): 759–771. <https://doi.org/10.1093/sysbio/syw028>
- Garrison NL, Rodriguez J, Agnarsson I, Coddington JA, Griswold CE, Hamilton CA, Hedin M, Kocot KM, Ledford JM, Bond JE (2016) Spider phylogenomics: Untangling the Spider Tree of Life. *PeerJ* 4: e1719. <https://doi.org/10.7717/peerj.1719>
- Gertsch WJ (1958) The spider family Hypochilidae. *American Museum Novitates* 1912: 1–28.
- Gertsch WJ (1964) A review of the genus *Hypochilus* and a description of a new species from Colorado (Araneae, Hypochilidae). *American Museum Novitates* 2203: 1–14.
- Gittenberger E (1991) What about non-adaptive radiation? *Biological Journal of the Linnean Society* 43(4): 263–272. <https://doi.org/10.1111/j.1095-8312.1991.tb00598.x>
- Grabherr MG, Haas BJ, Yassour M, Levin JZ, Thompson DA, Amit I, Adiconis X, Fan L, Raychowdhury R, Zeng Q, Chen Z (2011) Full-length transcriptome assembly from RNA-Seq data without a reference genome. *Nature Biotechnology* 29(7): 644–652. <https://doi.org/10.1038/nbt.1883>
- Harvey MS (2002) Short-range endemism among the Australian fauna: some examples from non-marine environments. *Invertebrate Systematics* 16: 555–570. <https://doi.org/10.1071/IS02009>
- Harvey MS, Rix MG, Framenau VW, Hamilton ZR, Johnson MS, Teale RJ, Humphreys G, Humphreys WF (2011) Protecting the innocent: studying short-range endemic taxa enhances conservation outcomes. *Invertebrate Systematics* 25(1): 1–10. <https://doi.org/10.1071/IS11011>
- Harvey MG, Smith BT, Glenn TC, Faircloth BC, Brumfield RT (2016) Sequence capture versus restriction site associated DNA sequencing for shallow systematics. *Systematic Biology* 65: 910–924. <https://doi.org/10.1093/sysbio/syw036>
- Hedin MC (2001) Molecular insights into species phylogeny, biogeography, and morphological stasis in the ancient spider genus *Hypochilus* (Araneae: Hypochilidae). *Molecular Phylogenetics and Evolution* 18: 238–251. <https://doi.org/10.1006/mpev.2000.0882>
- Hedin M (2015) High-stakes species delimitation in eyeless cave spiders (*Cicurina*, Dictynidae, Araneae) from central Texas. *Molecular Ecology* 24(2): 346–361. <https://doi.org/10.1111/mec.13036>
- Hedin M, Wood DA (2002) Genealogical exclusivity in geographically proximate populations of *Hypochilus thorelli* Marx (Araneae, Hypochilidae) on the Cumberland Plateau of North America. *Molecular Ecology* 11: 1975–1988. <https://doi.org/10.1046/j.1365-294X.2002.01561.x>
- Hedin M, Carlson D, Coyle F (2015) Sky island diversification meets the multispecies coalescent–divergence in the spruce–fir moss spider (*Microhexura montivaga*, Araneae, Mygalomorphae) on the highest peaks of southern Appalachia. *Molecular Ecology* 24(13): 3467–3484. <https://doi.org/10.1111/mec.13248>
- Hedin M, Derkarabetian S, Alfaro A, Ramírez MJ, Bond JE (2019) Phylogenomic analysis and revised classification of atypoid mygalomorph spiders (Araneae, Mygalomorphae), with notes on arachnid ultraconserved element loci. *PeerJ* 7: e6864. <https://doi.org/10.7717/peerj.6864>

- Heled J, Drummond AJ (2010) Bayesian inference of species trees from multilocus data. *Molecular Biology and Evolution* 27(3): 570–580. <https://doi.org/10.1093/molbev/msp274>
- Herbert PD, Ratnasingham S, de Waard JR (2003) Barcoding animal life: cytochrome c oxidase subunit 1 divergences among closely related species. *Proceedings of the Royal Society of London Series B, Biological Sciences* 270(suppl. 1): S96–S99. <https://doi.org/10.1098/rsbl.2003.0025>
- Hoffman RL (1963) A second species of the spider genus *Hypochilus* from eastern North America. *American Museum Novitates* 2148: 1–8.
- Huff RP, Coyle FA (1992) Systematics of *Hypochilus sheari* and *Hypochilus coylei*, two southern Appalachian lampshade spiders (Araneae, Hypochilidae). *Journal of Arachnology* 20(1): 40–46.
- Hundsdoerfer AK, Lee KM, Kitching IJ, Mutanen M (2019) Genome-wide SNP data reveal an overestimation of species diversity in a group of hawkmoths. *Genome Biology and Evolution* 11(8): 2136–2150. <https://doi.org/10.1093/gbe/evz113>
- Jackman TR, Wake DB (1994) Evolutionary and historical analysis of protein variation in the blotched forms of salamanders of the *Ensatina* complex (Amphibia: Plethodontidae). *Evolution* 48(3): 876–897. <https://doi.org/10.1111/j.1558-5646.1994.tb01369.x>
- Janes JK, Miller JM, Dupuis JR, Malenfant RM, Gorrell JC, Cullingham CI, Andrew RL (2017) The K = 2 conundrum. *Molecular Ecology* 26(14): 3594–3602. <https://doi.org/10.1111/mec.14187>
- Jockusch EL, Martínez-Solano I, Hansen RW, Wake DB (2012) Morphological and molecular diversification of slender salamanders (Caudata: Plethodontidae: *Batrachoseps*) in the southern Sierra Nevada of California with descriptions of two new species. *Zootaxa* 3190: 1–30. <https://doi.org/10.11646/zootaxa.3190.1.1>
- Kalyaanamoorthy S, Minh BQ, Wong TK, Von Haeseler A, Jermiin LS (2017) ModelFinder: fast model selection for accurate phylogenetic estimates. *Nature Methods* 14(6): 587–589. <https://doi.org/10.1038/nmeth.4285>
- Kass RE, Raftery AE (1995) Bayes factors. *Journal of the American Statistical Association* 90(430): 773–795. <https://doi.org/10.1080/01621459.1995.10476572>
- Katoh K, Standley DM (2013) MAFFT multiple sequence alignment software version 7: improvements in performance and usability. *Molecular Biology and Evolution* 30(4): 772–780. <https://doi.org/10.1093/molbev/mst010>
- Keith R, Hedin M (2012) Extreme mitochondrial population subdivision in southern Appalachian paleoendemic spiders (Araneae: Hypochilidae: *Hypochilus*), with implications for species delimitation. *Journal of Arachnology* 40: 167–181. <https://doi.org/10.1636/A11-49.1>
- Kimura M (1980) A simple method for estimating evolutionary rates of base substitutions through comparative studies of nucleotide sequences. *Journal of Molecular Evolution* 16(2): 111–120. <https://doi.org/10.1007/BF01731581>
- Kopelman NM, Mayzel J, Jakobsson M, Rosenberg NA, Mayrose I (2015) Clumpak: a program for identifying clustering modes and packaging population structure inferences across K. *Molecular Ecology Resources* 15(5): 1179–1191. <https://doi.org/10.1111/1755-0998.12387>

- Kozak KH, Weisrock DW, Larson A (2006) Rapid lineage accumulation in a non-adaptive radiation: phylogenetic analysis of diversification rates in eastern North American woodland salamanders (Plethodontidae: Plethodon). *Proceedings of the Royal Society B: Biological Sciences* 273(1586): 539–546. <https://doi.org/10.1098/rspb.2005.3326>
- Lanfear R (2018) Calculating and interpreting gene- and site-concordance factors in phylogenomics. http://www.robertlanfear.com/blog/files/concordance_factors.html
- Lanfear R, Calcott B, Ho SY, Guindon S (2012) PartitionFinder: combined selection of partitioning schemes and substitution models for phylogenetic analyses. *Molecular Biology and Evolution* 29(6): 1695–1701. <https://doi.org/10.1093/molbev/mss020>
- Leaché AD, Fujita MK, Minin VN, Bouckaert RR (2014) Species delimitation using genome-wide SNP data. *Systematic Biology* 63(4): 534–542. <https://doi.org/10.1093/sysbio/syu018>
- Leavitt DH, Bezy RL, Crandall KA, Sites Jr JW (2007) Multi-locus DNA sequence data reveal a history of deep cryptic vicariance and habitat-driven convergence in the desert night lizard *Xantusia vigilis* species complex (Squamata: Xantusiidae). *Molecular Ecology* 16: 4455–4481. <https://doi.org/10.1111/j.1365-294X.2007.03496.x>
- Leavitt DH, Starrett J, Westphal MF, Hedin M (2015) Multilocus sequence data reveal dozens of putative cryptic species in a radiation of endemic Californian mygalomorph spiders (Araneae, Mygalomorphae, Nemesiidae). *Molecular Phylogenetics and Evolution* 91: 56–67. <https://doi.org/10.1016/j.ympev.2015.05.016>
- Ledford J, Derkarabetian S, Ribera C, Starrett J, Bond JE, Griswold C, Hedin M (2021) Phylogenomics and biogeography of leptonetid spiders (Araneae: Leptonetidae). *Invertebrate Systematics* 35(3): 332–349. <https://doi.org/10.1071/IS20065>
- Li J-N, Yan X-Y, Lin Y-J, Li S-Q, Chen H-F (2021) Challenging Wallacean and Linnean short-falls: *Ectatosticta* spiders (Araneae, Hypochilidae) from China. *Zoological Research* 42(6): 791–794. <https://doi.org/10.24272/j.issn.2095-8137.2021.212>
- Magalhaes ILF, Neves DM, Santos FR, Vidigal THDA, Brescovit AD, Santos AJ (2019) Phylogeny of Neotropical *Sicarius* sand spiders suggests frequent transitions from deserts to dry forests despite antique, broad-scale niche conservatism. *Molecular Phylogenetics and Evolution* 140: 106569. <https://doi.org/10.1016/j.ympev.2019.106569>
- Magalhaes IL, Azevedo GH, Michalik P, Ramírez MJ (2020) The fossil record of spiders revisited: implications for calibrating trees and evidence for a major faunal turnover since the Mesozoic. *Biological Reviews* 95(1): 184–217. <https://doi.org/10.1111/brv.12559>
- Magalhaes IL, Porta AO, Wunderlich J, Proud DN, Ramírez MJ, Pérez-González A (2021) Taxonomic revision of fossil Psilodercidae and Ochyroceratidae spiders (Araneae: Synspermiata), with a new species of *Priscaleclercera* from mid-Cretaceous Burmese amber, northern Myanmar. *Cretaceous Research* 121: 104751. <https://doi.org/10.1016/j.cretres.2020.104751>
- Marshall TL, Chambers EA, Matz MV, Hillis DM (2021) How mitonuclear discordance and geographic variation have confounded species boundaries in a widely studied snake. *Molecular Phylogenetics and Evolution* 162: 107194. <https://doi.org/10.1016/j.ympev.2021.107194>
- Marx G (1888) On a new and interesting spider. *Entomologica Americana* 4: 160–162.

- Mason NA, Fletcher NK, Gill BA, Funk WC, Zamudio KR (2020) Coalescent-based species delimitation is sensitive to geographic sampling and isolation by distance. *Systematics and Biodiversity* 18(3): 269–280. <https://doi.org/10.1080/14772000.2020.1730475>
- Minh B, Hahn M, Lanfear R (2018) New methods to calculate concordance factors for phylogenomic datasets. *Molecular Biology and Evolution* 37(9): 2727–2733. <https://doi.org/10.1093/molbev/msaa106>
- Niemiller ML, Near TJ, Fitzpatrick BM (2012) Delimiting species using multilocus data: diagnosing cryptic diversity in the southern cavefish, *Typhlichthys subterraneus* (Teleostei: Amblyopsidae). *Evolution: International Journal of Organic Evolution* 66(3): 846–866. <https://doi.org/10.1111/j.1558-5646.2011.01480.x>
- Nguyen LT, Schmidt HA, Von Haeseler A, Minh BQ (2015) IQ-TREE: A fast and effective stochastic algorithm for estimating maximum-likelihood phylogenies. *Molecular Biology and Evolution* 32(1): 268–274. <https://doi.org/10.1093/molbev/msu300>
- Paradis E, Schliep K (2019) ape 5.0: an environment for modern phylogenetics and evolutionary analyses in R. *Bioinformatics* 35: 526–528. <https://doi.org/10.1093/bioinformatics/bty633>
- Papenfuss TJ, Parham JF (2013) Four new species of California legless lizards (*Anniella*). *Breviora* 536(1): 1–17. <https://doi.org/10.3099/MCZ10.1>
- Pfenninger M, Schwenk K (2007) Cryptic animal species are homogeneously distributed among taxa and biogeographical regions. *BMC Evolutionary Biology* 7(1): e121. <https://doi.org/10.1186/1471-2148-7-121>
- Pritchard JK, Stephens M, Donnelly P (2000) Inference of population structure using multilocus genotype data. *Genetics* 155(2): 945–959. <https://doi.org/10.1093/genetics/155.2.945>
- Rambaut A, Drummond AJ, Xie D, Baele G, Suchard MA (2018) Posterior summarization in Bayesian phylogenetics using Tracer 1.7. *Systematic Biology* 67(5): 901–904. <https://doi.org/10.1093/sysbio/syy032>
- Ramírez MJ, Magalhaes IL, Derkarabetian S, Ledford J, Griswold CE, Wood HM, Hedin M (2021) Sequence capture phylogenomics of true spiders reveals convergent evolution of respiratory systems. *Systematic Biology* 70(1): 14–20. <https://doi.org/10.1093/sysbio/syaa043>
- Reilly SB, Wake DB (2015) Cryptic diversity and biogeographical patterns within the black salamander (*Aneides flavipunctatus*) complex. *Journal of Biogeography* 42(2): 280–291. <https://doi.org/10.1111/jbi.12413>
- Satler JD, Carstens BC, Hedin M (2013) Multilocus species delimitation in a complex of morphologically conserved trapdoor spiders (Mygalomorphae, Antrodiaetidae, *Aliatypus*). *Systematic Biology* 62(6): 805–823. <https://doi.org/10.1093/sysbio/syt041>
- Schönhöfer AL, McCormack M, Tsurusaki N, Martens J, Hedin M (2013) Molecular phylogeny of the harvestmen genus *Sabacon* (Arachnida: Opiliones: Dyspnoi) reveals multiple Eocene–Oligocene intercontinental dispersal events in the Holarctic. *Molecular Phylogenetics and Evolution* 66(1): 303–315. <https://doi.org/10.1016/j.ympev.2012.10.001>
- Singhal S, Hoskin CJ, Couper P, Potter S, Moritz C (2018) A framework for resolving cryptic species: a case study from the lizards of the Australian wet tropics. *Systematic Biology* 67(6): 1061–1075. <https://doi.org/10.1093/sysbio/syy026>

- Stamatakis A (2014) RAxML version 8: a tool for phylogenetic analysis and post-analysis of large phylogenies. *Bioinformatics* 30(9): 1312–1313. <https://doi.org/10.1093/bioinformatics/btu033>
- Starrett J, Derkarabetian S, Hedin M, Bryson RW, McCormack JE, Faircloth BC (2017) High phylogenetic utility of an ultraconserved element probe set designed for Arachnida. *Molecular Ecology Resources* 17(4): 812–823. <https://doi.org/10.1111/1755-0998.12621>
- Starrett J, Hayashi C, Derkarabetian D, Hedin M (2018) Cryptic elevational zonation in trapdoor spiders (Araneae, Antrodiaetidae, *Aliatypus janus* complex) from the California southern Sierra Nevada. *Molecular Phylogenetics and Evolution* 118: 403–413. <https://doi.org/10.1016/j.ympev.2017.09.003>
- Stockman AK, Bond JE (2007) Delimiting cohesion species: extreme population structuring and the role of ecological interchangeability. *Molecular Ecology* 16(16): 3374–3392. <https://doi.org/10.1111/j.1365-294X.2007.03389.x>
- Sukumaran J, Knowles LL (2017) Multispecies coalescent delimits structure, not species. *Proceedings of the National Academy of Sciences* 114(7): 1607–1612. <https://doi.org/10.1073/pnas.1607921114>
- Swofford DL (2003) PAUP*. Phylogenetic Analysis Using Parsimony (*and Other Methods). Version 4. Sinauer Associates, Sunderland, Mass.
- Talavera G, Castresana J (2007) Improvement of phylogenies after removing divergent and ambiguously aligned blocks from protein sequence alignments. *Systematic Biology* 56: 564–577. <https://doi.org/10.1080/10635150701472164>
- Templeton A, Shaw K, Routman E, Davis S (1990) The genetic consequences of habitat fragmentation. *Annals of the Missouri Botanical Garden* 77(1): 13–27. <https://doi.org/10.2307/2399621>
- Van der Auwera GA, Carneiro MO, Hartl C, Poplin R, Del Angel G, Levy-Moonshine A, Jordan T, Shakir K, Roazen D, Thibault J, Banks E (2013) From FastQ data to high-confidence variant calls: the genome analysis toolkit best practices pipeline. *Current Protocols in Bioinformatics* 43(1): 11–10. <https://doi.org/10.1002/0471250953.bi1110s43>
- Vera A, Clark PL (2002) English-Yowlumni dictionary. Tule River Yokuts Language Project. <https://tulerivertribe-nsn.gov/language/>
- Vieites DR, Min MS, Wake DB (2007) Rapid diversification and dispersal during periods of global warming by plethodontid salamanders. *Proceedings of the National Academy of Sciences* 104(50): 19903–19907. <https://doi.org/10.1073/pnas.0705056104>
- Weng YM, Kavanaugh DH, Schoville SD (2021) Drainage basins serve as multiple glacial refugia for alpine habitats in the Sierra Nevada Mountains, California. *Molecular Ecology* 30(3): 826–843. <https://doi.org/10.1111/mec.15762>
- Wunderlich J (2008) The dominance of ancient spider families of the Araneae: Haplogynae in the Cretaceous, and the late diversification of the advanced ecribellate spiders of the Entelegynae after the Cretaceous-Tertiary boundary extinction events, with descriptions of new families. *Beiträge zur Araneologie* 5: 524–674, 802–813.
- Zerbino D, Birney E (2008) Velvet: algorithms for de novo short read assembly using de Bruijn graphs. *Genome Research* 18(5): 821–829. <https://doi.org/10.1101/gr.074492.107>

Supplementary material 1

Appendix I

Authors: Erik Ciaccio, Andrew Debray, Marshal Hedin

Data type: xlsx. file

Explanation note: Specimens used in phylogenomic analysis.

Copyright notice: This dataset is made available under the Open Database License (<http://opendatacommons.org/licenses/odbl/1.0/>). The Open Database License (ODbL) is a license agreement intended to allow users to freely share, modify, and use this Dataset while maintaining this same freedom for others, provided that the original source and author(s) are credited.

Link: <https://doi.org/10.3897/zookeys.1086.77190.suppl1>

Supplementary material 2

Appendix II

Authors: Erik Ciaccio, Andrew Debray, Marshal Hedin

Data type: xlsx. file

Explanation note: Specimens examined and used for study of morphology.

Copyright notice: This dataset is made available under the Open Database License (<http://opendatacommons.org/licenses/odbl/1.0/>). The Open Database License (ODbL) is a license agreement intended to allow users to freely share, modify, and use this Dataset while maintaining this same freedom for others, provided that the original source and author(s) are credited.

Link: <https://doi.org/10.3897/zookeys.1086.77190.suppl2>

Corrigendum: The distribution and behavioral characteristics of plateau pikas (*Ochotona curzoniae*). ZooKeys 1059: 157–171. <https://doi.org/10.3897/zookeys.1059.63581>

Jun Qiu^{1,2}, Cang Ma³, Ying-Hui Jia⁴, Jin-Zhao Wang³, Shou-Kai Cao³, Fang-Fang Li^{1,4}

1 State Key Laboratory of Plateau Ecology and Agriculture, Qinghai University, Xining, 810016, China
2 State Key Laboratory of Hydrosience & Engineering, Tsinghua University, Beijing, 100084, China
3 School of Water Resources and Electric Power, Qinghai University, Xining, 810016, China
4 College of Water Resources & Civil Engineering, China Agricultural University, Beijing, 100083, China

Corresponding author: Fang-Fang Li (liff@cau.edu.cn)

Academic editor: Jesus Maldonado | Received 3 November 2021 | Accepted 12 January 2022 | Published 17 February 2022

<http://zoobank.org/E3507CBD-AF90-4182-96FC-7144F7BC6460>

Citation: Qiu J, Ma C, Jia Y-H, Wang J-Z, Cao S-K, Li F-F (2022) Corrigendum: The distribution and behavioral characteristics of plateau pikas (*Ochotona curzoniae*). ZooKeys 1059: 157–171. <https://doi.org/10.3897/zookeys.1059.63581>. ZooKeys 1086: 205–206. <https://doi.org/10.3897/zookeys.1086.77554>

Thanks to the letter by Li (2021), the authors were made aware of a mistake regarding the surface temperature reported in the paper above. The surface temperature reported in the paper refers to the temperature recorded in images detected by the temperature receptors of the field infrared camera, which did not reflect the actual surface temperature. As there was no shelter to the field infrared camera in alpine meadow grasslands, the temperature of the camera increased rapidly under direct sunshine. Thus, the conclusion that the preferable temperature for pikas may be approximately 31–35°C was incorrect, and the temperature reported in Figure 6 was also therefore incorrect. As there was no equipment to measure the surface temperature in the observation, it is difficult to restore the original surface temperature values. The data in Figure 6 should only be used to compare the behavior characteristics of plateau pikas at different relative temperatures.

The authors would like to declare that the temperature in the paper refers to the temperature recorded in images detected by the field infrared camera's temperature receptors, and does not reflect the actual surface temperature. The historic high air

temperature in Dari County was 23.2°C (Wang et al. 2018), so the temperatures cited in the paper can only be taken as a reference of the temperature of the cameras in the sun.

The authors would like to acknowledge Dr. Wen-Jing Li for pointing out this discrepancy in surface temperatures.

References

- Li WJ (2021) Letter for Qiu et al. (2021) regarding ‘The distribution and behavioral characteristics of plateau pikas (*Ochotona curzoniae*)’. ZooKeys.
- Wang H, Zhao Z-X, Wang X-Y (2018) Analysis of trends and periodicity of temperature change of Dari County from 1956–2015. Modern Agricultural Science and Technology 2018(18): 214–215. [In Chinese]